

Proceedings of the International V4 Waste Recycling 21 Conference

editor
Ljudmilla Bokányi



Miskolci Egyetem
2018

ISBN 978-963-358-173-5

CONTENTS

<i>Ljudmilla Bokányi:</i> Preface.....	7
<i>Peter Chrabák–Ernő Garamvölgyi:</i> Smart Urban Re-Use Flagship Alliances in Central Europe	9
<i>Denis Werner–Thomas Mütze–Hans-Georg Jäckel–Urs Alexander Peuker:</i> Mechanical Processing of Spent Lithium-Ion-Batteries from Electric Vehicles	20
<i>Valéria Má dai Üveges–Terézia Varga–Ljudmilla Bokányi:</i> Experimental Comparison: Acidic and Bio Solubilisation of Indium from Liquid Crystal Displays	28
<i>Dávid Jáger–Daniel Kupka–Miroslava Václavíková–Lucia Ivaničová–George Gallios:</i> Electrochemical Oxidation of Reactive Black 5 Azo Dye in Chloride Media.....	35
<i>Gergő Bodnár–Daniel Kupka–Dávid Jáger:</i> Triazine Pesticide Decomposition by Advanced Oxidation Processes	43
<i>Grozdana Bogdanović–Dragan Milojević–Anđelija Bogdanović an–Velizar Stanković:</i> Adsorption of Copper, Iron and Zinc Ions from Acid Mine Drainage by Natural Zeolite	45
<i>Katarina Balanović–Milan Trumić–Maja Trumić:</i> Comminution of Zeolite and its Potential Application	53
<i>Dominika Behunová–George Gallios–Miroslava Václavíková:</i> Environmental Applications of Graphene Oxide	62
<i>József Paulovics–Khishigsuren Natsagdorj–Ljudmilla Bokányi:</i> Comparison of Biowaste Derived and Algae Biosorbents for Heavy Metals Removal from Effluents.....	65
<i>Ivo Safarik–Jitka Prochazkova–Sindy Mullerova–Eva Baldikova–Kristyna Pospiskova:</i> Magnetically Responsive Biomaterials and their Application	75
<i>Inna Melnyk–Veronika Tomina–Nataliya Stoliarchuk–Anastasiya Lebed–Iryna Furtat– Maria Kanuchova–Miroslava Václavíková:</i> Effect of Synthesis Conditions on the Formation of Spherical Silica Particles with Amino Groups and their Investigation in Sorption and as Antibacterial Agents	76
<i>Sándor Nagy–Ljudmilla Bokányi–Valéria Üveges–Mária Ambrus–Stoyan Gaydardzhiev– Gábor Mucsi:</i> Influence of Various Mechanical Preparation Methods of LCD on the Leachability of Critical Elements	77
<i>Michal Marcin–Martin Sisol–Ivan Brezáni:</i> Effect of Different Activation Solution on Andesite Based Geopolymers	88

<i>József Fajtli–Barnabás Csőke–Roland Romenda–Zoltán Nagy–Szabolcs Németh:</i> Developing a Complex Processing Technology in Zalaegerszeg for RMSW Preparation to Decrease Landfilling.....	94
<i>Milan Trumić–Maja Trumić–Dragan Radulović:</i> The Effect of Sieve Loading and Particles Shape on the Results of Polymer Sieve Kinetics	105
<i>Christof Lanzerstorfer:</i> Composition of Cement Kiln Dust by Particle Size.....	115
<i>Roland Romenda:</i> Process Engineering Investigation of a Hungarian Developed NIR Separator.....	122
<i>Marta Wójcik–Feliks Stachowicz:</i> Possibility of the Utilization of Sewage Sludge and Different Waste in a Civil Engineering	133
<i>Ákos Pintér–Móricz–János Takács–Ljudmilla Bokányi:</i> Experimental Investigation of Applicability of Bakonyoszló Sub-Bituminous Coal in Sewage Sludge Treatment.....	150
<i>Tamás Kékesi:</i> Characterization and Complete Utilization of Aluminium Melting Dross	162
<i>Roland Szabó–Benjámín Gulyás–Gábor Mucsi:</i> Glass Foam from Waste Hollow Glass	178
<i>Vladimir Nikolić–Milan Trumić–Maja Trumić–Ljubiša Andrić:</i> Abbreviated Methods for Determining Bond Work Index	188
<i>Alena Sicakova:</i> Coatings a Possible Way to Improve the Recyclability of Waste Aggregates.....	205
<i>Guillermo Uquillas Giacometti:</i> Investigation of Rheological Behaviour of Different Bentonite-Water Suspensions for Tunnel Boring Application.....	218
<i>Paula Figueirido–Carina Ulsen–Maurício Bergerman–Gábor Mucsi:</i> Properties of Recycled Concrete Aggregate Produced by Different Comminution Methods.....	219
<i>Ida Balczár–Tamás Korim:</i> Alkali Activated Cement Production from Air-Cooled Slag Industrial Waste	228
<i>Kinga Korniejenko–Janusz Mikula–Michał Łach–Florencia Moure–Lucía Moreira Martín Duarte Guigou:</i> Characterization of Geopolymer Composites Reinforced with Plastic Wastes	229
<i>Thomas Mütze–Urs Alexander Peuker:</i> High-Performance Geopolymers by Wet Milling of Blast Furnace Slags.....	239

<i>Sándor Nagy–Quyên V. Trinh–Ljudmilla Bokányi–Anett Pintér–Tamás Fábrik:</i>	
Influence of Moisture Content and Temperature on Briquetting of Solar Dried Sewage Sludge	247
<i>Sándor Nagy–Quyên V. Trinh–Gábor Dóra:</i>	
Compression Time and Temperature Effectson PUR Agglomeration	258
<i>János Lakatos:</i>	
Comparison of Bauxite and Red Mud Leachability	268
<i>Tamás Madarász:</i>	
Changes and Leading Trends in Contaminated Site Rehabilitation	275
<i>János Lakatos–Tamás Török–Ljudmilla Bokányi:</i>	
Testing of Leachability of Elements of EAF Dust byAcidic and Alkaline Media.....	276

PREFACE

This volume contains papers of the **XXI International Waste Recycling Conference**.

This conference series is being organised by academic and research institutions of Visegrad 4 countries:

- Institute of Raw Material Preparation and Environmental Processing, University of Miskolc, Hungary;
- Institute of Geotechnics, Slovak Academy of Sciences, Kosice, Slovakia;
- Institute of Environmental Engineering, VSB-Technical University, Ostrava, Czech Republic;
- AGH-University of Science and Technology, Cracow, Poland;
- Cracow University of Technology, Cracow, Poland.

The V4 WR21 International Conference (22–23 November, 2018, University of Miskolc, Hungary) was organised in cooperation with the

- Mining Scientific Committee, Hungarian Academy of Sciences,
- Sub-committee on Mining, Earth- and Environmental Sciences, Sub-Commission on Preparation, Environmental Processing ,
- Mining and Energy and Association of Environmental Enterprises as well as
- „Sustainable Raw Material Management Thematic Network–RING 2017”, EFOP-3.6.2-16-2017-00010 PROJECT.

The papers presented covers all the topics of waste recycling science, technology and innovation:

- Recycling and utilisation of industrial wastes (metallurgical, power-engineering, mechanical engineering, chemical industrial, WEEE, end-of-life vehicles, plastics, demolishing waste, mining waste and tailings etc.);
- Treatment and recycling of municipal solid waste and biowaste;
- Recycling of critical raw materials from secondary sources;
- Decontamination and remediation of contaminated areas;
- Waste water treatment and air quality control;
- Business activities in waste recycling;
- Legislation issues of recycling and waste utilization.

The valuable contribution of all the authors, as well as organisers is highly appreciated.

Miskolc, November, 2018.

Dr. Ljudmilla Bokányi
editor
chair of the conference



SMART URBAN RE-USE FLAGSHIP ALLIANCES IN CENTRAL EUROPE

PETER CHRABÁK¹–ERNŐ GARAMVÖLGYI²

¹Senior Researcher, Bay Zoltán Nonprofit Ltd. for Applied Research, peter.chrabak@bayzoltan.hu

²Senior Researcher, Bay Zoltán Nonprofit Ltd. for Applied Research, erno.garamvolgyi@bayzoltan.hu

Abstract

Waste is an extremely relevant issue in urban areas. It can cause social conflicts in housing areas as waste collection schemes in public spaces is visible for citizens and has an impact on the living quality of urban spaces. Reuse is a highly relevant approach to tackle the challenges of Waste Prevention in urban areas and to implement sustainable production and consumption patterns in practice.

The INTERREG SURFACE project's main objective is to improve environmental management and quality of life of urban areas through the establishment of Multi-Stakeholder based Smart Re-Use parks (SRP) as a possible solution for increasing sustainability in selected pilot urban areas represented by project consortium partners. The change consists in the availability of a harmonized and evidence based decision making setting in the field of waste prevention and reuse in Central European area where: 1) reuse and waste prevention options become integrated options of environmental management strategies & action plans, 2) urban decision makers can share decisions, 3) multi-stakeholder cooperation schemes and Smart Re-Use Parks Action Plans can be shared and used; 4) tested and validated pilots can be studied and 5) an increased set of immediately usable instruments be adopted through twinning training schemes as showcases for further implementing the project results on other European urban locations as best practices.

Keywords: *Re-use, Smart re-use parks, Waste prevention, Functional Urban Area, Environmental sustainability.*

1. INTRODUCTION

Large volumes of waste and waste water, poor air and water quality, high levels of ambient noise, lack of integrated environmental management nowadays are relevant issues in modern urban living areas. Reuse, as the second priority step in the EU waste hierarchy is a highly relevant approach to tackle them. Despite recent improvements at transnational level there is still a highly fragmented decision making landscape in this field.

2. THE SURFACE PROJECT

The INTERREG SURFACE project (2017–2020) focuses on jointly creating the knowledge foundations of re-use related approach and demonstrate the potential of integrated reuse activities for urban resource efficiency and waste prevention strategies. SURFACE project plan to contribute for a more sustainable lifestyle by “mainstreaming” re-use as an alternative way of fulfilling customer needs. In this broad context re-use not only refers to waste management legislation but also has interfaces to a number of strategies, policies and concepts in the area of sustainable development (e.g. Europe 2020 Strategy, Circular Economy Strategy, Sustainable consumption and production and Sustainable Industrial Policy Action Plan, European Strategy on Sustainable Development).

The core project aim is to support the European Circular Economy Strategy by prolonging the product life time through re-use and subsequently saving resources and improving energy efficiency. The project concept is substantially based on the three dimensions of sustainable development:

- Ecological sustainability – Improving resource efficiency by reducing wastes and emissions by extending the lifetime of products.
- Social sustainability – The primary goals are the change of public behaviour towards a sustainable life style. Additionally creation of “green jobs” for low qualified / long-time unemployed people as well as providing good quality products for people with low income are also promoted.
- Economic sustainability – Strengthening regional economies by stimulating co-operations between different actors and development of new business fields and models (especially for social enterprises, SMEs and service providers) and supporting the sharing economy.

The demonstration of the potential of integrated re-use activities for urban resource efficiency and waste prevention strategies, as well as preparing the ground for the Pilot actions are supposed to illustrate re-use as a key driver for sustainable and environmentally conscious consumption.

More specifically the project SURFACE targets to improve the environmental management and quality of life in urban areas through the establishment of Multi-Stakeholder based “Smart Re-Use parks” as a possible solution for increasing sustainability in selected pilot urban areas delegated and represented by project partners, especially:

- fostering the exchange of know-how between countries and regions to be as efficient as possible with available resources.
- building up modular solutions for re-use centres and networks to fulfil the needs of all CE countries by easy adaption.
- promoting the setting up of a customised SRP considering the local/regional waste prevention plans and vice versa.
- defining a list of requirements on a basic and on an advanced level of an SRP development in order to adopt the concerned best practices.
- implementing pilots for testing the SRP concept in several CE countries.

With the successful implementation the re-use and waste prevention options may become integrated part of environmental management strategies and action plans, or local/regional waste prevention plans – in line with the Circular Economy strategy of the EU and multi-stakeholder cooperation

schemes and Smart Re-Use Parks action plans can be shared and used for supporting urban decision makers.

The project consortium consists of several partners from CE region countries as Austria, Croatia, Slovenia, Poland, Czech Republic, Hungary and Germany, Italy (with certain regions). The Hungarian partner is the Bay Zoltán Research Institute.

3. WHAT IS A “SMART RE-USE PARK”?

Ideally a “Smart Re-Use Park” (SRP) is a flexible and modular combinations of re-use oriented services – located in visible and liveable urban areas – organically embedded into urban waste prevention strategies. Depending on each urban context the modular structure of SRPs is guided by urban strategies and plans which define the combination of services best responding to urban waste prevention goals for instance: reuse-collection points and shops, repair cafes, repair and upcycling workshops, rental services, swapping platforms, educational labs, Fab Labs¹, online reuse market-places, exhibitions for different target groups (schools, environmental initiatives, general public, etc.). For the straightforward development of an SRP the next essential dimensions should be clearly addressed:

- Geographical area
- Concerned (local) stakeholders, cooperation
- Organisation structure of an SRP
- Available and additionally required infrastructure
- Implemented functions and services within an SRP.

4. SMART RE-USE PARK ACTIONS



Figure 1

The premise for awareness raising re-use centre of the FKF Nonprofit Zrt. in Budapest

¹ A fab lab (fabrication laboratory) is a small-scale workshop offering open access to (personal) digital fabrication. So a FabLab is a digital workshop which can be used by the public to create transform creative ideas into tangible prototypes. A FabLab comprises digitally controlled machines like a lasercutter, CNC-router, a 3D printer, a vinyl cutter and electronics with the aim to make “almost anything”. – source: <http://fablab.nl/wat-is-fablab/?lang=en>

The core concept of the SURFACE project is the formation of SRPs in five pilot regions (IT, AT, DE, PL, HU) and preparing the implementation in the other four regions (IT, CZ, SI, HR). The SRP will be a place where products, goods and materials will be given a new chance to get back into the product cycle instead of ending up as waste or as recycled material with a lower value. The SRP is not solely a place where goods get reused or upcycled, it also provides a space where people encounter each other and have the opportunity for exchange and knowledge transfer in the area of Re-Use. Courses and workshops can give leverage to reach new horizons in environment conservation. Figure 1 shows one of the two premises of the FKF Nonprofit Zrt., as the assigned pilot for the implementation of SURFACE aims in cooperation with Bay Zoltán Research Institute.

As a first step a comprehensive survey had been made for project partners and their feedbacks were evaluated to unfold the initial phase of each participated pilot urban area, including the statistical data and actual waste management situation. The fact sheet of the pilot areas are presented in Table 1 capturing the situation of 2017.

Table 1
Fact sheet on participated pilot areas

COUNTRY	GEOGRAPHICAL LOCATION	TYPE OF AREA	AREA (km ²)	POPULATION
Austria	Schwaz, Innsbruck Land and Innsbruck Stadt	Service area of the pilot host company	3 938.00	389 126
Croatia	Labin	Service area of the pilot host company	390.92	22 590
Czech republic	Stonavka and Brno	Service area of the pilot host company	314.87	386 594
Germany	Lindau and Kempten	Service area of the pilot host company	297 700	1 900
Hungary	Budapest	Service area of the pilot host company	525	1 860 000
Italy	Vicenza	Province	2 722	867 314
Italy	Rimini	Province	863.6	336 898
Poland	Torun	Municipality	115.57	193 000
Slovenia	Ljubljana	City	163.8	270 000

5. WASTE MANAGEMENT SITUATION IN THE PILOT AREAS

At the local level waste management practice is rather similar in all concerned areas due to similar legislative environment: The responsibility of waste management is mostly given to the municipalities or group of them and therefore the municipal solid waste collection is a public service. According to the conducted surveys, there are two possible options for bulky waste collection: in some of these areas citizens are entitled to the free removal of bulky waste once per year free of charge. In this case bulky waste should be placed at the designated location on the day agreed for bulky waste collection or one day before. If citizens have already used this service, they can either take their

bulky waste to the collection centre by themselves or they can order collection for payment. In other areas there is only an option for citizens to bring the bulky waste to the collection points for high volume waste by themselves or to give their re-usable goods to the re-use centres.

In SURFACE participated countries a general trend in quantity of waste is observed: it is noticeable that the amount of collected waste is rising while the percentage of disposed waste is significantly lower comparing to previous years.

6. DECISION MATRIX

Towards to achieve the project goals, important deliverable of the project has been developed: the **Decision Matrix** (DM) is assigned to scatter the built-up knowledge and know-how for a wider implementation of SRP concepts throughout in and outside the Central European territory. The DM is supposed to provide guidance about selection criteria to be adopted in other locations throughout Europe in order to implement the available practices via the project results. The DM is substantially based on the experiments of project partners to unfold and share their opinion and expertise, which are important for a common thinking.

In favour of the reason above, a survey was developed in cooperation with project partners for the widest consensus on guiding principles of an SRP. The survey comprises 8 categorized questions with predefined answers with marking from 1-5 at discrete steps of 1. The concerned categories are:

1. Legislation
2. Private business
3. State subsidy
4. Socio-economy aspects
5. Public awareness
6. Smart Re-Use Park implementation potential
7. Demand on second-hand items
8. Supply on second-hand items

The eight questions were then followed by three additional questions on implementation, where the answers here were also predefined by “Yes” or “No” options. For every question a free text cell was offered for making remarks and amendments.

In fact the predefined answers may have inhere certain limitations on making the most precise answers, however for an easier comparison and common understanding the answers from different partners it was considered to be the most proper option.

All questions had got a hint aiming common perception, as well as short description on all optional answers (grades). Every project partner having pilot activity was asked to apply the questions specifically to their pilot area and fill in accordingly. Their inherently subjective answers were presented automatically in an excel spider web diagram for an easier review and comparison. So, overall we had 9 complete surveys at the end (examples are shown on *Figure 1* and *Figure 2*).

The individual partner surveys were composed into one common table summarising the status-quo situation on each area assigned within SURFACE project. It presents as a comprehensive summary of the survey with the questions with their answering options and all the answers and

intends to serve as the **Decision Matrix (DM)**. The DM is aimed to contribute for a swift benchmarking of the current situations in SURFACE pilots from different aspects of re-use, i.e. legislation, economic conditions, public attitude. It can also transfer information for new associated partners, or stakeholders having interest to implement and/or operate SRPs, or solely a variety of single re-use activities.

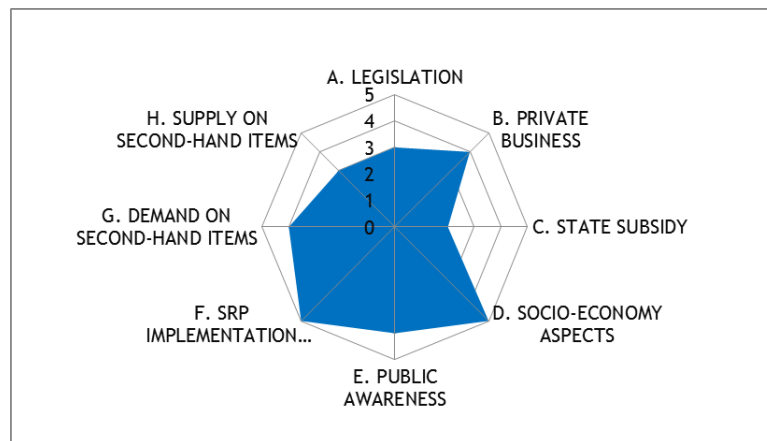


Figure 2
Austrian status-quo on Smart Re-Use Park implementation

Austria has got the most developed SRP infrastructure among the project partners. In this pilot area the strongest dimension concerning re-use is its socio-economy aspect: there are one or more social programmes linking directly to re-use. It is in close relation with a definitely positive public awareness and the dominant presence of private for-profit and non-for-profit businesses as well in the field of re-use. These positive givens leads to a relevant potential to the development of SRP in the region. This intention is also promoted by the already existing re-use related initiatives in the region, i.e.: repair and upcycling workshops, repair cafés, swapping platforms, rental services, fab labs, Library of Things², guided city tours with the focus on Re-Use. There are 62 recycling facilities in the region where re-usable items can be collected. The operators of an SRP are not restricted on legal status, so it can be hosted even by NGO, civil association and private company as well.

The willingness of citizens to transfer their obsolete items to re-use facilities is generally positive, but as long as there is a (well-known) company which makes profit out of the sale of re-use items the willingness may decline. So, the public is mainly motivated by environmental aspect to donate their obsolete items.

Concerning the demand on second-hand items, in the Austrian pilot region there is a strong striving for people beyond the green movement community to buy them. Although in the other districts of Tyrol, especially in the touristic areas the interest deteriorates drastically.

² Library of Things is an identical implementation of book library on any other items that can be found in a household, i.e. tools, sport equipment, toys, household appliances. The Library of Things movement is a growing trend in public in the United States and Western Europe.

The main drawback of the Austrian re-use system is the insufficient financial support, moreover the legislative background is also mentioned as a non-supportive factor.

As opposed Hungary has moderate tradition and public environmental consciousness as it is showed by *Figure 2*.

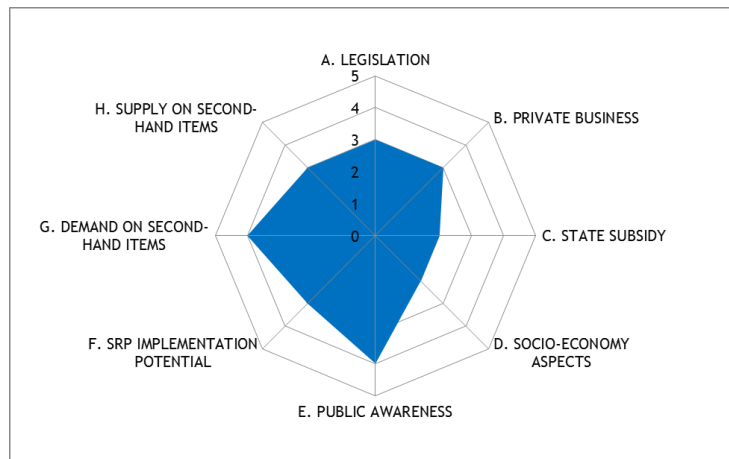


Figure 3
Hungarian status-quo on Smart Re-Use Park implementation

The Hungarian pilot area can be positioned in a fully average status from every aspect and can make a step forward in each category. The two most promising givens are the generally positive perceptions of the public on re-use issues and the dominantly positive acceptance of using second-hand products.

Nevertheless the two identified most relevant drawbacks refers to the engagement of state aiming to support: nor direct financial subsidy, nor direct social programmes exist supporting re-use initiatives.

Some elements as building blocks for an SRP already exist in the pilot region, i.e. rental service, online re-use marketplace, exhibition for different target groups. From venture aspects there is no restriction on the type of legal body to implement or to run an SRP.

7. OVERALL CONCLUSIONS ON DM RESULTS

The overall impression gained by the evaluation of the individual surveys above accurately reflects the re-use situations in the concerned areas. The overall consequences on each analysed dimensions are introduced in this chapter.

Legislation

From legislative aspects the German pilot area is in the most favourable position: its legislative measures exceed the mandatory provisions proactively. Italian region Emilia Romagna and Austrian Mid-Tyrol can be assumed to have a supportive legislation on re-use.

On the other end of the scale, the Croatian and Bohemian areas reported a rather passive and insufficient legislative system from re-use dimensions. The other locations are positioned themselves being in a neutral legal status, where the related obligations (derived from EU and national level) are fulfilled, however re-use is poorly addressed in the national and regional legislations.

Private business in re-use field

The presence of private actors in re-use field is mainly dominant in Austrian, Italian, Croatian and Slovenian regions. In Austria the private sector also involves private non-profit organisations. Most of the respondents claimed that the private share in re-use business is considerable, but still minor. In the Polish area the sector is mainly dominant by governmental organisations.

State subsidy

According to the reported answers of the surveys the most depressed aspect in re-use field is the deficient state subsidy. In most of the pilot areas there are some not significant financial supports; even they do not address re-use directly, even in the well exemplary region like Austria and Germany.

Socio-economy aspects

This analysed dimension shows the biggest deviation of answers: Austria and Italy can be considered having the most developed region, which are being reflected by the answers. Austria and Italy (Vicenza) reported that there are more social programmes linked directly to re-use, and also in German region there are more social programmes, but with indirect relation to re-use. In other pilot areas there are no social programmes at all, or if there are any, they indirectly linked to general waste management, but not re-use.

Public awareness

The public awareness on preparing for re-use activities is generally positive, but in Italian Emilia Romagna region it is assumed to be neutral, but not negative at all. In Austria and in Vicenza this awareness manifests in practice due to the existing re-use related shops having intensive visits by costumers and for a generally good reputation of re-use. In Croatian region the awareness is also very positive, however it is lacking of re-use shops.

SRP implementation potential

The givens in project SRPs are considered to be the most developed in Austria, Germany, Italy (Emilia Romagna, Vicenza) and Slovenia. It means that in these regions there are already relevant activities that can be easily integrated within an SRP. In these FUAs there are several specific re-use related activities are present i.e. repair and upcycling workshops, rental services, swapping platforms, fab labs.

Despite the very positive situation in Austria, they identified development potential in the region. According to their opinion the scientific approach and a more conscious public awareness is missing currently, which can promote far beyond the situation.

The Croatian pilot area starts from a very basic level, where there is only one textile sorting facility with a shop represents the re-use activity.

In the other areas, there are few SRP related activities are present. Hungarian partner reported that there are ongoing re-use related activities, however their integration into an SRP raises financial and legislative questions. From starting SRP as a business (implementation, operation) generally there is no restriction on the legal status of its host (NGO, civil association, private etc).

Demand and supply on second-hand items

The assessment of demand on second-hand items is the most ambiguous among the concerned areas: Austrian, German, Hungarian, and especially Polish partners reported that using and buying second-hand items are generally approved by the public. On the contrary Croatian, Italian (Emilia Romagna, Vicenza) and Slovenian partners shared that there is a massive negative opinion on using second-hand items. In Bohemian region there is ineligible experiment.

The feedbacks on supply of second-hand items reflect quite consistent situations in the concerned pilot areas. They generally assess that the public in the areas generally are conscious on the environmental gains of re-use, but as a common experience, they hardly turn it into practice, which means they do not make efforts to deliver their obsolete products to a re-use friendly option, i.e. collection centres, online marketing, etc.

8. IDENTIFICATION OF POTENTIAL STAKEHOLDERS

The recognition of concerned stakeholders in relation with urban waste prevention plan is organically linked to further, but practical steps of SURFACE project: the developed SRPs in dedicated areas highly require common thinking and interaction between project partners and external stakeholders from the beginning of the project implementation. For this aim, two main elements have to be integrated: on one hand the list of potential stakeholders having influence on the SRP development and on the other hand, a moderated platform for them to interact for changing information (**Multi-Stakeholder Forum, MSF**). Both actions are developed within the project.

The core concept of MSF is that each pilot area in the project should have its own group of interested actors (i.e. waste management companies, municipalities, policy makers) having direct relations on re-use activities in the concerned area. We can also call them as regional multi-stakeholder fora. However, in accordance with the practical implementation of re-use intentions on a higher (strategic) dimension, the long-term sustainability and boosting effect of project activities can be ensured by the involvement of actors having direct or indirect influence on regional (national) and/or local (urban) waste prevention plans. The waste prevention plans are strategic documents on an integrated approach of sustainable development of responsible waste management in the area bringing the national and European efforts closer to the local practice and also in consideration of urban givens.

The aim of the MSF is two-fold: it brings together all actors having role in waste management, especially in re-use and the stakeholders from strategic planning and legislation via regulations and plans. The MSF also serves as a conveyor for actors from level of implementation (actors having role on SRP development) with colligating their needs and expectations. Finally, a multilateral interaction of national and international stakeholders can lead to a cost and time effective cooperation with practical outcomes possessing the widest basement of their consensus.

For the sake of these aims, the first step would be to ask the project partners to think which stakeholders can be interested and which of them should and wants to participate in the regional

MSF. Here the focus is on urban Waste Prevention Plans, where all contacted partners should have preferably direct, but at least indirect interest on the development of regional/national Waste Prevention Plans. That is why partners with (potent) influence on Waste Prevention Plan (policy making) should have priority. This task is now ongoing in the project and supposed to have the result as list of stakeholders having relation on SRP development in each project area. Stakeholders from national dimension are not excluded from the list, however they should have influence on strategic planning related to re-use intentions. Finally, the MSF could be a communication platform for these actors, where they can keep contact and can discuss the topic in more details.

9. POTENTIALS AND VISIONS IN FUAS

In every pilot areas from all participating countries, there is at least one re-use joint activity which is already established and great potential for launching new initiatives. Short overview of the potentials in the field of repair and re-use in concerned areas, based on the findings from separate questionnaires for each project partner, can be seen in *Table 2*.

Table 2
Potentials in the field of repair and reuse in concerned FUAs

RE-USE JOINT ACTIVITIES	AUSTRIA	CROATIA	CZECH REPUBLIC	GERMANY	HUNGARY	ITALY (VICENZA)	ITALY (RIMINI)	POLAND	SLOVENIA
Repair and upcycling workshop	+	(-)*	+	+	+	+	+	+	+
Repair café	+	(-)*	-	+	(-)*	(-)*	+	(-)*	+
Rental services	+	(-)*	+	+	+	+	+	+	+
Swapping platforms	+	(-)*	+	+	N/A	+	+	+	+
Educational labs	(-)*	(-)*	+	+	(-)*	+	+	+	+
Fab Labs	+	(-)*	-	+	+	+	+	(-)*	(-)*
Online re-use marketplace	+	+	+	+	+	+	+	+	+
Exhibition for different target groups	-	-	(-)*	+	+	+	+	+	+
Other, please describe:	(+)*	-	(+)*	-	-	(+)*	-	-	-

(-)*: don't exist currently but are considered as a short or long term goal

(+)*: Austria –Library of things;

Czech Republic – Mini library;

Italy (Vicenza) – proposals of tourism dedicated to visiting areas dedicated to re-use, creation of local network of subjects engaged in re-use

Prevention of waste and preparing for re-use must have priority in waste management according to the waste hierarchy defined in the European Waste Framework Directive. Considering the different level of re-use related development in countries, dimensions should be determined on different level in order to make a distinction between the level of development, especially considering the organisational structure, the infrastructure and the offered services of an SRP.

Therefore the necessity and advantage of SRP establishment are evident among all countries and urban areas participating in the project. An SRP may include all three pillars of sustainability (mentioned above) by offering an opportunity for stakeholders to interact with each other. Main idea behind the implemented SRP has several key points:

- It must have social, economic and environmental impact;
- It should be designed as centre for a separate collection of reusable goods on the spot or/and via external collections which would contribute to waste reduction, resource savings and circular economy;
- It should offer high range of preparation for re-use and re-use activities for different materials - such as repairing, restoring, redesigning, renovation, refurbishment, workshops and education and other activities to raise awareness;
- It may offer basic vocational education and employment for socially excluded and vulnerable groups of population; re-use and repair activities hold a big potential for creating jobs for people with different level of skills.
- It should be entertaining for children, youth and adults as well;
- It must be open and accessible for citizens.

10. CONCLUSIONS AND NEXT STEPS

The project is still ongoing until the middle of 2020. The following tasks will make strong efforts to develop methodology tools in order to fertilize the SRP concept on other urban locations throughout Europe.

The tasks will include the development of a tool, named **Cooperation Matrix** aiming to support the selection process of the most appropriate relationships to be established between public authorities (responsible for waste prevention and management), private companies (offering services for waste management), social enterprises (providing workplaces for disadvantaged people at local level) for implementing and managing an SRP.

Additionally the SRPs **Activation Toolbox** will be developed. It is a decision support tool based on SURFACE evidences which will allow urban managers to establish if, when and how to implement SRPs as part of their waste prevention strategies.

The project will also eventuate in a “**Smart Re-Use Twinning Scheme**” for supporting a joint field training process which will allow transfer and implementation of SRP based systems in other locations outside the partnership.

ACKNOWLEDGEMENTS

This project is implemented through the CENTRAL EUROPE Programme co-financed by the ERDF. For more information and monitoring project progress, please visit the project website: <https://www.interreg-central.eu/Content.Node/SURFACE.html>



MECHANICAL PROCESSING OF SPENT LITHIUM-ION-BATTERIES FROM ELECTRIC VEHICLES

DENIS WERNER¹–THOMAS MÜTZE¹–HANS-GEORG JÄCKEL²–
URS ALEXANDER PEUKER¹

¹Institute of Mechanical Process Engineering and Mineral Processing,
TU Bergakademie Freiberg, Agricolastraße 1, 09599 Freiberg (Germany),
denis.werner@mvtat.tu-freiberg.de

²Institute of Mechanical Engineering – Recycling Machines,
TU Bergakademie Freiberg, Leipziger Straße 32, 09599 Freiberg (Germany)

Abstract

The development of high power and high energy lithium-ion-batteries in mobile applications lead worldwide to a steady growing amount of electric vehicles during the last years. When these batteries reach their end of life, an efficient recycling is required by European law 2006/66/EG in order to ensure environmental protection and sustainability as well as to close the material cycle. State of the art recycling is based on pyrometallurgical and hydrometallurgical processes focusing on the recovery of high valuable and strategic important components like copper, cobalt and nickel. Unfortunately, organic components are burned and metals like lithium and aluminium are lost in the slag. A combination of this state of the art with mechanical process technologies like comminution, screening and sorting, recycling efficiency can be increased.

The presentation focuses on the different preparation, pretreatment and processing steps within the recycling chain for Lithium-Ion-batteries in order to provide a safe and effective process. Batteries are collected and pre-sorted to separate them by type, size and cathode material avoiding any cross-contamination for subsequent process steps. After preparation, batteries are disassembled to needed depth of dismantling or further handling in respect to maximum size or volume of waste. Deactivation aims to remove residual chemically stored energy. Moreover, toxic and flammable electrolyte components are decomposed guaranteeing work and facility safety. Processing steps are depending on target output materials and requirements of metallurgical treatment. Methods and technologies from mechanical, chemical and thermal are used to generate first recycling products and provide concentrates for pyrometallurgical and hydrometallurgical refining. As a result, the proposed procedure allows to classify all available technologies for recycling lithium-ion batteries. As an example, chosen research and industrial approaches will be shown.

Keywords: *Lithium-Ion-batteries, recycling, mechanical processing, deformation, flow sorting*

1. INTRODUCTION

Since the beginning of the 1990s, rechargeable lithium ion batteries (LIBs) have been widely used as electro-chemical power sources in many types of portable electronic devices like smart phones, laptops and power tools. During the last few years, development of high power and high energy lithium-ion batteries have increased the amount of electric vehicles and hybrids, in total numbers as

well as in variety of types. Lithium-ion-batteries show big advantages due to their high energy and power density, low weight and small size, high operation voltage and wide range of operation temperature, long life cycles and low self-discharge rate (LEUTHNER 2013).

At the end of their lifespan, used batteries are marked as dangerous waste and European law 2006/66/EG requires a minimal recycling rate of 50%, respectively. Recycling rate is relevant for all kinds of lithium-ion batteries, although, they are classified by European law in respect to their application in three different categories. First category contains all portable batteries from consumer electronics, laptops, tablets or power tools. Batteries from bigger devices like electric vehicles, scooters or bikes as well as stationary energy storage systems are indicated as industrial batteries. Third category called automotive batteries includes starting and lightning batteries for vehicles.

State-of-the-art recycling processes for lithium-ion batteries are based on high energy and cost-intensive pyrometallurgical and/ or hydrometallurgical processes with limited capacities and low recycling rates (WUSCHKE et al. 2015). Target materials of recycling are high valuable and strategic important components like copper, cobalt and nickel. By contrast, low valuable organic components like solvents and separator are burned and metals like lithium and aluminium are lost in the slag in pyrometallurgical processes (HANISCH et al. 2015). These materials also have to be separated before hydrometallurgical treatment because of influencing process stability and recovery yield. Especially the growing amount of spent industrial batteries from electric vehicles consists of complex compounds and more peripheral components. Combining state-of-the-art processes with adequate preparation and pretreatment steps like presorting collected batteries by battery type or chemistry and disassembling peripheral parts, respectively, or technologies from mechanical processing are highly investigated topics. Therefore, additional deactivation steps are required to enable a safe and effective handling and processing. As a result, these efforts lead to creation of new business models, reducing materials which are lost in slag and increasing overall recycling efficiency and economic benefits.

2. COMPONENTS OF LITHIUM-ION-BATTERIES

Lithium-ion batteries consist of complex compounds, different subunits and various materials. Basic functional unit contains positive and negative electrodes, electrolyte and separator that are included by cell housing. In its most conventional structure, the electrodes formed by metal foils with duplex-coated active materials are divided by plastic separator foil. Cathode active materials were developed with valuable materials containing different amounts of cobalt like lithium cobalt oxide (LCO), lithium nickel cobalt aluminium oxide (NCA) and lithium nickel manganese cobalt oxide (NMC). These ultrafine lithium metal oxides are toxic, respirable and, especially nickel and cobalt, carcinogenic to humans (HANISCH et al. 2015). Furthermore, they contaminate soil and ground water when disposed incorrectly. However, the amount of used these materials is gradually being decreased and replaced by non-toxic and low valuable lithium iron phosphate (LAROCHE et al. 2018). Anode active materials typically consist of natural or synthesized graphite. The liquid electrolyte is composed of organic solvents (PC, EC, DMC, DEC), conductive salt like lithium-hexafluorophosphate and other additives (HARTNIG 2013). Some of the electrolyte components are corrosive and easily flammable. Under inconvenient conditions, they even tend to form explosive atmospheres. Moreover, the chemical properties of organic solvents affect human health and cause

toxic chemical reaction products with materials of cathode when treated mechanically or pyrometallurgically. To guarantee safe function, electrodes, separator and electrolyte is imbedded by housing made of aluminium, stainless steel or plastics. Several of basic functional units (cells) are electrically and mechanically connected forming the next higher subunit (module). Depending on application, modules are further connected to battery systems or directly implemented into final product as battery block. However, battery systems and blocks are equipped with several peripheral components like final housing, power electronics, battery management system and cooling or heating systems. Besides toxic and potentially hazardous materials in lithium-ion-batteries, remaining electric energy and high voltage of battery systems has to be removed before disassembling and mechanical processing.

3. UNIFORM INDICATION FOR RECYCLING PROCESSES OF LITHIUM-ION BATTERIES

Recycling of spent Lithium-ion batteries arises interest of researchers and recyclers all over the world. The used units operations, like mechanical, pyrometallurgical and hydrometallurgical, mainly do the characterization of recycling processes (HANISCH et al. 2015). Nevertheless, with this designation, not all process technologies can be defined explicitly. Different deactivation or disassembling approaches are missing as well as presorting steps indicating the dedication for Lithium-ion batteries or their subtypes. Focusing on recovering of especially cathode active materials, previous process steps are often not further classified in detail. Thus, they are summarized and simply called as pre-treatment. In there, mechanical treatment steps are termed as secondary treatment, followed by deep recovery steps (ZENG et al. 2014). In addition, material flows can vary tremendously within mechanical processing depending on recycling company, their strategy and nearby markets for secondary raw materials. Hence, there exist several different recycling technologies for Lithium-ion batteries worldwide, abstract terms like gas control, direct, physical or chemical processes are assigned only for selected processes (VEZZINI 2014; ROMBACH 2014; ORDOÑEZ et al. 2016). However, these terms do not allow uniform indication. In contrast, Martens developed a procedure to classify any recycling technology, autonomous from waste material (MARTENS 2016). By adopting the hierarchical outline level of macro processes developed for mechanical processing of solid primary raw materials, unambiguous assignment of recycling processes for Lithium-ion batteries is possible.

4. RECYCLING OF LITHIUM-ION BATTERIES

4.1 Generic recycling chain of Lithium-ion batteries

Recycling of lithium-ion batteries follows the generic recycling chain with preparation, pretreatment, processing and refining step (*Figure 1*) (MARTENS 2016). Lithium-ion batteries are collected and transported for pre-sorting. In most cases, portable lithium-ion batteries are collected with other battery types like NiMH or alkaline batteries (SCROSATI et al. 2015). As an outcome of first sorting step, other battery types are separated by optic, granulomere or electromagnetic properties. A potential second sorting uses different cathode active materials as sorting characteristic. The effort of sorting is depending on present collection system and final refining technology. Refining only provide stable process conditions and economically acceptable secondary raw material qualities when impurities are kept to a low level (LEBEDEVA et al. 2016).

In the subsequent pre-treatment step, lithium-ion batteries are disassembled and deactivated. According to the amount of subunits and peripheral parts of the battery system, disassembling is necessary to reach the maximal geometries of subsequent process steps (pack, module, cell or electrode). Disassembling takes place manually, automatically or semi automatically when manual work is supported by robots or machines. However, various battery designs caused by multi sourcing of production as well as fine components and complex compounds are challenging this process step. Main goals of disassembling are recovering materials to generate first recycling products, like wires and electronics from battery management system or thermal management increasing overall recycling efficiency. Furthermore, throughput for consecutively processing steps can be reduced. During disassembling process, analysing the current battery status can also lead to separation of batteries for second life applications.

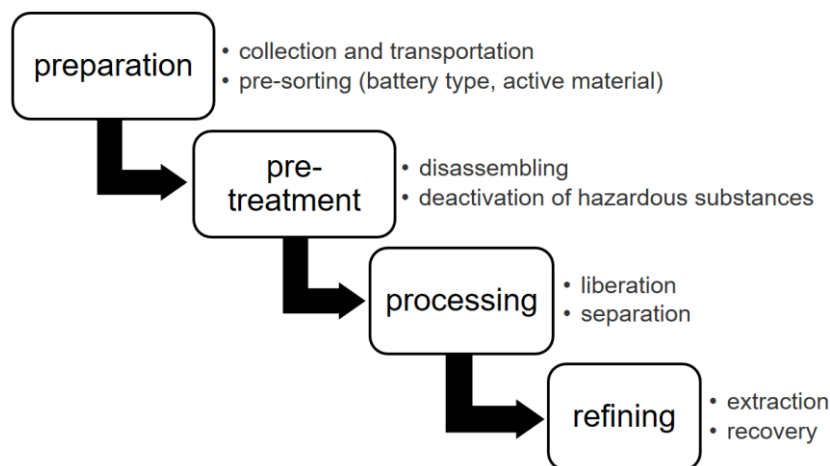


Figure 1
Generic recycling chain

When cells are further disassembled or liberated by mechanical stressing, deactivation steps play a crucial role for facility and work safety. The main objective of deactivation is to remove hazardous substances threatening further processing and contaminating recycling products. Deactivation is carried out by removing remaining energy and decomposing flammable components of liquid electrolytes. Therefore, discharging batteries with electrical resistance or in brine solution removes remaining electric energy. Each method shows differences in discharge efficiency, process time, temperature behaviour and chemical reactions with electrical connections. For a secure disassembling and mechanical processing, a complete removal of the residual energy is recommended to avoid short circuits, electric shocks or thermal runaway (HANISCH et al. 2015). Especially batteries from industrial applications like electric vehicles or stationary storage devices with high voltage and energy can be harmful. Elimination of potential risks from electrolyte are addressed by thermal or cryogenic treatment. Thermal treatment uses high temperature technologies like pyrolysis or calcination decomposing not only hazardous components of liquid electrolytes but also all other organic components like binder or separator. Although thermal treatment is energy intensive and organic materials cannot be recovered, it protects subsequent processing and refining against pollutants and

reduces uncontrolled reactions and emissions. Cryogenic treatment decreases speed of reactions and enable a safe liberation (GANA 2014). However, it requires special equipment for further handling of electrolyte released at increasing temperatures during further processing

Processing includes mechanical, chemical or thermal liberation and separation of lithium-ion battery packs, modules, cells or components. Main goals of processing, preferably technologies from mechanical liberation and sorting due to low energy and support material requirements, are enriching components and materials in concentrates for material recycling and reducing pollutants for metallurgical treatment. The adequate technology for processing depends on depth of disassembling, method of deactivation and chemical and physical composition of input material. Liberation is the basic requirement for any physical, chemical or thermal separation process. Due to non-brittle material characteristics, spent lithium-ion battery wastes are mechanically stressed by shearing, cutting, tearing or electrohydraulic fragmentation. Depending on type of stressing, liberated particles and components are sorted by suitable sorting characteristics like size, density and electromagnetic properties. Practically, this can be performed in multistage comminution and sorting steps combined with chemical and thermal processes. Chemical and thermal processes mainly liberate active materials from current collector foils or separating remaining electrolyte components.

Refining is the last step in the recycling chain recovering materials or raw materials by means of pyrometallurgical or hydrometallurgical technologies. Especially metals contained in battery cell housing and electrodes are target materials for refining processes. Other materials like housing and current collector foils, enriched in concentrates previously, are treated in established recycling processes. In pyrometallurgical processes, input material is fully smelted gaining three phases: slag, alloy and dust (MARTENS 2016). Transferring valuable metals like copper, cobalt, iron and nickel into an alloy is the main goal of pyrometallurgical treatment. Contained lithium, manganese and aluminium is concentrated in slag and added as construction material (HANISCH et al. 2015). In principle, recovering lithium is technically possible, but nowadays due to raw material price of lithium economically not feasible. Hydrometallurgical treatment applies techniques from extractive metallurgy. Main steps are leaching, concentration and purification and recovery of metals as salt compounds. Theoretically, this kind of process allows recovery of each component present in input but requires special pre-treatment and additional substances enabling desired reactions.

As a result, adjusted recycling chain for lithium-ion batteries is proposed (*Figure 2*). This ideal procedure allows classifying all available technologies for recycling lithium-ion batteries. Furthermore, it is possible to characterize different process routes and distinguish between dedicated and non-dedicated processes for lithium-ion batteries. Moreover, achieved recycling efficiency, needed specific energy and support material demand can be added with appropriate data enabling a resilient and comparable identification of the most efficient recycling process for Lithium-ion batteries.

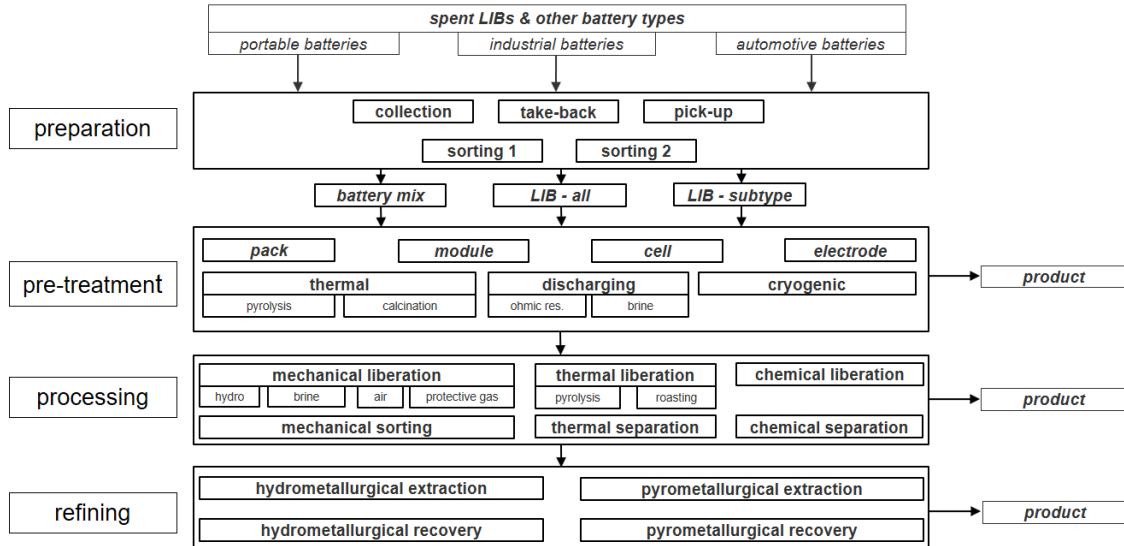


Figure 2
Recycling chain of spent Lithium-ion batteries

4.2 Classification of industrial approaches

Several different recycling processes and routes exist in industrial scale with predominant pyrometallurgical technologies (MESHRAM et al. 2014). These approaches do not adopt all steps of generic recycling chain due to existing technology, infrastructure and business area. With support from literature data, chosen established recycling processes for Lithium-ion batteries are characterized in respect to the four steps of recycling chain and their sub steps (Table 1).

Table 1
Categorized process steps for chosen companies with battery recycling division (tt+: Thermal treatment at high temperature, tt-: thermal treatment at low temperature; d: discharging; CO₂, N₂, Ar, air: comminution medium; p: pyrometallurgical process; h: hydrometallurgical process; 1, 2: processing order) (Meshram et al. 2014, Lv et al. 2018)

company	process steps of recycling chain							
	preparation		pre-treatment		processing		refining	
	collection	pre-sorting	disassembling	deactivation	liberation	separation	extraction	recovery
Umicore	-	-	x	-	-	-	x (p1; h2)	x (p1; h2)
Batrec	-	-	-	-	x (CO ₂)	x	x (h)	x (h)
Glencore	-	-	-	-	-	-	x (p1; h2)	x (p1; h2)
Accurec	-	-	x	x (tt+)	x (air)	x	x (p1; h2)	x (p1; h2)
AkkuSer	-	x	-	-	x	x	-	-
Redux	-	x	x	x (d, tt+)	x (air)	x	-	-
Düsenfeld	-	-	x	x (d)	x (N ₂)	x	x (h)	x (h)
Retriev	-	-	-	x (tt-)	x (air)	x	x (h)	x (h)
Recupyl	-	-	x	-	x (CO ₂ Ar)	x	x (h)	x (h)

Collection is not conducted by any of the selected companies. In addition, only two companies are sorting their input materials. Consequently, business models for preparation steps play an unimportant role for recycling companies focusing on processing and recovering materials. Normally, logistics and pre-sorting is, besides some exceptions, carried out by specialized companies. During first pre-treatment step, mainly industrial battery packs are dismantled to modules or cells for further processing. Deactivation is performed by thermal treatment at low or high temperatures. In case of Redux, also discharging process is carried out. On the other hand, Düsenfeld renounces fully any thermal treatment and only discharges batteries before further liberation. Liberation is exclusively by means of mechanical treatment varying with medium of comminution. When Lithium-ion batteries are liberated, protective gases like CO₂, Ar or N₂ are used. Besides, air is chosen for liberation when batteries are thermally deactivated. Active materials enriched in concentrates are processed on the one hand with a combination of pyrometallurgical and hydrometallurgical extraction and recovery. On the other hand, refining is performed directly in hydrometallurgical process.

5. CONCLUSIONS

Lithium-ion-batteries present the current most favourable energy storage device for mobile application. Growing production and increasing demand, especially for electric vehicles, will lead to sufficient amount of spent batteries allowing economic feasible recycling activities. State-of-the-art recycling technologies mainly base on high energy and cost-intensive, but robust hydrometallurgical and/ or pyrometallurgical processes with low recycling efficiencies. Combining with disassembling and mechanical processes, share of overall material recovery can be increased but also require special handling in respect to deactivation methods. As a result, former classification of processes is not enough. Therefore, generic recycling chain developed by Martens for any waste material can help to characterize and distinguish various approaches for recycling lithium-ion batteries. By means of chosen companies, their recycling procedures are classified with respect to steps and sub steps of generic recycling chain. This structure can contribute to a better understanding of the different and complex forms of Lithium-ion battery recycling. Furthermore, requirements for subsequent process steps determine process routes and recycling strategies avoiding misunderstandings in further discussions.

REFERENCES

- [1] GANA, M. (2014): *European Li-Ion Battery Advanced Manufacturing For Electric Vehicles – ELIBAMA*.
- [2] HANISCH et al. (2015): Recycling of Lithium-Ion Batteries (Chapter 27). In: YAN, J.(ed.), *Handbook of Clean Energy Systems, Volume 5 Energy Storage*. Wiley & Sons, Ltd, pp. 2865–2888.
- [3] HARTNIG, C., Schmidt, M. (2013): Elektrolyte und Leitsalze (Chapter 6). In: KORTHAUER, R. (ed.): *Handbuch Lithium-Ionen-Batterien*. Frankfurt, Springer, pp. 61–77.
- [4] LAROUCHE et al. (2018): Recycling of Li-Ion and Li-Solid State Batteries: The Role of Hydrometallurgy, *Extraction, 2018*, pp. 2541–2553. (10.1007/978-3-319-95022-8_214)
- [5] LEBEDEVA et al. (2016): Lithium ion battery value chain and related opportunities for Europe. European Commission. Petten.

-
- [6] LEUTHNER, S. (2013): Übersicht zu Lithium-Ionen-Batterien (Chapter 2). In: KORTHAUER, R. (ed.): *Handbuch Lithium-Ionen-Batterien*. Frankfurt, Springer, pp. 13–20.
- [7] LV et al. (2018): A Critical Review and Analysis on the Recycling of Spent Lithium-Ion Batteries. *ACS Sustainable Chemistry & Engineering*, 6 (2), pp. 1504–1521.
- [8] MARTENS, H., GOLDMANN, G. (2016): *Recyclingtechnik*. Wiesbaden, Springer.
- [9] MESHAM et al. (2014): Extraction of lithium from primary and secondary sources by pre-treatment, leaching and separation: A comprehensive review. *Hydrometallurgy*, 150, pp. 192–208. (10.1016/j.hydromet.2014.10.012).
- [10] ORDÓÑEZ et al. (2016): Processes and technologies for the recycling and recovery of spent lithium-ion batteries. *Renewable and Sustainable Energy Reviews*, 60, pp. 195–205.
- [11] ROMBACH, E. FRIEDRICH, B (2014): Recycling of Rare Metals (Chapter 10). In: WORREL, E. (ed.): *Handbook of Recycling*, Elsevier, pp. 95–111.
- [12] SCROSATI et al. (2015): Recycling lithium batteries (Chapter 20). In: SCROSATI et al.: *Advances in Battery Technologies for Electric Vehicles*, Woodhead Publishing, pp. 503–516.
- [13] VEZZINI, A., PISTOIA, G. (2014): Manufacturers, Materials and Recycling Technologies (Chapter 23). In: PISTOIA, G. (ed.): *Lithium-Ion Batteries Advances and Applications*. Amsterdam, Elsevier, pp. 529–551.
- [14] WUSCHKE et al. (2015): Recycling of Li-ion batteries – a challenge. *Recovery*, 4, pp. 48–59.
- [15] ZENG et al. (2014): Recycling of Spent Lithium-Ion Battery: A Critical Review. *Critical Reviews in Environmental Science and Technology*, 10 (44), pp. 1129–1165.



EXPERIMENTAL COMPARISON: ACIDIC and BIO SOLUBILISATION OF INDIUM FROM LIQUID CRYSTAL DISPLAYS

VALÉRIA MÁDAI ÜVEGES¹–TERÉZIAVARGA¹LJUDMILLA BOKÁNYI¹

University of Miskolc, Institute of Raw Material Preparation and Environmental Processing,
3515 Miskolc-Egyetemváros, Hungary;

Abstract

The recovery of indium from the ITO (indium-tin-oxide) layer of waste Liquid Crystal Display (LCD) panels is a very important task to sustain the strategic materials, as well as to create the circular economy in the EU.

After mechanical pretreatment, the indium can be recovered from the glass substrate by chemical solubilisation. To study the leaching of ITO, laboratory experiments were carried out. The particle size of the ITO glass was <5mm, S/L ratio was 1:1 and the rotation speed of the shaker was 150 rpm. The leaching efficiency of 1M HCl and 1M H₂SO₄ solution was evaluated at different temperature and retention time. Another possibility for the solubilisation of indium is bioleaching. The experiments were carried out with discarded LCD panels, after the same mechanical pretreatment as compared with chemical leaching experiments. In this case several strains of the *Acidithiobacillus* bacteria were used for the leaching. Bioleaching was investigated applying a shaker at 150rpm, at 30°C. The initial pH of the experiments was around 2,5. S/L ratio was 1:10 and the retention time was 7 days in each case.

The chemical solubilisation and the bioleaching results are compared, and it was revealed, that the efficiency of the chemical leaching could be as high as 100%, and although the results of the microorganisms assisted leaching reached only 75%, this method is a very promising and nevertheless meets the concept of the green chemistry and circular economy.

Keywords: *waste LDC, indium, leaching, Acidithiobacillus*

1. INTRODUCTION

In 2008 the European Commission drew attention to the strategic importance of defining policies for raw materials by launching the raw materials initiative. Within this framework, various actions were taken to address sustainable access to raw materials both within and outside the EU, as well as on resource efficiency and recycling. In the beginning, the Commission has identified 14 critical raw materials (CRMs) at EU level, and the meaning of “criticality” was also defined: “Critical raw materials are those which display a particularly high risk of supply shortage in the next 10 years and which are particularly important for the value chain” (web1). The list of CRMs was revised and expanded in every 3 years, and now it contains 27 materials, with some material groups, such as the rare earths, and the elements of platinum group for example.

The background of our present research is served by the “CriticEI” R&D project, wherein the Institute of Raw Material Preparation and Environmental Processing investigated the recycling of critical raw materials from different secondary material sources, such as the waste electronic equipment. Within this field the indium recovery from the indium-tin-oxide layer of the waste LCD panels was examined, by a mechanical preparation followed by a chemical treatment method. In present research work, we are preferably dealing with the possibilities of the bioleaching of the indium from the same material source, hence bio-hydrometallurgy has many advantages. It fits to the concept of green chemistry considering that the microorganisms serve as a renewable solvent, and the costs and the energy consumption can be lower compared with the chemical dissolution using mineral acids.

In the field of bioleaching of In from LCD panels, there are only few available papers. A recently released work of M.J. JOWKAR et al. (2018), in which *Acidithiobacillus thiooxidans* was used for the bioleaching of In from waste LCD screens of laptops presented very impressive results. After the adaptation of the bacterium to the ground waste LCD the maximum extraction for In was 100%, and 10% for Sr. There are research results, when mixed bacteria cultures are used for the metal extraction. In a recent work of J. Willner, et al. (2018), LCD panel from spent mobile phones was directed to biological leaching with a mixed culture of *A. ferrooxidans* and *A. thiooxidans*. The best results of this group were obtained at 30 °C, 32 days of retention time, with 1:5 solid waste to solvent ratio, when the In content of the solution was 11,1 mg/L.

2. MATERIALS AND METHODS

2.1. Mechanical pre-treatment and composition of the secondary raw material

For the chemical leaching experiments a representative sample was prepared from the collected LCD TVs and monitors. For the bioleaching experiments, new sample of discarded TV-s was processed. The mechanical pre-treatment of the LCD panels was developed by our Institute and it was applied in both cases. During the mechanical pre-treatment, firstly the televisions and monitors were isolated into parts (e.g. plastics, PCBs) by manual dismantling. Then the polarizing film was removed from the panels by a thermal treatment at 225 °C. After stripping the polarizing film the panels were crushed below 10mm with a rotary shear shredder. In order to ensure a more efficient leaching process, the next step of the pre-treatment was the separation of the liquid crystal by ultrasonic cleaning. Finally, the waste glass substrate with ITO layer was crushed below 5mm for the solubilisation tests with a hammer crusher (NAGY S. et al. 2014). The chemical composition of the applied sample can be seen in *Figure 1* wherein critical elements are signed with red.

The chemical composition of the waste sample is rather complex. It contains high amount of Al, B, Ba, Ca, Fe, Si, Sr. It also contains in quite low concentration several critical elements, like REEs and In. Based on our experiences, metals concentration of the LCD panel varies with the type of electric equipment, but the differences in the In content especially are not so pronounced. The In content of the sample used for the former chemical leaching tests was 128mg/kg, and it is equal to the indium content of the recently processed sample for bioleaching. This shows that the role and the manufacturing process of ITO layer in the LCD panels are still the same, so the importance of this secondary raw material source in In recycling will not diminish, at least in the near future.

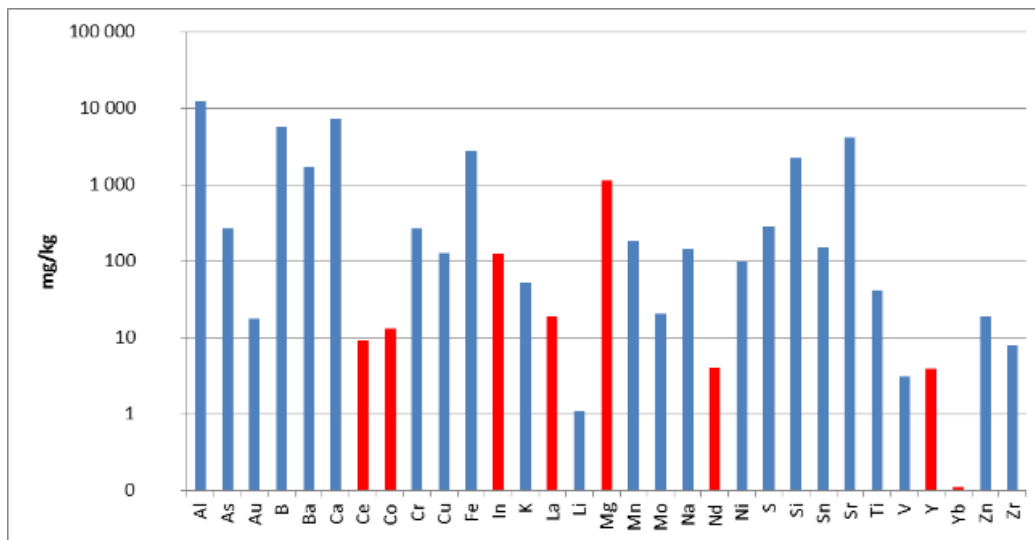


Figure 1

Chemical composition of the waste LCD panels after dismantling and stripping

2.2. Solvents and methods used for chemical and biological leaching

In the case of chemical leaching experiments 1M HCl and 1M H₂SO₄ solutions were applied for the single stage leaching and the effect of the temperature and residence time was investigated, furthermore the multistage leaching was also studied using a weak (0.5M) acetic acid in the first stage for selective Fe removal and 1M HCl solution in the second stage in order to recover indium (BOKÁNYI et al. 2014).

The aim of our preliminary research in the field of bioleaching was to investigate the possibility of indium recovery from pre-treated waste LCD panels by *A. ferrooxidans* Karitas. Related to the literature, the simultaneous use of different bacteria species can be fruitful, so a mixed culture of bacteria species was also tested for the bioleaching of indium. Since *A. albertensis* was first time isolated from gold mine subsurface environment by a research group in Slovakia (J. KISKOVÁ et al. 2018) and we could have the opportunity to make examinations with this bacteria species (courtesy of Professor Jana Kaduková-Sedlaková), a mixed culture of Karitas and *A. albertensis* without preliminary adaptation to the material source was also tested.

A. ferrooxidans can oxidize ferrous ions, and also elemental sulphur, thiosulphates and sulphids. The mechanisms of bioleaching by *A. ferrooxidans* are usually discussed in terms of direct bacterial attack on sulphide minerals and indirect oxidative dissolution of minerals by Fe³⁺. This bacteria was inoculated for 5 days before the experiments in Silverman-Lundgren (9K) nutrient solution. Mineral solution contained (NH₄)₂ SO₄, KCl, K₂HPO₄, MgSO₄·7H₂O, and Ca(NO₃)₂·4H₂O was autoclaved and FeSO₄·7H₂O solution was filter sterilized before inoculation. The leaching ability of the 9K solution without bacteria was also investigated.

A. albertensis are acidophilic, mesophilic, obligatory chemoautotrophic, aerobic, Gram-negative rods. Its closest relative is *A. thiooxidans*, the main energy source is oxidation of S^0 and/or S^{2-} , $S_2O_3^{2-}$ and $S_4O_6^{2-}$ reduction (XIA et al. 2007). The optimum temperature for their growth is between 25–30 °C and the optimum pH is 3.5–4, but they grow down to pH 2, therefore the simultaneous use with the highly acidophilic *A. ferrooxidans* is feasible. Since we do not have any detailed information about the growing characteristics of the mentioned *A. albertensis* bacterium yet, in case of it, the inoculation time was chosen to be two weeks in sterilized medium, consists of a mineral medium with KH_2PO_4 , K_2HPO_4 , $MgCl_2 \cdot 6H_2O$, $CaCl_2 \cdot 2H_2O$, NH_4Cl , Na_2CO_3 and 10% $Na_2S_2O_3$ in 90ml:10ml ratio. The mixed culture of *A. ferrooxidans* Karitas and *A. albertensis* was prepared in 1:1 ratio, just before the leaching experiments.

The temperature and the rotation speed were permanent during the 7 days of retention time, at 25 °C. pH measurements were carried out after 1, 4 and 7 days in order to follow the bacterial work. The leaching experiments were carried out in Wise Cube shaker (shown in Figure 2a) where the rotation speed was 150 rpm. Figure 2b shows the photos of the bioleaching experiments after 4 days of retention time. Since at the start of the experiments the flasks showed the same picture, the changes denote, that there should be differences between the metal content of the solutions.

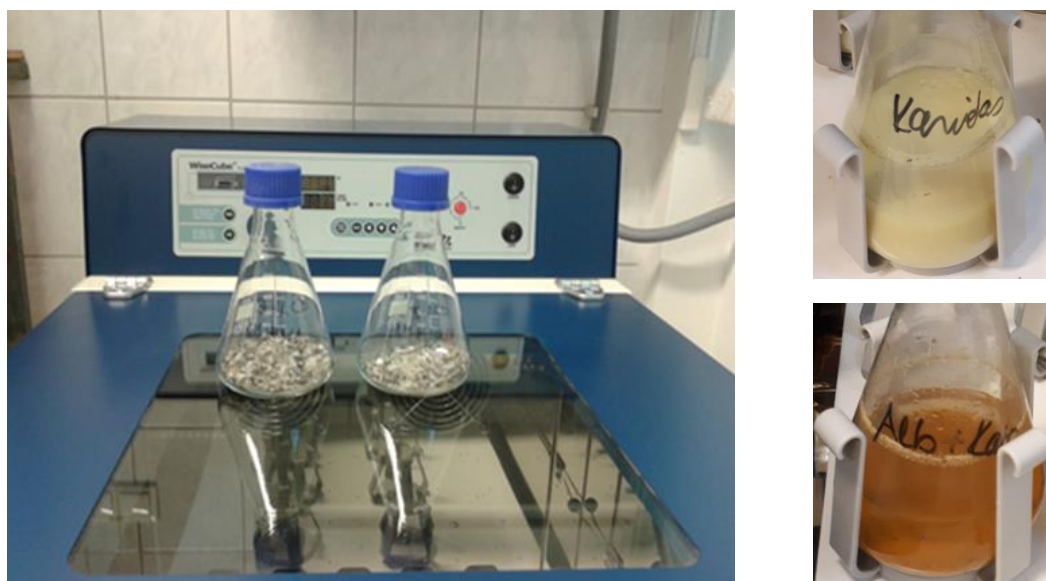


Figure 2

- a. photo of the Wise cube rotation shaker with the pre-treated LCD samples;
- b. photo of the flasks during bioleaching experiments

After the mentioned retention time, the solid/liquid separation was carried out by paper filtration and the solutions were directed to chemical analyses by ICP-OES spectrometry.

3. RESULTS AND DISCUSSION

Based on the chemical analyses of the solutions from chemical leaching tests, it was revealed, that the 1M HCl solvent was more effective for In solubilisation from the LCD glass as compared with 1M H₂SO₄ since the recovery values were higher at many circumstances and the In recovery was almost complete, as it is shown in *Figure 3*. The recovery of indium by 1M H₂SO₄ dissolution reached only in one case 99.73%, when the leaching took 1 hour and 55°C was used. Otherwise the recovery results for In were near 70%. Considering that at the further solution treatment phase the lower other metals concentration was to be desired, the best leaching parameters were chosen as follows: 1 hour retention time, 55 °C and 1M HCl as solvent. There was another attempt when the selective solubilisation of iron with weak acetic acid was the main goal at first, and In should be dissolved in the second stage in HCl. The results showed, that only a few amount of iron was recovered in the first step, and the total leaching efficiency for iron was almost the same compared to the one-stage experiments, only 15%, independently from the applied temperature. In was slightly dissolved in acetic acid, in 16-19% depending on the temperature, and the total In recovery of the multistage process was 97–98%. The optimal circumstances of the selective dissolution of iron should be further investigated.

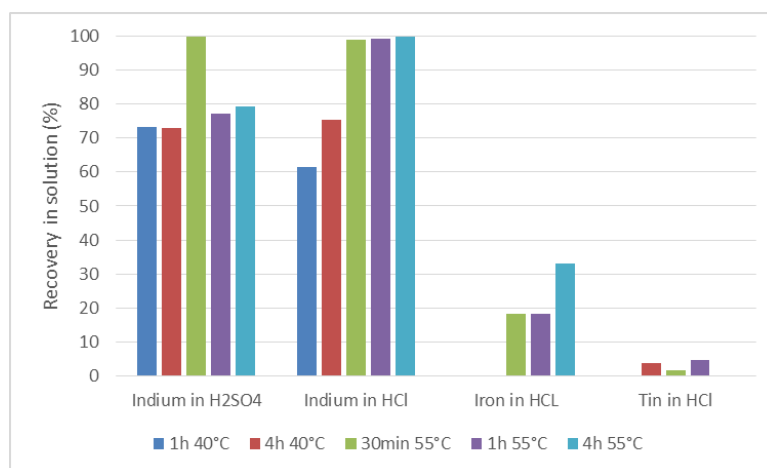


Figure 3
Recovery of the elements from dismantled and stripped LCD panel sample using 1M HCl and 1M H₂SO₄ solution

The recovery results of In and Sn, as the main components of the ITO layer of the LCD panel are shown in Table 1. Based on the chemical analyses of the solutions after 7 days of retention time, it was revealed, that the FeSO₄ itself was efficient solvent for the recovery of In, since it reached 68.46%. Although, when *A. ferrooxidans* Karitas was used, the efficiency of the leaching was increased by 7%, but still much lower, compared to the chemical leaching results with HCl. When the *A. ferrooxidans* and *A. albertensis* bacteria were used together, the dissolution rate was very poor. In

case of tin, comparing the results of the chemical leaching experiments, it can be concluded, that by biological leaching, the dissolution of the Sn was even lower in every case.

Table 1
Recovery of metals in different solvents during bioleaching experiments

Solvent	R _{In} (%)	R _{Sn} (%)
9K	68.46	0.57
Karitas	75.53	0.62
Karitas+albertensis	1.94	0.27

The reason of this phenomenon should be further investigated, but as a first approximation, there can be inhibition issues in the background, considering the complex composition of the LCD panel. Another explanation can be given related to the changes of the pH values, which were measured in the solution during bioleaching. Based on the curves, can be seen in Fig 4, it was clear, that while in case of Karitas strain was used alone, the pH curve shows regressiveness from the first day as it was expected, but the pH of the Karitas+albertensis leaching system first rose above pH 3, and then started decreasing. The pH changed in this case from the initial 2.8 to 2.5 which end value was not enough low. Based on this results, further experiments has to be carried out, in the field of bacterium adaptation to the material source and also the effect of a prolonged retention time should be examined.

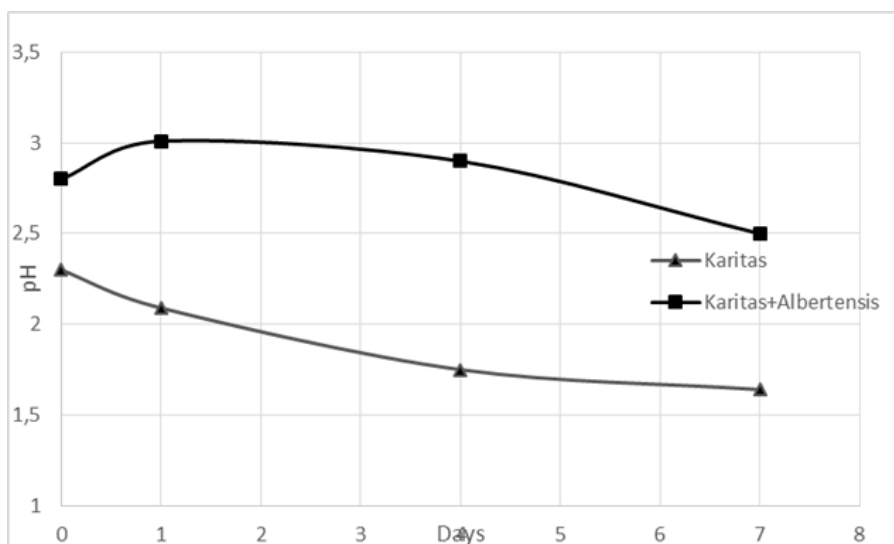


Figure 4
Changes in pH values during leaching experiments

4. CONCLUSIONS

Indium recovery from the pre-treated LCD panels was investigated via chemical and biological leaching experiments. It was revealed, that using 1M HCl as solvent, for 1hour retention time and with 55 °C temperature, was very effective for the dissolution of the In from the ITO layer, since the In recovery was complete. By biological leaching, our preliminary results showed that only 75.53% of the In was recovered in the solution, but this is promising, because there is a big potential in the bioleaching technique, since it meets the requirements of the green chemistry and the concept of the circular economy. Further investigations are needed to be done in order to achieve the same results using suitable microorganisms compared to the very effective chemical leaching method, though these developments can give better answer to the challenges of the future.

ACKNOWLEDGMENT

The described work/article was carried out as part of the “Sustainable Raw Material Management Thematic Network – RING 2017”, EFOP-3.6.2-16-2017-00010 and FIKP projects in the framework of the Széchenyi 2020 Program. The realization of this project is supported by the European Union, co-financed by the European Social Fund

REFERENCES

- [1] L. BOKÁNYI et al. (2014): Recovery of In as a critical element from waste LCD panels. *Proceedings of the 14th International Mineral Processing Symposium*, pp:645–651.
- [2] FAITLI J.–MAGYAR T. (2014): Az LCD-kijelző felépítése, működési elve. In: CSÓKE B.–BOKÁNYI Lj.–FAITLI J.–NAGY S. (eds.) *Elektronikai hulladékok előkészítése a stratégiai elemek visszanyerése érdekében*. Miskolc: Milagrossa Kft., pp. 14–21.
- [3] M. J. JOWKAR et al. (2018): Bioleaching of indium from discarded liquid crystal displays. *Journal of Cleaner production*, 180, pp. 417–429.
- [4] J. KISKOVA et al.: Analysis of autotrophic sulphur oxidising bacteria from Slovak gold mine Hodrusa-Hámre. *Proceedings of 5th Biotechnology and Metals Conference*, p. 34.
- [5] S. NAGY et al. (2014): Mechanical preparation of LCD TVs and monitors. In: Juan YIANATOS, Alex-DOLL,–Cesar GOMEZ (eds.): *XXVII International Mineral Processing Congress*. Santiago de Chile, Chile, 2014-10-20–2014-10-24. pp. 200–209.
- [6] J. WILLNER et al. (2018): Influence of temperature on indium and tin extraction from LCD glass during chemical and biological leaching. *Proceedings of 5th Biotechnology and Metals Conference*, p.102.
- [7] XIA, J. J. et al. (2007): A new strain *Acidithiobacillus albertensis* BY-05 for bioleaching of metal sulfides ores. *Transaction of Nonferrous Metals Society of China*, 17 (1), pp. 168–175.
- [8] web 1: Communication from the Commission to the European Parliament, the Council, the European Economic and Social Committee and the Committee of the Regions tackling the challenges in commodity markets and on raw materials/* com/2011/0025 final



ELECTROCHEMICAL OXIDATION OF REACTIVE BLACK 5 AZO DYE IN CHLORIDE MEDIA

DÁVID JÁGER¹–DANIEL KUPKA¹–MIROSLAVA VÁCLAVÍKOVÁ¹–
LUCIA IVANIČOVÁ¹–GEORGE GALLIOS²

¹ Institute of Geotechnics, Slovak Academy of Sciences, Watsonova 45, 040 01,
Kosice, Slovakia, e-mail: jager@saske.sk

² Aristotle University of Thessaloniki, School of Chemistry,
Lab. Chemical & Environmental Technology, University Campus, 54124, Thessaloniki, Greece

Abstract

Breakdown of commercial grade Reactive Black 5 (RB5) azo dye by chemical and electrochemical treatment was studied using a dimensionally stable anode and stainless steel cathodes as electrode materials, with NaCl as supporting electrolyte. The electrochemical treatment was compared to the chemical treatment with hypochlorite. The compounds present in the commercial grade RB5 azo dye and the products of its electrochemical degradation were separated using ion-pairing high performance liquid chromatography (HPLC) on reversed phase. The separated species were detected by diode array detector and identified utilizing high resolution mass spectrometry (HRMS) and tandem mass spectrometry (MS/MS). A suitable ion-pairing reversed phase HPLC-MS method with electrospray ionization for identification and quantification of the components was developed. The accurate mass of the parent and fragment ions were used in the determination of the empirical formulas of the components and degradation products. Structural formulas of degradation products were proposed using these information and principles of organic chemistry and electrochemistry.

Keywords: *Azo dyes; Decolorization; Electrochemical oxidation; HPLC-MS analysis; Water treatment*

1. INTRODUCTION

Reactive Black 5 (RB5) is one of the most common dyes that have been used in textile industries. Reactive dyes contain functional groups that form a covalent bond with the fiber, achieving extremely high wash fastness properties [1]. Most reactive dyes fall in the category of azo dyes. Azo dyes are aromatic compounds with one or more azo functional groups (see *Figure 1*). Azo dyes constitute the largest class of synthetic dyes [2]. Great amount of these compounds is lost during the dyeing process, resulting in azo dye contaminated effluents. Dyes are generally recalcitrant to biodegradation [3]. Different techniques of dye removal from waste effluents have been developed. Conventional processes applicable for this purpose include adsorption, coagulation, membrane filtration and ion exchange [4]. In fact, these approaches only transfer the contaminants from wastewater to solid wastes that have to be disposed.

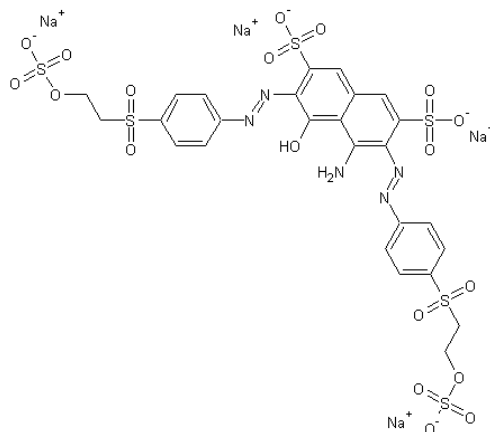


Figure 1
Structural formula of the RB5 molecule

Electrochemical oxidation is a modern technology for treatment of various wastewaters [5–9]. Oxidants are produced during the process *in situ* either directly at the electrode surface or indirectly from chemicals in the treated water. The electrode material strongly influences both the selectivity and the efficiency of the process [10, 11]. Titanium based mixed metal oxide anodes have received wide application in wastewater treatment due to their structural and chemical stability over a wide range of electrical potentials. In the presence of chlorides the electrochemical treatment can be carried out at lower potentials compared to those required for the direct anodic oxidation [12]. A significant disadvantage of electrolysis in chloride media is the formation of chlorinated organics. Indeed, chlorinated organic compounds are detected during electro-chlorination, but in most cases they are degraded during further electrolysis [13]. The exact nature of the electrochemical and chemical reactions that take place during electrolytic treatment in chloride media is complex and not entirely known [11]. The degradation mechanism of RB5 during electrolysis with NaCl as supporting electrolyte has not been fully described so far. The identification of degradation products is important in order to ensure that the treated wastewater is not toxic [14]. The objective of this study was to identify the products of electrochemical degradation of RB5 dye using HPLC-MS. The accurate mass of the parent and fragment ions was used in the determination of the empirical formulas of the components using the mass spectra. Structural formulas were suggested using these spectra.

2. MATERIALS AND METHODS

2.1. The electrochemical system

Electrolysis of RB5 solutions was performed under galvanostatic conditions in an undivided electrochemical cell. Titanium-based dimensionally stable anode DSA[®] coated by mixed oxides of RuO₂/IrO₂/TiO₂ was placed in the center of the cell and was surrounded by two stainless steel cathodes. The geometric area of the anode was 73 mm × 100 mm. With an applied current of 1.5 A, the approximate current density is 100 A m⁻². The electrolysis was carried out at room temperature in a batch mode. The solution was mixed by up-flow gas lifting (see Figure 2). The reaction cell was

gas tight sealed by the lid with openings for excurrent gas sampling and occasional withdrawal of liquid samples. Synthetic aqueous solution of RB5 was prepared by dissolving 300 mg L⁻¹ commercial grade Reactive Black 5 in 8 mM NaCl electrolyte. Color disappearance during chemical and electrochemical reaction was measured at 597 nm by UV-VIS spectrometer Helios gamma (Thermo Electron Corporations).

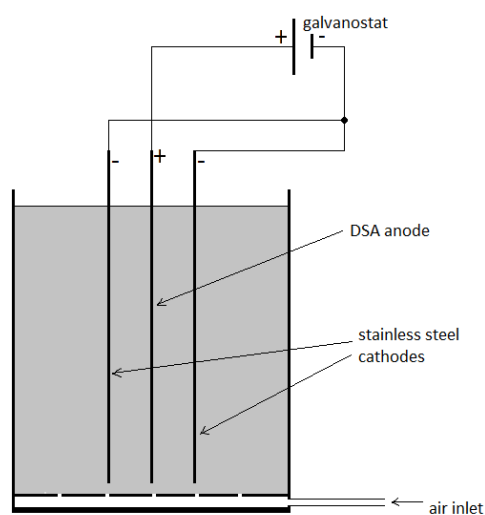


Figure 2
The configuration of the electrolytic cell

2.2. Solvents and reagents for HPLC-MS

Ultrapure water (18.2 MΩ), analytical grade sodium chloride, HPLC and LC-MS grade reagents and solvents (methanol, triethylamine and acetic acid) were used for the eluents preparation. The solvents were degassed in ultrasonic bath prior the HPLC analyses. Triethylammonium acetate (TEAA), the ion-pairing reagent, was prepared by mixing equimolar amounts of triethylamine and acetic acid.

2.3. Identification of the organic species using HPLC-MS

Samples were withdrawn from the electrolytic cell during the electrolysis for chromatographic and mass spectrometric analyses. The samples were filtered using 0.22 μm PTFE syringe filters before analysis. The HPLC-MS analysis of reaction products were performed using DIONEX UltiMate 3000 HPLC system linked with micrOTOF-Q II quadrupole-time of flight hybrid mass spectrometer (Bruker Daltonics). The separation of the compounds was performed using ionpairing reversed-phase HPLC with Acclaim™ 120-3 C18, 150 mm × 2.1 mm column (Thermo Scientific), by multistep gradient elution with a mixture of water (A) and methanol (B) with 2.5 mM TEAA, a volatile cationic ion-pairing reagent as eluent. Flow rate was adjusted at 250 μL min⁻¹. The mobile phase composition during the elution was following: 0-30 min 10→70% B, 30-40

min 70→10% B, 40-45 min 10% B. The column temperature was set at 40 °C. The injection volume was 50 μ L. The HPLC eluate was further analyzed by MS. The mass spectrometer was equipped with electrospray ion source which was used in negative mode. The sum formulas were determined and possible structures of the species were suggested using the accurate masses of the molecular and fragment ions. The mass deviations (experimental vs. theoretical) were below 5 ppm for every m/z.

3. RESULTS AND DISCUSSION

The typical ESI mass spectra of sulfated dyes are complex, with many fragment ions being present in the first-order spectra [15–17]. The mass spectrum of polysulfated dyes, like RB5, usually shows an extensive fragmentation with typical neutral losses of H₂O, SO₂, SO₃ and sulphuric acid, and reduced relative abundance of single charged[M-H]⁻ pseudomolecular ions [16–18]. In the ESI mass spectra of polysulfated dyes multiple charged quasimolecular ions are present, which are usually more intensive than the single charged deprotonated pseudo-molecular ion. Adducts of the species with triethylammonium and sodium cations are also present in the spectra.

4. REACTIVE BLACK 5

Commercial dyestuffs that are placed on the market are not pure compounds. They usually contain other substances, additives that improve the product's application properties. A number of impurities such as precursors of the synthesis, products of partial azo-coupling, products of hydrolysis as well as compounds formed by elimination reactions of the main RB5 component are present. The impurities are formed during dye manufacturing as well as during storage. *Figure 3* depicts the UV chromatogram of the dye solution. The peaks corresponds to specific compounds. Nine compounds were identified. 3 compounds that corresponds to the major peaks are shown in the *Table 1*. In the table the m/z ratios of the detected fragment and adduct ions are indicated too.

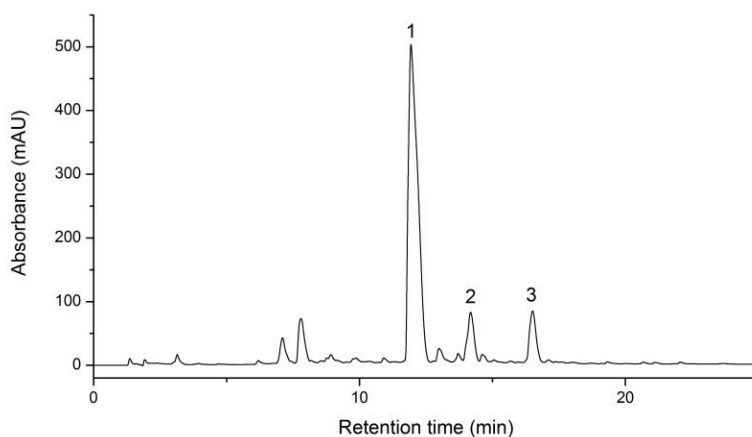
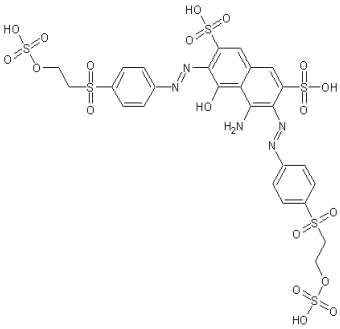
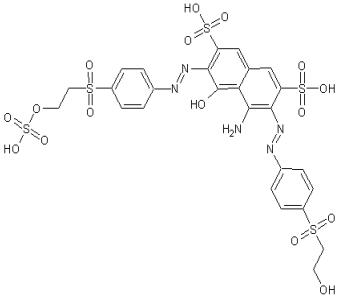
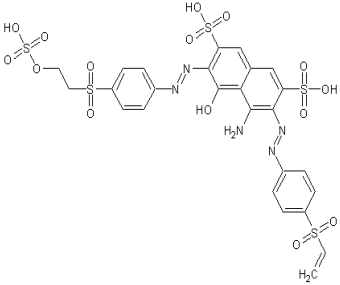


Figure 3

UV chromatogram at 254 nm from the HPLC-DAD analysis of the dye solution

Table 1.

The suggested structural formula of the compounds that correspond to the 3 major peaks of the UV and TIC chromatograms from the HPLC-ESI-MS analysis of the dye solution.

Retention-time (min)	m/z (monoisotopic) of the detected molecular ion(s) and charge	m/z (monoisotopic) of the detected fragment and adduction(s) and charge	Empirical formula and the suggested structure of the neutral compound
12.9	450.465 [M-2H] ²⁻ 299.976 [M-3H] ³⁻	401.483 [M-2H-H ₂ SO ₄] ²⁻ 461.458 [M-3H+Na] ²⁻ 501.027 [M-2H+TEA] ²⁻ 410.489 [M-2H-SO ₃] ²⁻ 1003.058 [M-H+TEA] ⁻	C ₂₆ H ₂₅ N ₅ O ₁₉ S ₆  RB5
14.6	821.984 [M-H] ⁻ 410.489 [M-2H] ²⁻	843.966 [M-H+Na] ⁻ 923.102 [M-H+TEA] ⁻ 421.479 [M-3H+Na] ²⁻ 370.510 [M-2H-SO ₃] ²⁻	C ₂₆ H ₂₅ N ₅ O ₁₆ S ₅  One of the 2 possible isomers
16.4	803.972 [M-H] ⁻ 401.482 [M-2H] ²⁻	825.951 [M-2H+Na] ⁻ 905.092 [M-H+TEA] ⁻ 412.473 [M-3H+Na] ²⁻ 361.501 [M-2H-SO ₃] ²⁻	C ₂₆ H ₂₃ N ₅ O ₁₅ S ₅  One of the 2 possible isomers

M – neutral molecule

TEA –triethylamine

5. ELECTROCHEMICAL DEGRADATION

The variability of compounds that are already present in the initial solution makes the identification of the species formed during electrolytic treatment more complicated. Two concurrent processes take place during the electrolysis of azo dyes: heterogeneous direct oxidation/reduction on the surface of electrodes and indirect homogeneous reactions, which occur in the bulk solution. During electrolysis with DSA anode in chloride media the decolorization of the RB5 solution was rapid (see *Figure 4*). After 15 min of electrolytic treatment the concentration of the dye was under the HPLC-MS detection limit. The decolorization is caused by the changes in the chemical structure of the dye molecule: by oxidation of the functionalities or by interruption of the conjugated system of double bonds in the structure. Despite the complete color removal, azo compounds were still present among the degradation products with molecular weight between 400–600 Da.

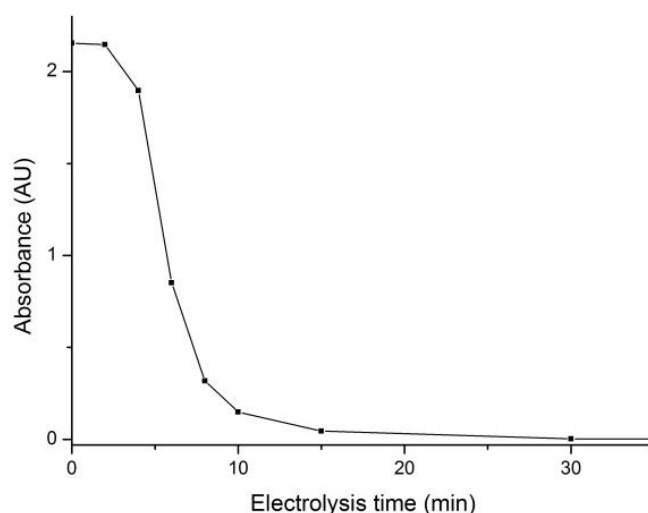


Figure 4

Absorbance of the solution at 597 nm during electrolysis

The chemical oxygen demand (COD) of the solution decreased also. The production of CO₂ and the decrease of total organic carbon (TOC) of the solution is negligible. The initial compounds were degraded/ transformed to highly polar and smaller products that show the least retention on a reversed stationary phase. Some halogenated organic products were identified. The chlorinated products are produced by the action of the active chlorine species that are generated in the solution during electrolysis, such as Cl₂ and hypochlorous acid. These chloro derivatives were degraded during further electrolysis. The exact mechanisms of the formation of the small polar compounds are in fact complex. No opening and mineralization of the aromatic rings was observed during the experiments. The small aliphatic products were probably formed from the aliphatic parts of the RB5 molecule. Nitrates were identified after treatment, as oxidation products of the azo or amine functionalities.

6. CONCLUSIONS

Electrochemical oxidation using a DSA anode was employed to treat a synthetic solution of RB5 azo dye. The study showed that almost complete color disappearance was achieved within 15 min by electrolysis. Despite decolorization azo compounds were still detected after long treatment, but their quantity was reduced considerably. Chlorinated organics were detected among by products during the electrolysis. Using the described HPLC-MS method we identified 40 degradation by products that formed during the electrolysis of the dye solution. In order to identify all compounds with high accuracy and to distinguish between structural isomers, different analytical techniques such as ^1H and/or ^{13}C nuclear magnetic resonance are required. The proposed chemical formulas of identified species could serve as a starting point for the study of toxicity of treated wastewaters. Measuring of the absorbance and chemical oxygen demand of these solutions after treatment is not enough for toxicity assessment of these solutions.

ACKNOWLEDGEMENTS

This work has been supported by the Marie Curie Programme FP7-People-2013-IAAP-WaSClean project No 612250, ERDF GeoCex project No ITMS 26220120064-Centre of Excellence for Integrated Research of the Earth's Geosphere, Slovak R&D Agency project No APVV-10-0252-WATRIP, as well as Greek national support project No 40124, and R&D support project (MVTs) of Slovak Academy of Sciences.

REFERENCES

- [1] TAPPE, H. et al. (2000): *Reactive Dyes*, in *Ullmann's Encyclopedia of Industrial Chemistry*. Wiley-VCH Verlag GmbH & Co. KGaA.
- [2] HUNGER, K.–P. MISCHKE–W. RIEPER (2000): *Azo Dyes, 1. General*, in *Ullmann's Encyclopedia of Industrial Chemistry*. Wiley-VCH Verlag GmbH & Co. KGaA.
- [3] PAGGA, U.–D. BROWN (1986): The degradation of dyestuffs: Part II Behaviour of dyestuffs in aerobic biodegradation tests. *Chemosphere*, 15 (4), pp. 479–491.
- [4] FORGACS, E.–T. CSERHÁTI–G. OROS (2004): Removal of synthetic dyes from wastewaters: a review. *Environ. Int.*, 30 (7), pp. 953–971.
- [5] SIRÉS, I. et al. (2014): Electrochemical advanced oxidation processes: today and tomorrow. A review. *Environmental Science and Pollution Research*, 21 (14), pp. 8336–8367.
- [6] BRILLAS, E.–C. A. MARTÍNEZ-HUITLE (2015): Decontamination of wastewaters containing synthetic organic dyes by electrochemical methods. An updated review. *Applied Catalysis B: Environmental*, 166–167, pp. 603–643.
- [7] MARTÍNEZ-HUITLE, C. A. et al. (2015): Single and Coupled Electrochemical Processes and Reactors for the Abatement of Organic Water Pollutants: A Critical Review. *Chemical Reviews*, 115 (24), pp. 13362–13407.

- [8] SÄRKKÄ, H.–A. BHATNAGAR–M. SILLANPÄÄ (2015): Recent developments of electro-oxidation in water treatment – A review. *Journal of Electroanalytical Chemistry*, 754, pp. 46–56.
- [9] MOREIRA, F.C. et al. (2017): Electrochemical advanced oxidation processes: A review on their application to synthetic and real wastewaters. *Applied Catalysis B: Environmental*, 202, pp. 217–261.
- [10] CHRISTOS, C. et al. (2008): Advanced oxidation processes for water treatment: advances and trends for R&D. *Journal of Chemical Technology & Biotechnology*, 83 (6), pp. 769–776.
- [11] PANIZZA, M.–G. CERISOLA (2009): Direct And Mediated Anodic Oxidation of Organic Pollutants. *Chemical Reviews*, 109 (12), pp. 6541–6569.
- [12] BONFATTI, F. et al. (2000): Electrochemical Incineration of Glucose as a Model Organic Substrate. II. Role of Active Chlorine Mediation. *Journal of the Electrochemical Society*, 147 (2), pp. 592–596.
- [13] FÓTI, G. et al. (1999): Oxidation of Organics by Intermediates of Water Discharge on IrO₂ and Synthetic Diamond Anodes. *Electrochemical and Solid-State Letters*, 2 (5), pp. 228–230.
- [14] MADSEN, H. T.–E. G. SØGAARD–J. MUFF (2014): Study of degradation intermediates formed during electrochemical oxidation of pesticide residue 2,6-dichlorobenzamide (BAM) at boron doped diamond (BDD) and platinum–iridium anodes. *Chemosphere*, 109, pp. 84–91.
- [15] ANSORGOVÁ, D.–M. HOLČAPEK–P. JANDERA (2003): Ion-pairing high-performance liquid chromatography-mass spectrometry of impurities and reduction products of sulphonated azodyes. *Journal of Separation Science*, 26 (11), pp. 1017–1027.
- [16] SAKALIS, A. et al. (2004): Analysis of sulphonated azodyes and their degradation products in aqueous solutions treated with a new electrochemical method. *International Journal of Environmental Analytical Chemistry*, 84 (11), pp. 875–888.
- [17] HOLČAPEK, M.–K. VOLNÁ–D. VANĚRKOVÁ (2007): Effects of functional groups on the fragmentation of dyes in electrospray and atmospheric pressure chemical ionization mass spectra. *Dyes and Pigments*, 75 (1), pp. 156–165.
- [18] VANĚRKOVÁ, D. et al. (2006): Analysis of electrochemical degradation products of sulphonated azo dyes using high-performance liquid chromatography/tandem mass spectrometry. *Rapid Communications in Mass Spectrometry*, 20 (19), pp. 2807–2815.

TRIAZINE PESTICIDE DECOMPOSITION BY ADVANCED OXIDATION PROCESSES

GERGŐ BODNÁR¹–DANIEL KUPKA¹–DÁVID JÁGER¹–MIROSLAVA VÁCLAVÍKOVÁ¹

¹Institute of Geotechnics, Slovak Academy of Sciences, Watsonova 45, 040 01 Košice, bodnar@saske.sk

Abstract

In recent decades awareness of the problematics of environmental pollution was rising. This has been reflected on the importance of developing new methods of remediation. The complexity of industrial waste effluents, which contains a broad variety of organic and inorganic compounds, requires the development of effective, fast and financially affordable methods. A vast amount of xenobiotics are used in a daily manner, which can present a risk for human health and environmental risk. One of these numerous types of compounds are pesticides from the group of triazine class.

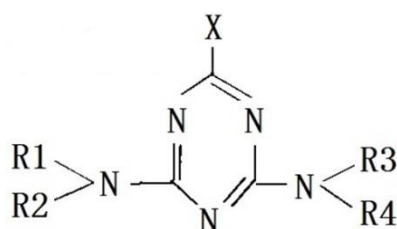


Figure 1

The general structural formula of triazine pesticides

These triazine class pesticides were sold under various commercial brands. Atrazine ($C_8H_{14}ClN_5$) is an organic compound consisting of an s-triazine-ring. Its main role is to eliminate the broadleaf weed from crop fields and increase their agricultural output. The effectiveness of atrazine is based on blocking the plastoquinone-binding protein in photosystem II and to accelerate the oxidative damage by breaking down the electron transport system.

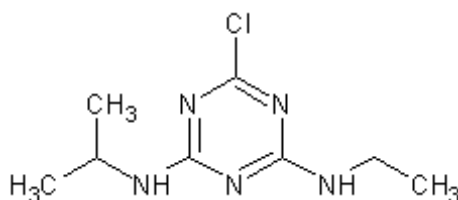


Figure 2

The structural formula of Atrazine

Atrazine is a commonly used selective herbicide of the triazine class. It has been widely used in the world. Atrazine was banned in the European Union in 2004, because of its endocrine disruptor effects, possible carcinogenic effect, and negative environmental impact when the contamination in groundwater exceeds the safety levels stated by the EU. The need of ecologically clean methods makes electrochemical advanced oxidation processes (EAOPs) ideal. Advanced oxidation processes are modern, clean and efficient technologies used for remediation of groundwater and wastewaters contaminated with persistent pollutants. Electrochemical oxidation (EO) is the most popular procedure among the electrochemical advanced oxidation processes. The basic principle of these methods is in generating non-selective highly reactive species, such as hydroxyl radicals ($\cdot\text{OH}$). These ($\cdot\text{OH}$) radicals are able to oxidise persistent pollutants ultimately to carbon dioxide, water, inorganic ions and low molecular weight carboxyl acids, which are biodegradable. Degradation of atrazine by electrochemical oxidation was examined using galvanostatic conditions in an undivided cell. Two different types of anodic materials were used for the treatment. Titanium mesh coated by mixed metal oxides RuO_2 , IrO_2 and TiO_2 (MMO anode) and niobium mesh coated by boron doped diamond layer (BDD anode).

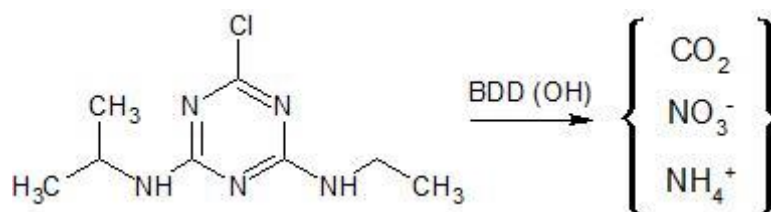


Figure 3

Mineralization of atrazine on BDD anode

The products of electrochemical degradation of atrazine were separated using high performance liquid chromatography (HPLC) on reversed phase. The separated species were detected by diode array detector (DAD) and electrospray ionization mass spectrometry (ESI-MS).

Keywords: Atrazine, Electrochemical Oxidation, Boron doped diamond electrode

ACKNOWLEDGEMENTS

This work has been supported by the *Marie Curie Programme* FP7-People-2013-IAAP-WaSClean project No 612250, the Slovak Grant Agency VEGA, project No 2/0145/15, and the Operational Programme Research and Development through the project: Centre of Excellence for Integrated Research of the Earth's Geosphere (ITMS: 26220120064).



ADSORPTION OF COPPER, IRON AND ZINC IONS FROM ACID MINE DRAINAGE BY NATURAL ZEOLITE

GROZDANKA BOGDANOVIĆ¹–DRAGAN MILOJEVIĆ²–
ANĐELIJA BOGDANOVIĆ³–VELIZAR STANKOVIĆ¹

¹University of Belgrade, Technical Faculty in Bor, VJ 12, 19 210 Bor, Serbia; gbogdanovic@tf.bor.ac.rs

² Student at University of Belgrade, Technical Faculty in Bor, VJ 12, 19 210 Bor, Serbia

³ Student at University of Belgrade, Faculty of Chemistry, Studenski trg 12-16, 11000 Beograd, Serbia

Abstract

Mining and processing operations of metal ores could cause the devastation of large areas of land at the mine surroundings by depositing huge amounts of mining waste on dumps. Acid mine drainages (AMDs), originated either from such dumps or from active or abandoned heavy metal mines, contain considerable amount of heavy metal ions and sulphuric acid, produced as a consequence of bio- and chemical processes between oxygen, rainfalls and minerals present therein. Currently, active and abandoned copper mines from the RTB Bor Co. produce huge amounts of mine waters (~ 4 to $5 \cdot 10^6$ m³/year) in various locations. The main toxic constituents of these waters are copper ions, the concentration of which varies mainly from 5 to 500 ppm, but in some cases > 1000 ppm and sulphuric acid (pH ≈ 3.5 to 4). Ferric/ferrous ions, then zinc and manganese could be, beside copper ions, recovered and commercialised in an acceptable form. In this study, the adsorption features of natural zeolite (clinoptilolite) have been studied in order to determine its applicability for treating AMDs containing Cu²⁺, Fe²⁺ and Zn²⁺ ions. In order to determine both the rate of adsorption and the metal uptake at equilibrium a series of experiments were performed under batch conditions from single ion solutions. Parameters that were varied, are: the initial pH and the initial concentration of metal ion solution. Obtained results showed a considerably fast increase in metal uptake that is ended, in general, in the first 40 minutes, corresponding to 50– 80% of total removal. After this initial rapid period, the rate of adsorption is decreases. Data obtained from the equilibrium experiments are interpreted in terms of Langmuir and Freundlich isotherms. Langmuir model showed better fitting with the experimental data. Maximum metal uptake was achieved at pH value around 4.5.

Keywords: *mining waste, acid mine drainage, copper, zinc, adsorption, zeolite*

1. INTRODUCTION

Over the last one hundred years, mining as the main industrial branch in the town of Bor has had a significant impact not only on the environment of the town itself but also on the environment of the whole region. The harmful effect of mining activities is reflected in degradation of large areas of land (open pits), disposal of huge volumes of solid waste (mine overburden, waste rock and flotation tailings) as well as the occurrence of acid mine drainage.

Pyrite is one of the most abundant minerals in polymetallic heavy metal sulphide deposits, mine overburden, flotation tailings and at the same time the most reactive one in the natural processes of chemical and biochemical degradation. Pyrite oxidation results in the formation of sulphuric acid and iron (III) sulphate, causing oxidation of other less abundant sulphide minerals, during which the ions of other heavy metals (Cu, Zn, Pb, As, Cd, Ni, Mn etc.) enter the solution, depending on the mineral composition of the ore (CHANDRA and GERSON 2010; STANKOVIC et al. 2009; BOGDANOVIĆ et al. 2016). The generation of acid mine drainage (AMD) and uncontrolled release of dissolved heavy metals is of the greatest concern in mining industry due to restrictions established by law regulations for discharge of wastewater into natural recipients.

In Copper Mines Bor, Serbia, there are a few AMDs containing heavy metal ions such as: copper, iron, zinc, nickel as well as sulphuric acid. These are so-called „blue waters“, from underground mine, from AMDs collected at the bottom of the open pits in Bor, Veliki Krivelj and Cerovo as well as seepages from flotation tailing dumps in Bor and Veliki Krivelj. These amounts come into the Krivelj River and via the Timok River to the Danube, damaging them heavily and permanently. In some sources of waste water copper ion concentrations are such that a serious consideration should be given to its extraction and recovery not only for the purpose of reducing a threat to the streams and the river in their proximity but also for the purpose of achieving economic benefits of its commercialization (BOGDANOVIĆ et al. 2013a.).

Heavy metal ions can be removed from wastewaters by various methods, where the adsorption is one of them. The adsorption as a technique is relatively well described in the literature and the focus of research has shifted to examining the efficiency of different types of natural adsorbents such as zeolite bentonite, clay or various types of natural or activated carbonaceous materials (low-quality coal, waste of various types of deciduous and coniferous trees, etc.) (ANTIC, D. V. et al. 2012; BAILEY, S. E. et al. 1999; MOSHOESHOE, M. et al. 2017).

This paper presents the results of heavy metal ions adsorption by zeolite, from synthetic solution containing single metal ionic specie. Different parameters were changed, as: the initial pH and the initial concentration of metal ions solution. Equilibrium data were evaluated from adsorption isotherms.

2. MATERIALS AND METHODS

2.1. Adsorbent

Natural zeolite from Serbia (Deposit “Igroš”, Kopaonik) was used in the experiments as an adsorbent for copper, iron and zinc ions removal from synthetic solutions. In order to improve the reactivity of the sample, micronization grinding of the sample was performed out in a laboratory vibrating mill with rings of the type “Siebtechnik TS -250” at a speed of 1,000 rpm for the time of 120 s. The particle size distribution is shown in *Table 1*.

Table 1
Particles size distribution of the zeolite samples

Size fraction (µm)	+212	– 212+150	–150+106	–106+75	–75+30	– 30+20	–20+10	–10+5	–5+0
W,%	0.57	0.60	2.27	6.20	0.32	1.27	0.07	0.23	88.48

The specific surface area was determined by used particle sizing instrument Malvern Instruments Mastersizer 2000. The value of the specific surface was found $0.787 \text{ m}^2 \cdot \text{g}^{-1}$. The chemical composition of natural zeolite is shown in the *Table 2*.

Table 2
Chemical composition of the zeolite samples

Component	SiO ₂	Al ₂ O ₃	Fe ₂ O ₃	CaO	MgO	Na ₂ O	K ₂ O	Ignition loss
Content, %	65.1	14.86	2.34	2.72	1.64	0.59	0.79	10.83

The cation exchange capacity was determined by the standard method (MATIJAŠEVIĆ and ĐAKOVIĆ 2009) using a solution of NH₄Cl concentration of $1 \text{ mol} \cdot \text{dm}^{-3}$. Type and content of exchangeable cations in the initial sample is shown in *Table 3*. The total cation exchange capacity was determined as the sum of particular ones.

Table 3
Content of exchangeable cations and cation exchange capacity (CEC)

Exchangeable cation (Me ^{z+})	Ca ⁺	K ⁺	Mg ⁺	Mg ⁺	CEC
Content, (mmol/100g)	68,47	7,95	16,13	8,94	101,49

Mineralogical composition of the samples was determined by optical microscopic and X-ray (XRPD) analysis, showing that in zeolite tuff the predominant mineral is clinoptilolite, while the trace minerals are mica and quartz.

2.2. Chemicals

Stock solutions of the chosen Me²⁺ ions were prepared by dissolving the corresponding sulphate salts of the metals in 1,000 ml distilled water in an amount to obtain an initial concentration. Lower concentrations were then prepared when required by further dilution of the stock solution with distilled water. Initial pH of prepared solutions was adjusted by adding sulfuric acid and controlled by pH-meter. All chemicals were of analytical grade.

2.3. Experimental procedure

The adsorption experiments were performed in a batch mode in a series of beakers equipped with magnetic stirrers by stirring 1 g of the zeolite with 50 ml of metal ion solution. Zeolite sample and aqueous phase were suspended by magnetic stirrer at 300 rpm. The agitation time was varied from 5–120 minutes. At the end of the predetermined time, the suspension was filtered and the filtrate was analyzed. The initial and remaining concentrations of metal ions were determined by Optical emission spectrometers with inductively coupled plasma. All experiments were performed at room temperature. Based on material balance, the adsorption capacity was calculated by using the following expression:

$$q(t) = (C_0 - C(t)) \cdot \frac{V}{m} \quad (1)$$

where: $q(t)$ is the mass of adsorbed metal ions per unit mass of adsorbent (mgg^{-1}); C_0 and $C(t)$ are the initial and final metal ion concentrations (gdm^{-3}), respectively; V is the volume of the aqueous phase (dm^3); m is the mass of adsorbent used (g).

Degree of adsorption, in percentage, is calculated as:

$$\text{AD}(\%) = \left(1 - \frac{C(t)}{C_0}\right) \cdot 100 \quad (2)$$

3. Results and discussion

Effect of the initial pH value of the solution on the metal uptake by zeolite

Influence of the initial pH value of the solution on adsorption capacity copper, iron and zinc ions was examined through the series of experiments, by varying the initial pH of solution from 2.0 to 5.0. The initial concentration of metals ions was kept constant ($C_i = 200 \text{ mg dm}^{-3}$). Mass of adsorbent used was 1g while the total time of adsorption was 60 minutes. Obtained results are shown in *Figure 1*.

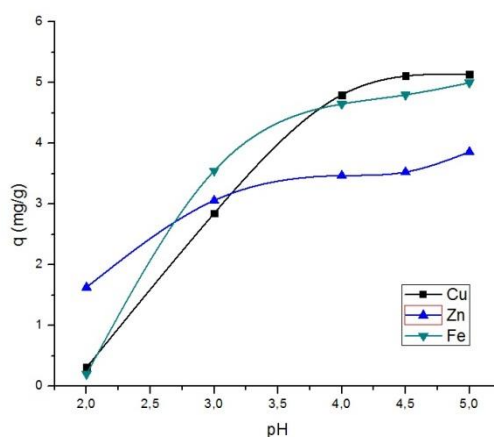


Figure 1

The effect of pH on adsorption capacity of Cu^{2+} , Ni^{2+} and Fe^{2+} ions

As can be seen from *Figure 1*, changes of the initial pH of solution strongly affects the adsorption capacity of zeolite in such way that the capacity increases with pH for all investigated ions, what is in agreement with the previously reported results (CABRERA et.al. 2005; BOGDANOVIĆ et al. 2013b). At lower pH values (pH 2), the adsorption capacity of zeolite for copper and iron ions was 0,31 i 0,2 mg g^{-1} , respectively. The adsorption capacity of zeolite for zinc ions rises from 1.63 mg g^{-1} to almost 3.86 mg g^{-1} by increasing pH from 2 to 5.0. Generally, adsorption capacity is low at lower pH, because zeolite primarily adsorbs hydrogen ions whose concentration is far higher than the metal concentration. Decreasing of aqueous phase acidity lowers the concentration of hydrogen ions which favours the adsorption of metals ions. The maximum adsorption capacity

for metals ions occurs in pH range between 4.0 and 5.0. Maximal adsorption capacity of copper ions obtained at pH = 5.0 is 5.14 mg g⁻¹. The achieved copper adsorption degree is almost 51%, while the adsorption degree of iron was 51.55%. Corresponding achieved capacity is 5.00 mg g⁻¹ at pH = 5.0. Increasing the mass of zeolite in the suspension increased the adsorption degree due to an increased number of active sites available to adsorb metal ions. Obtained results showed that after 40 minutes reached degree of adsorption is 80% for copper, when using 5 g of adsorbent.

4. ADSORPTION ISOTHERMS

Distribution of metals ions at equilibrium between aqueous phase and solid adsorbent is quantified by adsorption isotherm. Several equilibrium models have been developed to describe adsorption isotherm relationships. The two main isotherm models used in this work are the Langmuir and Freundlich models. Langmuir model is obtained under an assumption of a totally homogeneous adsorption surface, whereas the Freundlich isotherm is suitable for a highly heterogeneous surface (OTER and AKCAY 2007; PANAYOTOVA 2001). To determine adsorption isotherm, a fixed amount of zeolite (1g) was mixed for 60 minute with a constant volume of solution (50 cm³) containing metal ions in the range from 25 to 400 mg dm⁻³ (initial pH = 4.5). All other parameters were kept constant as described above. The adsorption isotherm results, for all considered ions, are shown in *Figure 2* (left column) and linear Langmuir plots were presented in *Figure 2* in the right column next to the correspond isotherm. The adsorption isotherm parameters are summarized and presented in *Table 3*, together with the regression coefficients R², for both considered models.

Table 4
Adsorption parameters calculated from linearized form of adsorption isotherms

Metal ion	Linear form of Langmuir equation	Evaluated Langmuir parameters		
		K _L , (dm ³ ·mg ⁻¹)	q _m , (mg·g ⁻¹)	R ²
Cu ²⁺	C _e /q _e =10,70663 + 0,168C _e	0.07	7.54	0.944
Fe ²⁺		0.175	5.8	0.987
Zn ²⁺		0.04	5.6	0.946
	Linear form of Freundlich equation	Evaluated Freundlich parameters		
		K _f , (dm ³ ·mg ⁻¹)	n, (g·dm ⁻³)	R ²
Cu ²⁺	log q _e = -0,24589 + 0,35498 log C _e	2.64	5.82	0.54
Fe ²⁺		1.42	6.57	0.984
Zn ²⁺		1.2	3.76	0.967

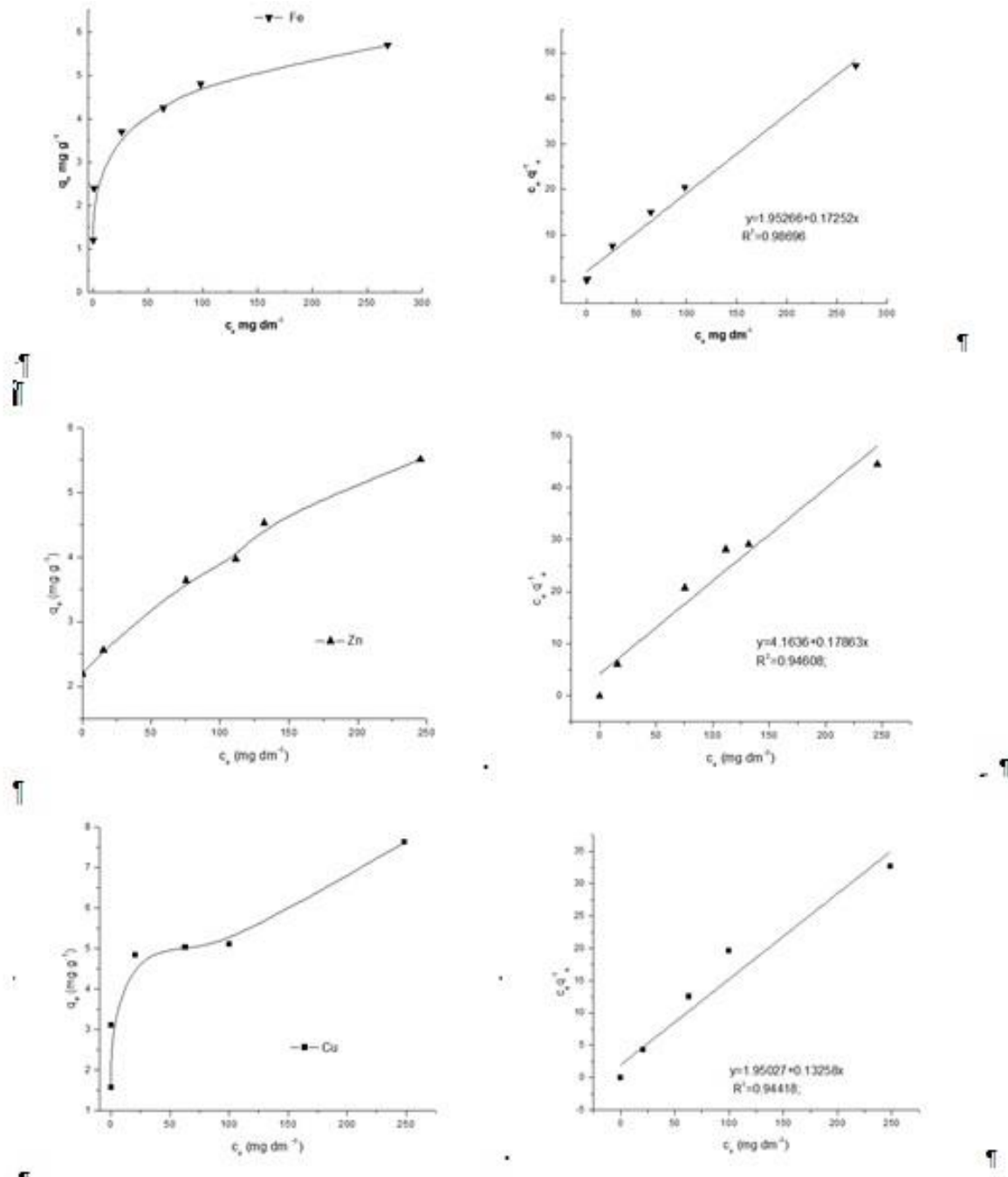


Figure 2
Adsorption isotherms (left) and their linear Langmuir plots (right) for each considered ion

According to the regression coefficients, the experimental results for adsorption isotherm provide a better fitting to the Langmuir model for copper and iron ions. Adsorption data for zinc ions in linearized form gave satisfactory correlation coefficient, $R^2 = 0.946$ for Langmuir and $R^2 = 0.967$ for Freundlich model for covered concentration range. Comparison of the linear correlation coefficients indicated that Freundlich adsorption model better fits the experimental data for zinc ions ($R^2 = 0.967$). The Freundlich isotherm constants K_F and n were 1.2 and 3.76 respectively. The numerical value of $1/n < 1$ indicates that adsorption capacity is only slightly suppressed at lower equilibrium concentrations (ERDEM 2004).

5. CONCLUSION

The adsorption of copper, iron and zinc ions from solution onto natural zeolite occurs efficiently. The adsorption rate strongly depends on the initial pH value of the solution. The adsorption decreases in more acidic solutions (pH 2), for all investigated ions due to a feature of hydrogen ions to be adsorbed and a competition between them and metal ions in solution. Better adsorption conditions were achieved at higher pH values (pH 4–5 for all investigated ions). Adsorption isotherms of metal ions showed that the adsorption equilibrium could be modelled better by Langmuir than by Freundlich equation. Maximal achieved adsorption capacity were 7.54 mg g^{-1} , 5.8 mg g^{-1} and 5.6 mg g^{-1} for copper, iron and zinc ions, respectively. It could be pointed out that all investigated metal ions would be adsorbed from mixed solutions, as acid mine drainage generally are.

ACKNOWLEDGEMENTS

The authors acknowledge the financial support from the Ministry of Education, Science and Technological Development of the Republic of Serbia (Projects No. 172031).

REFERENCES

- [1] ANTIĆ, D. V. et al. (2012): Removal of copper ions from acid mine drainage using anthracite coal. In: MARKOVIĆ, Z. S. et al. (eds.): *20th Int. Scientific and Professional Meeting "Ecological Truth"*, Zaječar, Serbia, 30 May–02 June, pp. 271–280.
- [2] BOGDANOVIĆ, G. et al. (2013a): Mine Waters from Mining & Smelting Basin Bor – A Resource for the Recovery of Copper or Polluter of the Environment. *Recycling and Sustainable Development*, 6 (1), pp. 37–43.
- [3] BOGDANOVIĆ, G. et al. (2013b): Adsorption of copper and zinc ions from acid mine drainage by natural zeolite. *Proceedings of the XV Balkan Mineral Processing Congress*, Volume II, Sozopol, Bulgaria, June 12–16, pp. 989–993.
- [4] BOGDANOVIĆ, G. et al. (2016): Leaching of Low – Grade Copper Ores: A Case Study for Kraku Bugaresku-Cementacija.
- [5] Deposits (Eastern Serbia). *Journal of Mining and Metallurgy*, 52A (1), pp.45–56.
- [6] BAILEY, S. E et al. (1999): A Review of Potentially Low-cost Sorbents for Heavy Metals. *Water Research*, 33(11), pp. 2469–2479.

- [7] CABRERA, C. et.al. (2005): Sorption characteristics of heavy metal ions by a natural zeolite. *Journal of Chemical Technology and Biotechnology*, 80, pp. 477–481.
- [8] CHANDRA, A. P–GERSON, A. R. (2010): Review. The mechanisms of pyrite oxidation and leaching: A fundamental perspective. *Surface Science Reports*, 65, pp. 293–315.
- [9] ERDEM, E. et al. (2004): The Removal of Heavy Cations by Natural Zeolites. *Journal of Colloid and Interface Science*, 280, pp. 309–314.
- [10] MATIJAŠEVIĆ, S.–DAKOVIĆ, A. (2009): Adsorption of Uranyl Ion on Acid – Modified Zeolitic Mineral Clinoptilolite. *Chemical Industry*, 63, pp. 407–414.
- [11] MOSHOESHOE, M. et al. (2017): A Review of the Chemistry, Structure, Properties and Applications of Zeolites. *American Journal of Materials Science*, 7, pp. 196–221.
- [12] OTER, O–AKCAY, O. (2007): Use of natural clinoptilolite to improve water quality: sorption and selectivity studies of lead(II), copper(II), zinc(II), and nickel(II). *Water Environment Research*, 79, pp. 329–335.
- [13] PANAYOTOVA, M. I. (2001): Kinetics and thermodynamics of copper ions removal from wastewater by use of zeolite. *Waste Management*, 21, pp. 671–676.
- [14] STANKOVIĆ, V. et al. (2009): Heavy metal ions adsorption from mine waters by sawdust. *Chemical Industry and Chemical Engineering*, 15 (4), pp. 237–249.



COMMINUTION OF ZEOLITE AND ITS POTENTIAL APPLICATION

KATARINA BALANOVIĆ–MILAN TRUMIĆ–MAJA TRUMIĆ

University of Belgrade, Technical Faculty in Bor, V.J. 12, 19210 Bor, Serbia,
kbalanovic@tfbor.bg.ac.rs, mtrumic@tfbor.bg.ac.rs, majatrumic@tfbor.bg.ac.rs

Abstract

Natural zeolites are widely used in wastewater treatment, construction, agriculture and livestock farming, veterinary medicine, food, textile and other industries. Properties, such as low melting temperature and low hardness, allow the substitution of quartz sand with zeolite to a certain extent in the production of porcelain and concrete. Thus significantly improves their physical and mechanical characteristics. For this purpose, zeolites that have previously adsorbed heavy metals from wastewater can also be used. Natural zeolites are often used as adsorbents because of their high porosity and large specific surfaces. By reducing the zeolite grain size, the metal adsorption rate increases, which does not have effect on zeolite adsorption capacity. For this reason, the zeolite grinding test should be carried out. In this paper the zeolite grinding kinetics in a ball mill with charge of different ball size was analyzed. By analyzing the obtained results, it was observed that the highest value of the zeolite grinding efficiency (wide range of zeolite particle size) was achieved by using the charge with the ball smallest diameter.

Keywords: *zeolites, comminution, ball mill, charge*

1. INTRODUCTION

Natural zeolites are hydrated aluminosilicate of alkali and alkaline earth cations. They have a crystal structure composed of tetrahedra AlO_4 and SiO_4 which are bound with oxygen atoms (DEMIRKIRAN et al. 2010). Because of their widespread in the world and interesting properties such as hydration and dehydration, ion exchange, ability of sorption of gases, liquids and steam, they have been widely used in various fields. Zeolites are widely used as building materials, for the production of cement and porcelain, for the treatment of municipal, industrial and drinking water, for the removal of Cs and Sr from the waters of nuclear plants, in agriculture and livestock farming, veterinary medicine, in food and other industries (FREDERICK 1999). During the production of porcelain, by substitution of quartz sand with a zeolite with a grain size of 0.075 mm in a certain extent, improve some properties such as an increase of the electrical resistance of porcelain and improvement of the sintering conditions. Adding zeolite reduces the activation energy needed to begin sintering the porcelain. With a decrease in activation energy, the sintering temperature decreases from 1350 °C to 1250 °C, resulting in significant savings in production and price reduction of product (DEMIRKIRAN et al. 2008). Also, using zeolite, porcelain with slightly higher values of electrical resistance at room temperature is obtained. Another advantage is that zeolite

is more easily grinding compared to quartz, which additionally saves energy in the grinding process (DEMIRKIRAN et al. 2010). With the decreasing zeolite particle size, the surface area for potential chemical reactions increases. Since zeolites have a considerable amount of silica, they are suitable for use in cement production. By adding zeolite with grain size $(-0.5+0)$ mm in the cement production process, some characteristics of the product are improved. Using finer particles of zeolite, they fill the voids between cement and aggregates grain, making the concrete tighter. Also, reducing the grain size of the zeolite slows down the reaction of hydration, which reduces time after which the concrete starts to set (CZAPIK and CZECHO-WICZ 2017). In addition to natural zeolites, as additive in cement production, zeolites that have previously adsorbed metals from wastewater can be used, provided that this does not affect the mechanical properties of concrete and that such a concrete later does not affect the environment. Natural zeolites are especially suitable for purification of wastewater by the ion exchange method because they contain non-toxic compounds K, Ca, Na, and Mg (MEDVIDOVIĆ et al. 2006). In this way wastewater containing lead, chromium, cadmium, nickel, copper, mercury, silver as well as acid mine drainage, can be treated (PANSINI 1996). For this purpose, zeolites with a wide range of particle size, $(-5+0)$ mm, can be used (SEKULIĆ et al. 2013). By reducing the size of the zeolite grain, the metal adsorption rate increases, which does not have effect on zeolite adsorption capacity (TRGO et al. 2015).

For this reason, in this paper, the zeolite grinding test was performed. The zeolite grinding kinetics in a ball mill with charge of different ball size was analyzed. The equation of the grinding kinetics law for the first order grinding was used. The differential form of the first order grinding kinetics equation is (MAGDALINOVIĆ 1999):

$$\frac{dR}{dt} = -kR \quad (1)$$

where
is:

$\frac{dR}{dt}$	– grinding speed of a large class
R	– the content of the wide class in the mill at the moment (t)
t	– grinding time
k	– grinding rate constant

The integral form of equation (1) is:

$$R = R_0 \cdot e^{-kt} \quad (2)$$

Equation (2) can be written in the form:

$$\ln R_0 - \ln R = kt \quad (3)$$

or otherwise:

$$\ln \frac{R_0}{R} = kt \quad (4)$$

Equation (4) represents the equation of the linear line in the coordinate system $[t; \ln(R_0/R)]$, with the coefficient of direction (k):

$$k = \text{tg}\alpha = \frac{Y}{X} = \frac{\ln \frac{R_0}{R_2} - \ln \frac{R_0}{R_1}}{t_2 - t_1} \quad (5)$$

2. MATERIALS AND METHODS

The test was carried out on samples of zeolite from the deposit "Igroš" - Kopaonik. The chemical composition of zeolite was tested in the Institute for Technology of Nuclear and Other Mineral Raw Materials in Belgrade and is shown in *Table 1*. The zeolite density is 2186 kg/m³, and the Bond working index is $W_i = 9.20$ kWh/t.

Table 1
Chemical composition of the zeolite sample

Component	Content (%)
SiO ₂	64.05
TiO ₂	15.29
Fe ₂ O ₃	4.82
Al ₂ O ₃	2.52
MgO	1.33
Na ₂ O	1.27
K ₂ O	0.77
Other	9.95

Three samples of 200 g (wide range of particle size $(-1.18+0)$ mm) were formed, which the particle size distribution before grinding was given in *Table 2*. Grinding kinetics were monitored at the following time intervals: 0.5 min, 1 min, 2 min, 4 min, 8 min, 15 min.

Table 2
Particle size distribution of zeolite samples before grinding

Size fraction, d (mm)	Zeolite	
	W %	R %
-1.18+0.850	16.05	16.05
-0.850+0.600	14.45	30.50
-0.600+0.425	10.35	40.85
-0.425+0.300	9.35	50.20
-0.300+0.212	6.75	56.95
-0.212+0.106	13.05	70.00
-0.106+0.075	6.45	76.45
-0.075+0	23.55	100.00
Σ	100.00	

Grinding experiments were carried out in a laboratory ball mill with the following characteristics:

- mill diameter $D = 158$ mm
- mill length $L = 198$ mm
- relative rotational rate of the mill $\Psi = 0.85$ n_k

- coefficient of ball mill loading $\varphi = 0.40$
- inside surface of cylinder mill ribbed
- grinding method dry

The ball mill (*Figure 1*) is rolling using a roller device (*Figure 2*). Inside surface of mill is ribbed to prevent sliding of the ball during operation of the mill (*Figure 3*).



Figure 1
Outside view of the mill



Figure 2
Device with rollers



Figure 3
Ribbed inside surface of the mill

Balls were made from steel: S4146, extra high quality, having hardness 62 ± 2 HRC according to Rockwell. The mill ball loading was constant in all grinding experiments and amounted to 40% by volume. Three different charge of balls were used (*Figure 4*), where each individual charge was composed of balls of the same diameter. The ball charge characteristics are given in *Table 3*.

Table 3
Characteristics of ball charge

Ball diameter in charge (mm)	Charge mass (g)	Number of balls in charge	Ball mass (g)
10	6775.8	1562	4.34
15	6945.1	482	14.41
24	6921.8	127	54.50



Figure 4
Three different charge made of balls of diameter 24, 15 and 10 mm

3. RESULTS AND DISCUSSION

The results of the zeolite sample grinding kinetics with a 24 mm ball diameter charge, are shown in *Figure 5*. In *Table 4*, the values of the grinding rate constant and the correlation coefficients, are given.

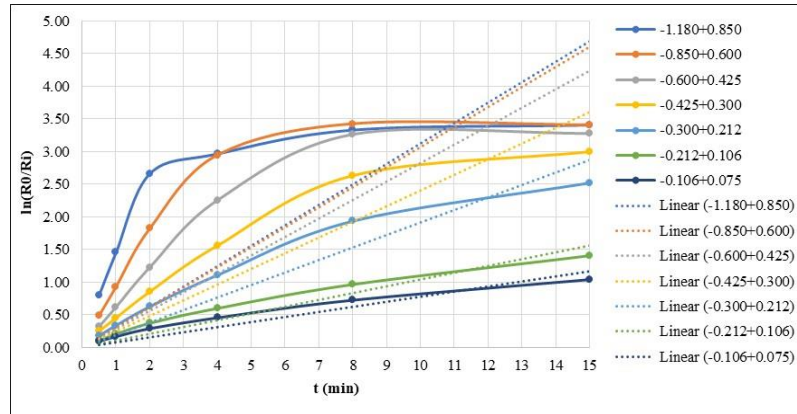


Figure 5

Zeolite grinding kinetics with 24 mm ball diameter in charge

Table 4

Grinding rate constant and the correlation coefficients obtained by the zeolite grinding with 24 mm ball diameter in charge

Size fraction, d (mm)	Grinding rate constant, k	Correlation coefficient, R ²
-1.180+0.850	0.312	-0.969
-0.850+0.600	0.307	0.110
-0.600+0.425	0.282	0.550
-0.425+0.300	0.241	0.782
-0.300+0.212	0.192	0.885
-0.212+0.106	0.104	0.904
-0.106+0.075	0.078	0.876

By analyzing the values from *Table 4*, it can be noticed that the grinding rate constant with 24 mm ball diameter in charge decreases with the reduction zeolite sample size. The highest grinding rate constant was obtained at the largest size fraction (-1.180+0.850) mm. The correlation coefficients for the narrow size classes (-1.180+0.850) mm and (-0.850+0.600) mm are smaller than the minimum correlation coefficient that is $R^2_{\min}=0.569$ (VOLK 1965), which means that this model cannot describe the grinding kinetics for these two narrow classes.

In *Figure 6*, the results of the zeolite sample grinding kinetics with 15 mm ball in a charge are shown. In *Table 5*, the values of the grinding rate constant and the correlation coefficients, are given.

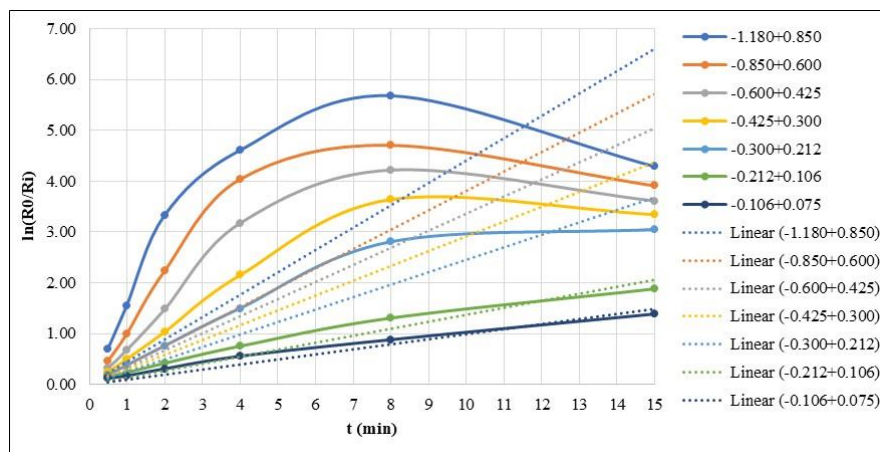


Figure 6
Zeolite grinding kinetics with 15 mm ball diameter in charge

Table 5
Grinding rate constant and the correlation coefficients obtained
by the zeolite grinding with 15 mm ball diameter in charge

Size fraction, d (mm)	Grinding rate constant, k	Correlation coefficient, R ²
-1.180+0.850	0.440	-0.404
-0.850+0.600	0.381	0.028
-0.600+0.425	0.336	0.360
-0.425+0.300	0.292	0.623
-0.300+0.212	0.245	0.807
-0.212+0.106	0.138	0.937
-0.106+0.075	0.099	0.946

The values in Table 5 show that in case of grinding with 15 mm ball diameter in charge, the values of the grinding rate constant are reduced by decreasing zeolite sample size, same as at grinding with 24 mm ball diameter in charge. The highest grinding rate constant was achieved with the largest size fraction (-1.180+0.850) mm. The correlation coefficients for the narrow size classes (-1.180+0.850) mm, (-0.850+0.600) mm and (-0.600+0.425) mm are smaller than the minimum coefficient of correlation which is $R^2_{\min} = 0.569$ (VOLK 1965), which means that this model can not described grinding kinetics for these three narrow classes. The problem when calculating the grinding kinetics constant is that the grains of the sample are sticking together and increasing their size after 8 minutes of grinding, which can be seen by the fall of the curves in Figure 6.

In Figure 7, the results of the zeolite sample grinding kinetics with 10 mm ball diameter in charge are shown. In Table 6, the values of the grinding rate constant and the correlation coefficients, are given.

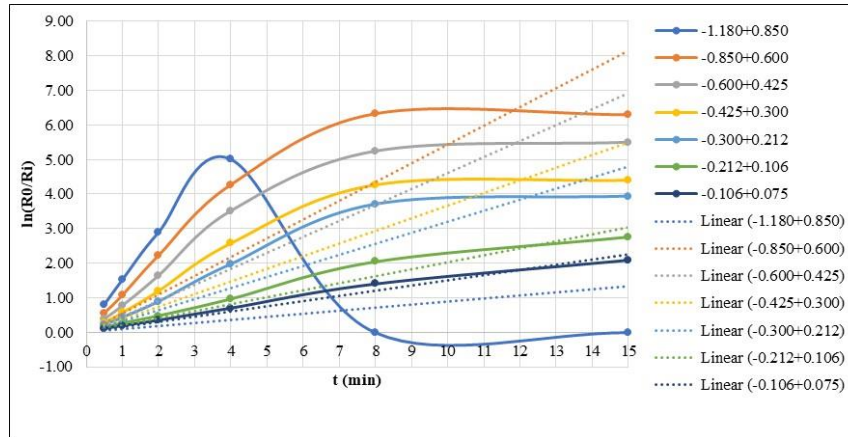


Figure 7
Zeolite grinding kinetics with 10 mm ball diameter in charge

Table 6
Grinding rate constant and the correlation coefficients obtained
by the zeolite grinding with 10 mm ball diameter in charge

Size fraction, d (mm)	Grinding rate constant, k	Correlation coefficient, R ²
-1.180+0.850	0.090	-0.786
-0.850+0.600	0.542	0.589
-0.600+0.425	0.460	0.687
-0.425+0.300	0.367	0.730
-0.300+0.212	0.319	0.806
-0.212+0.106	0.203	0.951
-0.106+0.075	0.150	0.973

In this case, as in the previous two, the value of the grinding rate constant decreases with the decrease in the sample size. The highest grinding rate constant was achieved with the size fraction (-0.850+0.600) mm. By comparing the results of grinding with 24 mm, 15 mm and 10 mm ball diameter in charge, the higher values of the constant were obtained with 10 mm ball diameter in charge. Figure 7 looks slightly different from Figure 6 and Figure 5, because of anomaly in the size class (-1.180+0.850) mm. This class disappeared after 4 minutes of grinding and this anomaly can explain such a low coefficient of correlation for a given size class.

In Table 7 and Figure 8, grinding kinetics with a different ball diameter in charge is given for each narrow size class, of which a wide size class (-1.180+0) mm is formed.

By analyzing the data from Figure 8, it is concluded that the maximum value of the grinding rate constant is obtained with 10 mm ball diameter in charge and the smallest with 24 mm ball diameter in charge, for each narrow size class. The results confirmed that larger diameter ball is

required for larger grains, and with the reduction in the size of the grain, the required diameter of the ball decreases. From here it follows that for smaller grains of smaller size classes and less hardness, a smaller diameter ball is required (MAGDALINOVIĆ et al. 2012).

Table 7
Grinding rate constant of narrow size classes
with a different ball diameter in charge

Size fraction, d (mm)	Ball diameter in charge (mm)		
	24	15	10
–1.180+0.850	0.312	0.440	0.090
–0.850+0.600	0.307	0.381	0.542
–0.600+0.425	0.282	0.336	0.460
–0.425+0.300	0.241	0.292	0.367
–0.300+0.212	0.192	0.245	0.319
–0.212+0.106	0.104	0.138	0.203
–0.106+0.075	0.078	0.099	0.150

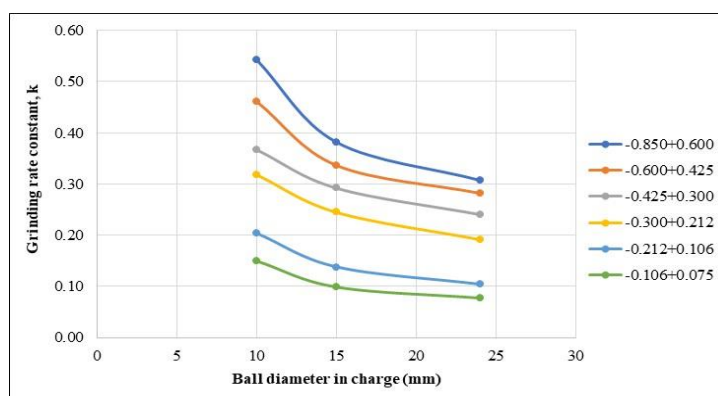


Figure 8

Grinding rate constant of narrow size classes with a different ball diameter in charge

4. CONCLUSION

By comparing the results of the value grinding rate constant with different ball diameter in charge (24 mm, 15 mm and 10 mm), it was concluded that in all cases the highest values of the constant were realized in the largest narrow size class, and that constant decreases with the decrease in the sample size. Also, the highest value of the zeolite grinding efficiency was obtained by using the charge with the smallest diameter (10 mm) ball. Bearing in mind that the sample was composed of more fine narrow size classes and that the zeolite has a lower value of the Bond working index, and

that for smaller grains which are less hardness are required smaller diameter ball, the obtained results indicate that for such a raw material really needed a charge composed of smaller diameter balls.

By further research, it would be possible to determine whether a second charge of balls of even smaller diameter could correspond to a wide size class (-1.180+0) mm.

REFERENCES

- [1] CZAPIK, P.–CZECHOWICZ, M. (2017): Effects of natural zeolite particle size on the cement paste properties. *Structure and Environment*, 9 (3), pp. 180–190.
- [2] DEMIRKIRAN, A. Şükran. et al. (2008): Effect of natural zeolite addition on sintering kinetics of porcelain bodies. *Journal of materials processing technology*, 203, pp. 465–470. (doi:10.1016/j.jmatprotec.2007.10.053).
- [3] DEMIRKIRAN, A. Şükran. et al. (2010): Electrical resistivity of porcelain bodies with natural zeolite addition. *Ceramics International*, 36(3), pp. 917–921. (doi:10.1016/j.ceramint.2009.10.029).
- [4] FREDERICK, A. M. (1999): La roca magica: Uses of natural zeolites in agriculture and industry. In: Proc. Natl. Acad. Sci. USA, Vol. 96, *National Academy of Sciences colloquium "Geology, Mineralogy, and Human Welfare"*, Irvine, California, 8–9 November. Arnold and Mabel Beckman Center in Irvine, pp. 3463–3470.
- [5] MAGDALINOVIĆ, N. (1999): Usitnjavanje i klasiranje, Nauka Beograd, pp.195–205.
- [6] MAGDALINOVIĆ, N. et al. (2012): The optimal ball diameter in a mill. *Physicochemical Problems of Mineral Processing*, 48(2), pp. 329–339.
- [7] MEDVIDOVIĆ, N. Vukojević. et al. (2006): Column performance in lead removal from aqueous solutions by fixed bed of natural zeolite–clinoptilolite. *Separation and Purification Technology*, 49(3), pp. 237–244. (doi:10.1016/j.seppur.2005.10.005).
- [8] PANSINI, M. (1996): Natural zeolites as cation exchangers for environmental protection. *Mineralium deposita*, 31 (6), pp. 563–575. (DOI:10.1007/BF00196137).
- [9] SEKULIĆ, Ž. et al. (2013): Defining the size class as the quality parameter of zeolite assortment of products. *Mining and Metallurgy Engineering Bor*, 3, pp. 13–32. (DOI: 10.5937/mmeb1303013S).
- [10] TRGO, M. et al. (2015): Influence of zeolite particle size and initial lead concentration on sorption kinetic study by batch experiments. *The Holistic Approach to Environment*, 5 (3), pp. 105–118.
- [11] VOLK, W. (1965): Statystyka stosowana dla inżynierów. *Wydawnictwa Naukowo-Tekniczne*.



ENVIRONMENTAL APPLICATIONS OF GRAPHENE OXIDE

DOMINIKA BEHUNOVÁ¹–GEORGE GALLIOS²–MIROSLAVA VÁCLAVÍKOVÁ¹

¹Institute of Geotechnics SAS, Watsonova 45, 040 01 Košice, Slovakia

²Aristotle University of Thessaloniki, School of Chemistry, Lab. General & Inorganic Chemical Technology, 54124 Thessaloniki, Greece
vaclavik@saske.sk

Abstract

Nanomaterials exhibit remarkable properties in numerous areas of interest including the environmental remediation. The environmental remediation process is the act of removing pollutions or contaminants from environmental media, such as water or soil (HU et al. 2014; MEUSER 2012). The effective strategies of waste water treatment can be treated with adsorption using graphene oxide-based composites, which shows strong binding with these pollutant species.

Graphene oxide (GO), the functionalized graphene containing epoxy and hydroxyl chemical groups, has a special physico-chemical properties such as large surface area, mechanical stability, tunable optical, thermal and electrical properties (NOVOSELOV et al. 2004; GEIM et al. 2007). The advantage of this material is based on the amphiphilic character which allows remove inorganic and organic molecules at nanoscale dimension. Hence, heavy metal ions (Cd^{2+} , Pd^{2+} , Hg^{2+} , Cr^{6+} , As^{3+} etc.), synthetic or natural organic molecules (dyes), pharmaceuticals (antibiotics), agriculture molecules (pesticides), biomolecules (proteins, DNA etc.), mixtures (oil/petrol), are potentially removed by GO (PENDOLINO et al. 2017).

Graphene and its derivatives are used as adsorbing materials thanks to their structure and, mainly to the presence of oxygen groups on GO surface. The **solid phase** of GO can be designed to two forms, membrane and foam (sponge) and both are very attractive for high-efficiency separation applications including water purification and desalination (PENDOLINO et al. 2017). TAN et al. 2015 reported a successful adsorption of Cu^{2+} , Cd^{2+} and Ni^{2+} on a GO/PVA membrane. The equilibrium was reached in a short time and the membrane was regenerated more than six times. On the other hand KIM et al. 2017 observed special GO-polymer membrane which showed excellent water flux and salt rejection (a NaCl of 99.9%), alongside excellent mechanical stability and chlorine tolerance for the osmosis process. NAIR et al. 2012 prepared a non-selective GO membrane by spray or spin-coating on copper substrate. This membrane was able to selectively reject all molecules except H_2O . They tested ethanol, hexane, acetone, decane, and propanol by weight during several days, without any visible changes. This kind of membrane can be used for a clear nanofiltration of pure water.

The solid phase of GO is more convenient form to be used in environmental application, the **liquid phase** represents an alternative approach to purify water. In addition, both faces of GO layer are efficiently employed to create weak or chemical bonds. The presence of hydroxyl, epoxy and alkoxy groups on GO allows many of conventional organic synthesis to add an auxiliary functionality. A typical example of organic dye removal using liquid GO dispersion involves a prototype contaminant, methylene blue dye (MB). The result exhibits a removal contaminant range of 95% with GO having a concentration of 100 times lower than that of the dye (ZHAO et al. 2017). Similar result was obtained by YANG et al. 2011 to

purify water system from MB via GO adsorption. Authors reported a removal efficiency of 99% for a concentration of MB below 200mg/L and a maximum absorption capacity of 714 mg/g.

Considering studies and excellent properties of GO were interesting for researcher over the world, that's why we decided to create a new research to **collect the liquid phase of GO and turned into solid phase on stainless steel** (SS) electrode using electrophoretic deposition. It is expected that new surface cover by GO layer of the SS electrode will provide more active surface area and increase efficiency of electrochemical oxidation technique. Using electrochemical oxidation is effective and simple process for treatment of assorted wastewaters. Oxidants are produced during the technique directly at the electrode surface and/or indirectly from chemical compounds in the treated waste water (JAGER et al. 2018).

The latest research shows that removals of chemical hazardous material using GO are a quite novel approach in the treatment of wastewater. This unique material offers unconventional physico-chemical properties that can work in removal technology restricting the negative impact to the environment and human health. GO is capable of simultaneously removing of a broad class of molecules and display strong affinity for the adsorption of contaminants to convert it in to the harmless products.

Keywords: wastewater treatment, graphene oxide, electrochemical oxidation, degradation, water purification

ACKNOWLEDGEMENTS

This work has been supported by the Marie Curie Programme FP7-People-2013-IAAPWaSClean project No 612250 as well as H2020-MSCA-RISE-2016-NANOMED project No 734641. The support of Slovak R&D Agency project No APVV-10-0252-WATRIP, Science and Scientific Grant Agency VEGA project No. 2/0158/15, VEGA project No. 2/0055/17, Greek national support project No 40124 and R&D support project (MVTs) of Slovak Academy of Sciences are greatly acknowledged as well.

REFERENCES

- [1] GEIM, A. K.–NOVOSELOV, K. S. (2007): The rise of graphene. *Nature Materials*, 6, pp. 183–191.
- [2] HU, A.–APBLETT, A. (2014): Nanotechnology for water treatment and purification. Heidelberg, Springer.
- [3] JAGER, D.–KUPKA, D.–VACLAVIKOVA, M.–IVANICOVA, L.–GALLIOS, G. (2018): Degradation of Reactive Black 5 by electrochemical oxidation. *Chemosphere*, 190, pp. 405–416.
- [4] KIM, S.–LIN, X.–OU, R.–LIU, H.–ZHANG, X.–SIMON, G. P.–EASTON, Ch. D.–WANG, H (2017): Highly crosslinked, chlorine tolerant polymer network entwined graphene oxide membrane for water desalination. *Journal of Materials Chemistry A*, 4.
- [5] MEUSER, H. (2012): *Soil remediation and rehabilitation, treatment of contaminated and disturbed land*. Vol. 23, Dordrecht, Springer Science and Business Media.
- [6] NAIR, R. R.–WU, H. A.–JAYARAM, P. N.–GRIGORIEVA, I. V.–GEIM, A. K. (2012): Unimpeded permeation of water through helium-leak-tight graphene-based membranes. *In Science*, 335 (6067), pp. 442–444.

- [7] NOVOSELOV, K. S.–GEIM, A. K.–MOROZOV, S. V. et al. (2004): Electric Field Effect in Atomically Thin Carbon Films. *Science*, 306, pp. 666–669.
- [8] PENDOLINO, F.–ARMATA, N. (2018): *Graphene Oxide in Environmental Remediation Process*. Springer Briefs in Applied Sciences and Technology.
- [9] TAN, P.–SUN, J.–HU, Y.–FANG, Z.–BI, Q.–CHEN, Y.–CHENG, J. (2015): Adsorption of Cu^{2+} , Cd^{2+} and Ni^{2+} from aqueous single metal solutions on graphene oxide membranes. *J Hazard Mater*, 297, pp. 251–260.
- [10] YANG, S. T.–CHEN, S.–CHANG, Y.–CAO, A.–LIU, Y.–WANG, H. (2011): Removal of methylene blue from aqueous solution by graphene oxide. *J. Colloid Interface Sci*, 359 (1), pp. 24–29.
- [11] ZHAO, L.–YANG, S-T.–FENG, S.–MA, Q.–PENG, M.–WU, D. (2017): Preparation and Application of Carboxylated Graphene Oxide Sponge in Dye Removal. *Int. J. Environ. Res. Public Health*, 14, p. 1301.



COMPARISON OF BIOWASTE DERIVED AND ALGAE BIOSORBENTS FOR HEAVY METALS REMOVAL FROM EFFLUENTS

JÓZSEF PAULOVICS¹–KHISHIGSUREN NATSAGDORJ²–LJUDMILLA BOKÁNYI³,

¹KISANALITIKA Kft., 3792 Sajóbáony, Gyártelep, paulovics.jozsef@kisanalitika.hu

²University of Miskolc, 3515 Miskolc, Egyetemváros, mgl.khishgee@gmail.com

³University of Miskolc, 3515 Miskolc, Egyetemváros, ejtblj@uni-miskolc.hu

Abstract

Biosorption is a promising and versatile technique to remove dissolved species of heavy metals from industrial effluents. Different researchers have already accomplished a large number of laboratory investigations on biosorption aimed at the pollution removal from aqueous solutions with different kinds of biomass. The most investigated biosorbents are different micro- and macro algae, as well as various biowastes. The algae show relatively high metal-sequestering capacity, although there are very serious disadvantages of the algae biosorption process. In case of micro algae this is the necessity of effective and economically feasible separation of pregnant biosorbent from the solution, or of the algae immobilization. In case of the latter that is the disadvantageous composition of harvested and processed macro algae. Nevertheless, the economically feasible conversion of the biowaste into biosorbent results in the value-added product, as well as meets the endeavours of circular economy. There are countless research reports on the biosorption process using waste-based sorbents, although the mechanism of their biosorption is not fully revealed yet. The first objective of the present study was to investigate and compare the adsorption behaviour of biowastes (e.g. natural and chemically modified sunflower seed hulls and soybean hulls) and that of algae (e.g. *Lyngbyataylorii* micro algae and *Undariapinnatifida* macro algae) in mono-cationic systems containing lead and cadmium. Another objective was to reveal the mechanism of the Pb- and Cd-cations on biowastes above.

Present paper connects to our previous research. The investigated biowastes have lower metal adsorbing capacity than the algae, but the adsorption capacity of biowastes can be enhanced with base washing (BW) and citric acid (CA) modification according to more authors (ZHU et. al. 2008 and LI et. al. 2011), thus chemical modification of sunflower seed hulls (SFH) and soybean hulls (SBH) were carried out according to the similar method previously described by LI et. al. (2011). Previously we conducted the base washing (BW) and citric acid (CA) modification of SFH and SBH, but we didn't receive the expected improvement of the capacity, thus we conducted again this modification in case of SFH. Our new measurements with modified SFH haven't proved that the capacity of SFH can be increased by the applied base washing (BW) and citric acid (CA) modification. For the explanation of this phenomenon, and to understand the mechanism of metal uptake process BET specific surface, FT-IR analysis and ξ -potential measurements were used.

Keywords: *biosorption, sunflower, soybean, algae, cadmium, lead*

1. INTRODUCTION

Industrial effluents (i.e. effluents from machinery manufacturing, electroplating and battery factories, chemical manufacturing, waste incineration etc.) can be contaminated with different pollutants, among them heavy metals as well. However there are essential heavy metals (e.g. copper, zinc etc.), but most of them are toxic (including lead and cadmium) from minor concentrations and have the tendency to bio-accumulate.

Lead and cadmium are widely used in the industry and its release in water bodies may cause serious ecological and human health consequences. Because of their high risk to the environment and ecosystem, heavy metals should be removed as much as possible (with high efficiency). Conventional methods of heavy metal separation (e.g. chemical precipitation, oxidation/reduction, ion-exchange, electrolysis and membrane filtration) are well known, but each of them has significant disadvantages (e.g. expensive, only effective at higher concentrations, incomplete metal removal, etc.), thus the phenomenon of biosorption could be an appropriate alternative in the near future, because cheap and renewable biosorbents can be found easily, that can be regenerated and biosorption can be efficient at very low concentrations as well.

Biosorption is one of the most promising technologies involved in the removal of toxic metal, which allows reducing metal ion concentrations to environmentally acceptable levels (ZINICOVSCAIA et al. 2017).

Biosorption has been defined as the property of certain biomolecules to bind and concentrate selected ions or molecules from aqueous solution. As opposed to a much more complex phenomenon of bioaccumulation based on active metabolic transport, biosorption by dead biomass is passive and based mainly on the affinity between the biosorbent and sorbate (VOLESKY 2007).

Although there are countless research reports on the topic of biosorption process, the majority of them are still at laboratory scale. Nevertheless, finding the appropriate, cheap and effective industrial biosorbents is also an encouraging challenge.

Many kinds of biological materials have an affinity for binding inorganic and organic pollutants, so that there is an enormous biosorption potential within the countless types of biomaterials (DHANKHAR and HOODA 2011; GADD, 2009).

The most investigated biosorbents are different micro and macro algae, as well as various biowastes. As our previous investigations and research showed the algae (e.g. *Lyngbyataylorii* micro algae and *Undariapinnatifida* macro algae) show relatively high metal-sequestering capacity (PAULOVICS et al. 2008; BOKÁNYI and SAJBEN 2005), although there are very serious disadvantages of the algae biosorption process. In case of micro algae this is the necessity of effective and economically feasible separation of loaded biosorbent from the solution, or of the algae immobilization. In case of the latter that is the disadvantageous composition of harvested and processed macro algae. Nevertheless, the economically feasible conversion of the biowaste into biosorbent results in the value-added product, as well as meets the endeavours of circular economy.

There are countless research reports on the biosorption process using waste-based sorbents, although the mechanism of their biosorption is not fully revealed yet.

The first objective of the research presented was to investigate and compare the adsorption behaviour of biowastes (e.g. natural and chemically modified sunflower seed hulls and soybean hulls) and that of algae (e.g. *Lyngbyataylorii* micro algae and *Undariapinnatifida* macro algae) in mono-cationic systems containing lead and cadmium cations.

Present paper connects to our previous research. The investigated biowastes have lower metal adsorbing capacity than the algae, but the adsorption capacity of biowastes can be enhanced with base washing (BW) and citric acid (CA) modification according to more authors (ZHU et al. 2008 and LI et al. 2011), thus chemical modification of sunflower seed hulls (SFH) and soybean hulls (SBH) were carried out according to the similar method previously described by LI et al. (2011). Previously we conducted the base washing (BW) and citric acid (CA) modification of SFH and SBH, but we didn't receive the expected improvement of the capacity, thus we conducted again this modification in case of SFH. Our new measurements with modified SFH haven't proved that the capacity of SFH can be increased by the applied base washing (BW) and citric acid (CA) modification. For the explanation of this phenomenon, and to understand the mechanism of metal uptake process BET specific surface, FT-IR analysis and ξ -potential measurements were used.

2. MATERIALS AND METHODS/AREA DESCRIPTION

Biowastes as biosorbents

Biosorbent materials presented in this paper (i.e. sunflower seed hulls [SFH] and soybean hulls [SBH]) were originated from a vegetable oil production company located in North-Hungary.

Preparation of natural biosorbents

The sunflower seed hulls and soybean hulls were ground in Retsch SM 2000 cutting mill equipped with a 2 mm screen and afterwards sieved. Fractions between 200 and 315 μm were selected for our further experiments, and were repeatedly washed three times in deionized water (50 g of biomass with 3 times 200 mL of deionized water) in order to remove surface contaminations. The hulls were then dried at 80 °C for 24 h and cooled in a desiccator.

Modified (BW and CA) biosorbents

Adsorption capacity of different biowastes can be enhanced with base washing (BW) and citric acid (CA) modification according to ZHU et al. (2008), thus chemical modification of sunflower seed hulls and soybean hulls were carried out according to the similar method previously described by LI et al. (2011) (see *Figure 1*).

Solution preparation

Lead(II) solutions were prepared by dissolving solid lead(II) nitrate (VWR Chemicals company) in deionized water. Cadmium(II) solutions were prepared by dissolving solid cadmium nitrate tetrahydrate (SIGMA-ALDRICH) in deionized water. The initial pH values of the working solutions (before and after the biosorption) were adjusted between 5.0 and 5.2. Diluted 0.1 M NaOH or 0.1 M HCl were used for pH adjustment.

Biosorption experiments

Biosorption of cadmium and lead on the surface of SF, SB, modified SF (M-SF) and modified SB (M-SB) were investigated in mono-cationic systems. Batch equilibrium sorption experiments were performed in 250 mL Erlenmeyer flasks. The initial Pb^{2+} or Cd^{2+} concentration were 20; 50; 80; 100; 200; 300; 400; 600; 800; 1000; and 1500 mg/L. The concentration of biomass was 1 g/L

(100 mg biomass in 100 mL solution). The suspension was shaken at 150 rpm for 18 h at the temperature of 25°C by using adjustable incubator shaker WiseCube WIS-20.

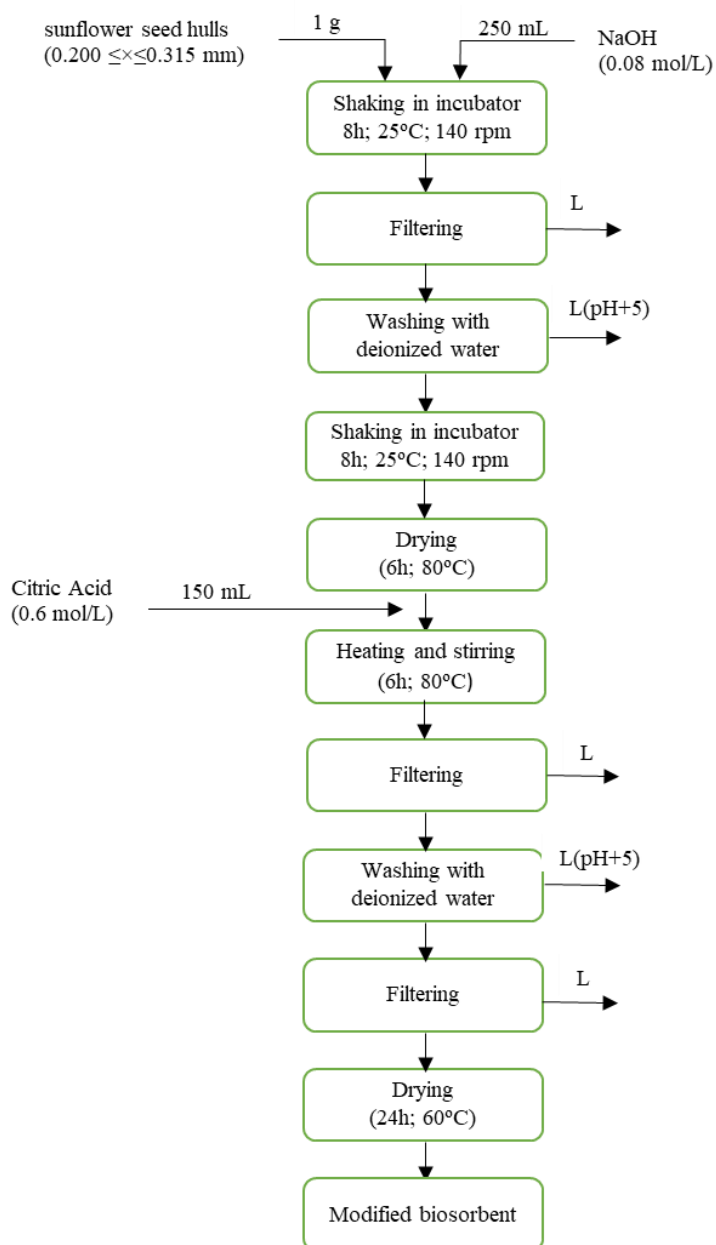


Figure 1
Combined (base washed (BW) and citric acid (CA)) modification of biowastes

Determination of sorption isotherm

Suspended solid particles were removed after the biosorption experiments by using filter paper (grade: 1,289; diameter: 150 mm; 84 g/m²). After the filtration some drops of HNO₃ were added to the separated liquid samples. Prior to the testing in ICP-OES or AAS, all the samples were refrigerated at approximately 4 °C.

The concentrations of the metals in liquid phase were subsequently determined by using inductively coupled plasma optical emission spectrometer (ICP-OES), type: SPECTRO CIROSVISION at KISANALITIKA Laboratory Services Ltd. in case of biosorption on natural biomass and modified SFH, and by using atomic absorption spectrometer (AAS) at Institute of Chemistry, University of Miskolc in case of the modified biomass.

The measured metal concentrations were used to calculate the adsorption capacity (q_{eq} [mmol g⁻¹]) of the biosorbent applying the following mass balance equation:

$$q_{eq} = (C_0 - C_{eq}) * V / m \quad (1)$$

where C_0 , C_{eq} , V and m are initial metal concentration (mmol/L), metal concentration at equilibrium (mmol/L), the volume (L) of the solution and weight (g) of adsorbent, respectively.

3. RESULTS AND DISCUSSION

Figure 2 shows the sorption capacity of the investigated algae (e.g. *Undaria pinnatifida* macro algae and *Lyngbya taylorii* micro algae). In the Figure 3 sorption capacity of investigated biowastes (i.e. natural and chemically modified sunflower seed hulls and soybean hulls) can be seen regarding the Pb²⁺ and Cd²⁺.

These algae show relatively high metal-sequestering capacity, although there are very serious disadvantages of the algae biosorption process. In case of micro algae this is the necessity of effective and economically feasible separation of loaded biosorbent from the solution, or of the algae immobilization. In case of the latter that is the disadvantageous composition of harvested and processed macro algae.

Figure 3 proves that the applied biowastes (sunflower seed hulls and soybean hulls) are able to reduce the Pb²⁺ and Cd²⁺ concentrations in model solutions, but these uptake capacities are not outstanding among other biosorbents.

Nevertheless, it can be worth studying their applicability as a biosorbents. Other authors (e.g. ZHU et. al. 2008) also reported that agricultural by-products are high volume, low value and underutilized lignocellulosic biomaterials, and contain high levels of cellulose, hemicellulose and lignin.

Adsorption capacity of crude agricultural by-products is low in general, but chemical modification has shown great promise in improving the adsorption and the cation exchange capacity of agricultural by-products. Citric acid (CA) is a low cost material used extensively in the food industry ZHU et. al. (2008).

Because of the above mentioned reasons we have also conducted the combined (BW and CA) modification of SFH and SBH according to LI et al. (2011). Our measurements didn't prove the increased capacity of SFH and SBH with this modification, and we experienced uncertainty when

the c_{eq} was greater than 3 mmol/L, thus we repeated the modification experiment with SFH (see Figure 4).

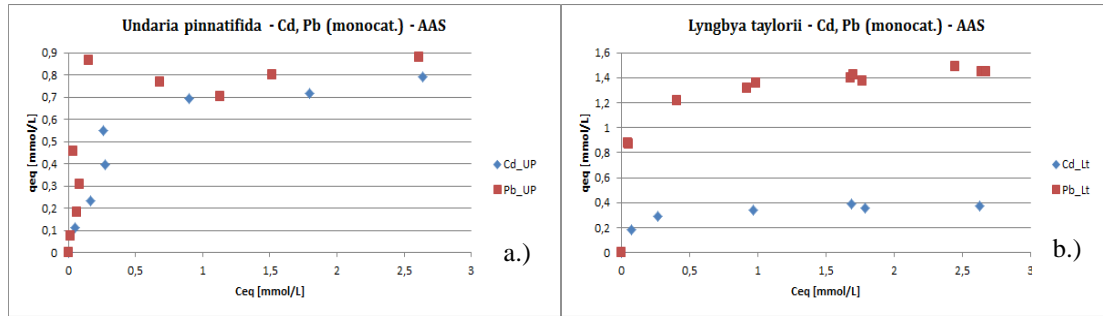


Figure 2a

Sorption capacity of *Undariapinnatifida* (PAULOVICS et. al. 2008);
(b) Sorption capacity of *Lyngbyataylorii* (BOKÁNYI and SAJBEN 2005)

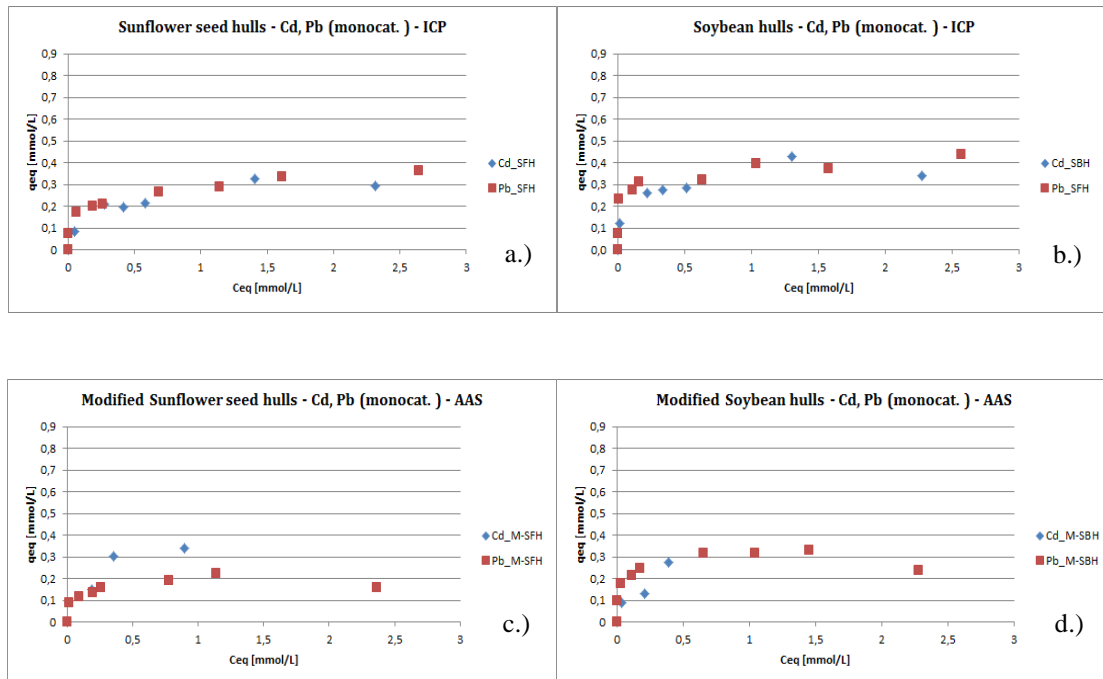


Figure 3a

Sorption capacity of sunflower seed hulls; (b) Sorption capacity of soybean hulls; (c) Sorption capacity of modified sunflower seed hulls; (d) Sorption capacity of modified soybean hulls

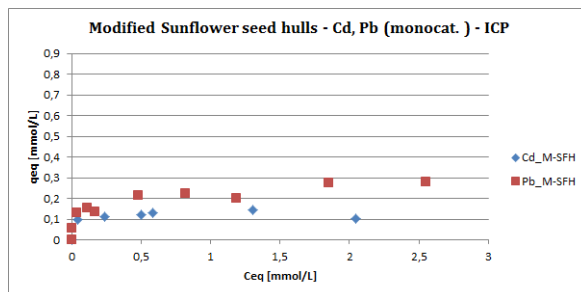


Figure4
Sorption capacity of modified sunflower seed hulls

From our previous (Figure 3 c and d) and repeated (Figure 4) investigation we can conclude that Pb^{2+} and Cd^{2+} sorption capacity of the investigated biowastes could not be increased by the applied modification, because natural biosorbents show higher capacities than the modified ones. For the explanation of this phenomenon, and to understand the mechanism of metal uptake process BET specific surface, FT-IR analysis and ξ -potential measurements were used.

According to ZINICOVSCAIA et al. (2017) the biosorption process includes physicochemical interactions between metal ions and several anionic ligands present on the biomass like carboxyl, phosphoryl, carbonyl and sulfhydryl. The efficiency of metal biosorption is strongly dependent on experiment parameters such as: pH, temperature, and the concentration of sorbate and sorbent. The pH value plays an important role in biosorption process, because it influences the speciation of metal in the aqueous solution, the ionization of surface functional groups, and the binding sites on the surface of the biomass (ZINICOVSCAIA et al. 2017; AMINI et al. 2013).

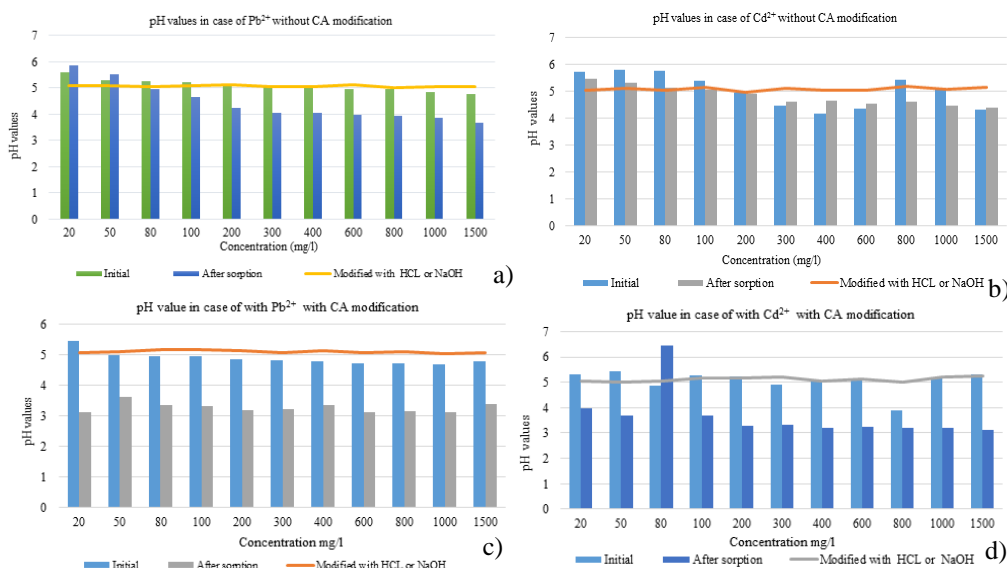


Figure 5
pH value measurements before (a. and b.) and after biosorption (c. and d.)

Effect of pH was studied in the range 1...7. The initial pH values, in case of untreated Pb^{2+} and Cd^{2+} solution, were above 5 pH value and values after adsorption were slightly decreased under pH 5 (see *Figure 5a* and *b*). After adsorption with combined modification, pH values significantly dropped under 3.5 for almost all solutions in case of Pb^{2+} and values decreased between 3.96 and 3.14 pH in case of Cd^{2+} (see *Figure 5c* and *d*).

One of the possible explanations for lower capacities in case of combined modification can be the significant decrease of pH value after biosorption, since the initial pH decreased from 5 to about 3.

This significant drop of pH values after biosorption can indicate that the citric acid hasn't modified the surface of the biowastes, but it has been adsorbed to the surface as a citrate salt, releasing the H^+ ions. Nevertheless the adsorbed citrate did not increase the adsorption capacity. The pH drop in turn led to the increase in the cations mobility and lower adsorption.

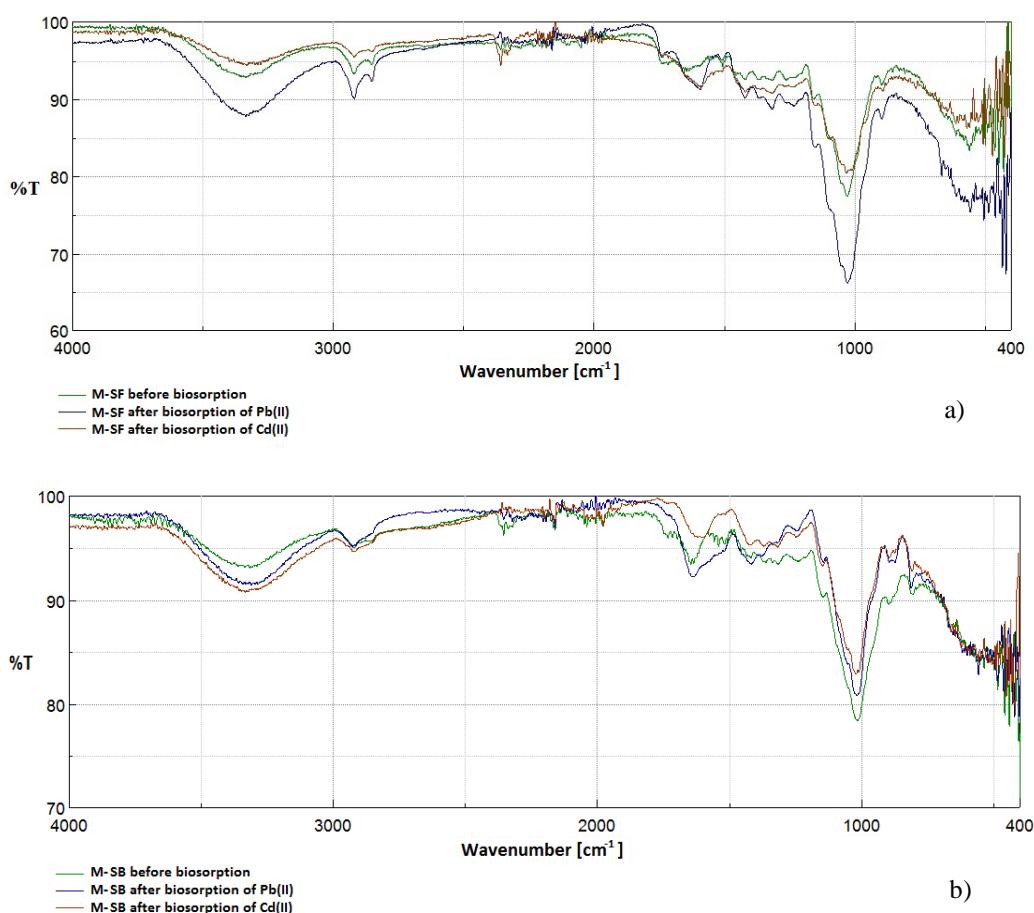


Figure 6
(a) FTIR spectra of modified SFH; (b) FTIR spectra of modified SBH

Functional groups responsible for metal binding were determined by Fourier transform infrared spectroscopy (see *Figure 6*). Both modified SFH and modified SBH have peaks at similar wavenumbers and when the biomasses were loaded with Pb^{2+} and Cd^{2+} , the FT-IR spectrum showed the adsorption of cations leads to the intensity and wave number shifting. The highest deviation from the unloaded biomasses curve appears at around 1030 cm^{-1} , which corresponds to $-C-O$ alcohols and carboxylic acids. The broad peak observed at 3444 cm^{-1} corresponds to the $O-H$ stretching vibrations of cellulose, pectin, absorbed water, hemicellulose and lignin. These infrared measurements also revealed the presence of such functional groups as amide groups (1651 cm^{-1}), $-C=O$ from carboxyl or ester groups (1739 cm^{-1}). Peaks appeared at similar wavenumbers in case of natural SFH and SBH, thus the applied modification did not considerably influence the appearing of newer functional groups responsible for binding (PAULOVICS and BOKÁNYI 2017).

4. CONCLUSIONS

Investigated biosorbents (i.e. natural sunflower seed hulls and soybean hulls as biowastes, *Lyngbyataylorii* micro algae and *Undariapinnatifida* macro algae) were able to reduce the Pb^{2+} and Cd^{2+} concentrations in model solutions. Uptake capacities of these biowastes are not outstanding among other biosorbents, but their application has several advantages (e.g. inexpensive, great abundance, macroscopic etc.), thus their further investigation is extremely justified.

According to ZHU et al. (2008) chemical modification has shown great promise in improving the adsorption and the cation exchange capacity of agricultural by-products, thus we tried to reproduce the experiments of LI et al. (2011) on SBH. We also applied this BW and CA modification on SFH, and conducted this experiment twice. None of our applied modifications provided the expected improved sorption capacities regarding Pb^{2+} and Cd^{2+} .

According to our measurements natural sunflower seed hulls and soybean hulls have higher adsorption capacity towards dissolved-cadmium and lead ions than chemically modified SFH and SBH.

One of the possible explanations for lower capacities in case of combined modification can be the significant decrease of pH value after biosorption, since the initial pH decreased from 5 to about 3. This significant drop of pH values after biosorption can indicate, that the citric acid did not modify the surface of the biowastes likely by adsorption of citrate and release of H^+ . Nevertheless the adsorbed citrate did not increase the adsorption capacity. The pH drop in turn led to the increase in the cations mobility and lower adsorption.

The main adsorption mechanism of Pb^{2+} and Cd^{2+} on sunflower seed hulls has electrostatic character, while the biosorption on soybean hulls took place by a specific sorption according to our zeta-potential measurements. These phenomena did not change after the chemical modification of biosorbents (PAULOVICS and BOKÁNYI 2017).

FT-IR spectra showed that sunflower seed hulls (SFH), soybean hulls (SBH), modified SFH and modified SBH have similar functional groups on their surface, like $-C-O$ alcohols and carboxylic acids, $O-H$ groups, amide groups and $-C=O$ carboxyl or ester groups, the adsorption of cations leads to intensity and wave number shifting.

ACKNOWLEDGEMENTS

This research was supported by the cooperation between the Institute of Raw Material Preparation and Environmental Processing, University of Miskolc and the KISANALITIKA Ltd., Hungary. The described work/article was carried out as part of the “Sustainable Raw Material Management Thematic Network – RING 2017”, EFOP-3.6.2-16-2017-00010 and FIKP Project in the framework of the Széchenyi2020 Program. The realization of this project is supported by the European Union, co-financed by the European Social Fund.

REFERENCES

- [1] AMINI, M. et al. (2013): Biosorption of U(VI) from aqueous solution by *Chlorella vulgaris*: equilibrium, kinetic, and thermodynamic studies. *J. Environ. Eng.*, 139, pp. 410–421.
- [2] BOKÁNYI, L.–SAJBEN, A. (2005): *Description of biosorption by isotherms. microCAD 2005 International Scientific Conference*. 10–11 March 2005, University of Miskolc, pp. 7–12.
- [3] DHANKHAR, R.–HOODA, A. (2011): Fungal biosorption – an alternative to meet the challenges of heavy metal pollution in aqueous solutions. *Environ. Technol.*, 32, 467–491.
- [4] GADD, G. M. (2009): Biosorption: critical review of scientific rationale, environmental importance and significance for pollution treatment. *J. Chem. Technol. Biotechnol.*, 84, 13–28.
- [5] LI, J. (2011): Biosorption of Pb²⁺ with Modified Soybean Hulls as Absorbent. *Chinese Journal of Chemical Engineering*, 19 (2), 334–339.
- [6] PAULOVICS, J. et al. (2008): Kontrolluntersuchungen der Biosorption an der freien Makroalge *Undaria pinnatifida*. M.Sc. thesis, University of Miskolc.
- [7] PAULOVICS, J.–BOKÁNYI, L. (2017): Biosorbent from Biowastes for Heavy Metals Removal from Industrial Effluents. *Acta Mechanica Slovaca*, 21 (3), 6–11.
- [8] VOLESKY, B. (2007): Biosorption and me. *Water Research*, 41, 4017–4029.
- [9] ZINICOVSCAIA, I. et al. (2017): Biosorption of lead ions by cyanobacteria *Spirulina platensis*: kinetics, equilibrium and thermodynamic study. *Nova BiotechnolChim*, 16 (2), 105–112; DOI: 10.1515/nbec-2017-0015
- [10] ZHU, B. et al. (2008): Adsorption of copper ions from aqueous solution by citric acid modified soybean straw. *Journal of Hazardous Materials*, 153, 300–308.



MAGNETICALLY RESPONSIVE BIOMATERIALS AND THEIR APPLICATIONS

IVO SAFARIK^{1,2}–JITKA PROCHAZKOVA¹–SINDY MULLEROVA¹–
EVA BALDIKOVA¹–KRISTYNA POSPISKOVA²

¹Department of Nanobiotechnology, Biology Centre, ISB, CAS, Na Sadkach 7, 370 05 Ceske Budejovice, Czech Republic; email: ivosaf@yahoo.com

²Regional Centre of Advanced Technologies and Materials, Palacky University, Slechtitelu 27, 783 71 Olomouc, Czech Republic; email: kristyna.pospiskova@seznam.cz

Abstract

Food, agriculture and wood industries are responsible for the production of huge amounts of biological waste materials. In many cases, these materials can be used as efficient biosorbents or low-cost carriers. In order to improve their properties, conversion into their magnetic derivatives can be very useful.

Diamagnetic biological materials (e.g. prokaryotic and eukaryotic microbial cells, lignocellulose materials, soluble and insoluble biopolymers etc.) can be magnetically modified in order to obtain smart biomaterials exhibiting an appropriate response to external magnetic field. Magnetic modification of originally diamagnetic biological materials is usually based on the attachment of magnetic iron oxides nano- and microparticles on the surface or within the pores of the treated material. Magnetic modification can be performed using different procedures, e.g. by magnetic fluid treatment, mechanochemical synthesis and by direct or indirect microwave assisted synthesis. The most general magnetization procedure employs magnetic iron oxides nano- and microparticles prepared by microwave assisted synthesis from ferrous sulfate. Magnetically responsive biomaterials have been efficiently used as adsorbents of both organic and inorganic xenobiotics, affinity adsorbents for isolation of target biomolecules, carriers of various affinity ligands, biologically active compounds and cells or whole-cell biocatalysts. The potential of magnetically responsive biomaterials will increase in the near future.

Keywords: *Biological waste, magnetic modification, magnetic adsorbents*



EFFECT OF SYNTHESIS CONDITIONS ON THE FORMATION OF SPHERICAL SILICA PARTICLES WITH AMINO GROUPS AND THEIR INVESTIGATION IN SORPTION AND AS ANTIBACTERIAL AGENTS

INNA MELNYK^{1,2}–VERONIKA TOMINA²–NATALIYA STOLIARCHUK²–
ANASTASIYA LEBED³–IRYNA FURTAT³–MARIA KANUCHOVA⁴–
MIROSLAVA VACLAVIKOVA¹

¹Institute of Geotechnics of SAS, Watsonova 45, 04001Kosice, Slovak Republic,
melnyk@saske.sk, vaclavik@saske.sk

²Chuiko Institute of Surface Chemistry of NAS of Ukraine, Generala Naumova 17, 03164 Kyiv, Ukraine,
stonata@ukr.net, v.v.tomina@gmail.com

³National University of Kyiv-Mohyla Academy, Skovoroda 2, 04070 Kyiv, Ukraine,
furtat.im@gmail.com, anastasia.lebed3@gmail.com

⁴Technical University of Kosice, Letna 9, 04200 Kosice, Slovak Republic,
maria.kanuchova@tuke.sk

Abstract

Spherical silica particles with amino groups are simple and unique, as well as convenient materials for application in catalysis, nanomedicine, separation processes, adsorption, or energy-storage technology. Usually, the procedure of producing aminosilica particles includes two stages: (1) production of pure silica particles and (2) their post-synthetic grafting using aminopropyltriethoxysilane (APTES). In our research we considered one-pot synthesis technique of obtaining aminosilica nanoparticles with different sizes, content of amino groups, specific surface areas, and combinations of hydrophobic and amino groups on the surfaces. Particles' morphology and composition of the surface layers were analyzed using SEM, IR spectroscopy, XPS, elemental analysis, z-potential measurements, and adsorption methods. Depending on the structure-forming (tetraethoxysilane or bridged silanes) and functionalizing agents (silanes with amino, methyl, and phenyl groups), the surfaces of such particles contain silanol, hydrophobic, and amino groups. Therefore, different types of interactions are possible during the adsorption processes on the surfaces of such materials. Such material could adsorb up to 3.2 mmol/g of copper(II) ions from aqueous solutions, as well as organic dyes, such as Acid red 88 (262 mg/g) and Methylene blue (146 mg/g). It was shown that 1% (v/v) water suspension of Cu(II)-containing silica nanoparticles demonstrated up to 98.7% of antibacterial activity against *S. aureus* in 120 min, 99.9% - *E.coli*, 99.9% - *P. aeruginosa*, 84.5% - *C. albicans*. In conclusion, the proposed approaches provide control over the properties of the final materials necessary to create sorptive nanomaterials.

The research is financed from the SASPRO Programme No. 1298/03/01.

Keywords: aminosilicamicroparticles, porosity, adsorbents, copper(II) ions, organic dyes, antibacterial agents



INFLUENCE OF VARIOUS MECHANICAL PREPARATION METHODS OF LCD ON THE LEACHABILITY OF CRITICAL ELEMENTS

SÁNDOR NAGY¹–LJUDMILLA BOKÁNYI²–VALÉRIA ÜVEGES³–
MÁRIA AMBRUS⁴–STOYAN GAYDARDZHIEV⁵, GÁBOR MUCSI⁶

¹University of Miskolc, 3515 Miskolc Egyetemváros, Hungary, ejtnagys@uni-miskolc.hu

²University of Miskolc, 3515 Miskolc Egyetemváros, Hungary, ejtblj@uni-miskolc.hu

³University of Miskolc, 3515 Miskolc Egyetemváros, Hungary, ontam@uni-miskolc.hu

⁴University of Miskolc, 3515 Miskolc Egyetemváros, Hungary, ejtmuva@uni-miskolc.hu

⁵University of Liege, Place du 20 Août 7, 4000 Liège, Belgium, s.gaydardzhiev@ulg.ac.be

⁶University of Miskolc, 3515 Miskolc Egyetemváros, Hungary, ejtmucsi@uni-miskolc.hu

Abstract

As various electrical and electronic equipment pieces are frequently replaced due to technological development or changes, the recycling of the generating in huge amount e-wastes is of outstanding importance. The research in this field is inevitable in the spotlight of creating the circular economy. The recycling strategy is generally aiming at the recovery of materials like plastics and metals, as well as of valuable, even critical elements and compounds along with the satisfactory treatment of toxic ones. For this sake the mechanical treatment is combined with the chemical/bio/thermal techniques.

Due to the numerous elements used for their manufacturing, LCD (Liquid Crystal Displays) display panels provide a wide range of valuable and critical, but also toxic elements. Thus, instead of disposal of waste LCD panels, the recovery of such elements can not only prevent possible environmental hazards but endorse the utilisation of secondary raw materials.

It was proved that the mechanical pre-treatment is an important step, first of all, to recycle materials like plastics and common metals. Furthermore, the chemical mass transfer is governed by the concentration gradient, the area exposed and the retention time. Nevertheless, the presence of the “alien” components in the mass transfer can dramatically decrease the concentration gradient, the contact surface, as well as the diffusion rate. And finally, the lower the material flow to be submitted for the chemical processing, the lower the specific reagents requirement and, therefore the costs of the process (BOKÁNYI 2014).

Thus, the mechanical removal of LCD polarizing film seems to be highly advisable; however is not easy, needs 200–250 °C high temperature as well. At the same time, the ITO (Indium-Tin-Oxide) surface layer at favourable conditions can be exposed for the diffusion even without removing polarizing foil.

Therefore, one experimental series of our current research was focused on the comparison of acidic leaching of the stripped and ground LCD panel with and without the polarizing film. Another experimental series was devoted to the effect of fineness on the leachability of indium, tin and other elements. Thereafter, ground LCD was produced with different fineness in Retsch ZM 200 centrifugal mill. Based on the data obtained, important conclusions were drawn.

Keywords: LCD panel, critical elements recycling, mechanical preparation, acidic leaching

1. INTRODUCTION

Nowadays, e-waste is one of the fastest growing waste streams. It was estimated that ~44.7 million tonnes of e-waste were generated in 2016 and, with an annual growth rate of 3–4%, is expected to reach ~52.2 million tonnes in 2021 (BALDÉ et al. 2017). E-wastes are a potential resource for various valuable materials and critical metals such as indium, rare earth elements, precious metals, lithium and cobalt, as these are widely consumed in the production of electric and electronic equipment (ZHANG et al. 2017). Liquid crystal displays (LCDs) are widely used in TVs, laptops, desktops and any other device with a screen. Thus, with the emergence and replacement of a great amount of LCD electronic devices, the recovery of certain elements, i.e. indium or tin, from the waste LCDs is a relevant research topic.

Numerous studies have been reported on the research of indium production from waste ITO targets (HSIEH et al. 2009; LI et al. 2011), but only a few deals with the indium recovery from waste LCD displays. That is why it is become a very important task nowadays. In case of this latter, the first and very important part of the process is the pre-treatment method, which involves the separation of the polarizing film, as well as the liquid crystal from the surface of the glass substrate. LI J. et al. studied the separation of the polarizing film by thermal shock, and ultrasonic cleaning was used for the removal of liquid crystal. For the dissolution of indium a mixture of hydrochloric and nitric acids was applied at 60 °C for 30 min (LI et al. 2009). After the thermal treatment and ultrasonic washing the effect of a high energy ball grinding was studied by Lee et al. The leaching process was carried out with The ground product was then leached with a mixed acid solution ($\text{H}_2\text{O}:\text{HCl}:\text{HNO}_3 = 50:45:5$) solution for 30 min. It was concluded that higher recovery of indium was achieved at room temperature after using high energy ball mill, than by using a conventional shredding machine (LEE et al. 2013). Based on the experimental results of Yang et al. 1M HCl and 1M H_2SO_4 solution was also proved to be suitable for the dissolution of indium (YANG et al. 2013). The selective recovery of indium from the acidic solution is also a key factor for an effective and economical technology. Precipitation is one of the possible ways, but cementation of indium on Al or Zn particles was also investigated (MURATANI et al. 2010), as well as the solvent extraction (VIROLAINEN et al. 2011; RUAN et al. 2012) is also used widely for the selective separation of indium in the experimental studies.

The effect of different pre-treatments has been examined for the separation and recovery of glass, plastic and various metals, mainly indium. Among thermal treatments, the pyrolysis was mainly used to remove organic materials, the recovery rate of indium in leaching was examined (FERELLA et al. 2017; WANG and XU 2016; ZHANG et al. 2015).

During the experiments of HASEGAWA et al. (2013), ITO-glass was crushed into approximately 30 mm × 50 mm pieces, then the size of particles was reduced by milling in a ceramic pot mill combined with alumina balls of different sizes. When milling was performed for 6 h at 150 rpm, the fine particles facilitated the rate of indium extraction with amino-polycarboxylate chelats. SILVEIRA et al. (2015) investigated the effect of the particle size of the panels on the dissolution efficiency of indium. For their experiments, a knife mill, hammer mill, and porcelain ball mill were used before acid leaching with H_2SO_4 . During leaching, the concentration, solid/liquid ratio, temperature and leaching time were also examined. It was concluded that one of the most important parameters affecting the dissolution efficiency is the size of the particles to be leached.

Thus, it can be concluded that mechanical pre-treatment is an important step in the processing of waste LCD panels.

For the experiments described in the article, an experimental series focused on the comparison of acidic leaching of the stripped and ground LCD panel with and without the polarizing film. Another experimental series was devoted to examining the effect of fineness on the leachability of indium, tin and other elements.

2. MATERIALS AND METHODS

A mixture of 12 LCD displays from various types and brands of dismantled televisions was used for each experiment. The structure and design of a standard LCD panel can be observed in Figure 1. An LCD panel consists of several layers in a sandwich structure: on the outside, polarising foils are adhered to 0.4–1.1 mm thick glass substrates, latter account for 40–50 wt.% of the panel. The inside of the panel, the liquid crystals and the conductive indium tin oxide (ITO) layer are enclosed in a colour filter (CF) and thin film transistor (TFT) layer which are approximately 140–150 nm thick. ITO is a mixture of indium(III) oxide (In_2O_3) and tin(IV) oxide (SnO_2), with 80–90 wt.% of In_2O_3 , and 10–20 wt.% of SnO_2 (FAITLI and MAGYAR 2014; UEBERSCHAAR et al. 2017; WANG et al. 2017).

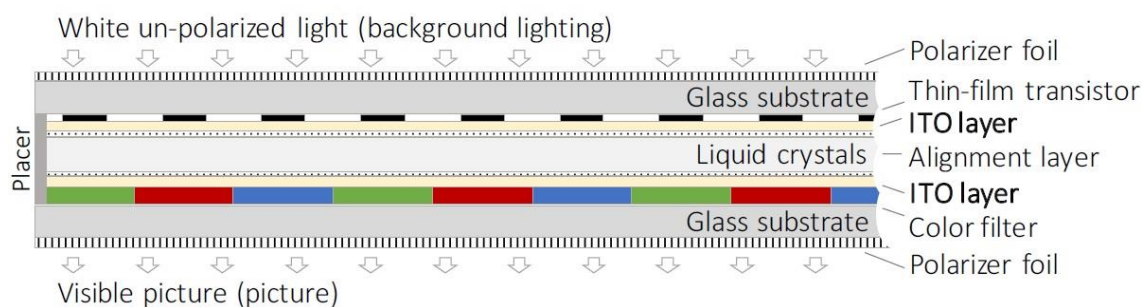


Figure 1
The structure of an LCD panel
(UEBERSCHAAR et al. 2017)

To compare the effect of the polarising foil on the properties of the ground panels and on the efficiency of acidic leaching, the experiments were carried out using LCD panels with (hereinafter LCD F) and without the polarising foil on (hereinafter LCD NF). Figure 2 summarises the processing flow sheets of both experiments.

When the foil wasn't removed (Figure 2.a), the stripped displays were first crushed using a hammer mill under 8 mm particle size, then ultrasonic washing at 40 Hz was carried out with a solution of surfactant at 40 °C for 30 minutes. The feed with particle size between 3.15–6.3 mm was further comminuted with Retsch SM 2000 cutting mill under 4 mm. Finally, before acidic leaching, the particle size was reduced below 1 and 0.5 mm with Retsch ZM 200 centrifugal mill at 14,000 rpm.

For the experiments with LCDs without foil (Figure 2b), the film removal and the ultrasonic washing of the LCD panels were carried out in accordance with the literature (LI et al. 2009;

MiŠKUFOVÁ et al. 2018). First, the panels underwent an ~ 230 °C thermal shock treatment for 2–3 minutes to remove the polarising film. Next, after ultrasonic washing (40 °C, 40 Hz, 30 minutes) with a solution of surfactant to remove liquid crystals, the ITO glass was crushed in a hammer mill under 8 mm. Finally, the particle size of product of the hammer milling was further reduced under 1 mm and 0.5 mm with Retsch ZM 200 centrifugal mill at 14,000 rpm.

The acid leaching of all samples was carried out with a 1:1 (g/mL) dilution ratio with 1 M HCl in Erlenmeyer flasks, using 150 min^{-1} intensive stirring in a shaking apparatus at 55 °C for 1 h using the elaborated earlier procedure (BOKÁNYI et al. 2014_1).

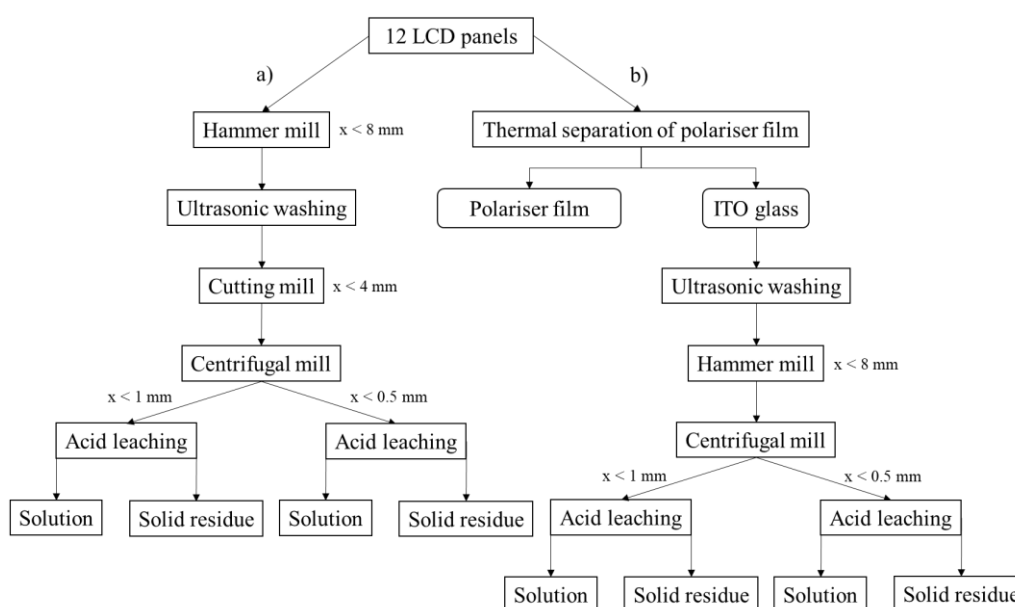


Figure 2

The processing flowsheet of LCD panels a) with and b) without polarising film

The particle size distributions were determined by sieve analysis (after hammer and cutting mill) and using a CAMSIZER X2 particle size and shape analyser (after centrifugal mill). The microscopic image was taken using a Zeiss Axioskop 2 MAT optical microscope.

The chemical analysis of the base materials and the acidic leachate solutions was carried out at the Institute of Chemistry, University of Miskolc, using ICP-OES analysis.

3. RESULTS AND DISCUSSION

3.1. Film separation

Both the CF and TFT layers of the various LCD panels (Figure 3) were used for the experiments. After the thermal treatment, most of the film could be removed from the glass and the pieces from which the film couldn't be separated were discarded. The mass balance of the panels after the foil removal with thermal shock treatment is summarised in Table 1.

Table 1
The mass balance after foil removal

Feed, wt. %	Glass, wt. %		Polarising film, wt. %		Discard, wt. %
	CF	TFT	CF	TFT	
100	43.36	42.03	6.21	5.68	2.62

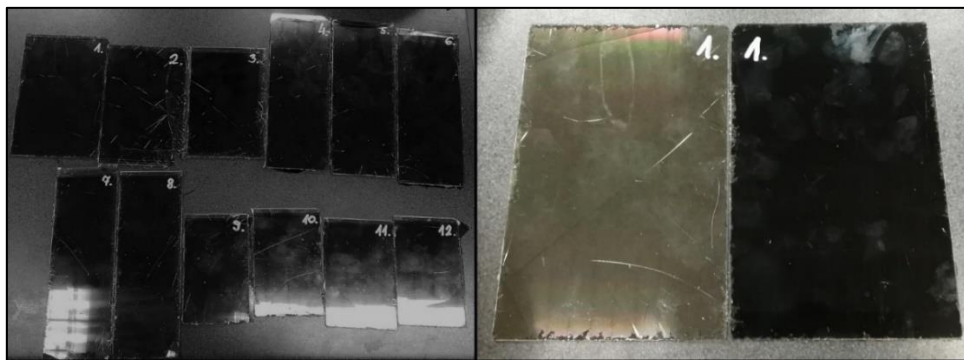


Figure 3
The 12 LCD displays (left) and the TFT and CF layers of the panels (right)

3.2. Comminution

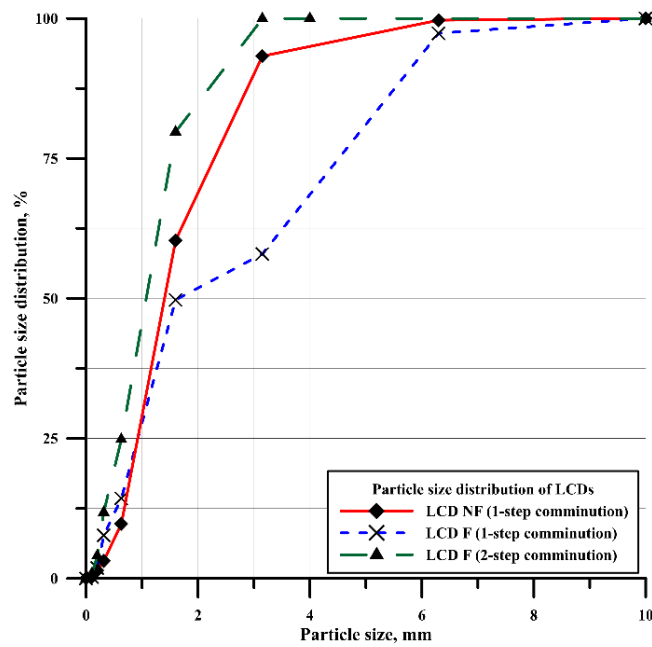


Figure 4
The particle size distributions of the LCDs after hammer and cutting milling

After film removal, the panels were crushed in a hammer mill with 8 mm sieve. Due to the different mechanical properties of the glass and the polarising film – the glass is brittle while the polarising film is flexible –, the particle size distribution of the hammer milled products were rather dissimilar. In case of the LCD F, over 40% of the particles were over 3.15 mm sized. On the other hand, the hammer milling of the LCD NF resulted in much finer particle size product, with only 6.7% of the particles over 3.15 mm and more than 80% between 0.63–3.15 mm.

To prepare an appropriate feed for the subsequent centrifugal milling, the LCD F panels were subjected to two-step comminution: the 3.15–6.3 mm LCD F particles were further ground using Retsch cutting mill under 4 mm. The acquired particle size distributions are illustrated in *Figure 4*.

Furthermore, some residual polarising film could be observed on certain >6.3 mm LCD NF particles; this was again confirmed by the optical microscopic analysis (*Figure 5*). Thus, the preliminary crushing of the LCD NF panels is not only applicable for the size reduction, but also for the separation of larger particles with some polarising film still adhered to the glass.



Figure 5

The >6.3 mm LCD NF particles (top), and the remaining foil (white) on the CF layer (bottom)

The size reduction of the samples under 1 and 0.5 mm was carried out using Retsch ZM 200 centrifugal mill: the <1 mm samples went through a 1-step comminution, while the <0.5 mm samples were first ground to under 1 mm and then under the desired particle size. The products of the milling processes can be observed in *Figure 6*.



Figure 6
The products of the centrifugal milling

As it can be seen in *Figure 6*, the colour of the finer particle sized products was considerably darker than the <1 mm sized samples. After centrifugal milling, the particle size distribution of the samples was examined as well (*Figure 7*).

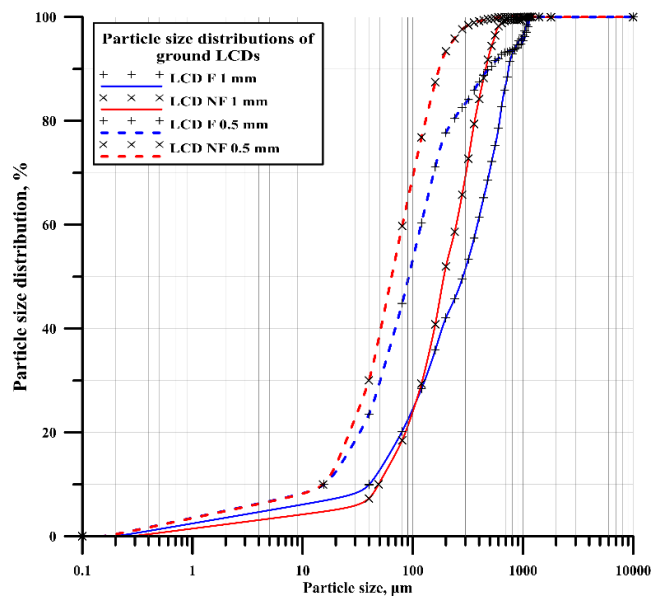


Figure 7
The particle size distributions of the LCDs ground in centrifugal mill

The examination of the particle size distributions revealed that the x_{10} values of the same-sized samples were almost identical, $x_{10} = 40.25 \mu\text{m}$ and $x_{10} = 48.86 \mu\text{m}$ for the $<1 \text{ mm}$ F and NF LCDs, and $x_{10} = 15.66 \mu\text{m}$ and $x_{10} = 15.30 \mu\text{m}$ for the $<0.5 \text{ mm}$ F and NF LCDs. However, the different trends of the particle size distributions get prominent as the particle size is increased. The median particle sizes of the LCDs without the polariser film are lower in both the $<1 \text{ mm}$ and $<0.5 \text{ mm}$ particle size ranges ($x_{50} = 192.09 \mu\text{m}$ and $x_{50} = 64.93 \mu\text{m}$, respectively), then the LCDs with the film on ($x_{50} = 284.76 \mu\text{m}$ and $x_{50} = 91.22 \mu\text{m}$, respectively). Moreover, the two LCD NF curves indicate that the yield of coarse particles is similar in both samples. Thus, it can be stated that due to the film is still attached to the glass, the LCD NF samples have finer particle size distributions than the LCD F samples.

3.3. Chemical processing

After acid leaching with 1 M HCl solution, the acquired leachate solutions of the $<0.5 \text{ mm}$ samples showed a strong green discolouration in case of both the LCD F and LCD NF samples (*Figure 8*). The material composition of the leachate solutions is summarised in *Table 2*.

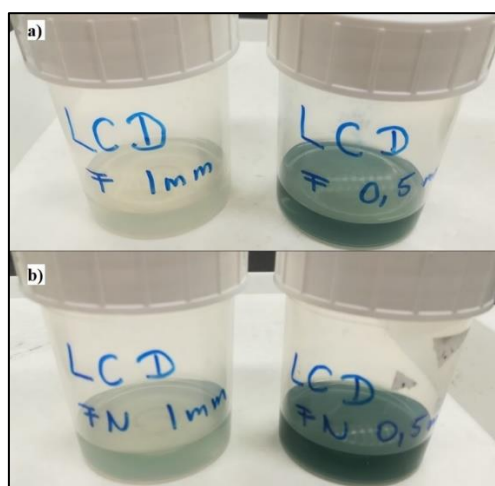


Figure 8

The acquired acidic leachate solutions of the a) LCD F and b) LCD NF samples

Table 2

The material composition of the acidic leachate solutions

Examined material	As	Cu	Fe	In	Mn	Sn	Sr
	mg/L						
LCD F $<1 \text{ mm}$	0.124	8.15	731	40.9	22.2	11.8	233
LCD F $<0.5 \text{ mm}$	0.213	2.08	4310	33.7	95.1	11.1	369
LCD NF $<1 \text{ mm}$	0.220	2.34	1553	139.0	35.9	19.2	285
LCD NF $<0.5 \text{ mm}$	0.602	2.32	6866	122.0	156.0	15.1	465

Based on our earlier results (BOKÁNYI et al. 2014_2) and chemical analyses, it was clearly revealed, that the mass transport is definitely hindered by the foil in both examined particle size ranges. The enrichment of the presented metals was in every case higher, when the foil was removed before the leaching tests, with one exception in case of the copper, when the recovery was almost 4 times higher from the sample LCD F <1mm compared to the other experiments. For example, in case of Mn, In, Fe and As, the leachability was much higher without the foil, about twice as many. In case of Sr, and Sn the effect of the foil removal showed not so remarkable changes in enrichment values. The effect of particle size reduction for the efficiency of the leaching was not the same comparing the recovery of the presented metals. In case of Sr, Mn, Fe and As it is proved, that the finer particle size enhanced the metal dissolution. Nevertheless, regarding the results related to Sn and In it is clear, that the further particle size reduction was maleficent. The explanation for this phenomena can be found, considering that the In and Sn is presented in the ITO layer on the surface of the glass substrate. The best results were obtained for In, in LCD NF< 1mm case, when the indium dissolution was complete.

4. CONCLUSIONS

The examination of the effect of mechanical preparation of LCD panels on metal recovery with acidic leaching is presented in the article. The effect of both removing and keeping the polarising film on the metal recovery was also taken into consideration. Using thermal treatment, most of the polarising film can be removed from the panels. In case of LCD NF samples, the mechanical treatment of the panels was less complicated than the comminution of LCD F samples. The comminution of LCD F samples required two-step crushing to produce the appropriate particle size for the centrifugal milling. Based on the particle size distribution of the product of the centrifugal mill, it can be concluded that the LCD F samples have more coarse particles than the LCD NF samples.

Thus, the polarising film not only affects the comminution procedure to be used, but the parameters of the ground products as well.

ACKNOWLEDGEMENTS

The research work was performed in the Centre of Excellence in Sustainable Natural Resource Management at the Faculty of Earth Science and Engineering, University of Miskolc. The described article was carried out as part of the „Mechanically controlled particle properties for enhancing leachability of certain components from EOL waste products (TÉT_14_VL-1-2015-0001) Science and Technology Wallonia – Hungarian co-operation project.

REFERENCES

- [1] BALDÉ, C.P. et al. (2017): *The global e-waste monitor – 2017*. Bonn/Geneva/Vienna: United Nations University (UNU), International Telecommunication Union (ITU) & International Solid Waste Association (ISWA).
- [2] https://collections.unu.edu/eserv/UNU:6341/Global-E-waste_Monitor_2017_electronic_single_pages_pdf

- [3] Ljudmilla, BOKÁNYI (2014): Innovative mineral processing techniques in waste recycling pp. inv55-inv62. In: ÜNER, Ipekoglu; VEDAT, Arslan; SEZAI, Sen (eds.): *Proceedings of the 14th International Mineral Processing Symposium*. Izmir, Turkey, Turkish Mining Development Foundation.
- [4] Ljudmilla BOKÁNYI– Terézia–VARGA–Valéria MÁDAI–ÜVEGES (2014_1): Experimental Investigation of Indium Recovery from Waste LCD Panels by Chemical Solubilisation Paper: WR18papers-Bokányi, p. 8. In: GOMBKÖTŐ, Imre (ed.) 18th International Conference on Waste Recycling Miskolc, Hungary, University of Miskolc.
- [5] Ljudmilla BOKÁNYI–Terezia VARGA–Valeria MADAI–UVEGES–Anita BRUNCSZLIK–Karolina GARAI (2014_2): Recovery of indium as a critical element from waste LCD panels pp. 645–651. In: ÜNER, Ipekoglu; VEDAT, Arslan; SEZAI, Sen (eds.) *Proceedings of the 14th International Mineral Processing Symposium*. Izmir, Turkey, Turkish Mining Development Foundation.
- [6] CSÖKE, B.–BOKÁNYI, L.–FAITLI J.–NAGY S. et al. (2014): A possible source of indium – LCD display panels. In: FÖLDESSY, J. (ed): *Basic research of the strategic raw materials in Hungary*. CriticEL 10. (Miskolc) MilagrossaKft., pp. 103–113.
- [7] FAITLI, J.–MAGYAR, T. (2014): Az LCD kijelzőfelépítése, működésielve. In: CSÖKE B.–BOKÁNYI, L.–FAITLI, J.–NAGY, S. (eds.): *Elektronikai hulladékok előkészítése a stratégiai elemek visszanyerése érdekében*. CriticEL 7(Miskolc): MilagrossaKft., pp. 14–21.
- [8] FERELLA, F. et al. (2017): Separation and recovery of glass, plastic and indium from spent LCD panels. *Waste Management*, 60, pp. 569–581.
- [9] HASEGAWA, H. et al. (2013): Recovery of indium from end-of-life liquid-crystal display panels using aminopolycarboxylatechelants with the aid of mechanochemical treatment. *Microchemical Journal*, 106, pp. 289–294.
- [10] HSIEH, S.-J.–CHEN, C.-C.–SAY, W. C. (2009): Process for recovery of indium from ITO scraps and metallurgic microstructures. *Materials Science and Engineering B*, 158, 82.
- [11] IŞILDAR, A. et al. (2018): Electronic waste as a secondary source of critical metals: Management and recovery technologies. *Resources, Conservation and Recycling*, 135, pp. 296–312.
- [12] LEE, C-H. et al. (2013): Recovery of indium from used LCD panel by a time efficient and environmentally sound method assisted HEBM. *Waste Management*, 33 (3), pp. 730–734.
- [13] LI, J. et al. (2009): Recovery of valuable materials from waste liquid crystal display panel. *Waste Management*, 29 (7), pp. 2033–2039.
- [14] MIŠKUFOVÁ, A. et al. (2018): Recovery of indium from LCD displays. *World of Metallurgy – ERZMETALL*, 71 (1), pp. 31–36.
- [15] MURATANI, T.–HONMA, T.–MAESETO, T.–SHIMADA, M. (2010): Method and apparatus for recovering indium from waste liquid crystal displays; US Patent Application Publication, Pub. No.: US 2010/0101367 A1.

- [16] RUAN, J.–GUO, Y.–QIAO, Q. I. (2012): Recovery of indium from scrap TFT-LCDs by solvent extraction. *Procedia Environmental Sciences*, 16, p. 545.
- [17] SILVEIRA, A. V. M. et al. (2015): Recovery of indium from LCD screens of discarded cell phones. *Waste Management*, 45, pp. 334–342.
- [18] UEBERSCHAAR, M. et al. (2017): Potential and Recycling Strategies for LCD Panels from WEEE. *Recycling*, 2 (7). DOI:10.3390/recycling2010007
- [19] VIROLAINEN, S. et al. (2011): Recovery of indium from indium tin oxide by solvent extraction. *Hydrometallurgy*, 107 (1–2), pp. 56–61.
- [20] WANG, R.–XU, Z. (2016): Pyrolysis characteristics and pyrolysis products separation for recycling organic materials from waste liquid crystal display panels. *Journal of Hazardous Materials*, 302, pp. 45–56.
- [21] WANG, S. et al. (2017): Recovery of valuable components from waste LCD panel through a dry physical method. *Waste Management*, 64, pp. 255–262.
- [22] YANG, J. et al. (2013): Indium recovery from discarded LCD panel glass by solvent extraction. *Hydrometallurgy*, 137, pp. 68–77.
- [23] ZHANG, K. et al. (2015): Recycling indium from waste LCDs: A review. *Resources, Conservation and Recycling*, 104 (A), pp. 276–290.
- [24] ZHANG, S. et al. (2017): Supply and demand of some critical metals and present status of their recycling in WEEE. *Waste Management*, 65, pp. 113–127.



EFFECT OF DIFFERENT ACTIVATION SOLUTION ON ANDESITE BASED GEOPOLYMERS

MICHAL MARCIN¹–MARTIN SISOL¹–IVAN BREZÁNI¹

¹Technical University of Košice, Faculty of Mining, Ecology, Process Control and Geotechnologies,
Institute of earth resources, Department of mineral processing, Park Komenského 19, 042 00,
Košice, Slovak Republic,
e-mails: michal.marcin@tuke.sk, martin.sisol@tuke.sk, ivan.brezani@tuke.sk,

Abstract

Andesite stone is widely used in civil engineering and architectural applications. Andesite contains SiO₂ as the main component. Therefore, andesite may be used as material for geopolymerization. This work describes changing of activation solution parameters on final strengths of alkali activated binders – geopolymers made from andesite filler. Samples were tested after 90 days.

Keywords: *andesite, geopolymers, compressive strength, flexural strength*

1. INTRODUCTION

Natural stones are classified, such as metamorphic (marble, gneiss etc.), sedimentary (limestone, travertine etc.), or magmatic (granite, basalt, andesite etc.) according to their generation properties. Andesite is classified as a volcanic rock, a subtype of magmatic rock. Andesite is used in many areas in the world, especially in civil engineering and architectural applications such as pavement, parquet, frame, coat, and dripstone manufacturing. Dust and aggregate are produced as byproducts during cutting and polishing processes of natural stone for decorative purposes. Broad scale andesite production generates significant amount of waste material; 70% of the andesite is wasted during mining, processing and polishing stages [1–3].

Andesite can be used as alkali activated materials and utilized in synthesis of geopolymers. The term geopolymer was first used by Joseph Davidovits. He defined the material that is formed in inorganic polycondensation called geopolymerization. In geopolymerization reaction, three-dimensional structures of AlO₄ and SiO₄ tetrahedra are created. According to him, only material with peak at about 55 ppm in ²⁷Al NMR spectrum may be called geopolymer. Only materials produced by alkaline activation of metakaolin comply with this condition. Later the term geopolymer was used for all alkali activated aluminosilicate. Nowadays, research in field of geopolymers is focused mostly on using secondary raw materials like fly ash [4, 5].

Geopolymers now represent a new group of organic substances, because they have significant environmental and energy potential. They belong in a group of the inorganic polymer covalently bound macromolecules with the chain consisting of -Si-O-Al-O-. Geopolymers are obtained from

the chemical reaction of alumino-silicate oxides with sodium silicate solutions in a highly alkaline environment. As an alkali activating solution, strongly alkaline aqueous solution of sodium or potassium hydroxide is most commonly used [5, 6].

Geopolymer structure is created by silicate network which is composed of SiO_4 and AlO_4 tetrahedron, which are connected to each other through its own oxygen atoms. The empirical formula of geopolymers, also known as poly(sialates) is $\text{Mn}\{-(\text{SiO}_2)_z-\text{AlO}_2\}_n \cdot w\text{H}_2\text{O}$, where M is a cation such as K^+ , Na^+ , or Ca^{2+} ; n is the degree of polycondensation and z is 1, 2, or 3 [4, 7].

Geopolymerization is a complex multi-stage process. The reaction rate and chemical composition of the final reaction products is dependent on a numbers of factors which can be properties of the feed material, such as chemical and phase composition, grain size, and material composition of the activating solution, such as, the water content and the presence of soluble silicates [8].

Geopolymers are materials with many excellent properties such as high mechanical strength, resistance to low and high temperatures, resistance to aggressive environments or flame resistance [9].

In this paper, we describe an alkaline activation of andesite with the changing of activation solution parameters.

2. MATERIALS AND METHODS

Material used for alkali activation was andesite filler (AF). Alumosilicate component (68%) is significant factor for geopolymers preparation. Material was homogenized before alkali activation. No other treatment was applied to material. Partial chemical analyses of the andesite filler is indicated in *Table 1*.

Table 1
Partial chemical composition of used materials.

Material	SiO_2	Al_2O_3	CaO	Fe_2O_3	MgO	LOI	Other	$\text{SiO}_2/\text{Al}_2\text{O}_3$
AF	52.01	16.43	8.55	5.5	1.31	3.71	12.3	3.2

The activation solution was prepared by mixing solid NaOH pellets with Na-water glass and water. Sodium water glass from the Kittfort Praha Co. with the density of 1.328–1.378 g/cm³ was used. It contains 36–38% Na_2SiO_3 and the molar ratio of $\text{SiO}_2/\text{Na}_2\text{O}$ is 3.2–3.5. Solid NaOH with the density of 2.13 g/cm³ was obtained from Kittfort Praha Co. containing at least 97%–99, 5% of NaOH.

Particle size analysis (*Figure 1*) showed that almost 100% of sample is below 120 μm , which is one of condition to successful geopolymerization process. Plan of experiments and activation solution parameters are showed in *Table 2*. AF mixture was stirred with activation solution for 10 minutes, until creation of homogenous mixture. Mixture was then filled into prismatic molds with the dimensions 40 × 40 × 160 mm and compacted on the vibration table VSB-40. The pastes were cured in a hot air drying chamber at 80 °C for 6 hours. Thereafter, the samples were removed from the forms, marked, and stored in laboratory conditions till the moment of the strength test. The values of compressive strength were determined after 7, 28, and 90 days according to the Slovak Standard STN EN 12390-3. Mechanical properties were examined only on 90th day of ageing. The

compressive and flexural strengths of the hardened samples was determined after 90 days using the hydraulic machine Form+Test MEGA 100-200-10D.

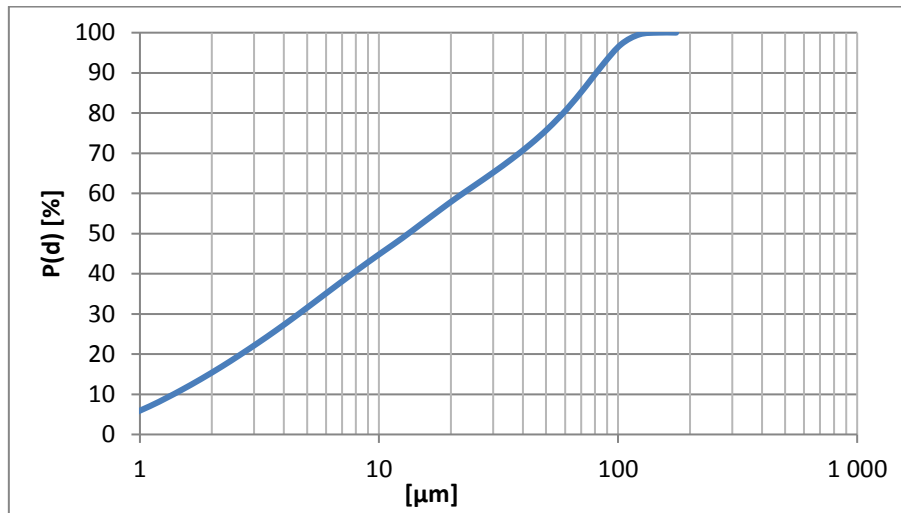


Figure 1
Particle size analysis

3. RESULTS AND DISCUSSION

Properties and composition of feed material plays an important role in alkali activation. The aim of this experiment was to find out the effect of main activation solution parameters. Compressive and flexural strengths after 90 days are shown in *Figures 2 and 3*.

Table 2
Plan of experiment

Sample	Na ₂ O [%]	Ms [mol/mol]	w [%]
AF1	5	0	0.25
AF2	6	0	0.25
AF3	7	0	0.25
AF4	8	0	0.25
AF5	5	0.25	0.25
AF6	6	0.25	0.25
AF7	7	0.25	0.25

Sample	Na₂O [%]	Ms [mol/mol]	w [%]
AF8	8	0.25	0.25
AF9	5	0.5	0.25
AF10	6	0.5	0.25
AF11	7	0.5	0.25
AF12	8	0.5	0.25
AF13	5	0.75	0.25
AF14	6	0.75	0.25
AF15	7	0.75	0.25
AF16	8	0.75	0.25
AF17	5	1	0.25
AF18	6	1	0.25
AF19	7	1	0.25
AF20	8	1	0.25
AF21	5	1.2	0.25
AF22	6	1.2	0.25
AF23	7	1.2	0.25
AF24	8	1.2	0.25
AF25	5	1.4	0.25
AF26	6	1.4	0.25
AF27	7	1.4	0.25
AF28	8	1.4	0.25

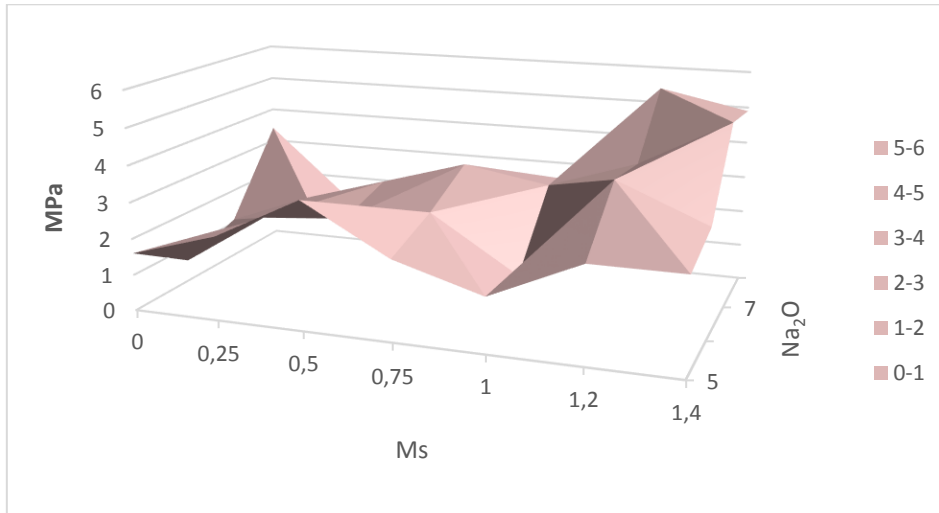


Figure 2
Flexural strength of andesite based geopolymers

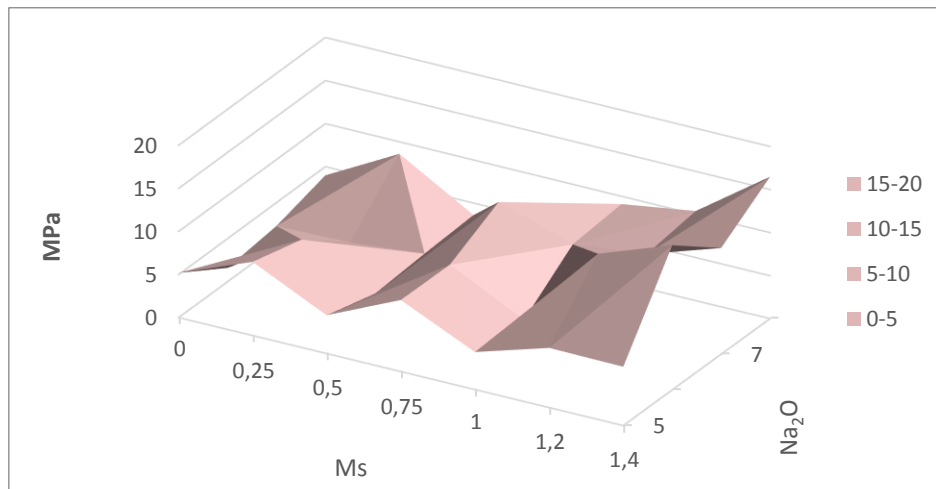


Figure 3
Compressive strength of andesite based geopolymers

From the flexural strengths graph is obvious that the highest strengths was achieved with higher amount of Na_2O in the activation solution (7% and 8%). 1.2 and 1.4 of modulus ratio was amounts were strengths were highest. Flexural strength achieved with these parameters was almost 5 MPa.

Compressive strengths is showed on *Figure 3*. This measurement showed very similar tendency, that higher amount of Na_2O and modulus ratio mean higher compressive strengths of andesite geopolymers. The highest value was 16.9 MPa.

4. CONCLUSIONS

Alkali activated materials – geopolymers, are a new generation of inorganic binders. Any aluminosilicate materials can be used to prepare geopolymers, including andesite. This paper describes possibilities of preparation of geopolymers from andesite with different activation solution used during preparation. The results shown, those activation solution parameters affect strengths of samples. Highest values of two main parameters meant highest strengths

ACKNOWLEDGEMENTS

This work was supported by there search grant project VEGA, no. 1/0843/15.

REFERENCES

- [1] DAVRAZ, M.–CEYLAN, H.–TOPCUN, I. B.–UYGUNOGLU, T. (2018): Pozzolanic effect of andesite waste powder on mechanical properties of high strength concrete. *Construction and Building Materials*, Vol. 165.
- [2] ALYAMAC, K. E.–INCE, R. (2009): A preliminary concrete mix design for SCC with marble powders. *Construction and Building Materials*.
- [3] SARIISIK, A.–SARIISIK, G.–SENTURK (2011): A. Applications of glaze and decor on dimensioned and esites used in construction sector. *Construction and Building Materials*, Vol. 25.
- [4] DAVIDOVITS, J. (1991): Geopolymers: In organic Polymeric new materials. *Journal of thermal analysis*, 37, pp. 1633–1656.
- [5] ŠKVÁRA, F. (2207): Alkali activated material sor geopolymers. *Ceramics – Silikáty*, 51/3, pp. 173–177.
- [6] XU, H.–VAN DEVENTER, J. S. J. (2000): The geopolymerisation of alumina-silicate materials. *Int. J. Miner. Process*, 59, pp. 257–266.
- [7] DAVIDOVITS, J. (2008): *Geopolymer: Chemistry and applications*. 2nd ed. France: Institut Géopolymère, p. 584.
- [8] XU, H.–VAN DEVENTER J. S. J. (2003): Effect of source materials on geopolymerization. *Ind Eng Chem Res*, 42, 1698–1706.
- [9] DUXSON, P.–FERNÁNDEZ-JIMÉNEZ, A.–PROVIS, J. L.–LUKEY, G. C.–PALOMO, A.–VAN DEVENTER, J. S. J. (2007): Geopolymer technology: the current state of the art. *J. Mater. Sci.*, 42, 2917–2933.
- [10] PHAIR, J. W.–VAN DEVENTER, J. S. J. (2001): Effect of silicate activator pH on the leaching and material characteristics of waste-based inorganic polymers. *Minerals Engineering*, Vol. 14, pp. 289–304.



DEVELOPING A COMPLEX PROCESSING TECHNOLOGY IN ZALAEGERSZEG FOR RMSW PREPARATION TO DECREASE LANDFILLING

JÓZSEF FAITLI¹–BARNABÁS CSÓKE²–ROLAND ROMENDA³–
ZOLTÁN NAGY⁴–SZABOLCS NÉMETH⁵

¹Associate Professor, ²Professor Emeritus, ³PhD Student, ⁴CEO, Project Leader, ⁵Executive Designer
University of Miskolc, Institute of Raw Material Preparation and Environmental Processing¹²³
3B Hungária Kft., Hungary, Zalaegerszeg⁴⁵
Hungary, 3515 Miskolc - Egyetemváros, ejtfajtj@uni-miskolc.hu

Abstract

In 2016, a Hungarian planning and manufacturing company, the 3B Hungária Ltd. started a project with the Institute of Raw Materials and Environmental Processing, University of Miskolc to reduce waste land-filling in the western Hungarian region. A new, almost completely Hungarian developed and produced waste processing plant has been built in Zalaegerszeg (Búslakpuszta) to treat residual municipal solid wastes (RMSW) of the region (60 000 tons/year). The designed mechanical-physical technology contains a bag opener machine, a drum sieve to separate the so called “bio” fraction, a hammer crusher for pre-comminution of the >200 mm fraction, the newly developed KLME (combined air flow, magnetic and eddy-current separator, KLME is the Hungarian abbreviation), two NIR sorters, the final shredder and all the necessary auxiliary equipment. Main products of the technology are the bio and inert fractions (land-filled at this stage), material streams for recycling, Fe, Al, PET and PVC and the secondary fuel material (RDF) for energetic utilisation. Paper reports about the commissioning and process engineering tests of the new plant.

Keywords: *KLME separator, residual municipal solid wastes (RMSW), separation efficiency, hammer mill, rotary shear.*

1. INTRODUCTION

Modern lifestyles result in significant municipal waste generation and if we would like to maintain or even improve the achieved living standards, sustainable waste management is necessary. According to European environmental policy, notably the European Commission’s Roadmap to a Resource Efficient Europe (EC 2011) and the EU’s Waste Framework Directive (EU 2008), landfilling of municipal solid wastes (MSW) is the least preferred waste management option. The non-contaminated (dry) part of MSW is typically collected strictly separately from the contaminated residual municipal solid waste (RMSW) (RADA et al. 2009). Even developed countries have to take the long-term generation of residual municipal solid wastes into account, because even with the application of a sophisticated selective collection system there are still large amounts of residual materials that have to be non-selectively collected and handled (AICH and GHOSH 2016). The social, natural and

economic features of local communities are quite diverse; therefore, beneficial managing options for the RMSW materials might be specific to a particular community (HANC et al. 2011; MONTEJO et al. 2011). *Figure 1* illustrates the historical change of the European development of waste management options of MSW handling (POMBERGER et al. 2017).

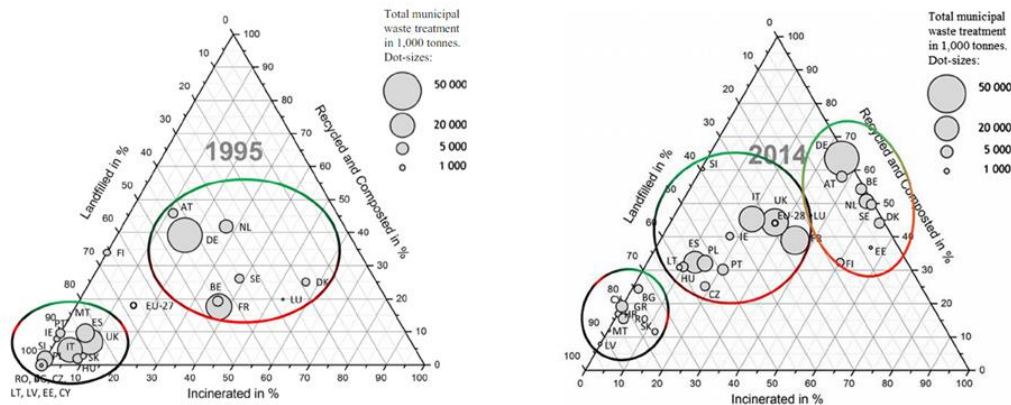


Figure 1
Different waste management options and MSW quantities of the EU member states in 1995 and 2014

Figure 1 shows two ternary diagrams. At a given point on a ternary diagram the sum of the percentages of the three fundamental waste treatment methods is always 100%. In 1995, one of the large groups of countries typically applied only landfilling, while the other group did already around 30-30% incineration and recycling. By 2014, the countries were splitted into three parts. The so called "landfilling" countries still landfilled almost 100% of their wastes. Among the "developing" countries, Hungary landfilled 60%, incinerated 10% and recycled-composted about 30% MSW. Afterword the EU has developed even a more conceptual plan. According to Directive 2008/98/EC, 2015/0275 (COD), until 2030, the gradual reduction of landfilling below 10% and the increasing of recycling and composting above 65% have been targeted for all generated wastes. This is a very serious challenge for the "developed" countries too mentioned earlier – not to mention – the "landfilling" and "developing" countries!

Nearly 50% of municipal solid wastes are still landfilled in Hungary today, although major improvements have been made over the past period. More than 3,000 old landfills and dumps had been closed and recultivated. Some new regional up-to-date landfills had been constructed. Almost everywhere around the country, selective "to house" collection systems had been introduced to collect the "dry" or "packaging" materials and the "bio" materials, however food wastes are still generally collected with the residual MSW. About 8–12 years ago intensive research was focused on the biological – mechanical treatment of RMSW, however, mainly mechanical – physical RMSW processing plants had been installed. There are more than 20 operating mechanical – physical and mechanical – biological RMSW processing plants in Hungary recently (LEITOL 2017). The applied typical mechanical – physical technology flowsheet is shown on *Figure 1*.

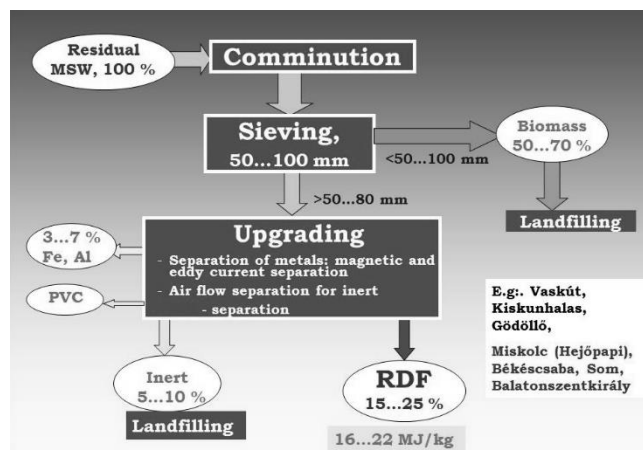


Figure 2

Typical mechanical – physical RMSW processing technology and its main products in Hungary recently
(BOKÁNYI et al. 2017; LEITOL 2017)

Figure 2 shows not only the technology but its main products and general product yields as well. The so called “bio-fraction” is the fine product of the drum sieve. The bio-fraction product represents high quantity, because generally 50–70 % (by mass) of the feed goes into this product. Unfortunately, the bio-fraction is still generally landfilled in Hungary. There are two places, namely Pécs and Győr, where the bio-fraction is stabilised by an aerobic biological process. The aerobic bio-stabilisation is advantageous because the mass of the waste stream is decreasing, therefore less landfill volume is necessary and the stabilised material is easier to handle on the landfill and the biomass is transformed into CO₂ instead of CH₄, therefore the greenhouse effect is smaller. However, the released thermal energy heats the environment and that is a serious disadvantage from a general environmental and economic standpoint. Intensive research is focusing right now on the local thermal co-utilisation of the bio-fraction and the RDF (refuse derived fuel) products. Another common feature of recent Hungarian RMSW processing plants, that they can separate only a low percentage of material streams for recycling. The Fe (ferrite), Al (aluminium), PET and PVC are separated in some places. In Miskolc there is a manual sorting cabin after the air flow separator, but generally nothing is sorted because there is no market and downstream industry to buy these secondary raw materials. If Hungary would like to approach the 2008/98/EC 2015/0275 (COD) EU Directive both the waste management and the downstream industry will have to be improved. The 5–10% inert product is also landfilled generally; however the utilisation of these materials in the construction industry might be a later option too. The main product of recent Hungarian RMSW processing plants is the RDF. If there is a cement plant nearby, the thermal utilisation of this waste by substituting fossil fuels is advantageous, but in many places the produced RDF has to be transported into long distances, into e.g. the Mátra Lignite Power Plant. The consortium described afterward has set the target of the local utilisation of the regional RMSW.

The municipality of Zalaegerszeg decided on the improvement of the MSW management of the region according to the mentioned EU directives. Nowadays 100% of the RMSW is landfilled in the up-to date landfill of the community. A consortium formed from a machine and technology

producer (3B Hungary Ltd.), a scientific partner (the Institute of Raw Materials Preparation and Environmental Processing, University of Miskolc), and a public waste managing service company (Zala-Müllex Ltd.) has started the development and construction of an RMSW processing technology targeting no-landfilling for this waste stream (FAITLI et al. 2018). The development and construction of the mechanical-physical processing plant as the first stage is supported by an EU-funded grant.

2. MATERIALS AND METHODS/AREA DESCRIPTION

Before designing a technology, quality and quantity data about the generating RMSW is necessary. Three sampling campaigns had been carried out. Sampling was based on the Hungarian Standards MSZ 21420 Parts: 28 and 29, however, a more detailed analysis was necessary for the design of the RMSW processing technology. On 10–14 October 2016, 5 waste collecting vehicles, on 8–15 January 2018, 17 vehicles and on 5–12 March 2018, another 17 vehicles from the region were selected for sampling. In each case an average sample of generally 500–800 kg RMSW was taken and processed by sieving manually and by a drum sieve machine, by hand sorting, manual sample splitting and drying at 105 °C in a heating chamber. *Table 1* shows a combined RMSW composition result that was used for the calculations to determine the yields of the technology.

Table 1
Combined results of three RMSW sampling campaigns in the area

Dry composition		Zalaegerszeg region																						
		> 200 mm																						
Category	1a food	b non-foomixed fo	1d bio	2 paper	cardboar	composit	5 textile	hygienic	7a 2D	7b PET	7c 3D	ombustit	9 glass	10a Fe	10b Al	10c Cu	11 inert	! hazardo	!3 <20 mm	extraneous	%	%		
Total	0.41	0.08	0.03	0.09	0.39	0.47	0.00	2.88	0.18	1.47	0.00	0.24	1.78	0.00	0.07	0.05	0.01	0.06	0.05	0.00	0.30	Σ	11.94	%
Packaging from this	0.00	0.00	0.00	0.00	0.07	0.43	0.00	0.00	0.00	1.39	0.00	0.09	0.13	0.00	0.00	0.00	0.01	0.01	0.05	0.00	0.00	Σ	4.68	%
		100 - 200 mm																						
Category	1a food	b non-foomixed fo	1d bio	2 paper	cardboar	composit	5 textile	hygienic	7a 2D	7b PET	7c 3D	ombustit	9 glass	10a Fe	10b Al	10c Cu	11 inert	! hazardo	!3 <20 mm	extraneous	%	%		
Total	2.01	0.53	0.19	0.22	4.62	0.68	1.23	0.97	4.44	3.50	1.79	1.69	1.56	0.51	1.45	0.44	0.01	0.19	0.03	0.00	0.11	Σ	24.31	%
Packaging from this	0.00	0.00	0.00	0.00	0.50	0.68	1.23	0.00	0.00	3.50	1.79	0.87	0.28	0.49	1.39	0.44	0.00	0.00	0.02	0.00	0.00	Σ	10.91	%
		50 - 100 mm																						
Category	1a food	b non-foomixed fo	1d bio	2 paper	cardboar	composit	5 textile	hygienic	7a 2D	7b PET	7c 3D	ombustit	9 glass	10a Fe	10b Al	10c Cu	11 inert	! hazardo	!3 <20 mm	extraneous	%	%		
Total	2.01	1.62	0.99	0.36	5.73	0.15	0.33	0.33	2.82	2.04	0.96	1.68	0.51	1.31	0.87	0.70	0.00	0.34	0.20	0.00	0.01	Σ	21.39	%
Packaging from this	0.00	0.00	0.00	0.00	0.94	0.15	0.33	0.00	0.00	2.04	0.66	1.33	0.23	1.23	0.87	0.70	0.00	0.00	0.17	0.00	0.00	Σ	9.91	%
		20 - 50 mm																						
Category	1a food	b non-foomixed fo	1d bio	2 paper	cardboar	composit	5 textile	hygienic	7a 2D	7b PET	7c 3D	ombustit	9 glass	10a Fe	10b Al	10c Cu	11 inert	! hazardo	!3 <20 mm	extraneous	%	%		
Total	1.31	5.92	0.40	0.94	7.17	0.02	0.00	0.17	0.38	0.49	0.01	0.49	0.30	2.02	0.14	0.33	0.00	0.68	0.17	0.00	0.02	Σ	15.80	%
Packaging from this	0.00	0.00	0.00	0.00	1.04	0.02	0.00	0.00	0.00	0.49	0.01	0.26	0.11	1.49	0.11	0.32	0.00	0.00	0.13	0.00	0.00	Σ	4.57	%
		< 20 mm																						
Category																				13 <20 mm	%	%		
Total																				21.34	Σ	26.57	%	
Packaging from this																					Σ	0.00	%	
Category	1a food	b non-foomixed fo	1d bio	2 paper	cardboar	composit	5 textile	hygienic	7a 2D	7b PET	7c 3D	ombustit	9 glass	10a Fe	10b Al	10c Cu	11 inert	! hazardo	!3 <20 mm	extraneous	%	%		
Total	5.75	8.14	1.62	1.60	17.92	1.31	1.56	4.35	7.82	7.49	2.77	4.10	4.16	3.85	2.54	1.52	0.01	1.27	0.45	21.34	0.44	Σ	100.00	%
Packaging from this	0.00	0.00	0.00	0.00	2.55	1.27	1.56	0.00	0.00	7.41	2.46	2.56	0.74	3.21	2.37	1.46	0.00	0.01	0.36	0.00	0.00	Σ	30.08	%

The named material categories and sub-categories in Table 1 are as follows: 1. BIOLOGICALLY DEGRADABLE WASTES; 1a.-eatable food waste, 1b. -non-eatable part of food, 1c. –mixed food waste (eatable and non-eatable together), 1.d. -other biologically degradable; 2. PAPERS; 3. CARDBOARDS; 4. COMPOSITES; 5. TEXTILES; 6. HYGIENIC WASTES; 7. PLASTICS; 7a.

-2D (foils), 7b. -PET, 7c. -3D (other plastics); 8. OTHER NON-CATEGORISED COMBUSTIBLES; 9. GLASSES; 10. METALS; 10a. -Fe, 10b. -Al, 10c. -Cu; 11. OTHER NON-CATEGORISED NON-COMBUSTIBLES (INERT); 12. HAZARDOUS; 13. FINE FRACTION (< 20 mm); 14. EXTRANEIOUS MATERIALS. *Table 1* shows the size- as well as the material composition of the RMSW. A “2” sieve series was used and five size fractions were measured. The material composition of each size fraction was measured too.

Figure 3 shows the flowsheet of the designed technology. It follows the concept of the general Hungarian RMSW mechanical – physical technology shown in *Figure 2*, however there are some new elements as well. Before the drum sieve the waste bags must be opened. Generally a rotary pre-shredder is applied for this task; however it has a serious disadvantage, namely this machine makes the Fe and plastic particles to be intergrown and that is a huge problem for the downstream separation. The energy need of a rotary pre-shredder is also significant. A bag opener machine (*Figure 4*) was developed and made here. The big rotor with teeth of the bag opener rotates opposite compared to the moving floor conveyor; therefore the bags are lifted and torn into the hydraulically supported standing teeth.

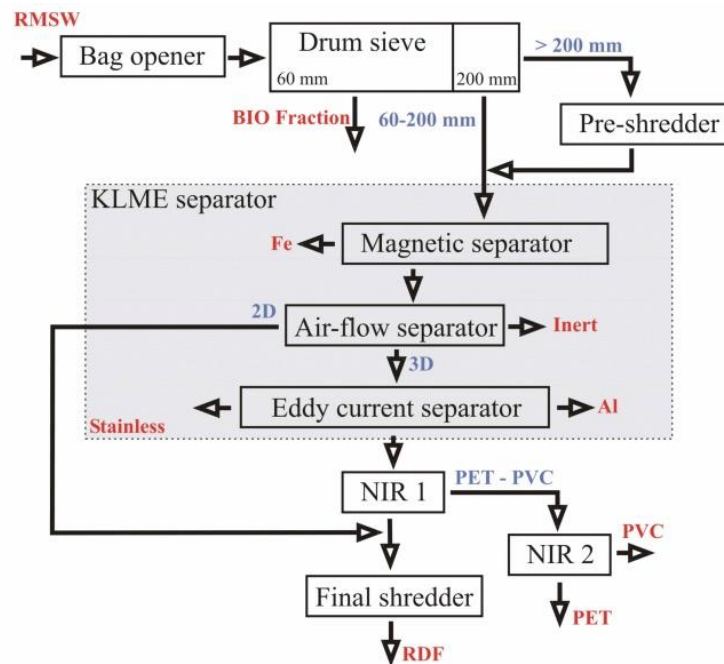


Figure 3

The designed mechanical – physical RMSW processing technology

The industry standard drum sieve (*Figure 5*) has two drum shaped screens, one with 60 mm and the other with 200 mm circular openings. The separated bio-fraction (< 60 mm) will be still landfilled after this first stage of development. The coarse fraction (> 200 mm) goes into a newly developed hammer mill (*Figure 7*) and its braked product is refeed into the 60–200 mm intermediate fraction before the KLME separator (*Figure 5* and 6).

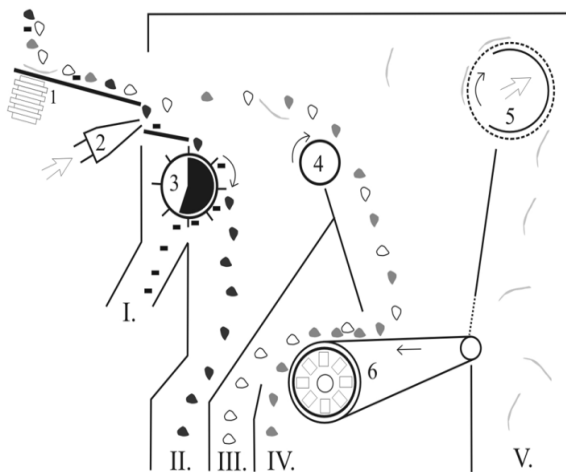


Figure 4. The moving floor conveyor and the bag opener



Figure 5. The drum sieve (back) and the KLME separator (front)

Figure 6 shows the schematics of the KLME separator.



Main technological units:

1. Vibrated feeder
2. Air nozzle
3. Magnetic drum
4. Rotated auxiliary cylinder
5. Exhaust cage
6. Eddy current separator

Numbers and short names of products:

- I. Magnetic
- II. Inert
- III. Al
- IV. 3D
- V. 2D

Figure 6
The KLME separator schematics

The 60–200 mm intermediate size fraction is fed into the KLME separator by a vibrated feeder. The air nozzle is located into the bottom of the first part of the vibrated plateau. Heavy particles fall through the air jet onto the magnetic drum. Magnetic particles are dragged into the Fe product, heavy inert particles, such as rocks, bricks and so on, as well as wet, therefore heavy books; shoes, etc. fall into the inert product. Light particles are blown and transported by the air jet. The operation of the KLME air separators is so complex, details are published elsewhere. When a particle falls

into the air jet, the initial acceleration part of particle settling is dominant, but afterwards when the particle is transported by the air jet, the particle settles in it and it has sufficient time to settle, therefore the terminal settling velocity is dominant. Another point is that the so called particle (body) density determines both the initial and terminal particle settling and not the material density. The material density of the aluminium cans and the PET bottles are significantly different, however their particle densities might be similar depending on how they had been compressed previously. Therefore the 2D (foils) and 3D (aluminium, plastics) shaped light particles are also blown by the air jet. The 3D plastics and aluminium particles settle out from the jet and then an eddy-current separator separates them into two products. The 2D like foils are sucked into the surface of the exhaust cage, because there is a strong suction from the middle of this cage. The rotating cage transports the 2D particles into the 2D output.



Figure 7. New hammer mill as pre-shredder



Figure 8. NIR sorters

Before the end of the technology there are two NIR sorters (near infrared). The first one is set to remove the PET and PVC particles and the second one cleans the PET product from this stream by removing the PVC. By this way the technology separates the Al, PET and Fe materials for waste-to-material recycling and the PVC is also removed from the produced RDF, because that is necessary for the thermal utilisation. The last machine of the technological flowsheet is a one rotor shredder produced by Metso. This is the only non-Hungarian made machine in the built RMSW processing plant.

3. RESULTS AND DISCUSSION

The first industrial test with the complete processing plant was carried out on 23 May, 2018. At that time continuous operation was maintained for about an hour and materials were produced in all the outputs of the technology, but minor operational clogging and mechanical engineering problems were arose. After some experimental development a more successful industrial test was performed on 24 July, 2018. Main technical parameters are shown in *Table 2*.

Table 2
Main technical parameters of the 24 July, 2018 industrial test

Parameter	Value
Moving floor conveyor speed	0.05 m/s
Revolution number of the bag opener rotor	4.8 1/min
Tangential speed of the drum sieve perimeter	1.13 m/s
KLME air nozzle air flow rate (blow in)	4800 m ³ /h
air flow rate, sucked out from the KLME	7400 m ³ /h
Revolution number of the eddy-current separator pole motor	2800 1/min
NIR1 and NIR2 feed belt conveyor speed	3 m/s
Belt conveyor speed before the Metso rotary-shredder	1 m/s

Detailed process engineering tests have not been carried out yet, when the products are analysed and yields and efficiencies are determined, because mechanical and process engineering developments are still ongoing. Another reason is that different engineering options are also tested, namely three different KLME separator constructions (exhaust cage 2D separator, spiked roller 2D separator and Coanda roller 2D separator) have been tested so far. Each of the constructions worked well, but each has different advantages – disadvantages. Figure 9 shows photos about some products of the 24 July, 2018 industrial test.



Figure 9
Photos about some products of the 24 July, 2018 industrial test

Figure 9 shows, that these products are fairly cleans. The eddy-current separator worked fine, because it is clearly visible to the naked eye that there are only a few extraneous particles in this product. The photo of the Fe product proves the success of the design concept of selecting the bag

opener machine instead of the rotary pre-shredder, because plastic is not captured in the Fe particles. The produced RDF is good quality, *Figure 9* simply shows it.

4. CONCLUSIONS

The municipality of Zalaegerszeg has decided to improve their MSW managing in the future, namely they would like to decrease landfilling near to 0%. The first stage of this conceptual plan is almost fulfilled because a new, almost completely Hungarian made mechanical-physical RMSW processing plant was inaugurated on 13 July, 2018 at Búslakpuszta, Hungary. There are still ongoing mechanical and process engineering development work to improve the technology and to gain industrial experience about different solutions and machine constructions.

ACKNOWLEDGEMENTS

The described work was supported by the projects GINOP-2.1.1-15-2016-00904 “Development of new equipment production for the low and medium capacity RMSW processing technologies” and the “Sustainable Raw Material Management Thematic Network – RING 2017”, EFOP-3.6.2-16-2017-00010. The realization of these projects is supported by the Hungarian Government and the European Union in the framework of the Széchenyi 2020 program supported by the European Structural and Investment Fund.

REFERENCES

- [1] AICH, A.–GHOSH, S. K. (2016): Application of SWOT analysis for the selection of technology for processing and disposal of MSW. *Procedia Environmental Sciences*, 35. pp 209–228.
- [2] BOKÁNYI Lj.–CSŐKE B.–GOMBKÖTŐ I.–NAGY S.–PINTÉR-MÓRICZ Á. (2018): „Hulladékból Energia” Kutatások a ME Nyersanyagelőkészítési és Környezeti Eljárástechnikai Intézetében. („Waste-to-energy” Research in the Institute of Raw Materials Preparation and Environmental Processing). *Műszaki és menedzsment tudományi közlemények*, 3 (1), pp. 49–57.
- [3] EC, 2011, Communication from the Commission to the European Parliament, the Council, the European Economic and Social Committee and the Committee of the Regions — Roadmap to a Resource Efficient Europe, COM (2011) 571 final, Brussels, 20. 9. 2011.
- [4] EU, 2008, Directive 2008/98/EC of the European Parliament and of the Council of 19 November 2008 on waste and repealing certain Directives, OJ L 312, 22.11. 2008, pp. 3–30.
- [5] EVERETT, J. W.–PEIRCE J. J. (1990): The development of pulsed flow air classification theory and design for municipal solid waste processing. *Resources, Conservation and Recycling*, 4. pp. 185–202.
- [6] FAITLI, J.–CSŐKE, B.–ROMENDA, R.–NAGY, Z.–NÉMETH, S. (2018): Developing the combined magnetic, electric and air flow (KLME) separator for RMSW processing. *Waste Management & Research*, doi.org/10.1177/0734242X18770251.

- [7] FAITLI J.–ROMENDA R.–SZÜCS M., (2017): Egyedi TSZH szemcsék mozgásának vizsgálata modell légáramkészülékben. (The examination of the motion of single MSW particles in a model air flow separator) In: SZIGYÁRTÓ I. L.–SZIKSZAI A. (eds.): XIII. Kárpát-Medencei Környezettudományi Konferencia. Kolozsvár, Romania, 5–8 April 2017, Ábel Kiadó, pp 228–237.
- [8] GOMBKÖTŐ, I.–NAGY, S.–CSÓKE, B.–JUHÁSZ, G. (2012): Effect of particle shape and orientation on separation efficiency of eddy current separator. In: *Indian Institute of Metals* (ed.): XXVI International Mineral Processing Congress, Proceedings. New Delhi, India, 24–28. September 2012, paper 538.
- [9] GUNDUPALLI, S. P.–HAIT, S.–THAKUR, A. (2017): A review on automated sorting of source-separated municipal solid waste for recycling. *Waste Management*, 60. pp 56–74.
- [10] Gy, P. M. (1979): *Sampling of Particulate Materials – Theory and Practice*. Elsevier Scientific Publishing Company, New York.
- [11] HANC, A.–NOVAK, P.–DVORAK, M.–HABART, J.–SVEHLA, P. (2011): Composition and parameters of household bio-waste in four seasons. *Waste Management*, 31. pp. 1450–1460.
- [12] Hungarian standard: MSZ 21420-28, (2005): Characterization of wastes. Part 28: Investigation of municipal wastes. Sampling.
- [13] Hungarian standard: MSZ 21420-29, (2005): Characterization of wastes. Part 29: Investigation of municipal wastes. Preparation of sample, characterization of material composition by the selection of material categories.
- [14] KAARTINEN, T.–SORMUNEN, K.–RINTALA, J. (2013): Case study on sampling, processing and characterization of landfilled municipal solid waste in the view of landfill mining. *Journal of Cleaner Production*, 55. pp. 56–66.
- [15] LEITOL, Cs. (2017): Visszacsatoláson alapuló több szempontú műszaki, környezeti és közgazdasági elemzés alkalmazása a mechanikai-biológiai hulladékkezelő művek technológiai tervezésében. (The application of multi standpoint technical, environmental and economic analysis in the feedback technique design of mechanical – biological MSW processing plants). PhD-Thesis, Pécs Science University.
- [16] LUNGU, M. (2005): Separation of small nonferrous particles using an angular rotary drum eddy-current separator with permanent magnets. *International Journal of Mineral Processing*, 78. pp. 22–30.
- [17] MARASPIN, F.–BEVILACQUA, P.–REM, P. (2004): Modelling the throw of metals and non-metals in eddy current separations. *International Journal of Mineral. Processing*, 73. pp. 1–11.
- [18] MILLER, S.–MILLER, R. (2009): *Air separation of recyclable materials*. United States Patent, Patent No. US7,584,856 B2.
- [19] MILLER, S.–MILLER, R. (2013): *Separation system for recyclable material*. United States Patent, Patent No. US8,618,432 B2.

- [20] MONTEJO, C.–COSTA, C.–RAMOS, P.–DEL CARMEN MARQUEZ, M. (2011): Analysis and comparison of municipal solid waste and reject fraction as fuels for incineration plants. *Applied Thermal Engineering*, doi: 10.1016/j.applthermaleng.2011.03.041.
- [21] PAP, Z.–GOMBKÖTŐ, I.–NAGY, S.–DEBRECZENI, Á. (2014): Determination of separability of different particles by eddy current separator: A statistical approach. In: YIANATOS, J.–DOLL, A.–GOMEZ, C. (eds.): *XXVII International Mineral Processing Congress, Proceedings*, Santiago de Chile, Chile, 20-24 October 2014, pp. 141–149.
- [22] R. POMBERGER–R. SARC–K. E. LORBER (2017): Dynamic visualisation of municipal waste management performance in the EU using Ternary Diagram method. *Waste Management*, 61. pp. 558–571.
- [23] RADA, E.–ISTRATE, I.–RAGAZZI, M. (2009): Trends in the management of residual municipal solid waste. *Environ. Technol.*, 7. pp. 651–61. Doi: 10.1080/09593330902852768.
- [24] ZHANG, S.–FORSSBERG, E.–ARVIDSON, B.–MOSS, W. (1999): Separation mechanisms and criteria of a rotating eddy-current separator operation. *Conservation and Recycling*, 25. pp. 215–232.



THE EFFECT OF SIEVE LOADING AND PARTICLES SHAPE ON THE RESULTS OF POLYMER SIEVE KINETICS

MILAN TRUMIĆ¹–MAJA TRUMIĆ¹–DRAGAN RADULOVIĆ²

¹University of Belgrade, Technical Faculty Bor, V.J. 12, 19210 Bor, Serbia,
mtrumic@tfbor.bg.ac.rs, majatrumic@tfbor.bg.ac.rs

²ITNMS, Franše d'Eperea 86, 11000 Belgrade, Serbia,
d.radulovic@itnms.ac.rs

Abstract

An experimental investigation has been made into the effects of different factors on the results of screening efficiency of polymer samples. The used polyvinyl chloride (PVC) samples have equal content of `small`, `large` and `small-to large` particles and filled the whole area of the sieve in one, two and four characteristic layers during the screening. Visual examination showed that the particle shape was similar in whole particle size distribution in the one sample tested. In addition to the aforementioned variable, the other factors studied included samples shape, vibrating amplitude and the duration of screening. Analysis of the obtained results of the screening rate in laboratory conditions was performed by applying the classical and modified model of the first order screening kinetics. The results showed that high loading of the sieve requires a larger vibrating amplitude for good classification and that the high layer reduction of sample is a more effective remedy for good efficiency than prolongation of sieving time. It has also been shown that the particles shape has a significant impact on the screening rate. The modified kinetics model (Magdalinović–Trumić) of the first order describes polymer screening kinetics with very good correlation coefficient in all cases. The application of the classical model is not adequate for determining a screening rate constant since the correlation coefficients are smaller than the minimum correlation coefficient.

Keywords: *polymer, screening, kinetic model, screening rate constant*

1. INTRODUCTION

Sieving or screening is the process which separate materials usually according to its particle sizes using a perforated area, so that small particle sizes (undersize product - between particle with average size smaller than average aperture size) pass through and larger sizes (oversize product - particles larger in size than average aperture size) stay on the surface perforated area (LIU 2009; YEKELER et al. 2014). TRUMIĆ and MAGDALINOVIĆ (2011) was give the definition of mentioned particles: `small`, (particles with the middle, diameter (ds) smaller than $0.75a$, where a is the aperture size, $0 < ds < 0.75a$), `small-to-large` (particles with mean diameter (dsl) larger than $0.75a$ and smaller than a , $0.75a < a$), and `large` (particles with the middle diameter (dI) larger than a and smaller than $1.5a$, $a < dI < 1.5a$). One can observe that there is not sharp cut between particle size classes because some larger particles may have passed through the aperture and

some smaller particles than aperture size remain in the oversize product. The explanation can be found in the analysis of the influence parameters that determine the efficiency of screening, like proportions of small and small to large particles in the particle size range (TRUMIĆ and MAGDALINOVIĆ 2011), particle shape (BEUNDER and REM 1999; KRUGGEL-EMDEN and ELSKAMP 2014; ELSKAMP, et al. 2017), and the density of raw materials (TRUMIĆ et al. 2016). It is also important to take into account the operating parameters (vibrating amplitude, duration of sieving, sieve loading) of the device in which the screening is done.

Most of the works regarding screening and sieving kinetics, i.e. the rate process, were studied from a different point of view. Generally it has been studied in terms of the rate of sieving of near-aperture particles for the terminal stages of sieving when the total load on the sieve does not change appreciably with time (STANDISH, 1985). For this condition for mathematical interpolation of screening and sieving kinetics, several models are proposed in literature.

The models used in this paper are the first order rate law given by Eq.(1) and Eq.(2) (STANDISH, 1985; TRUMIĆ and MAGDALINOVIĆ, 2011) and the modified first order rate law - model Magdalinović-Trumić (TRUMIĆ and MAGDALINOVIĆ, 2011) given by Eq.(3) and Eq.(4).

The first order screening kinetics:

$$dm / dt = - km \quad (1)$$

where dm / dt is the rate particles of size $(-a + 0)$ pass through the screen in time t , k the screening rate constant, m the mass of the particles of size $(-a + 0)$ on the screen at time t , and a is the aperture size.

The Eq.(2) represents a straight line in the coordinate system $[t; \ln 1 / 1-E]$

$$\ln (1 / 1 - E) = - kt \quad (2)$$

where E is screening efficiency- undersize recovery.

The modified first order screening kinetics:

$$dm / dt = - kmk_p \quad (3)$$

where dm / dt is the rate particles of size $(-a + 0)$ pass through the screen in time t , k the screening rate constant, m the mass of the particles of size $(-a + 0)$ on the screen at time t , and a is the aperture size and k_p is the change of the probability of screening coefficient.

The Eq.(4) represents a straight line in the coordinate system $[t; E / 1-E]$

$$\ln (1 / 1 - E) = - kt \quad (4)$$

where E is screening efficiency- undersize recovery which may be given by the following formula:

$$E = 1 - m / m_0 \quad (5)$$

where m is the mass of particles of size $(-a + 0)$ on the screen at time t , a the aperture size, m_0 the initial mass of a particle $(-a + 0)$.

2. MATERIALS AND METHODS

Experiments of sieving kinetics were carried out on PVC pipe and PVC insulation with equal content of `small`, `large` and `small-to large` particles. The samples filled the whole area of the sieve in one, two and four characteristic layers during the experiments. The density of PVC pipe is 1400 kg/m^3 and PVC insulation is 1350 kg/m^3 . As can be seen on the *Figure 1a, 1b*, PVC raw materials differ in particles shape. The PVC pipe has mostly cubical, while PVC insulation has a mostly needle shape particles. Experiments were performed using a sieve and sieve shaker ,Retsch' (*Figure 2a, 2b*). The sieving surface used in the experiments was square with openings of 1,7 mm. Mass of sample in one layer was 80 g. Particle size distribution of samples is given in Table 1. The variable operating parameters were vibrating amplitude in range 0.2 to 1.4, duration of sieving – 180 s total, sieve loading from 80g to 320 g.



Figure 1
PVC samples a) insulation and b) pipe



Figure 2
Laboratory Retsch devices: a) sieve shaker b) sieve

Table 1
Particle size distribution of PVC samples

d (mm)	Samples
-3.35 + 2.36	10
-2.36 + 1.7	30
-1.7 + 1.18	30
-1.18 + 0.85	20
-0.85 + 0.60	10
Σ	100%

*screening was done in one (1L), two (2L) and four (4L) layers

3. RESULTS AND DISCUSSIONS

The results of the screening kinetics investigation of the PVC pipes were analyzed using classic and modified model of the first order. The application of the classical model is not adequate for determining a screening rate constant since the correlation coefficients are smaller than the minimum correlation coefficient. The modified kinetics model (Magdalinović-Trumić) of the first order describes PVC pipe screening kinetics with a very good correlation coefficient for all tasted variables. Due to a reliable analysis of the vibrating amplitude value influence on the screening rate constant and the height of the raw material layer on the sieve, the obtained results will be shown only using a modified model.

The dependance of vibrating amplitude value and screening rate constant for one, two and four characteristic layers during the sieving are shown in *Table 2* and *Figure 3*.

Table 2
Dependance of vibrating amplitude and screening rate constant value for PVC pipe

Vibrating amplitude, A	one	two layers	four
	layer 1L	2L	layers 4L
Screening rate constant, k			
0.20	0.009	0.006	0.001
0.40	0.231	0.049	0.007
0.60	0.799	0.373	0.024
0.80	0.493	0.408	0.047
1.00	0.18	0.15	0.04
1.20	0.134	0.095	0.034
1.40	0.108	0.058	0.027

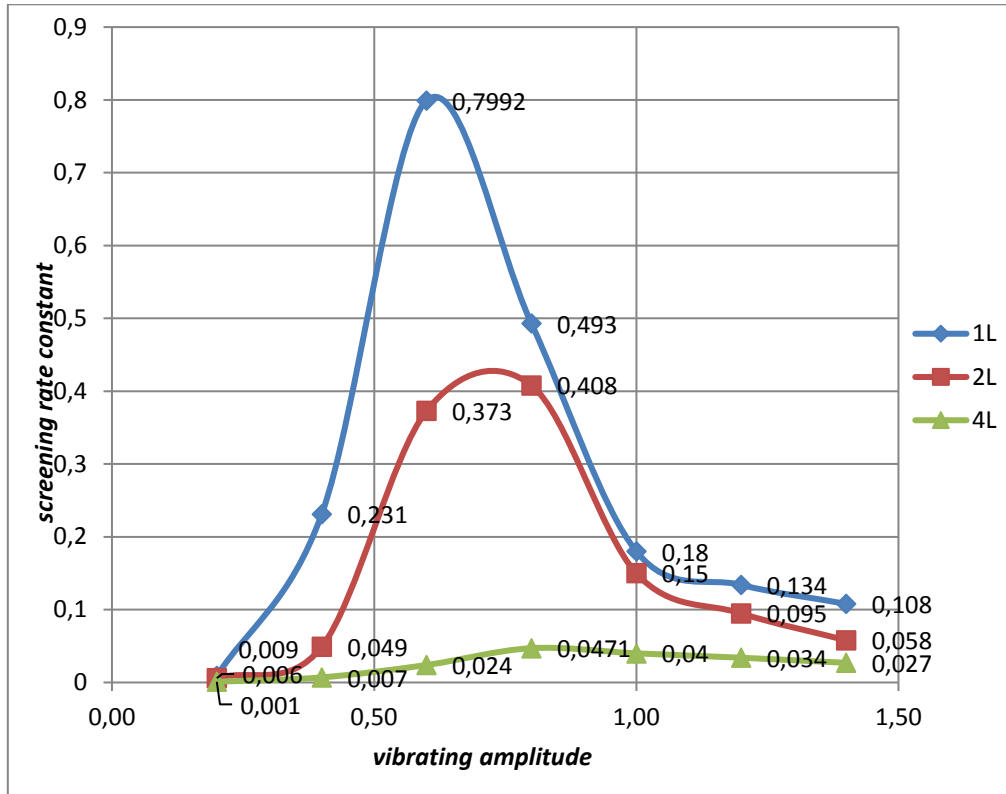


Figure 3

Dependance of vibrating amplitude and screening rate constant value for PVC pipe

It can be clearly seen that there is an optimal range of vibrating amplitude at which the screening rate constant has maximum value. If the screening is done in one characteristic layer, the optimal amplitude value is 0.6. With the increase in the height of the layer on the sieve, the value of the optimal amplitude increases, and for two and four layer it is value of 0.8.

Also, it is can be seen from the *Figure 3*. that in the entire tested amplitude range, the highest values for screening rate constant k , are achieved when the PVC pipe is screened in one layer, and at the optimum amplitude $k = 0.7992$. The doubly less absolute values for screening rate constant are achieved when the screening is done in two layers and at the optimal amplitude value $k = 0.408$. Drastically lower values for screening rate constant are achieved in the case of four-layer screening, and the maximum value for k in this case is 0.0471. Generally, based on the analysis, it can be said that screening in four layers on the sieve is not efficient because of the low rate of screening. It should also be noted that the influence of the height of the raw material layer on the sieve is not negligible.

On *Figure 4* and *Figure 5* are shown the screening kinetics for optimum amplitude values at the characteristic layer heights of PVC pipe on the sieve, by classical and modified model of the first order.

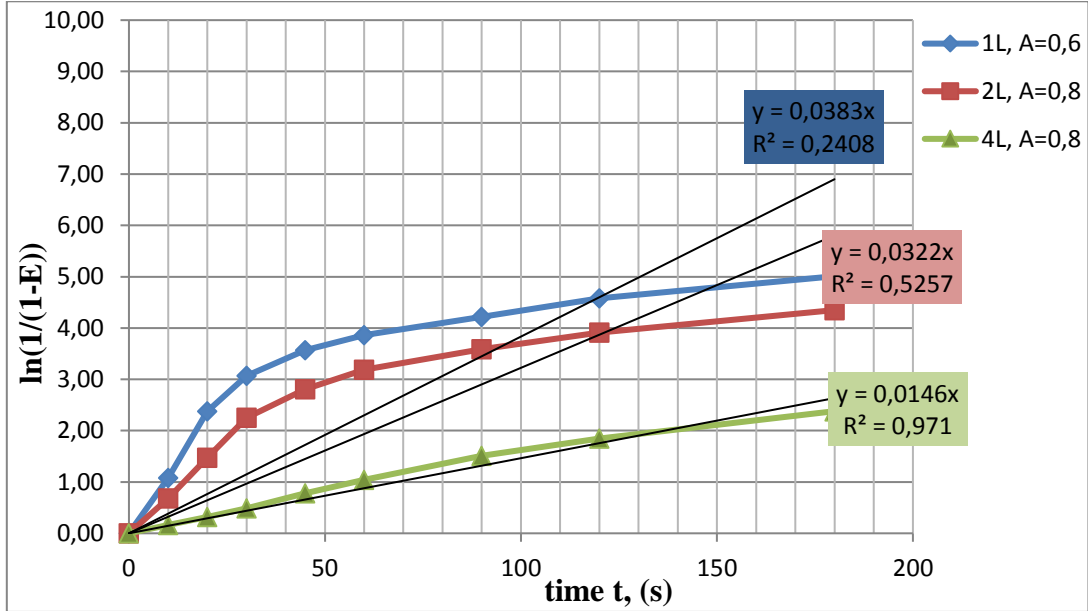


Figure 4
PVC pipe screening kinetics by classical model of the first order

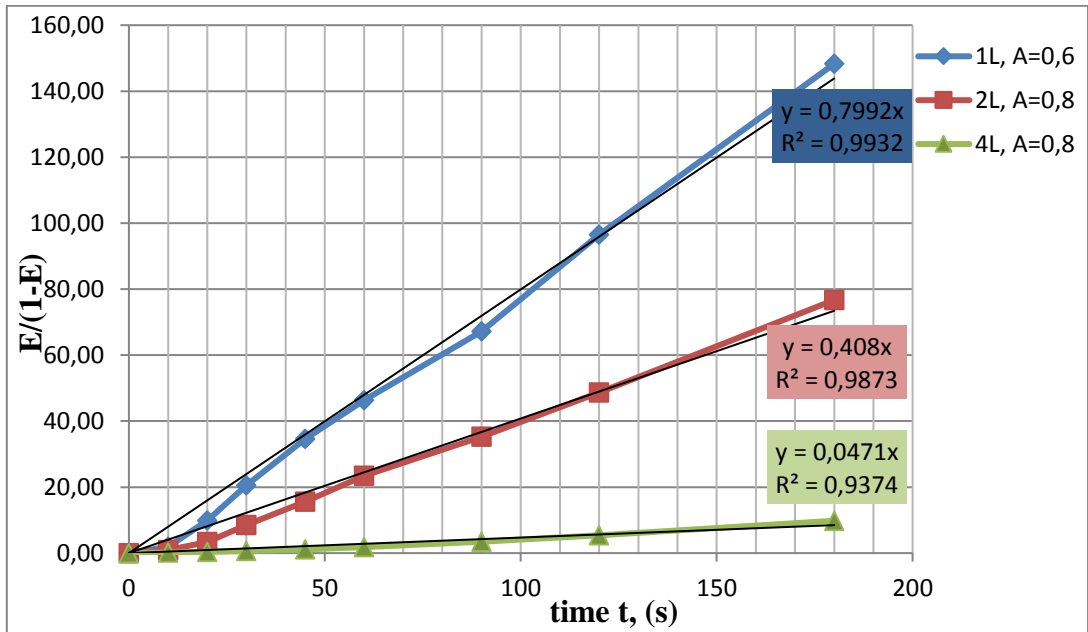


Figure 5
PVC pipe screening kinetics by modified model of the first order

Considering that the minimum value of correlation coefficient is $R^2_{\min} = 0,443$ (VOLK 1965), it can be said that both models describes screening kinetics with good correlation coefficient for two and four characteristic layers. It should be emphasized that for the entire tested range of amplitude values, as well as for all tested characteristic heights of the material on the sieve, only the modified model has a very high correlation coefficient over 0.9. These results confirm previous research of testing modified model screening kinetics Magdalinović-Trumić (TRUMIĆ and MAGDALINOVIĆ 2011; STOJANOVIĆ et al. 2015a; STOJANOVIĆ et al. 2015b; TRUMIĆ et al. 2016).

The second part of investigation is based on analysis of particle shape influence on screening kinetics.

The results of the screening kinetics investigation of the PVC insulation were analyzed using classic and modified model of the first order only in optimal range of vibrating amplitude value and were shown on *Figure 6* and *Figure 7*.

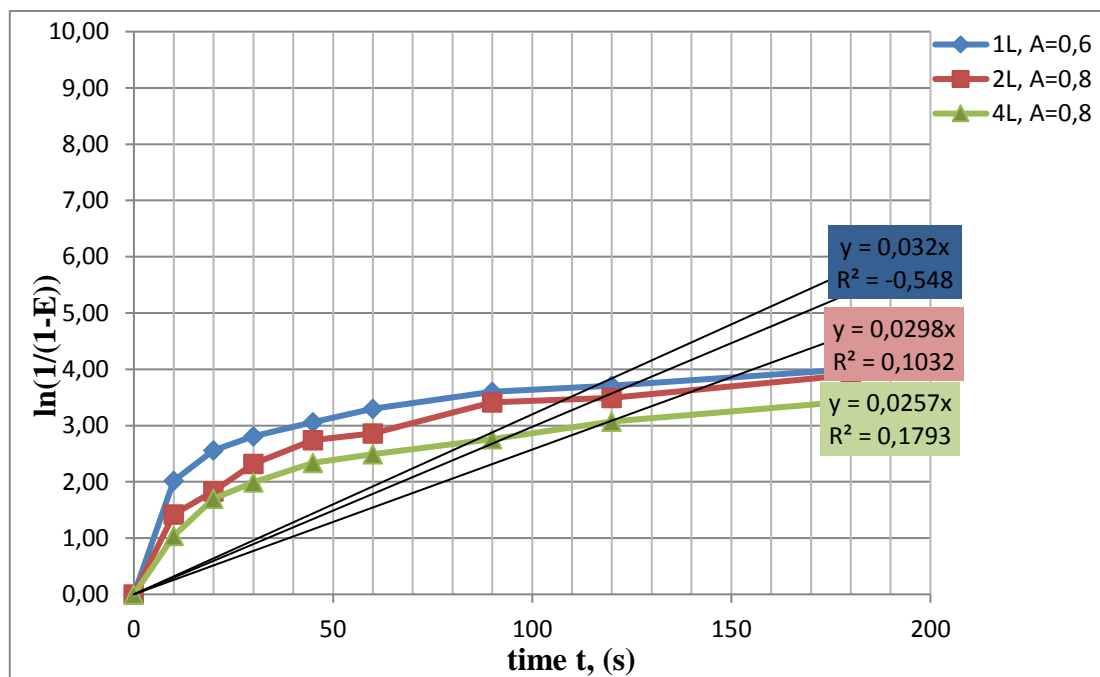


Figure 6
PVC insulation screening kinetics by classical model of the first order

Since the minimum value of the correlation coefficient is $R^2_{\min} = 0.443$, it can be concluded that the classical model does not describe the screening kinetics with a reliable correlation coefficient, even for optimal parameters. From the *Figure 7* can be seen that the modified model has a very high correlation coefficient over 0.9, which generally indicates that this modified model can be used for the reliable determination of the screening rate constant of raw materials of different shapes, in different loading of the sieve as well as in wide amplitude range.

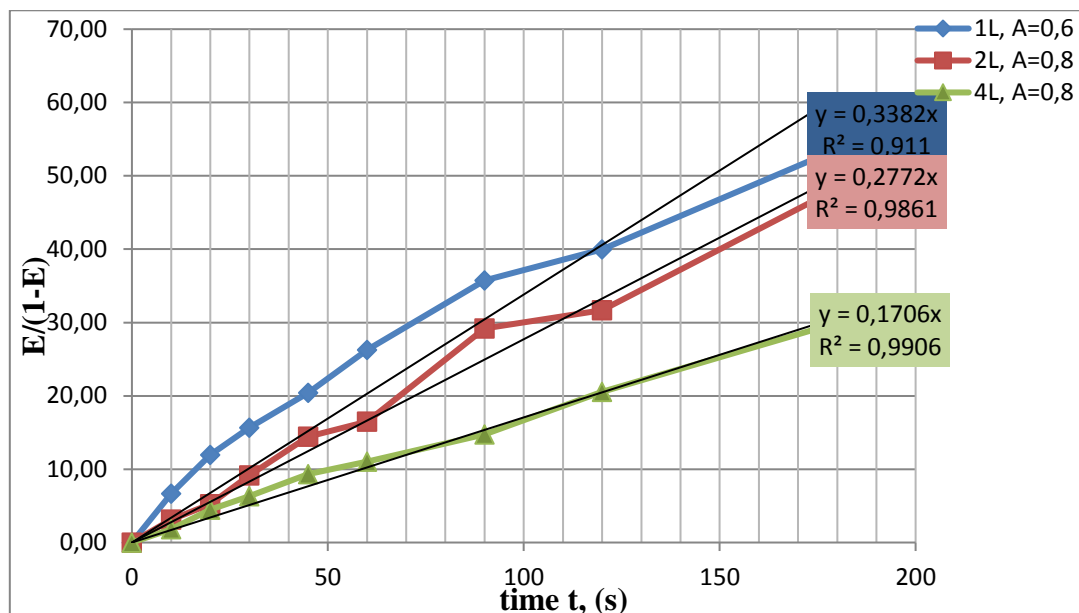


Figure 7

PVC insulation screening kinetics by modified model of the first order

Table 3

Values of screening rate constant for PVC pipe and PVC insulation using modified model

	PVC pipe	PVC insulation
1L; A = 0.6	0.799	0.338
2L; A = 0.8	0.408	0.277
4L; A = 0.8	0.047	0.171

Table 3 shows the values of the rate constant of screening k , of tested PVC samples in 1L, 2L and 4L on the sieve. It can be observed that k decreases with increasing layers on the sieve, which further states that the effect of the height of the raw material layer on the sieve is not negligible.

Also, the data show that PVC insulation sample with mostly needle particles shape have the smaller value of k in comparison with the PVC pipe sample with mostly cubic particles shape, which points to the significant impact of the shape of the particles on the screening rate.

4. CONCLUSION

Based on the experimental data presented in this paper and the analysis of screening kinetics of PVC samples – pipe and insulation, can be concluded:

- The modified kinetics model (Magdalinović–Trumić) of the first order describes polymer screening kinetics with very good correlation coefficient in all cases.
- The application of the classical model is not adequate for determining a screening rate constant since the correlation coefficients are smaller than the minimum correlation coefficient.
- There is an optimal range of vibrating amplitude at which the screening rate constant has maximum value.
- High loading of the sieve requires a larger vibrating amplitude for good classification.
- Secondary raw material with mostly needle particles shape has a smaller value of k in one and two characteristic layer, compared to secondary raw material with mostly cubic particles shape.

ACKNOWLEDGMENTS

This investigation was supported by Serbian Ministry of Education, Science and Technological Development and it was conducted under following projects: TR 33007 and OI 172031.

REFERENCES

- [1] BEUNDER, E. M.–REM, P. C. (1999): Screening kinetics of cylindrical particles. *International Journal of Mineral Processing*, 57, pp. 1–81.
- [2] ELSKAMP, F. et al. (2017): A strategy to determine DEM parameters for spherical and non-spherical particles. *Granular Matter*, 19 (3), p. 46.
- [3] KRUGGEL-EMDEN, H.–ELSKAMP, F. (2014): Modeling of screening processes with the discrete element method involving non-spherical particles. *Chemical Engineering and Technology*, 37 (5), pp. 847–856.
- [4] LIU, K. (2009): Some factors affecting sieving performance and efficiency. *Powder Technology*, 193 (2):25, pp. 208–213.
- [5] STANDISH, N. (1985): The Kinetics of Battih sieving. *Powder Technogy*, 41, pp. 57–67.
- [6] STOJANOVIĆ, A. et al. (2015a): Screening kinetics analysis of PVC insulation and copper wire. *X International Symposium on Recycling Technologies and Sustainable Development Proceedings*, Bor, Serbia, 04–07 November. pp. 80–85.
- [7] STOJANOVIĆ, A. et al. (2015b): The influence of particle shape on screening kinetics, *47th International October Conference on Mining and Metallurgy Proceedings*, Bor Lake, Serbia, 04–06 October. pp. 95–100.
- [8] TRUMIĆ, M.–MAGDALINOVIĆ, N. (2011): New model of screening kinetics. *Minerals Engineering*, 24 (1), pp. 42–49.

- [9] TRUMIĆ, M. S. et al. (2016): Influence of Secondary Raw Material Density and Grain Shape on Screening Kinetics, *XI International Symposium on Recycling Technologies and Sustainable Development Proceedings*, Bor, Serbia, 02–04 November, pp. 171–176.
- [10] VOLK, W. (1965): Statystyka stosowana dla inżynierów, *Wydawnictwa Naukowo – Techniczne*, Warszawa.
- [11] YEKELER M. (2014): Correlation of the Particle Size Distribution Parameters with Sieving Rate Constant. *Particulate Science and Technology: An International Journal*, 32 (2), pp. 118–122.



COMPOSITION OF CEMENT KILN DUST BY PARTICLE SIZE

CHRISTOF LANZERSTORFER¹

¹ University of Applied Sciences Upper Austria, Stelzhamerstraße 23,
A-4600 Wels Austria, c.lanzerstorfer@fh-wels.at

Abstract

In cement mills large amounts of dust are separated from the kiln off-gas by the de-dusting filters. According to the Best Available Techniques (BAT) Reference Document for the Production of Cement, Lime and Magnesium Oxide from 2013 the specific generation of cement kiln dust (CKD) is in the range of 50-200 kg per tonne of cement clinker produced. In some mills this dust can be mixed to the product, while in other mills it has to be utilized elsewhere or it is sent to landfill, depending on the chemical composition of the dust. In this study, the CKDs from three different cement mills were investigated with the focus on the size dependence of the composition. Prior to chemical analysis the CKDs were split into four size fractions by air classification. After digestion, the concentration of various metals (Ca, Cd, Co, Fe, K, Mg, Mn, Pb and Zn), of total carbon (TC) and anions (Cl⁻ and SO₄²⁻) was determined. For the heavy metals Cd, Pb and Zn a pronounced size dependence was found with considerably higher concentrations in the fine size fractions. A similar but less pronounced size dependence was found also for the anions and for K. The concentration of Ca, Fe and TC showed no distinct size dependence. Thus, air classification might be applied for CKD pre-processing in CKD-utilization, for example to produce heavy metal reduced or chloride and sulphate reduced fractions.

Keywords: *Cement kiln dust, CKD, heavy metals, chloride, sulphate*

1. INTRODUCTION

In the burning of clinker in rotary kilns for cement production large amounts of dust are generated. The dust is separated from the kiln off-gas by means of electrostatic precipitators (ESPs) or fabric filters before it is released to the atmosphere. The specific generation of cement kiln dust (CKD) is in the range of 50–200 kg per tonne of cement clinker produced (Institute for Prospective Technological Studies, 2013). In several cement plants the CKD can be re-incorporated in the clinker production cycle. However, this can only be done when the limits on the alkali and chloride concentration in cement are not exceeded. Otherwise, alternative ways of CKD utilization have to be found or the CKD has to be deposited off in landfill sites (MASLEHUDDIN et al. 2008). Such alternative applications include agriculture (potash/lime source), civil engineering (soil stabilization), building materials (lightweight aggregates, low-strength concrete), sewage and water treatment (coagulation aid, sludge stabilization) and pollution control (sulfur absorbent, waste

treatment) (LACHEMI et al. 2008; MACKIE et al. 2010; PAVIA and REGAN 2010; PEETHAMPARAN et al. 2008). There is even the standard ASTM D 5050 – 08 available guiding the use of CKD.

CKDs from cement kilns with a cyclone preheater system are quite fine grained powders. The reported mass median diameters are in the range from 10 μm to 18 μm (PEETHAMPARAN et al. 2008; MACKIE et al. 2010). The chemical composition of CKD was described in several studies (LACHEMI et al. 2008; PEETHAMPARAN et al. 2008; MACKIE et al. 2010; PAVIA and REGAN 2010). However, there is no information available on the size dependence of the dust composition.

Air classification is a cost-effective pre-treatment method, which can be applied to separate fine grained material into different size fractions (LANZERSTORFER et al. 2018). This can be beneficial when the composition of the material is size dependent. Therefore, in this study the composition of the CKDs from three cement mills was investigated by particle size.

2. MATERIALS AND METHODS

The CKD samples investigated were collected from the dry de-dusting systems of three different industrial cement plants. The samples investigated were collected at the dust discharge of the de-dusting systems of the cyclone preheater kiln systems. Sample A was collected when the kiln system was in direct operation mode where the kiln off-gas is de-dusted directly after the cyclone preheater outlet. Samples B and C were collected when the off-gas from the cyclone preheaters was utilized in a combined raw meal grinding and drying unit. The sample volumes of approximately 2 dm³ was reduced to an amount suitable for the various laboratory tests using sample dividers, which were applied repeatedly (Haver RT 12.5, Quantachrome Micro Riffler).

A laboratory air classifier 100 MZR from Hosokawa Alpine was used for dry classification of the CKD samples. In the first classification step, the finest size fraction was separated from the bulk of the dust. The remaining coarse fraction was used as feed material in the next classification step, where the classifier was operated at reduced speed. A detailed description of such a sequential classification procedure can be found elsewhere (LANZERSTORFER and KRÖPPL 2014). The speed of the classifier in the three classification runs was 21,000 rpm, 11,000 and 6,000 rpm and the air flow through the classifier was 50 m³/h.

The dust particle size distribution was measured using a Sympatec HELOS/RODOS laser diffraction instrument with dry sample dispersion. The instrument was calibrated using a SiC-P600'06 standard from Sympatec.

The total carbon content (TC) was determined using a vario TOC select system in solid mode from Elementar Analysensysteme. For calibration of the system an Elementar Analysensysteme soil standard with 4.1% TOC/TC was used. The loss on ignition (LOI) was determined at 850 °C using a muffle furnace.

The concentration of Cl⁻ in the samples was determined by leaching in de-ionized water and subsequent analysis by ion chromatography (IC).

For analysis of metals and sulphate the samples were digested using aqua regia, while for the determination of the Cl⁻ content the samples were leached with deionized water. The concentrations of various metals (Cd, Co, Cr, Fe, Mn, Ni, Pb and Zn) was determined by inductively coupled plasma optical emission spectroscopy using a Horiba Jobin Yvon Ultima 2 system. The concentration of K, Mg, Ca, Cl⁻ and SO₄²⁻ was measured by ion chromatography. Details of the analytical method can be found elsewhere (LANZERSTORFER 2015a). The measured concentrations

of Cr and Ni cannot be used because the dust gets contaminated with these elements during the classification procedure due to some erosion of the classifier wheel (LANZERSTORFER 2015b).

3. RESULTS AND DISCUSSION

The mass median diameter of the size fractions produced were quite similar because the operation parameters in the classification procedure were the same for all three CKDs. The mass median diameters of SF1, SF2, SF3 and SFG4 were $1.3\pm 0.1\ \mu\text{m}$, $3.0\pm 0.5\ \mu\text{m}$, $6.5\pm 1.3\ \mu\text{m}$, $17.4\pm 3.0\ \mu\text{m}$, respectively. The slightly different size distributions of the CKDs resulted in somewhat different mass fractions of the size fractions (*Table 1*). The particles size distributions of the size fractions of CKD A are shown in *Figure 1* exemplarily.

Table 1
Mass fractions of the various size fractions

CKD	SF1	SF2	SF3	SF4
A	0.196	0.284	0.390	0.130
B	0.183	0.299	0.397	0.121
C	0.233	0.428	0.252	0.087

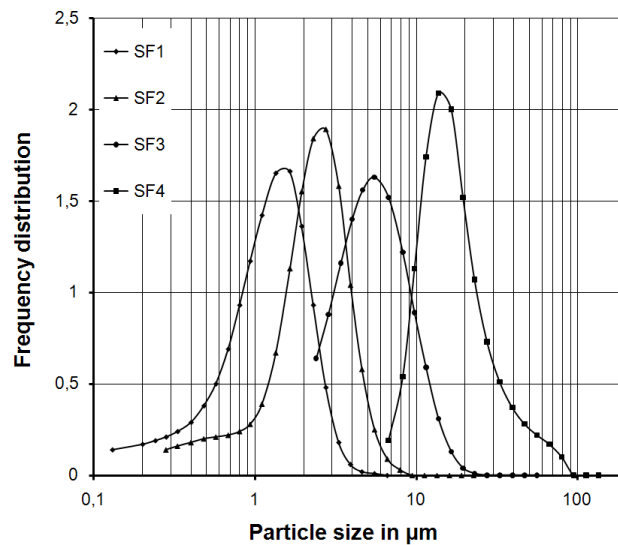


Figure 1

Particles size distributions of the size fractions produced from CKD sample A

The mass fractions of the size fractions and the results of the chemical analysis are summarized in *Table 2* (main components) and *Table 3* (heavy metals). The recovery of the components in the size fractions was in the range of 90% to 110%. An exception from this is evident for the recovery of Cr and Ni where the recovery was significantly higher. This is a result of some erosion of the classifier wheel, which is made of stainless steel (LANZERSTORFER 2015b).

The main component in the CKDs was Ca. The carbon (TC) contained in the dust can be assumed to be present as carbonate. Thus, the amount of CO₂ calculated from the TC fits well with the measured value of the LOI. The molar ratio of Ca+Mg to the calculated CO₂ was close to 1.0.

Table 2

Composition of CKD size fractions: Main components in g/kg dry dust

	Ca	Mg	TC	K	Cl	SO ₄ ²⁻	Fe	LOI
CKD A	284	2.0	95	11.50	9.6	11.0	8.3	353
SF1	264	1.5	86	15.5	11.8	20.0	10.0	330
SF2	296	1.5	93	11.0	8.5	12.0	8.0	350
SF3	318	2.0	100	9.1	8.1	6.0	8.0	369
SF4	315	2.0	95	13.1	12.4	4.5	10.3	363
Recovery	106%	93%	100%	104%	100%	90%	104%	101%
CKD B	280	2.0	97	4.0	3.1	8.90	9.7	350
SF1	313	2.0	90	3.5	4.0	15.00	10.8	340
SF2	329	2.0	95	4.1	3.0	9.00	10.0	344
SF3	256	2.0	94	3.9	3.2	8.00	10.2	344
SF4	326	3.0	91	3.5	1.7	9.00	13.4	338
Recovery	106%	106%	96%	96%	100%	109%	109%	98%
CKD C	334	2.2	105	4.9	4.8	4.0	6.5	381
SF1	320	2.0	107	5.1	5.9	6.0	8.2	384
SF2	355	2.0	106	4.5	5.3	4.0	7.1	387
SF3	331	3.0	104	4.0	4.2	3.0	5.5	378
SF4	311	4.0	98	3.8	3.7	2.5	5.7	355
Recovery	101%	110%	100%	91%	104%	102%	106%	100%

Table 3.

Composition of CKD size fractions: Heavy metals in mg/kg dry dust

	Mn	Cd	Co	Cr	Ni	Pb	Zn
CKD A	472	0.48	1.9	26.0	7.5	14.8	n.a.
SF1	379	0.90	2.4	29.4	14.4	24.6	n.a.
SF2	408	0.61	2.0	26.9	11.3	18.7	n.a.
SF3	500	0.32	1.7	30.9	10.5	11.6	n.a.
SF4	973	0.13	1.6	55.8	12.0	3.6	n.a.
Recovery	108%	102%	103%	126%	156%	102%	n.a.
CKD B	662	0.48	2.6	27.6	13.0	41.8	n.a.
SF1	591	0.94	3.9	33.1	26.6	82.0	n.a.
SF2	585	0.52	2.2	30.9	16.6	44.5	n.a.
SF3	768	0.45	2.4	36.7	16.8	35.0	n.a.
SF4	1083	0.16	2.2	54.1	19.3	17.2	n.a.
Recovery	109%	109%	100%	132%	145%	106%	n.a.
CKD C	192	0.68	2.1	12.6	15.1	57.1	47.8
SF1	211	0.94	2.4	21.8	25.1	78.8	77.9
SF2	197	0.81	2.5	17.9	18.7	53.3	49.3
SF3	184	0.32	1.1	15.1	14.9	34.3	29.6
SF4	184	0.13	0.5	16.4	14.6	29.8	15.0
Recovery	102%	97%	93%	142%	125%	92%	101%

n.a. not analyzed

The results show little dependence of the concentration on the particle size for the main components Ca and TC (*Figure 2*). This is quite reasonable because CaCO_3 is usually the main component in CKDs (LACHEMI et al. 2008; PEETHAMPARAN et al. 2008; MACKIE et al. 2010; PAVIA and REGAN 2010).

For the anions Cl^- and SO_4^{2-} some size dependence of the concentrations was found. This dependence is more expressed for SO_4^{2-} than for Cl^- (*Figure 3*). In the coarsest size fraction of CKD A the concentration of Cl^- was increased. For this deviation from the general trend no explanation was found for the moment. The concentration of K showed a similar trend.

The concentration of the heavy metals Pb and Cd shows distinct size dependence with increased concentrations in the finest size fractions (*Figure 4*). The same was observed for Zn (*Table 3*). These metals are volatile at cement kiln conditions, which means that they leave the kiln as gaseous components. When the kiln off-gas cools down in the preheater the heavy metals re-condense on the surface of the dust. Since the finer particles have a larger specific surface area higher concentrations of these heavy metals result in the finer size fractions.

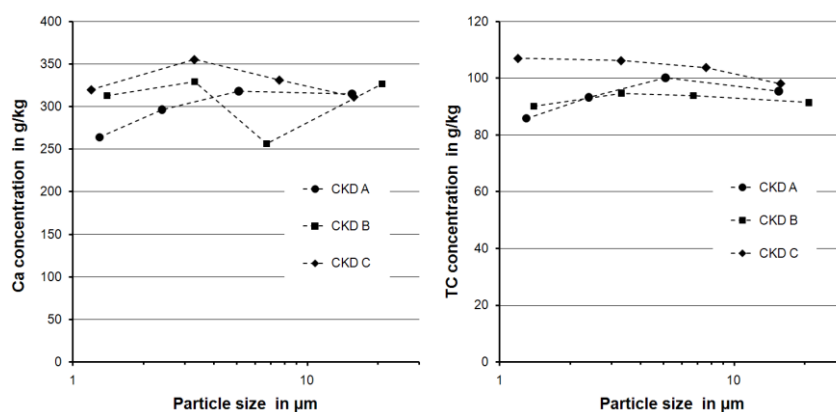


Figure 2.
Size dependence of the concentration of Ca and TC

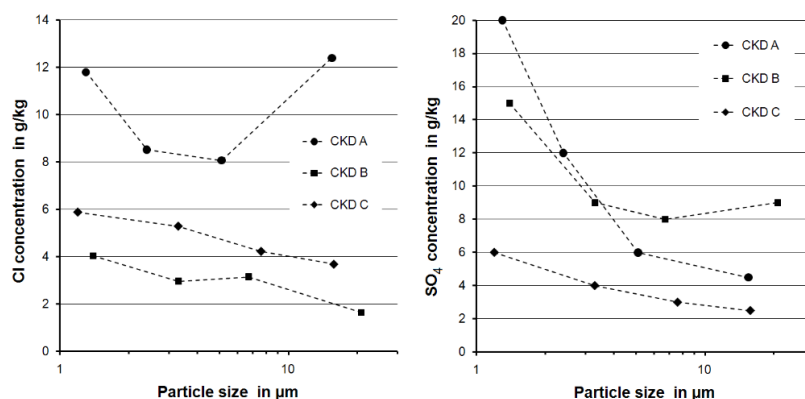


Figure 3
Size dependence of the concentration of Cl^- and SO_4^{2-}

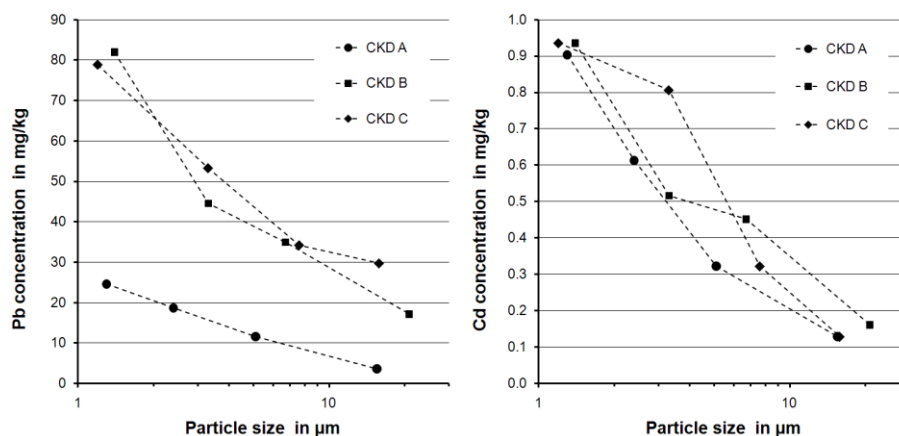


Figure 4
Size dependence of the concentration of some heavy metals

4. CONCLUSIONS

The classification experiments with CKD from three different cement mills showed that the size dependence of the concentration of various elements is quite similar for the different CKDs. For the heavy metals Cd, Pb and Zn a pronounced size dependence was found with considerably higher concentrations in the finest size fractions. For the anions Cl^- and SO_4^{2-} as well as for K the size dependence was less. The concentrations of Ca, Fe and TC showed no distinct size dependence at all. Thus, air classification might be applied for CKD pre-processing in CKD-utilization, for example to produce heavy metal reduced or chloride and sulphate reduced fractions.

ACKNOWLEDGEMENTS

Laboratory work by D. Lampl is gratefully acknowledged.

REFERENCES

- [1] Institute for Prospective Technological Studies (eds) (2013): *Best Available Techniques (BAT) Reference Document for Production of Cement, Lime and Magnesium Oxide*. Sevilla (Spain), European Commission.
- [2] LACHEMI, M. et al. (2008): Controlled low strength materials incorporating cement kiln dust from various sources. *Cement and Concrete Composites*, 30 (5), pp. 381–392.
- [3] LANZERSTORFER, C. et al. (2014): Air classification of blast furnace dust collected in a fabric filter for recycling to the sinter process. *Resources, Conservation and Recycling*, 86, pp. 132–137. DOI:10.1016/j.resconrec.2014.02.010.
- [4] LANZERSTORFER, C. (2015a): Chemical composition and physical properties of filter fly ashes from eight grate-fired biomass combustion plants. *Journal of Environmental Sciences*, 30, pp. 191–197. DOI:10.1016/j.jes.2014.08.021.

-
- [5] LANZERSTORFER, C. (2015b): Investigation of the contamination of a fly ash sample during sample preparation by classification. *International Journal of Environmental Science and Technology*, 12 (4), pp. 1437–1442. DOI:10.1007/s13762-014-0586-z.
- [6] LANZERSTORFER, C. et al. (2018): Feasibility of Air Classification in Dust Recycling in the Iron and Steel Industry. *Steel Research International*, 89 (7), 1800017, 1–6. DOI:10.1002/srin.201800017
- [7] MACKIE, A. et al. (2010): Physicochemical characterization of cement kiln dust for potential reuse in acidic wastewater treatment. *Journal of Hazardous Materials*, 173, pp. 283–291. DOI:10.1016/j.jhazmat.2009.08.081.
- [8] MASLEHUDDIN, M. et al. (2008): Usage of cement kiln dust in cement products – Research review and preliminary investigations. *Construction and Building Materials*, 22 (12), pp. 2369–2375. DOI:10.1016/j.conbuildmat.2007.09.005.
- [9] PAVIA, S. et al. (2010): Influence of cement kiln dust on the physical properties of calcium lime mortars. *Materials and Structures*, 43 (3), pp. 381–391. DOI:10.1617/s11527-009-9496-9
- [10] PEETHAMPARAN, S. et al. (2008): Influence of chemical and physical characteristics of cement kiln dusts (CKDs) on their hydration behaviour and potential suitability for soil stabilization. *Cement and Concrete Research*, 38, pp. 803–815. DOI:10.1016/j.cemconres.2008.01.011



PROCESS ENGINEERING INVESTIGATION OF A HUNGARIAN DEVELOPED NIR SEPARATOR

ROLAND ROMENDA

PhD-student,

University of Miskolc, Institute of Raw Materials Preparation and Environmental Processing
Hungary, 3515 Miskolc, Egyetemváros, ejtrom@uni-miskolc.hu

Abstract

The huge amount of plastic waste generation is a serious problem nowadays. The great variety of different plastic materials causes difficulties for human sorters during waste preparation. A better solution for the problem might be the so-called sensor based sorting, where a sensor identifies particles and an actuator sorts them into different products with good efficiency. In the western Hungarian region, – in Zalaegerszeg – a newly developed mechanical-physical municipal solid waste (MSW) processing plant has been built aiming minimal landfilling. There are two Near-Infrared (NIR) separators in this plant – they had been designed and manufactured by the 3B Hungária Ltd. Systematic process engineering investigation has been carried out with single- and multi MSW particles with the NIR separators. Single particles were fed many times; yield was defined as the probability of getting into a product. Main effects of improper sorting was analysed statistically.

Keywords: *NIR separator, municipal solid waste (MSW), optical separation, sensor based sorting, plastic waste*

1. INTRODUCTION

Today, in Hungary, the plastic waste ratio in the residual municipal solid waste (RMSW) is about 10–15%, but if the selectively collected plastic waste is also considered, the whole amount can easily reach 20%. At this time a significant portion of this material stream is recovered into the so-called RDF (refuse derived fuel) product, the remaining is landfilled, while recycling of this materials still accounts for a very small proportion (CSŐKE et al. 2006). At the beginning of 2018, the European Commission put forward a new proposal on plastic wastes. This proposal refers to the 10 most commonly used single-use plastic products and fishing gears in European seas and coasts, accounting for 70% of all marine waste. The regulation will seek to reduce plastic waste on several sides, on the one hand by banning certain products (e.g. disposable plastic cutlery) and on the other hand reducing consumption by consumers (e.g. food storage containers and cups) and manufacturers (e.g. filter tobacco, plastic bags) (European Commission 2018).

There are a number of methods for processing these wastes, ranging from low-efficiency density separators to high-efficiency sensor based sorters (FAITLI et al. 2010; OSBORNE et al. 1986;

GUNDUPALLI et al. 2017). The fundament of separation might be many different material features: colour, density, magnetic susceptibility, heat conductance, etc. (FAITLI et al. 2015 a. and b.). There are many types of known optical separators. The 3D camera sorter is a commonly used separator, but in its operation, it ignores many tangible properties of the material such as colour, texture, size, shape. One option is to examine the samples delivered on a tape using a 3D camera and a weighing tape, which means that the granules are identified and sorted according to the shape and density of the material.

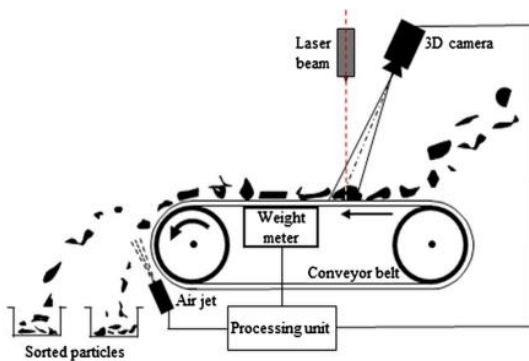


Figure 1
Optical sorter with 3D camera and weight meter (GUNDUPALLI et al. 2017)

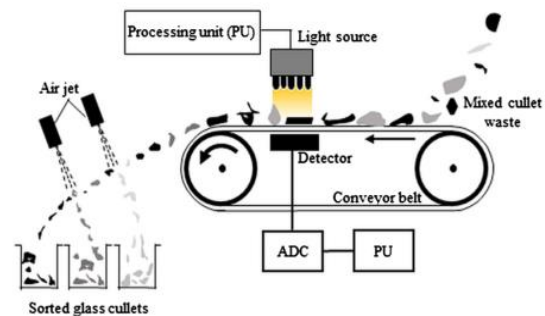


Figure 2
Optical sorter for colour identifying the glass wastes (GUNDUPALLI et al. 2017)

Another, more commonly used method is that the samples are illuminated by a constant light source and either detects a beam passing through the sample or reflecting on the sample (BOTONJIC-SEHIC et al. 2008; COLLEL et al. 2010; DAVIES 2005; SHAW & MANTSCH 1999). In the arrangement shown in Figure 2, the analogue signal captured by the detector placed under the tape is proportional to the amplitude of the beam of light. According to the figure, sorting is provided with two air jet nozzles, so there are three products at a given time moment of the sorting device. The particle motion of the blown particles is also important for sensor based sorting; therefore fundamental particle settling studies are also relevant (FAITLI et al. 2017).

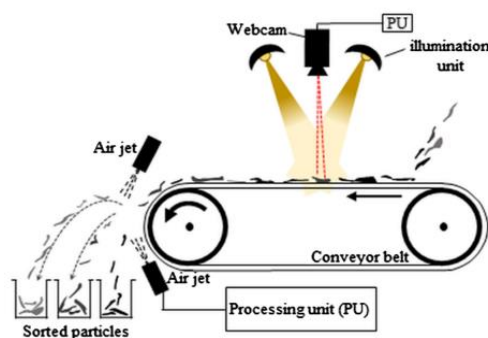


Figure 3
An ordinary optical separator.
(GUNDUPALLI et al. 2017)

In the arrangement according to *Figure 3*, particles coming from the belt are illuminated from two sides with a corresponding wavelength light. For the detection of reflected light beams, NIR or other optical sensors are used, after which the identification of the particles is followed by the analysis of the signal and then the sorting of the products in three products by means of air jets.

The consortium comprising of the 3B Hungária Ltd. and its scientific partner, the Institute of Raw Materials Preparation and Environmental Processing is working on the construction of a processing plant for RMSW preparation for the Zalaegerszeg region (FAITLI et al. 2018). There are two near-infrared NIR sorters in the plant that can be used to sort a large number of waste types. At present, the selection of PET and PVC is set to produce high-quality RDF and recycled PET, but lately these machines will be able to be used for the recycling of other waste streams, because the plant has been developed in a modular system. Today, RDF utilization enjoys priority, but as time goes on, – according to EU priorities as well – recycling will be more important.

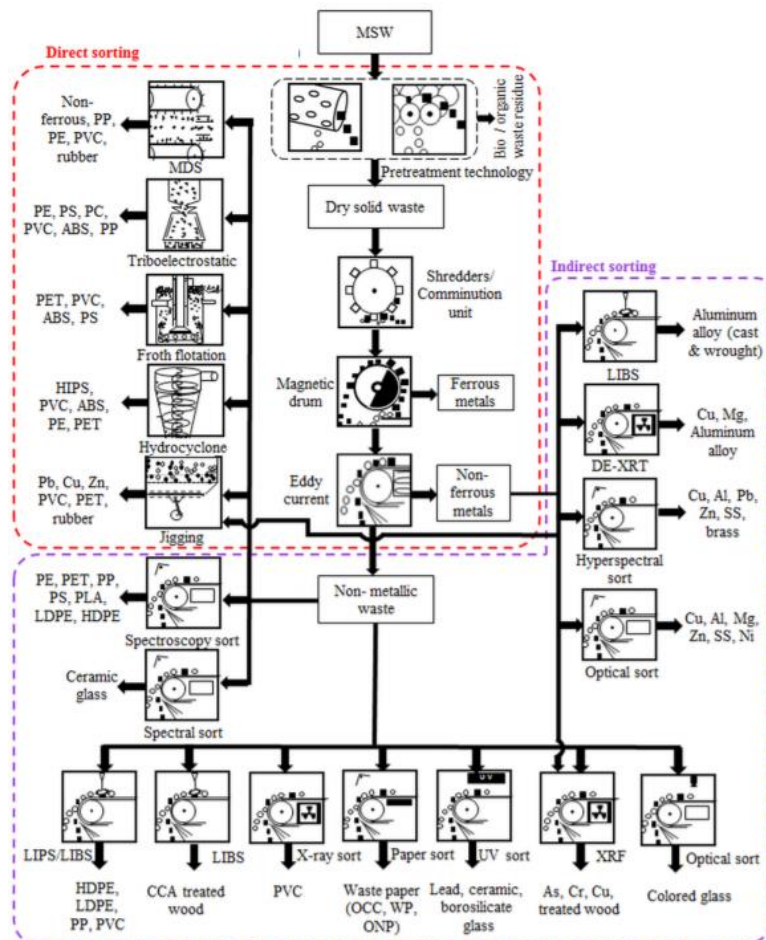


Figure 4
Direct and indirect separation.
(GUNDUPALLI et al. 2017)

2. MATERIALS AND METHODS

The examination with the industrial size NIR sorting equipment made by the 3B Hungária Ltd. was carried out on 26–28 July, 2017. Figure 5 shows the main parts of the machine. The central part of the equipment is a 3 m wide accelerator conveyor belt with its driven sprocket to the opposite side of the optical part. The fed particles are illuminated by two-row filament lamps with visible white and near-infrared (NIR) wavelengths. The filament lamps must be cooled by air flow and this air stream is also “blown” towards to the tape. The particles absorb or reflect a special wavelength NIR light according to their material quality. Reflected light passes through the gap between the two lamp lanes to the top, where the hyperspectral NIR camera is installed. The NIR camera is connected to the control computer through an appropriate interface, which analyses and compares spectra with the reference spectrum database. When authenticated, the computer signals to the air nozzle control valves and the short air jet impulse overflows the identified particle through the separating roller.



Figure 5
The Near-infrared separator.

The main properties of the NIR separator during examination:

- Nozzles: JAA 1385T1 (<http://monojet-ipar-technika.hu>)
- Pressure in the nozzles: 7.7 bar
- Type of the Camera: LLA – PMAmsi 2000/LR50
- Software: LLA – KUSTA 1.9MSI
- Setting: 96 track (96 nozzle, 25 mm space)
- Speed of belt: 3 m/s
- Diameter of the pulley: 220 mm
- Diameter of the separating roller (rotating opposite direction than the pulley!): 90 mm
- Distance between the axes of the separating roller and the pulley: 660 mm
- The upper point level of the separating roller from the belt: – 90 mm

During the No 1–4 tests, only PVC and PET particles were used. *Table 1* and *Figure 6* show the material, name and photo of the model particles used in tests No 5 and 6.

Table 1
Used model particles in NIR tests No 5 and 6.

PVC	Paper	HDPE	PET	PS	PP	PE(2D)
I/1	II/1	III/1	IV/1	V/1	VI/1	VII/1
I/2	II/2	III/2	IV/2	V/2	VI/2	VII/2
I/3	II/3	III/3	IV/3	V/3	VI/3	VII/3
I/4	II/4		IV/4		VI/4	VII/4
			IV/5		VI/5	VII/5
			IV/6			



Figure 6
The model particles

Model particles were tested individually and together. Depending on the machine a particle could get into the so-called “Dropped” product or if it was blown out of the separation roll into the so-called “Blown” product. Yield (ratio of blown particles) was calculated as pieces ratio (number of blown particles over number of fed particles) as well as weight ratio (mass of blown particles over mass of fed particles). During test No 5, each material group was examined separately 5 times, and the numbers of the dropped and blown particles were calculated. Finally, during the last, sixth test all particles were thrown to the belt at a time and in each series a new material type was set to be blown out by the NIR sorter.

3. RESULTS AND DISCUSSION

The following tables present results of examinations.

Table 2

NIR test No 1 results, only PVC particles were fed and PVC was set to be blown out.

Product	Pieces (pcs.)	Weight (kg)	Pieces ratio (%)	Weight ratio (%)
A, series				
Dropped	4	0.045	20.0	17.0
Blown	16	0.220	80.0	83.0
Total	20	0.265	100.0	100.0
B, series				
Dropped	0	0.265	20.0	17.0
Blown	20	0.265	80.0	83.0
Total	20	0.265	100.0	100.0
C, series				
Dropped	1	0.045	20.0	17.0
Blown	19	0.220	80.0	83.0
Total	20	0.265	100.0	100.0
D, series				
Dropped	2	0.045	20.0	17.0
Blown	18	0.220	80.0	83.0
Total	20	0.265	100.0	100.0
E, series				
Dropped	3	0.045	20.0	17.0
Blown	17	0.220	80.0	83.0
Total	20	0.265	100.0	100.0
Mean				
Dropped			20.0	17.0
Blown			80.0	83.0
Total			100.0	100.0

Table 3

NIR test No 2 results, only PET particles were fed and PET was set to be blown out.

Product	Pieces (pcs.)	Weight (kg)	Pieces ratio (%)	Weight ratio (%)
A, series				
Dropped	3	0.025	27.3	5.7
Blown	8	0.410	72.7	94.3
Total	11	0.435	100.0	100.0
B, series				
Dropped	2	0.070	20.0	17.1
Blown	8	0.340	80.0	82.9
Total	10	0.410	100.0	100.0
C, series				
Dropped	2	0.125	20.0	30.1
Blown	8	0.290	80.0	69.9
Total	10	0.415	100.0	100.0

Product	Pieces (pcs.)	Weight (kg)	Pieces ratio (%)	Weight ratio (%)
Mean				
Dropped			22.4	17.6
Blown			77.6	82.4
Total			100.0	100.0

Table 4

NIR test No 3 results, PET and PVC particles were fed and PET and PVC were set to be blown out.

Product	PVC				PET			
	Pieces (pcs.)	Weight (kg)	Pieces ratio (%)	Weight ratio (%)	Pieces (pcs.)	Weight (kg)	Pieces ratio (%)	Weight ratio (%)
A, series								
Dropped	0	0.000	0.0	0.0	1	0.030	27.3	5.7
Blown	10	0.130	100.0	100.0	9	0.410	72.7	94.3
Total	10	0.130	100.0	100.0	10	0.435	100.0	100.0
B, series								
Dropped	2	0.020	20.0	15.4	0	0.070	20.0	17.1
Blown	8	0.110	80.0	84.6	10	0.340	80.0	82.9
Total	10	0.130	100.0	100.0	10	0.410	100.0	100.0
C, series								
Dropped	0	0.000	0.0	0	1	0.125	20.0	30.1
Blown	10	0.130	100.0	100.0	9	0.290	80.0	69.9
Total	10	0.130	100.0	100.0	10	0.415	100.0	100.0
Mean								
Dropped			6.7	5.3			22.4	17.6
Blown			93.3	94.7			77.6	82.4
Total			100.0	100.0			100.0	100.0

Table 5

NIR test No 4 results, PET and PVC particles were fed and PET was set to be blown out.

Product	PVC				PET			
	Pieces (pcs.)	Weight (kg)	Pieces ratio (%)	Weight ratio (%)	Pieces (pcs.)	Weight (kg)	Pieces ratio (%)	Weight ratio (%)
A, series								
Dropped	6	0.080	60.0	0.0	3	0.080	30.0	20.5
Blown	4	0.055	40.0	100.0	7	0.310	70.0	79.5
Total	10	0.135	100.0	100.0	10	0.390	100.0	100.0
B, series								
Dropped	10	0.130	100.0	15.4	2	0.070	20.0	16.7
Blown	0	0.000	0.000	84.6	8	0.325	80.0	83.3
Total	10	0.130	100.0	100.0	10	0.395	100.0	100.0

Product	PVC				PET			
	Pieces (pcs.)	Weight (kg)	Pieces ratio (%)	Weight ratio (%)	Pieces (pcs.)	Weight (kg)	Pieces ratio (%)	Weight ratio (%)
C, series								
Dropped	9	0.120	90.0	0	3	0.090	30.0	22.5
Blown	1	0.005	10.0	100.0	7	0.310	70.0	77.5
Total	10	0.125	100.0	100.0	10	0.400	100.0	100.0
Mean								
Dropped			83.3	85.1			26.7	19.9
Blown			16.3	14.9			73.3	80.1
Total			100.0	100.0			100.0	100.0

Table 6

Results of separately examined particle samples with the correctly set option ("set option" means the material stream that has been set on the NIR computer for sorting out)

Sample	Dropped	Blown	Observation (reason of improper separation)
Set option: PVC			
I/1	0	5	perfect yield
I/2	0	5	
I/3	0	5	
I/4	0	5	
Set option: Wood			
II/1	1	4	slipping on the belt slipped on the belt slipped on the belt
II/2	4	1	
II/3	4	1	
II/4	4	1	
Set option: PE			
III/1	0	5	perfect yield
III/2	0	5	
III/3	0	5	
Set option: PET			
IV/1	0	5	NIR identification error too much air flow, blown to the roof and bounded back
IV/2	0	5	
IV/3	0	5	
IV/4	1	4	
IV/5	0	5	
IV/6	1	4	
Set option: PS			
V/1	0	5	perfect yield
V/2	0	5	
V/3	0	5	
Set option: PP			
VI/1	0	5	

Sample	Dropped	Blown	Observation (reason of improper separation)
VI/2	0	5	
VI/3	1	4	NIR identification error, rolled sample
VI/4	1	4	NIR identification error, rolled sample
VI/5	0	5	
Set option: PElow			
VII/1	5	0	NIR identification error and slipped samples
VII/2	4	1	
VII/3	4	1	
VII/4	4	1	
VII/5	5	0	

Table 7

Test results of the mixed sample examinations with different "to be blown" set options during the series

Blown sample	Set option						
	PVC	Wood	PE	PET	PS	PP	PElow
PVC	100 %	0 %	0 %	0 %	25 %	0 %	0 %
Paper	0 %	25 %	0 %	0 %	75 %	0 %	0 %
HDPE	0 %	0 %	100 %	0 %	0 %	33 %	0 %
PET	0 %	0 %	50 %	100 %	17 %	50 %	17 %
PS	0 %	0 %	30 %	0 %	67 %	0 %	0 %
PP	0 %	0 %	0 %	0 %	20 %	80 %	20 %
PE(2D)	0 %	20 %	60 %	40 %	0 %	0 %	20 %

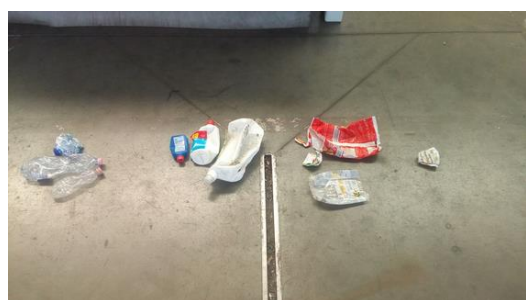


Figure 7

The blown samples during test No 6, set options PE (left) and PP (right)

4. CONCLUSION

Improper separation can be basically the consequence of the following three phenomena: a., *displacement on the belt after identification*. The speed of the accelerator belt has to be set properly, namely an identified particle must arrive at the place of the air jets just in time. If a particle slides or rolls on the belt surface this timing might be improper. Therefore cylindrical particles, such as

undamaged PET, Al, plastic bottles can roll on the belt causing improper sorting. Lightweight materials (e.g. foil) can slide on the belt. That is why the paper-foil separation was preferable with paper blowing, because paper was slightly stuck on the belt. The cooling air of the illuminating halogen lamps produces a slight blowing downward, which influenced the movement of some light particles. Proper space filling and distribution of the fed materials on the belt is also crucial, too many particles disturb identification and blowing, one particle might cover another one; but on the other hand an optimal concentration on the belt can hinder particle displacement after identification. b., *improper NIR camera identification*. During tests, often incorrect camera identification happened. If a particle is smaller than the resolution of the camera, identification problem is evident. It was tested with 20 mm wide paper strips. The NIR camera could not detect them, because its resolution is 25 mm. There are many overlapping between plastic materials and their sensing, like PE and PELow. The PET bottles were detected as HDPE due to their caps and the PETs were blown out. In two cases it was observed that the small particle was blown upwards by the nozzle on the upper wall of the machine, which dropped then into the wrong product indicating too high air jet velocity. In some other cases the opposite was observed, namely if a 3D like plastic bottle arrived in a wrong orientation to the jets, it was not blown into the “blown” product indicating too low air jet velocity. The camera must ignore the belt, so it cannot detect black PETs in the PET setting. The direction of rotation of the separating roll should be adjusted depending on the material. When blowing a hard bouncing material, it is advisable to rotate it backward; therefore the non-sorted soft particles will drop back into the “dropped” product.

ACKNOWLEDGEMENTS

The described work was carried out as part of the EFOP-3.6.1-16-2016-00011 “Younger and Renewing University – Innovative Knowledge City – institutional development of the University of Miskolc aiming at intelligent specialisation” project implemented in the framework of the Széchenyi 2020 program and the “Sustainable Raw Materials Management Thematic Network – RING 2017”, EFOP-3.6.2-16-2017-00010 project in the framework of the Széchenyi2020 Program. The realization of these projects is supported by the European Union, co-financed by the European Social Fund.

REFERENCES

- [1] BOTONJIC-SEHIC, E.–BROWN, C. W.–LAMONTAGNE, M.–TSAPARIKOS FORSENIC, M. (2008): *Application of Near-Infrared*.
- [2] BURNS, D. A.–CIURCZAK, E. W.: *Handbook of near-infrared analysis 3rd edition*. 836: CRC Press
- [3] COLLELL, C.–GOU, P.–PICOUET, P.–ARNAU, J.–COMAPOSADA, J. (2010): Feasibility of near-infrared spectroscopy to predict a(w) and moisture and NaCl contents of fermented pork sausages. *Meat Science*, 85 (2), pp 325–330.
- [4] CSÖKE, B.–FAITLI, J.–ALEXA, L.–FERENCZ, K. (2006): Production of secondary raw materials and fuels through the preparation of municipal wastes. In: N. Acarkan, Guven Onal (ed.): *Proceedings of the XXIII. International Mineral Processing Congress*. Istanbul, Turkey, 2006. 09. 03–2006. 09. 08. Promed Advertising Limited, pp 2230–2235

-
- [5] DAVIES, A. M. C. (2005): An introduction to near infrared spectroscopy. *NIR news*, (16), pp. 9–11
- [6] European Commission (2018): *Plastic Waste: a European strategy to protect the planet, defend our citizens and empower our industries*. Strasbourg, 16 January 2018.
- [7] J. FAITLI–B. CSÖKE–R. ROMENDA–Z. NAGY–S. NÉMETH (2018): Developing the combined magnetic, electric and air flow (KLME) separator for RMSW processing. *Waste Management & Research*, p. 9.
- [8] FAITLI, J. (2017): Continuity theory and settling model for spheres falling in non-Newtonian one- and two-phase media. *International Journal of Mineral Processing*, 169 (1), pp. 16–26.
- [9] J. FAITLI–A. ERDÉLYI–J. KONTRA–T. MAGYAR–J. VÁRFALVI–A. MURÁNYI (2015): Pilot Scale Decomposition Heat Extraction and Utilization System Built into the “Gyál Municipal Solid Waste Landfill”. In: R. COSSU–P. HE–P. KJELDSSEN–Y. MATSUFUJI–D. REINHART–R. STEGMANN (ed.): *15th International Waste Management and Landfill Symposium*. S. Margherita di Pula, Italy, CISA Publisher, Paper 262. p. 12.
- [10] J. FAITLI–T. Magyar–A. Erdélyi–A. Murányi (2015): Characterization of thermal properties of municipal solid waste landfills. *Waste Management*, 36 (1), pp. 213–221.
- [11] FAITLI, J.–NAGY, S.–ANTAL, G.–CSÖKE, B.–LUKÁCS, P. (2010): Laboratory-scale magneto-hydrostatic separator for high resolution density analysis of plastic and other wastes. In: *XXV International Mineral Processing Congress: Smarter Processing for the Future*. Brisbane, Australia, 2010-09-06 -2010-09-10. pp. 697–705.
- [12] GUNDUPALLI at al. (2016): A review on automated sorting of source-separated municipal solid waste for recycling. *Waste Management*, Volume 60, February 2017, pp. 56–74
- [13] MAYO, D. W.–MILLER, F. A.–HANNAH, R. W. (2003): Course notes on the interpretation of infrared and Raman spectra. 567, *John Wiley and Sons*.
- [14] NORRIS, K. H.–HART, J. R. (1965): Direct spectrophotometric determination of moisture content of grain and seeds. *International Symposium on Humidity and Moisture*, pp. 19–25
- [15] OSBORNE, B. G.–Fearn, T. (1986): “Introduction.” In *Near Infrared Spectroscopy in Food Analysis*, 1–19. Harlow: Longman Scientific & Tecnical.
- [16] SATHISH PAULRAJ GUNDUPALLI–SUBRATA HAIT–ATUL THAKUR (2017): A review on automated sorting of source-separated municipal solid waste for recycling. *Waste Management*, 60 pp. 56–74.
- [17] SHAW, R. A.–MANTSCH, H. H. (1999): “Near-IR Spectrometers.” In *Encyclopedia of Spectroscopy and Spectrometry* (Second edition), 1738–1747: Academic Press.
- [18] STARK, E.–LUCHTER, K. (2005): NIR instrumentation technology. *NIR news*, (16), pp. 13–16.
- [19] STOKES, L. (1979): Economical and practical evaluation of an online NIR instrument for controlling protein in soybean-meal. *Cereal Foods World*, 24 (9), pp. 460–460.



POSSIBILITY OF THE UTILIZATION OF SEWAGE SLUDGE AND DIFFERENT WASTE IN A CIVIL ENGINEERING

MARTA WÓJCIK¹, FELIKS STACHOWICZ²

¹Rzeszow University of Technology, Department of Materials Forming and Processing, Powstańców
Warszawy Av. 8, 35-959 Rzeszów, Poland, m.wojcik@prz.edu.pl

²Rzeszow University of Technology, Department of Materials Forming and Processing, Powstańców
Warszawy Av. 8, 35-959 Rzeszów, Poland, stafel@prz.edu.pl

Abstract

Due to the development of a sewerage system, as well as, the building of new treatment plants, the amount of generated sewage sludge is growing every year. The restrictions associated with the conventional utilization of sludge, for example in agriculture, result in the development of alternative methods. Sewage sludge alone or in conjunction with other waste indicates the usefulness in a production of different construction materials.

This paper shows the literature review associated with the application of sewage sludge and other fractions of waste in a civil engineering. The use of sewage sludge in a production of, for example cement, bricks and lightweight aggregates, is presented. The influence of waste on the characteristics of obtained materials was shown. The utilization of waste in a construction sector is an environmentally-friendly solution which can reduce the consumption of natural resources. Additionally, this utilization method promotes the idea of sustainable construction.

Keywords: *sewage sludge, waste, recycling, civil engineering, sustainable construction*

1. INTRODUCTION

Nowadays, the construction sector is one of the fastest-growing industries in the world. According to the General Statistical Office Report (2018), the production of new building materials grew of about 35% in the first quarter of 2018 and was the highest from 2007. The income from a construction sector generates approximately 10% of European Union Gross Domestic Product (GDP) (OKOYE 2016). The average person spends inside the building approximately 80% of his life (KRUSE 2016).

The construction sector also influences the environment in a significant way. For example, it consumes approximately 42% of the energy used in the world (MAZUR-WIERZBICKA 2014). The residential and commercial sector (homes and buildings) accounts for 30% of water and 50% of natural resources. Additionally, the construction sector is a main source of waste (PED-DAVENKATESU and NAIK 2016). According to The Statistical Office of the European Union (2016), the total amount of waste generated in the European Union in 2010 was over 2.5 billion

tonnes, of which almost 35% (860 million tonnes) derived from construction and demolition activities (*Figure 1*). In order to ensure the ecological safety, new technologies and materials in a building sector are required.

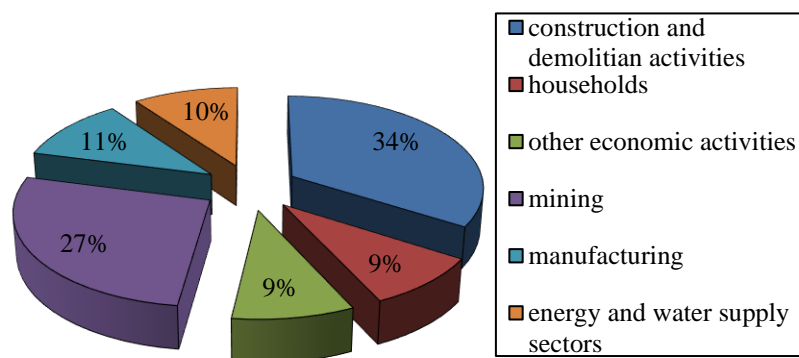


Figure 1
The production of waste in different sectors of economy

Nowadays, the construction sector is facing with the declining availability of raw materials, for example aggregates and sand. According to KOZIOŁ and KAWALEC (2008), the annual consumption of natural aggregates in Europe is approximately 6 tonnes per capita. The worldwide consumption of sand and gravel is 40 billion tonnes every year (MACHNIAK 2015). The perspective of the depletion of natural resources led to the development of a sustainable construction. The application of alternative sources in a production of different building materials is one of the main important aspects in a sustainable construction. In literature, the production of different construction materials, for example, bricks, concrete or ceramics with the application of waste is well known. BADR et al. (2012) produced bricks with the use of silica fume and rice husk biochar. CHIN et al. (1998) carried out the possibility of the production of construction materials by means of paper sludge. MOHAJERANI et al. (2017) described the production of asphalt with the use of cigarette butts. By means of that, waste might be converted into valuable constructive materials. The utilization of different fractions of waste in a civil engineering enables their recycling, as well as, promotes the idea of a sustainable development.

The use of sewage sludge in a construction sector is a promising concept. Sewage sludge is defined as a solid residue of wastewater treatment, which consists of water and suspended solids. With the increasing number of new residents attached to the sewerage system, the amount of generated sewage sludge is increasing every year (*Figure 2*). The statistics show that approximately 12 million tonnes of sewage sludge dry mass was produced in Europe in 2014 (The Statistical Office of the European Union 2016). Due to the introduction of general ban on sewage sludge landfilling in many European countries, new utilization methods are necessary. Economical, social, as well as environmental aspects caused the increasing interest of the application of sewage sludge in a construction industry. Sewage sludge alone or in conjunction of other waste might be used as a component for cement and bricks production or as an additive for cementitious inorganic binders. The

application of sewage sludge in a construction sector is also a promising approach to protect natural resources.

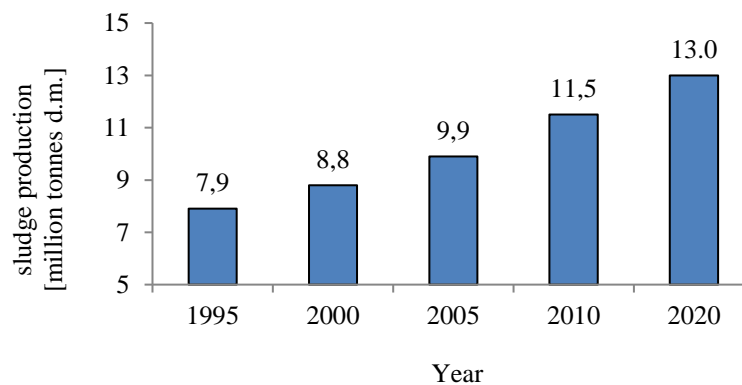


Figure 2

The production of sewage sludge in Europe

This paper presents the literature review associated with the production of sustainable construction materials with the application of sewage sludge and other waste. The selected physical and mechanical properties of obtained products were assessed. Recycling or recovery different fractions of waste in a construction sector might be a promising solution both in a civil and environmental engineering.

2. THE APPLICATION OF SEWAGE SLUDGE AND OTHER WASTE IN A CIVIL ENGINEERING

The following chapter presents the overall overview of previous research concerning the use of sewage sludge and other waste in a production of different construction materials. A number of experimental research were performed on the use of different materials in a construction sector. It was noted that waste indicates the usefulness in the production of, for example aggregates, bricks, cement or as an insulation (*Table 1, Figure 3*).

Table 1

The possible application of different waste in a construction sector

No.	Type of waste	Possible application
1.	Agro-industrial	<ul style="list-style-type: none"> – aggregates, – concrete, – bricks, – tiles, – insulation, – wall panels, – roof sheets

Table 1 (to be continued)

2.	industrial	<ul style="list-style-type: none"> – aggregates, – concrete, – bricks, – ceramic products, – surface furnishing materials
3.	Waste from mining	<ul style="list-style-type: none"> – aggregates, – concrete, – bricks, – blocks, – pavement materials

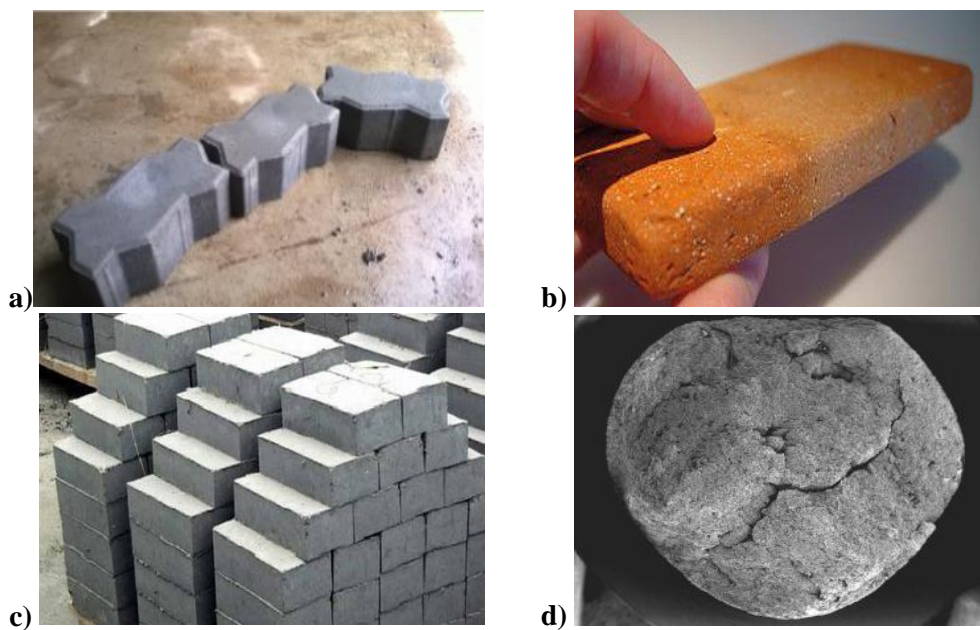


Figure 3

Examples of different building materials with the use of waste; pavement blocks contained sewage sludge ash (a); bricks contained sewage sludge (b); bricks produced with the use of sewage sludge ash and coal fly ash (c); aggregate obtained from sewage sludge ash and used motor oil (d); asphalt contained cigarette butts (e) (<https://www.slideshare.net/AmbaSasank/utilization-of-sewage-sludge-ash-in-construction-materials>; <https://www.treehugger.com/green-architecture/ecobrique-a-building-with-sewage.html>; <https://www.indiamart.com/proddetail/light-weight-fly-ash-brick-16687684062.html>; <https://ars.els-cdn.com/content/image/1-s2.0-S0958946510001009-gr8.jpg>)

Sewage sludge might be applied as a component in a brick production. Bricks contained different by-products might be even 30% cheaper than traditional products. TAY et al. (2002) noted that dried sewage sludge in conjunction with clay might be used in a brick production. The percentage share of dry sludge was in the range of 0 – 40%. The mixture of sludge and clay was grounded to fine particles with a diameter below 0.1 mm and formed. After that, the mixture was sintered. TAY et al. (2002) showed that the addition of sewage sludge resulted in the increase of the porosity of bricks. It was closely related with the decomposition of organic compounds contained in sewage sludge. But the aforementioned problem might be solved by the replacement of sewage sludge with sewage sludge ash. The compressive strength of bricks contained sewage sludge decreased as the sludge content increased (TAY et al. 2002).

ALLEMAN and BERMAN (1984) examined the properties of bricks obtained from sewage sludge, clay and shale. It was observed that conventional clay and shale might be supplemented with sewage sludge with a solid content of 15 –25%. The compressive strength of samples with sewage sludge was similar to conventional bricks. Additionally, obtained biobricks had the look, feel and smell of regular bricks (ALLEMAN and BERMAN 1984).

Ravikrishnan and Senthilselvan (2014) investigated the usefulness of sewage sludge and textile sludge in the manufacture of unburnt bricks. It was noted that sludge in a dosages of 5–25% might be a partial replacement for clay. The bricks contained sludge, were characterized by the higher compressive strength in comparison to conventional materials. For the dosages of sludge in the range of 5–20%, the aforementioned parameter was even 30% higher than for traditional bricks. But the optimal dosage of sludge was 10%. RAVIKRISHNAN and SENTHILSELVAN (2014) also noted that the porosity of bricks increased with the increase of the dosage of sludge. As a result, the water absorption increased and it was higher than for a control sample.

Sewage sludge ashes also indicate usefulness in a construction sector. Due to the increasing interest in thermal utilization methods, the aforementioned solution is a promising approach in waste management. JAMSHIDI et al. (2013) examined the possibility of the replacement of sand in a cement production by the use of sewage sludge ash (*Table 2*). In a laboratory research, dosages of 5, 10 and 20% were added. The results showed the decrease of a compressive strength with the increase of the dosage of ash after 28 and 90 days. The significant differences were observed for dosages of 10 and 20%. For 5% dosage of ash, the decrease of compressive strength was insignificant. It was also observed that the strength lost was proportional to the sewage sludge ash content. JAMSHIDI et al. (2013) also noted that the compressive strength of specimens with sewage sludge ash increased with curing time. The highest increase was noted for 20% dosage of sewage sludge ash. This could be explained by the fact that sewage sludge ash behaves like extra sites for the nucleation (PACHECO-TORGAL and GOMES 2006).

The application of sewage sludge ash in dosages of 5 and 10% did not influence the water adsorption in a significant way. However, the addition of 20% of ash resulted in the increase of the aforementioned parameter nearly twice. But it did not negatively influence the cement parameters (JAMSHIDI et al. 2013).

Table 2

The influence of the addition of sewage sludge ash on the selected parameters of cement (on the basis of studies carried out by JAMSHIDI et al. 2013)

No.	dosage of sewage sludge ash [%]	Compressive strength [MPa]	Flexural strength [MPa]	Capillary water adsorption coefficient [kg/m ² ·h·0.5]
1.	0	37.0	5.90	0.55
2.	5	35.0	5.10	0.57
3.	10	33.0	4.90	0.53
4.	20	29.0	4.20	0.95

MONZÓ et al. (1996) noted that sewage sludge ash is a reactive material which influences the change of mechanical properties of cement (Table 3). The addition of ash resulted in the decline of its workability with the increase of a dosage of ash. But this relationship was not linear. As reported by MONZÓ et al. (2003), the decrease of workability might be reduced by the application of plasticizers or super plasticizers.

The application of sewage sludge ash in the production of cement mortar also affected the increase of porosity and the water adsorption. This phenomenon was closely related with the addition of sewage sludge ash. The increase of water adsorption of mortar affects the deterioration of its mechanical properties. MONZÓ et al. (1996) noted that the compressive and flexural strength decreased as the dosage of sewage sludge ash increased. The application of sewage sludge ash in the highest tested dosage (30 wt.%) decreased the compressive strength by approximately 38% after 7 days and by approximately 23% after 28 days of curing. But all samples met the construction standards. The analysis of results also showed that specimens cured for 28 days indicated higher compressive strength than samples cured for 7 days. It was associated with the development of pozzolanic properties and the reactivity of sewage sludge ash which is a binding agent. It was also observed that specimens with the addition of 20 and 30% of sewage sludge ash indicated similar compressive strength after 28 days of curing (MONZÓ et al. 1996).

Table 3

The influence of the addition of sewage sludge ash on the selected parameters of cement mortars (on the basis of studies carried out by MONZÓ et al. 1996)

No.	dosage of sewage sludge ash [%]	Compressive strength after 7 days [MPa]	Compressive strength after 28 days [MPa]	Flexural strength [MPa]	water adsorption [%]
1.	0	45.0	52.0	8.0	8.2
2.	10	40.0	49.0	7.8	9.8
3.	20	34.0	42.0	7.0	11.0
4.	30	28.0	40.0	6.9	–

The properties of cement mortars contained sewage sludge ash were also examined by BAEZA-BROTONS et al. (2014). The obtained results showed that the addition of ash affected the decrease of density and water adsorption. The aforementioned parameters decreased with the increase of a dosage of sewage sludge ash. This phenomenon might be explained by the fact that fine particles of sewage sludge ash occupied the gaps between coarse aggregates. BAEZA-BROTONS et al. (2014) also showed the increase of porosity of cement mortars with the increase of a dosage of ash.

Sewage sludge, as well as, sewage sludge ashes indicates the usefulness in the production of lightweight aggregates. Lightweight aggregates are a granular material with bulk density below 1200 kg/m^3 . According to CHEESEMAN and VIRDI (2005), good quality aggregates should characterize by: (1) strong sintered ceramic core; (2) a dense surface layer with low water adsorption; (3) a nearly spherical shape. TUAN et al. (2013) examined the properties of aggregates obtained from sewage sludge and glass powder. The percentage share of sludge and glass powder was 70 and 30%; accordingly. Lightweight aggregates possessed a density of 1200 kg/m^3 , water adsorption of 1.2% and the crushing strength of 5.27 MPa. The addition of glass powder decreased the sintering temperature due to its low melting point. In other research, XU et al. (2006, 2008a, 2008b) tested aggregates derived from sewage sludge, clay and sodium silicate (Na_2SiO_3) in the amount of 22, 68 and 10%, respectively. Aggregates were sintered at a $1000 \text{ }^\circ\text{C}$. It was observed that Na_2SiO_3 in conjunction with sludge might be used as a binder in the production of lightweight aggregates. The usefulness of Na_2SiO_3 is associated with the fact that SiO_2 contained in Na_2SiO_3 enhances the formation of glassy phase of lightweight aggregates. The lightweight aggregate produced from sewage sludge, clay and Na_2SiO_3 had a bulk density of 575 kg/m^3 and the water adsorption of 10% (XU et al. 2006).

The usefulness of sewage sludge in the production of lightweight aggregates was also proved by LAU et al. (2017). The selected properties of aggregates obtained from sewage sludge, palm oil fuel ash and Na_2SiO_3 were examined (Table 4). Before the laboratory research, sewage sludge was treated with the use of lime (30 wt.%). The mixture was preheated at $200\text{--}800 \text{ }^\circ\text{C}$ with dwell time of 30 min. By means of that, the cracks on the sintered pellets were minimized. After that, pellets were sintered at $1200 \text{ }^\circ\text{C}$ with dwell time of 30 min.

The analysis of results showed that aggregates with higher content of sewage sludge indicated higher mass loss rate. It was closely related with the decomposition of organic compounds and the presence of CaO in sewage sludge. On the other hand, aggregates with a high content of palm oil fuel ash were characterized by the higher density. This is because palm ash possessed a lower melting point than sewage sludge. During sintering, palm oil fuel ash melted and formed a liquid phase which filled the gaps between particles. Depending on the content of sludge, palm fuel oil ash and Na_2SiO_3 , as well as the sintering temperature, the bulk density was in the range of $400\text{--}1300 \text{ kg/m}^3$. The density also increased with the increase of sintering temperature (LAU et al. 2017). According to KOCKAL and OZTURAN (2011), the increase of sintering caused that more voids were filled with more compounds. As a result, denser glassy and crystalline matrix was formed. The increase of density also affected the reduction of open pores in the aggregate matrix.

LAU et al. (2017) showed that aggregates produced from sewage sludge, palm oil fuel ash and Na_2SiO_3 were characterized by the different water adsorption. Depending on the content of sludge, palm fuel oil ash and Na_2SiO_3 , the water adsorption was from 2 to 75%. The aforementioned parameter increased as the dosage of sewage sludge increased. It could be explained by the fact that the high content of organic compounds in sewage sludge induces a higher loss of ignition and more

voids within an aggregate are created. As a result, water-permeable structure of aggregates was formed. However, the increase of sintering temperature resulted in the decline of water adsorption. The elevation of temperature caused the fusion of materials and contributed to a less water permeable surface (LAU et al., 2017). Aggregates contained a sodium silicate were characterized by the lower water adsorption. The presence of binder reduced the required sintering temperature to form glassy texture on the surface of aggregates. Such vitrified surface prevented the ingress of water into the aggregates bodies (WASSERMAN and BENTUR, 1997).

Depending on the chemical composition, mechanical properties of aggregates were different. LAU et al. (2017) noted that the crushing strength increased with the increase of a sintering temperature. It is associated with the forming a denser matrix at a higher temperature. Depending on the content of sludge, palm fuel oil ash and Na_2SiO_3 , the crushing strength was 5.0–8.1 MPa. It was also observed that the aforementioned parameter decreased as the content of sewage sludge increased. Because the presence of binder enhanced a vitrification, aggregates with sodium silicate were also characterized by the higher crushing strength than aggregates without binder. The presence of high glass-forming oxide (SiO_2) in the binder enhanced the viscosity of aggregates, forming a more vitrified surface which contributed to higher crushing strength (OJOVAN 2008).

Table 4

Selected parameters of aggregates produced from sewage sludge, palm oil fuel ash and Na_2SiO_3 (on the basis of studies carried out by LAU et al. 2017)

No.	Dosage [wt.%]			density [kg/m^3]	water adsorption [%]	shrinkage [%]	Crushing strength [MPa]	
	POFA	SS	Na_2SiO_3				1160°C	1180°C
1.	40	60	0	420	75	1.5	0.45	0.60
2.	50	50	0	440	68	2.0	0.50	0.92
3.	60	40	0	450	64	4.9	0.52	1.22
4.	40	60	10	500	57	6.0	0.55	1.40
5.	50	50	10	780	28	7.5	2.45	12.00
6.	60	40	10	785	25	12.0	2.50	25.00
7.	40	60	15	680	28	7.0	1.00	2.00
8.	50	50	15	1050	4.5	17.0	7.80	14.00
9.	60	40	15	1060	2	20.5	8.00	31.00
	limestone			≤ 1200	≤ 2.0	n/a	≈ 8.0	

SS – sewage sludge

POFA – palm oil fuel ash

n/a – not advisable

Due to the enhancement of sintering reaction, waste glass might be applied in a production of artificial aggregates (*Figure 4*). The waste glass contains a lot of Na_2O which influences the decrease of a sintering temperature. Properties of lightweight aggregates derived from sewage sludge and waste glass were examined by TUAN et al. (2013). The percentage share of sewage sludge and glass powder was 50–90% and 10–50%, respectively. The mixtures were sintered at 830–1100 °C. Before laboratory tests, glass powder was dried at 105 °C for 24 h and grounded in a ball mill to particle sizes of less than 150 μm . Natural stone was used as a control sample.

Depending on the percentage share of components, the characteristics of aggregates were different. The density was below 2 g/cm^3 for all samples. However, the density increased as a dosage of waste glass increased and decreased as the sewage sludge dosage increased. The water adsorption of aggregates decreased with the elevation of temperature. The significant reduction of water adsorption of aggregates with the increase of a dosage of glass was also observed. Depending on the dosage of glass and the sintering temperature, water adsorption was in the range of 1 – 45%. Na_2O in waste glass is melted at a relatively low temperature. Therefore, more viscous phases with lower viscosity are formed. As a result, the adsorption capacity is reduced (WEI et al. 2011). In a construction industry, the water adsorption below 20% is accepted.

TUAN et al. (2013) also examined the compressive strength of aggregates produced from sewage sludge and waste glass. It was noted that the average value of the aforementioned parameter was 49.46 MPa after 28 days. It meets the strength requirements of ASTM330 for structural lightweight aggregates. But granite aggregates were characterized by the higher compressive strength (approximately 67 MPa). Additionally, aggregates contained more waste glass were characterized by the higher compressive strength than other samples (TUAN et al. 2013).



Figure 4
Aggregates produced from sewage sludge and glass waste (an own source)

The ceramic tile industry indicates the potential for utilizing different waste, including sewage sludge. ZHOU et al. (2013) examined the microstructure and mechanical properties of tiles produced from sewage sludge, quartz, feldspar and kaolin. The content of sludge in tiles was in the range of 50–65 wt.%. The microstructure of obtained product was constructed by the crystal and vitreous phase.

The addition of sewage sludge also affected the properties of tiles. ZHOU et al. (2013) noted that when the content of sludge was lower than 60 wt.%, the water adsorption was below 1.5% and met the construction standards (below 3%). The water adsorption for commercial tiles was approximately 1%. The compressive strength increased as a dosage of sewage sludge decreased. For a

dosages of sludge below 60 wt.%, the compressive strength was approximately 25.5 MPa. Commercial tiles had a similar value of compressive strength (approximately 26 MPa).

ZHOU et al. (2013) also performed the leaching test of tiles contained sewage sludge (Table 5). The results were compared with findings for commercial tiles. It was noted that the leaching of all tested heavy metals from tiles with the addition of sludge was lower than the regulatory level. The low leaching of metals might be explained by their solidification and stabilization in the split tile body (ZHANG et al. 2007). The leaching of metals was also slightly higher than for conventional tiles.

Other applications of sewage sludge are related with a road construction. Sewage sludge ash indicates the usefulness as a portion of fine aggregates in hot mix asphalt paving. SAYED et al. (1995) examined the mechanical and chemical properties of asphaltic pavement mixes. It was noted that asphalt surface containing 2–2.5% of sewage sludge ash had similar mechanical parameters as traditional pavements. The usefulness of sewage sludge as a partial substitute for fine aggregates was also tested by JOSHI et al. (2016). VOUK et al. (2017) proved that sewage sludge in conjunction with grounded demolishing concrete might be used as a road layer. WÓJCIK et al. (2018) showed that unconventional material derived from sewage sludge, glass powder and quartz sand meets the construction standards and might be applied as a layer in a road construction (Figure 5).

Table 5

The leaching of selected heavy metals from tiles contained sewage sludge (on the basis of studies carried out by ZHOU et al. 2013)

No.	Metal	Leaching from tiles contained sewage sludge [mg/dm ³]	Leaching from commercial tiles [mg/dm ³]	Required level [mg/dm ³]
1.	Cu	0.23	0.06	-
2.	Cd	0.0009	0.0001	1.0
3.	Pb	0.014	0.005	5.0
4.	Cr	0.0009	0.0005	5.0
5.	Ni	0.15	0.11	-
6.	Ba	0.22	0.01	100.00
7.	Hg	ND	ND	0.2
8.	Be	0.0003	ND	-
9.	Zn	0.28	0.06	-
10.	Ag	ND	ND	5.0
11.	Se	0.0008	ND	1.0

ND – not detected



Figure 5

*Aggregates produced from sewage sludge, glass powder and quartz sand
(an own source)*

All aforementioned examples show the multidirectional applications of sewage sludge in a construction sector. The addition of different waste in the production of building materials is an economical and environmentally-friendly solution. However, it should be noted that the high dosages of sewage sludge (above 20–30 wt. %) influences the mechanical properties of final products negatively.

3. DISCUSSION

The possibility of the use of waste in a construction sector was proved by different researchers (see chapter above). Sewage sludge and other fractions of waste might be applied in a production of unconventional building materials. The major application of by-products is the production of lightweight aggregates and bricks. The least utilization is related with the manufacturing of tiles, ceramic materials, asphalt and cement.

Results obtained by different authors have shown that the most of final products contained waste meet the construction standards. On the basis of literature, it was stated that the addition of sewage sludge or other waste in the amount of below 20% of total mass has a different influence on the mechanical properties of final products (*Table 6*). The increase of compressive strength for small doses of waste was noted by MONZÓ et al. (2003) and VOUK et al. (2017). But the relationship was not linear. On the other hand, DONATELLO et al. (2010), PAN et al. (2003) and TAY (1986) showed the decrease of the aforementioned parameter after the addition of a small amount of sewage sludge. The influence of waste on the water adsorption of final products was also differential.

In any case, the high dosages of waste (above 40–50 wt. %) resulted in the decrease of mechanical characteristics of construction materials. Additionally, the addition of high dosages of sewage sludge might have a negative impact on the porosity of obtained products. This phenomenon is associated with the decomposition of organic compounds contained in sewage sludge. The porosity might be reduced by the replacement of sewage sludge by sewage sludge ash which is characterized by the lower content of organic compounds.

Table 6
The influence of the addition of waste on the compressive strength and the water adsorption of building materials

No.	building material	kind of waste	compressive strength	water adsorption	Source
1.	bricks	dry pulverized sludge	↑	↓	Yagüe et al. (2002)
2.	bricks	wastewater sludge	↑	n/a	Weng et al. (2003)
3.	artificial aggregates	dried industrial sludge	↓	n/a	Tay et al. (2002)
4.	cement	sewage sludge pellets	↑ for a dosages below 30% ↓ for higher dosages	n/a	Monzó et al. (2004)
5.	ceramic	sewage sludge	↑ for a dosages below 5% ↓ for higher dosages	↑ for a dosages below 30% ↓ for higher dosages	Martinez-Garcia et al. (2012)

↑ – increase of the parameter

↓ – decrease of the parameter

n/a – not advisable

Some researchers also examined the leaching of compounds from building materials contained waste. Sewage sludge or sewage sludge ash might be characterized by the high leaching of some metals, for example molybdenum, selenium or antimony. For some energetic waste, the high leaching of calcium, sodium and chlorine might be also observed (WÓJCIK et al. 2017). After the addition of different fractions of waste into construction materials, the increase of leaching of compounds was not noted. The samples contained by-products were characterized by the similar leachingability as control specimens (YIMING et al. 2012; LUCIANA et al. 2011; CHIANG et al. 2009). According to FRANUS et al. (2016), the sintering of materials contained waste results in the bonding of heavy metals in the aluminosilicate structure. Additionally, the heat-induced transformation caused the long-term stability of metals. By means of that, the utilization of waste in a construction sector might be considered as an environmentally-friendly solution.

A relatively new application of sewage sludge is the production of lightweight aggregates. Research carried out by different scientist has shown that aggregates contained sewage sludge, are characterized by the high porosity and the different structure (TUAN et al. 2013; WANG et al. 2009). It was closely related with the decomposition of organic compounds. But most of them meet the construction standards and might be used as a substitute of natural aggregates. Due to the shrinkage of supplies of natural aggregates, the aforementioned material is a promising option. Lightweight aggregates obtained from sewage sludge might be also applied in a production of cement or as a layer in a road construction.

4. CONCLUSIONS

The aforementioned literature review confirms the usefulness of sewage sludge and other waste in a civil engineering. The possibility of production different building materials with the use of waste was presented. The results presented in the paper show that sewage sludge in conjunction with other waste might be used in a production of:

- cement,
- bricks,
- ceramics and tiles,
- lightweight aggregates.

The application of different fractions of waste in a construction sector ensures their recycling in line with legal and environmental requirements. The utilization of waste in a civil engineering can also reduce the cost of the production of building materials while meeting the construction standards.

It can be concluded that the production of new construction materials with the addition of waste is a promising approach which can protect the natural resources. The idea of “sustainable construction” based on the production of alternative materials should be implemented and widely promoted.

REFERENCES

- [1] ALLEMAN, J. E.–BERMAN, N. A. (1984): Constructive sludge management: Biobrick. *Journal of Environmental Engineering*, 110 (2), pp. 301–311. DOI: 10.1061/(ASCE)0733-9372(1984)110:2(301).
- [2] BADR, E. D. E. H. et al. (2012): Incorporation of water sludge, silica fume and rice husk ash in brick making. *Advances in Environmental Research*, 1, pp. 83–96.
- [3] BAEZA-BROTOS, F. et al. (2014): Portland cement systems with addition of sewage sludge ash. Application in concretes for the manufacture of blocks. *Journal of Cleaner Production*, 82, pp. 112–124. DOI: 10.1016/j.clepro.2014.06.072.
- [4] CHEESMAN, C. R.–VIRDI, G. S. (2005): Properties of microstructure of lightweight aggregate produced from sintered sewage sludge ash. *Resources, Conservation & Recycling*, 45 (1), pp. 18–30. DOI: 10.1016/j.resconrec.2004.12.006.
- [5] CHIANG, K. Y. et al. (2009): Lightweight bricks manufactured from water treatment sludge and rice husks. *Journal of Hazardous Materials*, 171 (1-3), pp. 76–82. DOI: 10.1016/j.hazmat.2009.05.144.
- [6] CHIN, T. L. et al. (1998): A novel method to reuse paper sludge and co-generation ashes from paper mill. *Journal of Hazardous Materials*, 58, pp. 93–102.
- [7] DONATELLO, S. et al. (2010): Effect of milling and acid washing on the pozzolanic activity of incinerator sewage sludge ash. *Cement and Concrete Composites*, 32 (1), pp. 54–61. DOI: 10.1016/j.cemconcomp.2009.09.002.

- [8] FRANUS, M. et al. (2016): Utilization of sewage sludge in the manufacture of lightweight aggregate. *Environmental Monitoring and Assessment*, 188 (1), pp. 1–16. DOI: 10.1007/s10661-015-5010-8.
- [9] <https://ars.els-cdn.com/content/image/1-s2.0-S0958946510001009-gr8.jpg> (accessed: 17. 09. 2018).
- [10] <https://www.indiamart.com/proddetail/lightweight-fly-ash-brick-16687684062.html> (accessed: 17. 09. 2018).
- [11] <https://www.slideshare.net/AmbaSasank/utilization-of-sewage-sludge-ash-in-construction-materials> (accessed: 17. 09. 2018).
- [12] <https://www.treehugger.com/green-architecture/ecobrique-a-building-with-sewage.html> (accessed: 17. 09. 2018).
- [13] JAMSHIDI, A. (2013): Mechanical Performance of Concrete With Partial Replacement of Sand by Sewage Sludge Ash From Incineration. *Materials Science Forum*, 730-732, pp. 462-467.
- [14] JOSHI, M. S. et al. (2016): Utilization of Sewage Sludge in Construction Material. *Imperial Journal of Interdisciplinary Research*, 2 (7), pp. 277–279.
- [15] KOCKAL, N. U.–OZTURAN, T. (2011): Characteristic of lightweight fly ash aggregates produced with different binders and heat treatments. *Cement and Concrete Composites*, 33 (1), pp. 61–67. DOI: 10.1016/j.cemconcomp.2010.09.007.
- [16] KOZIOŁ, W.–KAWALEC, P. (2008). Kruszywa alternatywne w budownictwie. *Nowoczesne Budownictwo Inżynieryjne*, 4, pp. 34–37 (in Polish).
- [17] KRUSE, K. (2016): The 80/20 Rule and How It Can Change Your Life. <https://www.forbes.com/sites/kevinkruse/2016/03/0780-20-rule/> [access: 15. 09. 2018].
- [18] LAU, P. C. et al. (2017): Characteristics of lightweight aggregate produced from lime-treated sewage sludge and palm oil fuel ash. *Construction and Building Materials*, 152, pp. 558–567. DOI: 10.1016/j.conbuildmat.2017.07.022.
- [19] LUCIANA, C. S. H. et al. (2011): Characterization of ceramic bricks incorporated with textile laundry sludge. *Ceramics International*, 38 (2), pp. 951–959. DOI: 10.1016/j.ceramint.2011.08.015.
- [20] MACHNIAK, Ł. (2015): Przestrzenny rozkład zapotrzebowania na kruszywa w budownictwie jednorodzinym. *Zeszyty Naukowe Instytutu Gospodarki Surowcami Mineralnymi i Energią Polskiej Akademii Nauk*, 91, pp. 149–159 (in Polish).
- [21] MARTÍNEZ-GARCÍA, C. et al. (2012): Sludge valorization from wastewater treatment plant to its application on the ceramic industry. *Journal of Environmental Management*, 95, pp. S343–S348. DOI: 10.1016/j.envman.2011.06.016.
- [22] MAZUR-WIERZBICKA, E. (2014): Ecoinnovations – an Important Element of Sustainable Construction. *Handel Wewnętrzny*, 5 (352), pp. 138–148 (in Polish).

- [23] MOHAJERANI, A. et al. (2017): Physico-mechanical properties of asphalt concrete incorporated with encapsulated cigarette butts. *Construction and Building Materials*, 153, pp. 69–80. DOI: 10.1016/j.conbuildmat.2017.07.091.
- [24] MONZÓ, J. et al. (1996): Use of Sewage Sludge Ash (SSA)-Cement Admixtures in Mortars. *Cement and Concrete Research*, 26 (9), pp. 1389–1398.
- [25] MONZÓ, J. et al. (2003): Reuse of sewage sludge ashes (SSA) in cement mixtures: the effect of SSA on the workability of cement mortars. *Waste Management*, 23 (4), pp. 373–381. DOI: 10.1016/S0956-053X(03)00034-5.
- [26] MONZÓ, J. et al. (2004): Some strategies for reusing residues from waste water treatment plants: preparation of binding materials. In: VÁZQUEZ, E. et al. (eds.): *Proceeding of the Conference on the Use of Recycled Material in Building and Structures*. Barcelona, Spain, 8–11 November, International Union of Laboratories and Experts in Construction Materials RILEM, pp. 814–823.
- [27] OJOVAN, M.I. (2008): Viscosity and Glass Transition in Amorphous Oxides. *Advances in Condensed Physics*, 2008, pp. 1–23. DOI: 10.1155/2008/817829.
- [28] OKOYE, P. (2016): Imperatives of Economic Fluctuations in the Growth and Performance of Nigeria Construction Sector. *Microeconomics and Macroeconomics*, 4 (2), pp. 46–55. DOI: 10.5923/j.m2economics.20160402.02.
- [29] PACHECO-TORGAL, F. et al. (2006): Influence of physical and geometrical properties of granite and limestone aggregates on the durability of a C20/25 strength class concrete. *Construction and Building Materials*, 20, pp. 1079–1088. DOI: 10.1016/j.conbuildmat.2005.01.063.
- [30] PADDAVENKATESU, Y.–NAIK, B. H. (2016): Waste Minimisation in Construction Industry. *International Journal of Innovative Research in Science, Engineering and Technology*, 5 (10), pp. 18023–18030. DOI: 10.15680/IJRSET.2016.0510108.
- [31] PAN, S-C. et al. (2003): Reusing sewage sludge ash as adsorbent for copper removal from wastewater. *Resources, Conservation and Recycling*, 39(1), pp. 79-90. DOI: 10.1016/S0921-3449(02)00122-2.
- [32] RAVIKRISHNAN, S.–SENTHILSELVAN, S. (2014): Novel Green Bricks manufactured from Textile ETP Sludge. *International Journal of Scientific & Engineering Research*, 5 (6), pp. 76–81.
- [33] SAYED, M. H. Al. et al. (1995): Use of sewage sludge ash in asphaltic paving mixes in hot regions. *Construction and Building Materials*, 9 (1), pp. 19–23. DOI: 10.1016/0950-0618(95)92856-C.
- [34] TAY, J. H. et al. (2002). Potential reuse of wastewater sludge for innovative applications in construction aggregates. *Water Science and Technology*, 50 (9), pp. 189–196.
- [35] TAY, J-H. (1986): Potential use of sludge ash as construction material. *Resources and Conservation*, 13 (1), pp. 53–58. DOI: 10.1016/0166-3097(86)90006-4.

- [36] The statistical office of the European Union. Sewage sludge production and disposal from urban wastewater 2016.
- [37] TUAN, B. L. A. et al. (2013): Development of lightweight aggregate from sewage sludge and waste glass powder for concrete. *Construction and Building Materials*, 47, pp. 334–339. DOI: 10.1016/j.conbuildmat.2013.05.039.
- [38] VOUK, D. et al. (2017): Use of Sewage Sludge Ash in Cementitious Materials. *Reviews of Advanced Materials Science*, 49, pp. 158–170.
- [39] WANG, X. et al. (2009): Development of lightweight aggregate from dry sewage sludge and coal ash. *Waste Management*, 29 (4), pp. 1330–1335. DOI: 10.1016/j.wasman.2008.09.006.
- [40] WASSERMAN, R.–BENTUR, A. (1997): Effect of lightweight fly ash aggregate microstructure on the strength of concretes. *Cement and Concrete Research*, 27 (4), pp. 525–537. DOI: 10.1016/S0008-8846(97)00019-7.
- [41] WEI, Y-L. et al. (2011): Preparation of low water-sorption lightweight aggregates from harbour sediment added with waste glass. *Marine Pollution Bulletin*, 63 (5–12), pp. 135–140. DOI: 10.1016/j.marpolbul.2011.01.037.
- [42] WENG, C-H. et al. (2003): Utilization of sludge as brick materials. *Advances in Environmental Research*, 7 (3), pp. 679–685. DOI: 10.1016/S1093-0191(02)00037-0.
- [43] WÓJCIK, M. et al. (2017): The possibility of the application of fly ashes in order to the improvement of sewage sludge dewatering. *Journal of Civil Engineering, Environment and Architecture JCEEA*, 64 (1), pp. 377–393. DOI: 10.7862/rb.2017.35 (in Polish).
- [44] WÓJCIK, M. et al. (2018): Unconventional material from sewage sludge with a potential application in a road construction. In: SAMOŁYK, G. (eds.): *Progressive technologies and materials in mechanical engineering PRO-TECH-MA 2018*. Lublin, Poland, 21–23 June, Lublin University of Technology, pp. 11–13.
- [45] XU, G.R. et al. (2006): Utilization of dried sludge for making ceramsite. *Water Science & Technology*, 54 (9), pp. 69–79.
- [46] XU, G.R. et al. (2008a): Ceramsite Made with Water and Wastewater Sludge and its Characteristics Affected by SiO₂ and Al₂O₃. *Environmental Science & Technology*, 42 (19), pp. 7417–7423.
- [47] XU, G.R. et al. (2008b). Effect of sintering temperature on the characteristics of sludge ceramsite. *Journal of Hazardous Materials*, 31 (2), pp. 394–400. DOI: 10.1016/j.hazmat.2007.04.121.
- [48] YAGÜE, A. et al. (2002): Use of dry sludge from waste water treatment plants as an additive in prefabricated concrete brick. *Materiales de Construcción*, 52 (267), pp. 31–41. DOI: 10.3989/mc.2002v52.i267.324.

-
- [49] YIMING, L., et al. (2012): Utilization of municipal sewage sludge as additives for the production of eco-cement. *Journal of Hazardous Materials*, 213–214, pp. 457–65. DOI: 10.1016/j.hazmat.2012.02.020.
 - [50] ZHANG, H. Y. et al. (2007): Study on use of MSWI fly ash in ceramic tile. *Journal of Hazardous Materials*, 141, pp. 106–114. DOI: 10.1016/j.jhazmat.2006.06.100.
 - [51] ZHOU, J. et al. (2013): Direct-utilization of sewage sludge to prepare split tiles. *Ceramics International*, 39, pp. 9179–9186. DOI: 10.1016/j.ceramint.2013.05.019.



EXPERIMENTAL INVESTIGATION OF APPLICABILITY OF BAKONYOSZLOP SUB-BITUMINOUS COAL IN SEWAGE SLUDGE TREATMENT

ÁKOS PINTÉR-MÓRICZ¹–JÁNOS TAKÁCS²–LJUDMILLA BOKÁNYI³

¹Institute of Raw Material Preparation and Environmental Processing,
University of Miskolc and Research Institute of Applied Earth Sciences,
University of Miskolc 3515 Miskolc-Egyetemváros, pinter@afki.hu

²Institute of Raw Material Preparation and Environmental Processing,
University of Miskolc, 3515 Miskolc-Egyetemváros, ejttaki@uni-miskolc.hu

³Institute of Raw Material Preparation and Environmental Processing,
University of Miskolc, 3515 Miskolc-Egyetemváros, ejtblj@uni-miskolc.hu

Abstract

Superfast anaerobic stabilization of municipal sewage sludge being investigated at Institute of Raw Material Preparation and Environmental Processing of the University of Miskolc inheres involving the adsorbents. The adsorption of the water soluble compounds on the coal surface is a part of this stabilization process. Therefore, it is important to investigate the adsorption properties of the coal. Heavy metals can be suitable for determining adsorption properties since they are pollutants and they can be found in sewage sludge in mainly dissolved (ionic) form.

The adsorption of lead and cadmium heavy metal ions on the high humic acid containing Hungarian sub-bituminous coal was experimentally investigated as an adsorbent candidate. Coal of different particle size was used in the measurements. Initial concentrations of Cd- and Pb-nitrate and -acetate were varied as well. Constants of the Langmuir and the Freundlich type adsorption isotherms were calculated from the measured data, and the obtained isotherms were plotted. The effect of the heavy metal ions, the anions and the particle size, along with the changes in pH, are discussed. Further aims and directions of the research are also formulated.

Keywords: adsorption, cadmium, coal, isotherm, lead, sewage sludge.

1. INTRODUCTION

Sub-bituminous Bakonyoszlop coal is planned to be used in sewage sludge treatment as adsorbents. Therefore, the aim of our research work is to determine the adsorption properties of Hungarian sub-bituminous coal from Bakonyoszlop. This coal is reported by DUSZÉN Bányászati és Szolgáltatási Kft to have high humic acids content. Humic substances are known for their very good adsorption properties (FERRO-GARCÍA et al. 1998; KLUCÁKOVÁ and OMELKA 2004), thus, we can expect good adsorption properties of our coal sample as well. Before performing the experimental investigation of organic material adsorption, heavy metal ion adsorption on this high humic acid content coal was investigated. During our adsorption tests for removing heavy metal ions from their solution, different particle size Bakonyoszlopi brown coal was used as adsorbents.

2. ADSORPTION

Adsorption is defined as the adhesion of a chemical species onto the surface of solid particles. These components, even at extremely small concentrations, can be selectively captured and removed from gaseous or liquid phase. Adsorption takes place on active sites of the surface of the adsorbent.

The properties of the material being adsorbed and the properties of the surface of the adsorbent mutually determine the quality of adsorption.

Activated carbon is among the most widely used adsorbent (BERECZ 1988). The adsorption on activated carbon is a physical adsorption, which is usually referred to as physisorption. In the special literature activated carbon is the most frequently used carbon based adsorbent. However, carbon nanotubes are also applied. Adsorption on coal can be used for removing heavy metal ions from wastewater.

3. ADSORPTION ISOTHERMS

The curve where the variation in the amount of material adsorbed is plotted versus the concentration of the solution or the partial pressure of the gas component at constant temperature is called adsorption isotherm. The changes of equilibrium concentrations can be studied on the basis of the adsorption isotherms, thus, during an adsorption process the first step is the plotting of the equilibrium isotherm.

The adsorption isotherm can be characterized by three physical quantities: temperature (T), pressure (p) or concentration (c) and the fraction of the adsorption sites occupied (surface coverage, Γ).

The isotherm equations were basically developed for describing gas-solid system processes. However, they can be applied for description of liquid-solid systems as well, in some cases, as empiric equations. The isotherm equation that describes the given equilibrium the most properly should be determined.

A general adsorption isotherm equation valid for gases, gas mixtures and fluids was developed by Langmuir. He presumed that on the surface of adsorbents there are active sites (active centres) on the surface of the adsorbent. They are energetically equivalent. There is no interaction between the adsorbed molecules. Each active site adsorbs one molecule, thus, the layer is mono molecularly covered. Between the adsorption layer and the adsorbed medium an equilibrium occurs, where the speeds of the reverse processes are equal. The Langmuir equation for k adsorbed component, whose fluid phase concentration is c_k :

$$q_k = \frac{a_k \cdot c_k}{1 + b_k \cdot c_k}$$

where a_k, b_k : constants of the Langmuir equation

q_k : solid phase concentration of k component

c_k : liquid phase concentration of k component.

TÓTH (2001) introduced the Tóth isotherm constants:

$$\Theta = K_T p [1 + (K_T p)^t]^{-\frac{1}{t}}$$

where $\Theta = q/q_{\max}$, q and q_{\max} are the adsorption and the maximum adsorption, respectively, K_T and t are the Tóth isotherm equation constants, while p is the equilibrium pressure.

There is a q_{\max} at a certain c_k value from where the q_k is not increasing anymore. If there are significant differences between the obtained measurement data and the calculated isotherm equation data, other isotherms should be used.

Adsorption of polar components on polar adsorbent can be described with the Freundlich isotherm:

$$q_k = a_k \cdot c_k^{\frac{1}{n}}$$

where q_k : solid phase concentration of k component
 c_k : liquid phase concentration of k component
 n : constant
 a_k : constant (characteristic for the adsorbed component)

This equation is fully empirical. The plotted curve is infinite, there is no q_{\max} reached on it.

4. CHARACTERIZATION OF THE COAL

The Bakonyozslop coal belongs to the brown coal resources located in the Hungarian Transdanubian Mountains, as it was shown by PERGER (2009) and also written by Fekete and by Geománia. There Eocene and Oligocene brown coals can be found, which have high humic acids content. The Dudar coal, mined just next to the Bakonyozslop site, has as much as 60 percent humic acids content (as it was determined by DUSZÉN Bányászati és Szolgáltatási Kft.), which can worldwide be considered a high number.

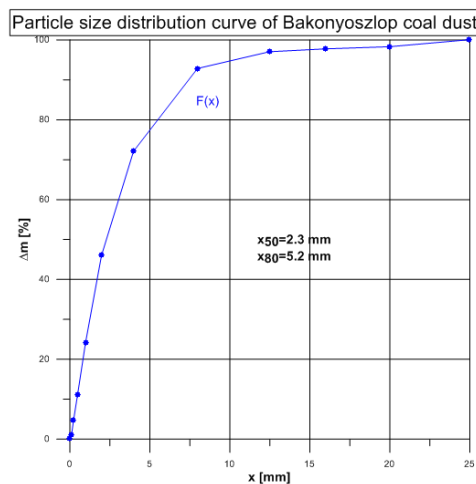


Figure 1
Particle size distribution
of the Bakonyozslop coal dust

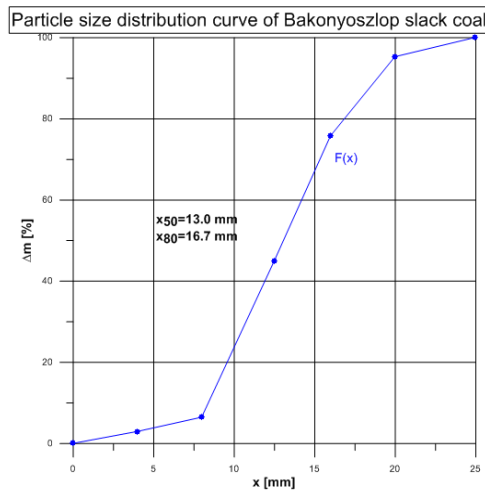


Figure 2
Particle size distribution
of the Bakonyozslop slack coal

Two coal samples were used for the experiments: slack coal from Bakonyoszlop and coal dust from Bakonyoszlop. Both coal types were analyzed, first, the particle size distribution of the samples was determined. The particle size distribution of the Bakonyoszlop coal samples are shown in Figures 1–2.

After the particle size analysis, two particle size intervals were selected per coal type. From the slack coal, the 12.5–20 mm particle size interval and the 4–12.5 mm particle size interval were chosen. From the coal dust, the 8–12.5 mm and the <8 mm particle size intervals were selected for further investigation. The aim of this was to investigate the effect of particle size on the adsorption capacity. The coal samples are shown in Figures 3–6.



Figures 3., 4., 5. and 6. (from left to right) Bakonyoszlop slack coal (12.5–20 mm) sample, Bakonyoszlop slack coal (4–12.5 mm) sample, Bakonyoszlop coal dust (8–12.5 mm) sample, Bakonyoszlop coal dust (<8 mm) sample

Before the adsorption measurements, the moisture and ash content of the 4 different particle size Bakonyoszlop coal samples were determined, which can be seen in *Table 1*.

Table 1
Moisture and ash content of the coal samples

Particle size of the coal	Moisture	Ash content (%)	
		dry	wet
Slack 12.5–20 mm	19.91	11.34	9.08
Slack 4–12.5 mm	22.33	8.57	6.66
Dust 8–12.5 mm	20.33	14.83	11.82
Dust <8 mm	20.48	19.77	15.72

The specific area of the 4 different particle size Bakonyoszlop coal samples were also determined before the adsorption measurements, these data are presented in *Table 2* (courtesy of Tibor Ferenczi).

Table 2
Specific area of the coal samples

Particle size of the coal	Single point BET m ² /g	Multi point BET m ² /g	Langmuir m ² /g
Slack 12.5–20 mm	12.5950	13.2517	18.4102
Slack 4–12.5 mm	39.9550	42.3417	59.5620
Dust 8–12.5 mm	29.0268	30.5753	42.8981
Dust <8 mm	17.1196	18.1722	25.4592

5. MATERIALS AND METHODS

The adsorption capacity of the Bakonyoszlop coal was investigated by determining the adsorption isotherms of two heavy metal ions, cadmium and lead, which both can occur in municipal sewage sludge. Cadmium and lead from nitrate and from acetate were also used for the measurement to investigate the adsorption in the presence of two different anions, one of which is originating from an organic acid. The applied salts (lead nitrate, lead acetate, cadmium nitrate, cadmium acetate) were of analytical purity and they were the products of VWR International (nitrates) and Sigma-Aldrich (acetates). Having 4 salts and 4 particle size fractions, 16 adsorption measurements were performed.

A Wise Cube WIS-20 shaking machine (see Figure 7) was used at 25 °C. The shaking speed was 150 1/min. The duration of the shaking was selected to be 4 hours (a preliminary measurement showed that between 2, 4, 6 and 8 hours of shaking there is no significant difference between the adsorbed heavy metal ions).

The weight of the added coal was 10.00 grams (coal dust under 8 mm) or ~10 grams (8–12.5 mm coal dust, 4–12.5 mm slack coal, 12.5–20 mm slack coal), which were weighed on a digital scale.

The measurements were performed with 20, 50, 80, 100, 200, 300, 400, 600, 800 and 1000 mg/L solutions of lead and cadmium ions. Stock solutions were first prepared, the necessary amount of metal salt for 1 dm³ of the highest concentration solution (1000 mg/l) was weighed on an analytical scale and it was diluted with distilled water. Then the dilution series were prepared by using this stock solution and distilled water. The coal samples and the solutions were put in 250 cm³ Erlenmeyer flasks. The amount of the heavy metal solutions was exactly ten times as much as the weight of the coal sample. The amounts of the necessary stock solution and distilled water were previously calculated. The diluted solutions were prepared in the Erlenmeyer flasks by using automated pipettes. Plastic cups were mounted on these flasks before measurements.

Before the adsorption tests the pH of the prepared solutions (20...1000 mg/L) were measured by a Mettler Toledo Seven Easy pH measurement device. Since the adsorption is strongly pH dependent, as it was explained by JEAN and BANCROFT (1986), the solutions had to be adjusted to approximately the same pH value. The adjusted pH-s were selected to be between 5.0–5.2. Very small amounts of 0.1 M sodium hydroxide or hydrochloric acid solutions were used for this process. The samples in the Erlenmeyer flasks were put in a vacuum drying oven for 30 minutes to ensure the penetration of the solution to the whole surface area of the coal grains.



Figure7
Wise Cube shaking machine used for the measurements

After stopping the shaking machine, the content of the flasks was filtered through a filter paper ($d = 150$ mm, specific weight = 84 g/mm²). The filtrate was split into two parts, they were put into plastic cups. To one of them, 2 ml concentrated (68%) nitric acid was added with pipette in order to preserve the sample, it was stored in a fridge at 4 °C till chemical analysis. The other part underwent pH measurement in order to observe any pH changes.

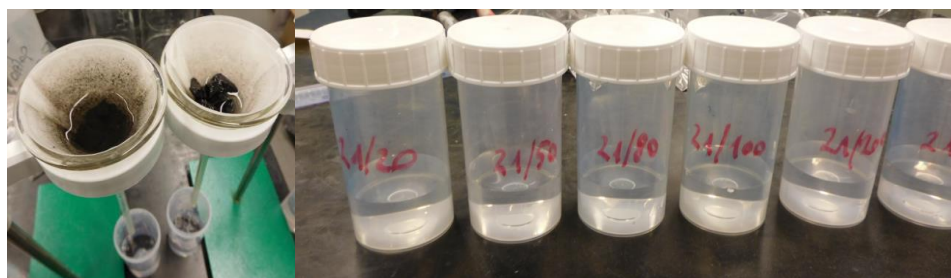


Figure8. (left) Filtering of the samples after shaking, Figure 9. (right) Samples before concentration analysis

The determination of Pb and Cd concentrations of the samples (stored in fridge) took place in the Department of Chemistry, University of Miskolc with the contribution of dr. János Lakatos by a Philips PU 9100 X atomic absorption spectrometer.

6. RESULTS AND DISCUSSION

The adsorption capacity of the coal (q_{eq} , mmol/g) at equilibrium state was calculated with the following relationship:

$$q_{eq} = \frac{(c_0 - c_{eq}) \cdot V}{m}$$

where c_0 : concentration before adsorption in the solution [mmol/L]
 c_{eq} : equilibrium metal ion concentration in the solution [mmol/L]
 V : volume of the solution [L]
 m : weight of the adsorbent [g]

Curves were fitted on the empirical measurement points in order to determine the constants of the Freundlich and Langmuir isotherm equations.

The following formulae and abbreviations were used to express the determined isotherm equations:
 Langmuir isotherm:

$$q_{eq} = q_{max} \frac{c_{eq}}{b + c_{eq}}$$

where q_{eq} : concentration in the adsorbed phase (on the surface)
 c_{eq} : concentration in the main fluid phase
 q_{max} : maximum adsorption capacity
 b : constant

Freundlich-isotherm

$$q_{eq} = K_F \cdot c_{eq}^n$$

where q_{eq} : concentration in the adsorbed phase (on the surface)
 c_{eq} : concentration in the main fluid phase
 K_F , n : constants.

The calculated constants of the isotherms are shown in *Tables 3–6* for all types and particle size coals.

Table 3
Constants of the obtained adsorption isotherms for cadmium from cadmium nitrate

Particle size of the coal	Langmuir isotherm		Freundlich isotherm	
	q_{max}	b	K_F	n
Slack 12.5–20 mm	0.01051	2.5384	0.00246	0.6512
Slack 4–12.5 mm	0.01491	0.7907	0.00573	0.6244
Dust 8–12.5 mm	0.01845	0.0821	0.02621	0.5612
Dust <8 mm	0.02312	0.0789	0.04694	0.6361

Table 4
Constants of the obtained adsorption isotherms for cadmium from cadmium acetate

Particle size of the coal	Langmuir isotherm		Freundlich isotherm	
	q_{\max}	b	K_F	n
Slack 12.5–20 mm	0.00712	2.5661	0.00220	0.8227
Slack 4–12.5 mm	0.01848	0.3060	0.00483	0.5573
Dust 8–12.5 mm	0.01485	0.1223	0.01549	0.4868
Dust <8 mm	0.14930	2.4524	0.04713	0.6582

Table 5
Constants of the obtained adsorption isotherms for lead from lead nitrate

Particle size of the coal	Langmuir isotherm		Freundlich isotherm	
	q_{\max}	b	K_F	n
Slack 12.5–20 mm	0.01507	0.1226	0.01403	0.3493

Table 6
Constants of the obtained adsorption isotherms for lead from lead acetate

Particle size of the coal	Langmuir isotherm		Freundlich isotherm	
	q_{\max}	b	K_F	n
Slack 12.5–20 mm	0.00812	0.06864	0.01120	0.4873

The isotherm data for the 4–12.5 mm slack coal and both coal dusts are missing for the lead salts, since no adsorption isotherms could be obtained from the measurement data. Almost all the lead ions were absorbed by the coal samples according to the atomic absorption spectrometry concentration measurements.

The correlation factor and correlation index between the measurement data and the calculated isotherm points was calculated for all isotherms. These results are shown in *Table 7*.

Table 7
Correlation factors and correlation indexes between the measurement points and the calculated isotherms

Particle size of the coal	Correlation factor		Correlation index	
	Langmuir	Freundlich	Langmuir	Freundlich
Cd nitrate, Slack 12.5–20	0.9192	0.8314	0.9171	0.7718
Cd nitrate, Slack 4–12.5	0.8158	0.8303	0.7931	0.8110
Cd nitrate, Dust 8–12.5	0.6951	0.9352	0.5113	0.9164
Cd nitrate, Dust <8 mm	0.8022	0.9823	0.5557	0.9723
Cd acetate, Slack 12.5–20	0.8251	0.6919	0.6584	0.4995

Particle size of the coal	Correlation factor		Correlation index	
	Langmuir	Freundlich	Langmuir	Freundlich
Cd acetate, Slack 4–12.5	0.9395	0.9442	0.9100	0.9425
Cd acetate, Dust 8–12.5	0.8524	0.9779	0.7525	0.9716
Cd acetate, Dust <8 mm	0.9915	0.9928	0.9724	0.9921
Pb nitrate, Slack 12.5–20	0.8471	0.7635	0.8112	0.7143
Pb acetate, Slack 12.5–20	0.8534	0.9830	0.7604	0.9765

The higher correlation factors and indexes are marked with bold letters. It can be seen from *Table 7* that the bold numbers occur much more frequently in the Freundlich isotherm columns (7:3 in both cases). It means that the Freundlich isotherms are closer to the measured data than the Langmuir isotherm, thus, we decided to use the Freundlich isotherms in the future. The obtained Freundlich adsorption isotherms are shown in Figures 10–16.

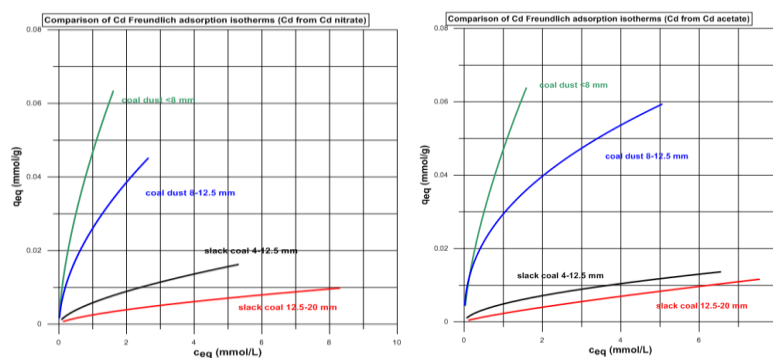


Figure 10. (left) Adsorption isotherms for cadmium from cadmium nitrate, Figure 11. (right) Adsorption isotherms for cadmium from cadmium acetate

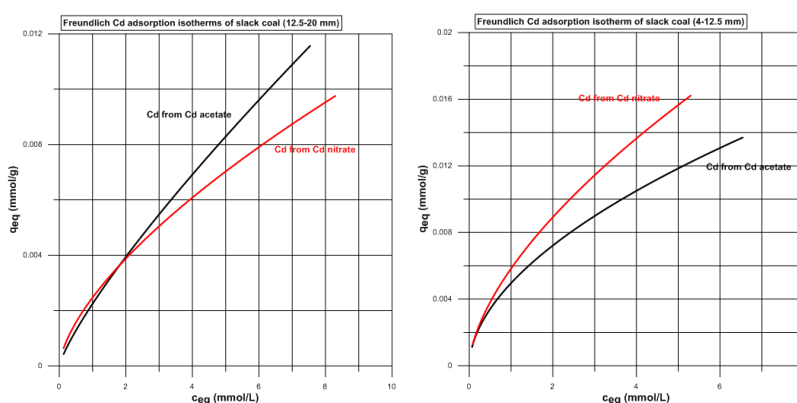


Figure 12. (left) Cadmium adsorption isotherms: 12.5–20 mm slack coal (Cd from nitrate and acetate), Figure 13. (right) Cadmium adsorption isotherms: 4–12.5 mm slack coal (Cd from nitrate and acetate)

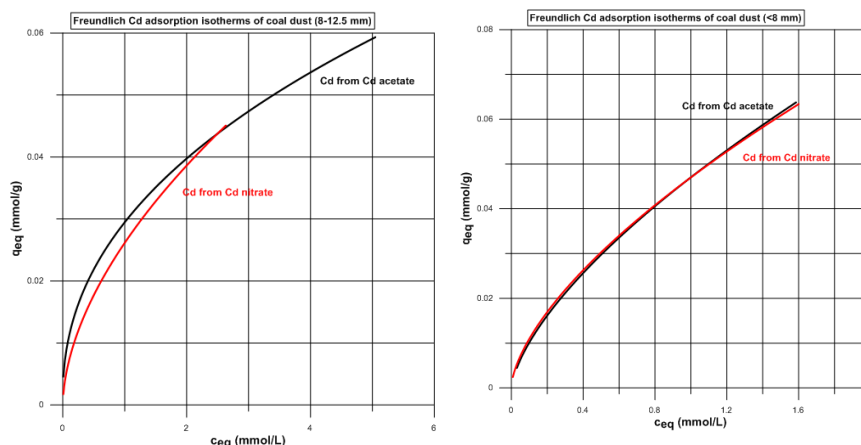


Figure 14. (left) Cadmium adsorption isotherms: 8–12.5 mm coal dust (Cd from nitrate and acetate), Figure 15. (right) Cadmium adsorption isotherms: <8 mm coal dust (Cd from nitrate and acetate)

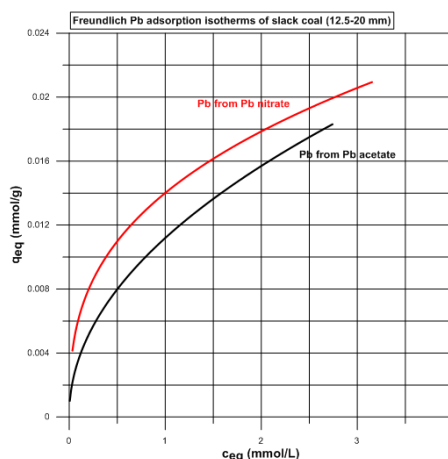


Figure 16
Lead adsorption isotherms: 12.5–20 mm slack coal (Pb from nitrate and acetate)

On the basis of our measurements and calculations it can be assessed that adsorption affinity of the lead is higher than the adsorption affinity of the cadmium at all particle size Bakonyoszlopi sub-bituminous coal samples (Tables 3–6, Figures 10–16).

The highest adsorption capacity could be calculated for <8 mm coal dust, the second highest for the 8–12.5 mm coal dust, the third highest for the 4–12.5 mm slack coal, while the lowest adsorption capacity was calculated for the 12.5–20 mm slack coal. Thus, it can be stated that higher maximum adsorption capacities could be calculated for smaller particle size coals (Tables 3–6, Figures 10–11). In Figure 12 it can be seen that the cadmium adsorption capacity of the 12.5–20 mm slack coal is higher when the Cd was from Cd nitrate than when it was from Cd acetate. On the other hand, in

Figures 13–14 it can be seen that the cadmium adsorption capacity of the 4–12.5 mm slack coal and the 8–12.5 mm coal dust was higher when the Cd was from Cd acetate than it was from Cd nitrate. In *Figure 15* (coal dust, <8 mm) the two determined isotherms are almost identical. As for the lead, in *Figure 16* it can be noticed that the Pb adsorption capacity is higher when the Pb was from Pb nitrate than when it was from Pb acetate. Overall, in two cases, the adsorption capacity was higher when the metal ion was from nitrate and in other two cases, the adsorption capacity was higher when the metal ion was from acetate, however, these differences are not high, thus, it can be concluded that there is no significant difference between heavy metal adsorption on Bakonyoszlop coal from heavy metal nitrate and from heavy metal acetate.

The pH values of the solutions after the measurement were very different from the initial values. Even pH values under 3 and above 9 were measured. Generally, it can be said that an increase in the pH value was slightly more frequent than a decrease of the pH value. Nitrate solutions suffered slightly greater pH value changes than acetate solutions. Overall, it can be said that no trend could be derived from the pH changes during adsorption measurements. The reason of the significant pH changes could be the mobilization of acidic/basic ions/substances from the coal.

7. CONCLUSIONS AND SUMMARY

During our research work the adsorption properties of high humic acids content Hungarian sub-bituminous coal from Bakonyoszlop is being investigated to evaluate its applicability in municipal sewage sludge treatment.

As a first part of this work, the adsorption isotherms of cadmium and lead on this coal was determined by using different particle size Bakonyoszlop coal samples and heavy metal ions from different salts. On the basis of all measured results and calculated data presented in this paper it can be said that this isotherm determination was successful for cadmium in all cases. However, the lead adsorption isotherm could be determined only in one case (12.5–20 mm slack coal). The presence of different anions (nitrate, acetate) did not significantly influence the heavy metal ion adsorption process on the coal.

Significant changes in pH were observed during the measurements, which could be attributed to the high amount of added coal and the mobilization of acidic/basic substance/ion from it.

Correlation factors and correlation indexes were calculated between measurement and calculated isotherm points. It could be concluded that for these adsorption tests, Freundlich isotherms can be more suitable than Langmuir isotherms.

As a solution to the lack of lead isotherms and the significant pH changes, it would be worthy to repeat the measurements with a lower amount of coal, for instance a 40:1 solution:coal ratio can be optimal instead of the applied 10:1 ratio. That may result in applicable lead adsorption isotherms for all particle size coals and also q_{eq} values of smaller particle size coals could be able to be obtained at higher c_{eq} values. That would also result in comparable data with adsorption isotherms of other coals. Nevertheless, these preliminary results can be considered promising for the application of this high humic acids content coal in municipal sewage sludge treatment.

ACKNOWLEDGEMENTS

The experimental work was carried out as a part of “Development of bio raw materials products range with a special regard to the local technology – research on the possibility of utilisation by

technological” optimisation GINOP-2.2.1-15-2017-00069R&D Project. The research was carried out partially in the framework of the GINOP-2.3.2-15-2016-00010 Development of enhanced engineering methods with the aim at utilization of subterranean energy resources (PULSE) project of the Research Institute of Applied Earth Sciences of the University of Miskolc in the framework of the Széchenyi 2020 Plan, funded by the European Union, co-financed by the European Structural and Investment Funds.

REFERENCES

- [1] BERECZ, E. (1988): *Fizikai Kémia*. Budapest, Tankönyvkiadó Vállalat.
- [2] FERRO-GARCÍA, M. A. et al. (1998): Adsorption of humic substances on activated carbon from aqueous solutions and their effect on the removal of Cr(III) ions. *Langmuir*, Vol. 14, No. 7, pp. 1880–1886.
- [3] JEAN, G. E.–BANCROFT, G. (1986): Heavy metal adsorption by sulphide mineral surfaces. *Geochimica et Cosmochimica Acta*, Vol. 50, Issue 7, pp. 1455–1463.
- [4] KLUCÁKOVÁ, M.–OMELKA, L. (2004): Study of sorption of metal ions on lignite and humic acids. *Chemical Papers*, Vol. 58, No. 3, pp. 170–175.
- [5] TÓTH, J. (2001): *Adsorption. Theory, Modeling, and Analysis*. New York, Basel, Marcel Dekker, Inc.

WEB REFERENCES

- [6] Duzsén Bányászati és Szolgáltatási Kft. Dudarittal a lúgos vörösiszap ellen. Környezetbarát talajjavítók, avagy DUDARIT-tal a lúgos vörösiszap ellen. [http://duszen.hu/hu/component/content/article/13-szines/11-dudarittal-a-lugos-voeroesisz ap-ellen](http://duszen.hu/hu/component/content/article/13-szines/11-dudarittal-a-lugos-voeroesisz-ap-ellen) (Visited: 2018-11-02)
- [7] Fekete, I. Eoszén Kft. <http://eoszen.hu/index.php?m=1> (Visited: 2018-11-02)
- [8] Geománia. Felhagyott szénbánya meddőhányói, Dudar, Bakony és Balaton-felvidék. <http://geomania.hu/lelohely.php?lelohely=322> (Visited: 2018-11-02)
- [9] PERGER, A. (2009): The role of coal in the Hungarian electricity sector with special attention to the use of lignite (Report). https://www.energiaklub.hu/files/brochure/lignite_hungary.pdf (Visited: 2017-04-25)



CHARACTERIZATION AND COMPLETE UTILIZATION OF ALUMINIUM MELTING DROSS

TAMÁS KÉKESI¹

¹Professor, University of Miskolc, Miskolc-Egyetemváros, H3515, kekesi@uni-miskolc.hu

Abstract

Aluminium scrap is a raw material of growing importance in the production of aluminium and its alloys. Due to the thermodynamic properties, melting the recycled metal of high specific surface generates significant amounts of dross consisting of an oxide matrix and a large proportion of entrapped liquid metal. This heterogeneous material is usually processed by a thermo-mechanical treatment with the addition of a large amount of NaCl-KCl based salt to recover the entrapped metal. The residual dross is currently considered as waste, and it is usually disposed of despite of its potentially valuable metallic and non-metallic components. We have examined the structure and composition of different residual dross types applying instrumental techniques and chemical leaching tests. The results pointed out the possibility of utilizing the chloride and the oxide components and removing the still remaining metals. A method of hydrometallurgical processing has been examined for the recycling of the basically NaCl-KCl salt content leaving a residue which may be suitable as an additive to rough ceramic materials used in the construction industry.

Keywords: *Aluminium melting, dross, salt recovery, metal content, ceramic material, hydrometallurgy*

1. INTRODUCTION

The restructuring of the Hungarian aluminium industry in the last decade to cut the primary production and to become based on primarily secondary raw materials was a pioneering change in a country of significant bauxite resources and a long tradition of primary technology development. The change corresponds to a global tendency indicated by the steady increase in the share of the secondary based aluminium production, currently approaching a global 35%. This share in Hungary is well beyond 70%, as primary metal – from import - is only used for technological reasons in the metallurgical production of the required compositions of usually low Fe and Si aluminium alloys. The global share of scrap as a raw material for aluminium production is expected to rise further, as re-melting consumes 95% less energy than primary production and the amount of scrap generated is increasing. Obsolete scrap, recycled from consumption represents a growing share in the charge of melting. It causes an increased dross formation in the usually applied gas fired melting furnaces because the thicker non-metallic surface layers on the usually large specific surface area entails higher degree of oxidation during melting (HAN et al. 2003). The molten drops of the metal are more isolated and the dispersed particles of the metal – implying larger specific surfaces – are faster oxidised. The oxidation of aluminium and – especially – of magnesium, a common

alloying component, is highly exothermic, possibly causing an extreme local superheating which, in turn, results in an increased rate of oxidation. TÓTH et al. (2013) have shown the significance of metal losses by dross formation. The highly negative Gibbs free energy change (< -900 kJ/mol O_2) associated with the oxidation of aluminium at the typical temperature (~ 750 °C) of melting results in an extremely high stability of its native oxide. Magnesium has an even more negative Gibbs free energy (< -1000 kJ/mol O_2) related to its oxidation at this temperature (GILCHRIST 1979). Oxidation is also highly likely by the main furnace gas components, CO_2 and H_2O arising from natural gas combustion. Therefore, oxidation during melting cannot be avoided, and the principal oxide component of the dross is Al_2O_3 and MgO or the spinel compound $MgAl_2O_4$ when melting of AlMg alloys. The latter compound causes a great structural changes, resulting in higher dross volumes. Due to the great exothermic heat of aluminium oxidation (< 1100 kJ/mol O_2), the surface of the melt can be superheated and such solid phases as AlN and Al_4C_3 can be also formed.

The oxides of aluminium and also of magnesium do not form a protective slag layer as they are solid at the temperature of aluminium melting. Although they have higher densities than that of the molten metal, their fine particular shape and the high surface tension results in the formation of the physically heterogeneous dross layer at the surface of the melt (HO and SAHAI 1990). The oxides represent a direct loss of the metal, but even more molten metal is entrapped physically in the heterogeneous dross layer, usually removed manually from the surface of the metal bath after melting. The structure of the aluminium dross is generally characterised by oxide particles and scales stuck together by the partly frozen metal. The metallic content of the dross may reach as high as 70–80% by weight, which is usually removed by a thermo-mechanical treatment (TÓTH et al. 2013) in a converter-type rotary furnace applying significant addition of NaCl-KCl based salts. Salt addition efficiently serves the separation and disintegration of the oxide coatings and to prevent excessive re-oxidation of the molten metal phase. The metal recovery by the hot processing is shown in *Figure 1*.

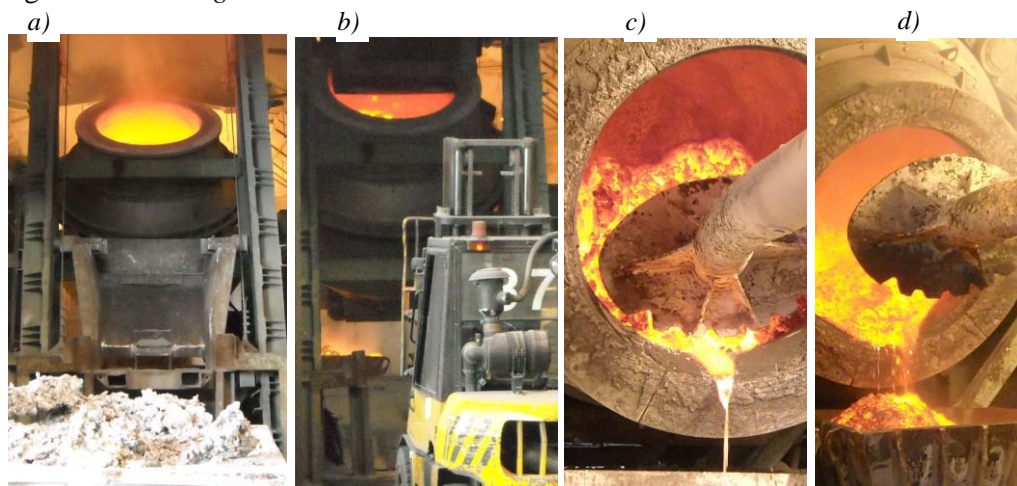


Figure 1

Thermo-mechanical treatment of the aluminium dross to recover the entrapped metal (a – dross charging, b – processing, c – tapping and retaining the residue, d – removing the residual dross)

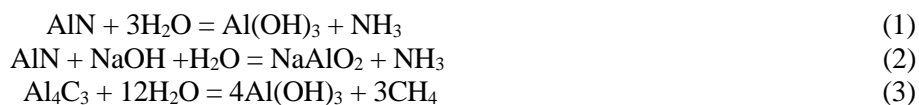
The heterogeneous material is heated by the jet flame of an oxy-fuel burner mounted in the lid, while the oxide structure is broken by the rotary movement of the furnace drum and the intermittently applied pushing force exerted by the plunging tool used in the tilted position of the furnace.

The tapped metal is aluminium, containing the less reactive alloying components, while Mg is lost by selective oxidation generating extra heat. As most of the entrained metal content can be recovered by this process, the residual dross usually consists of mostly the oxides and the salt components, accompanied by a low (2–10%) concentration of metal. The amount of this residual dross may be ~ 5 % of the produced metal, depending on the Mg content of the grades, reaching levels measured in thousands of tons in Hungary. As no significant metallic value can be recovered from it, and its oxide and chloride components cannot be utilised in this form, the major part of it is disposed of at landfill sites. In order to make the residue also useful it is imperative to separate the salt and the oxide constituents. The recovered salt can be recycled to the thermo-mechanical treatment of the primary aluminium dross. The salt-free final residue, containing mostly the oxides and a minor amount (a few per cent) of the aluminium metal could be utilized in different industrial technologies as:

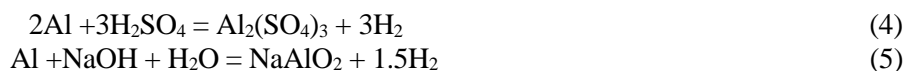
- slag forming agent in steel making (where the remaining Al content is also of benefit for the reducing effect)
- additive to special cements and concrete (to improve thermal insulating properties)
- additive to asphalt (to increase wear resistance)
- additive to produce glass foams (a novel structural material for heat insulation)
- ceramic production

However, all these novel applications would require an almost complete elimination of the chloride components from the residual dross (XIAO et al. 2005). The remaining aluminium content may be useful (as in steel making slag modification) or harmful (as in ceramic production), or indifferent in small quantities covered by a thick and firm oxide layer (as in the other noted potential applications). In order to meet the requirements of utilization the salt removal is a commonly critical condition, which, at the same time, may also serve the economy of dross processing by recycling.

The basically chloride salt content of the residual dross may be dissolved by pure water at ordinary temperatures. The obtained brine can be evaporated to yield the NaCl-KCl salt for recycling. The minor CaF₂ component - also present originally - may not be recovered, but can be supplied when the proper NaCl/KCl ratio is reset for the repeated application. Thus water leaching should be the fundamental initial step in a hydrometallurgical processing scheme after crushing and fine grinding the residual dross (“salt cake”) from the thermo-mechanical treatment of the primary melting dross. The preliminary grinding step may be followed by a physical separation of the larger malleable particles containing a predominant metallic core, or added directly to the leaching step to produce a brine of approx. 25% saturation for efficient dissolution, but also subsequently an energy saving removal of water by evaporation. Side reactions occurring as a result of the high-temperature treatment of the dross may occur, producing some noxious gases too:



If acidic or alkaline solutions are present, the minor metallic aluminium content may also be dissolved:



The reactions above – especially the last two – are exothermic, which will beneficially increase the temperature. These effects may also be present if the residual dross is disposed of in the environment.

There are proposed technologies (OLPER and KASPAR 1994) which are assumed to offer 99% recovery of the salt and a low (< 0.2 %) chloride content in the final residue, and the harmful gases evolved during the hydrometallurgical treatment are combusted. The generated heat of dissolution can be utilized for the evaporation of water. Although the proposed hydrometallurgical process may seem straightforward, there remain the questions of dissolution kinetics, efficiency of solid/liquid separation by decantation or filtering, solubility of metals, the application of acid or alkaline media, purity of the solid residue and the efficiency of evaporation. These questions required clarifications by fundamental experiments.

2. EXPERIMENTAL MATERIALS AND PROCEDURE

The raw materials for the experimental examinations were collected from the accumulated residual dross at an industrial site of the thermo-mechanical treatment of aluminium melting dross. There are basically two different extreme types that can be distinguished also by sight. One being light and the other dark in colour. Applying a special method (KULCSÁR and KÉKESI 2017) for determining the metal content (broken down into physically obtainable in the molten form or coarse pieces after granulating the hot treated residue, and the hidden metal content in the separated fine fraction after grinding), it has been pointed out that the lighter material had a metal content of 9.9%, and it was a mere 1.1 per cent in the fine (< 250 µm) fraction obtained after grinding. Whereas these values were 13.6 and 4.5 per cent in the dark material. No metal could be melted out of either samples whereas - after granulating the hot material in water - grinding and classifying resulted in a fine fraction of ~90% from both materials. The characteristic images and the relevant Energy Dispersive X-ray (EDS) and the X-ray Diffraction (XRD) spectra are shown in *Figure 2* and *3*.

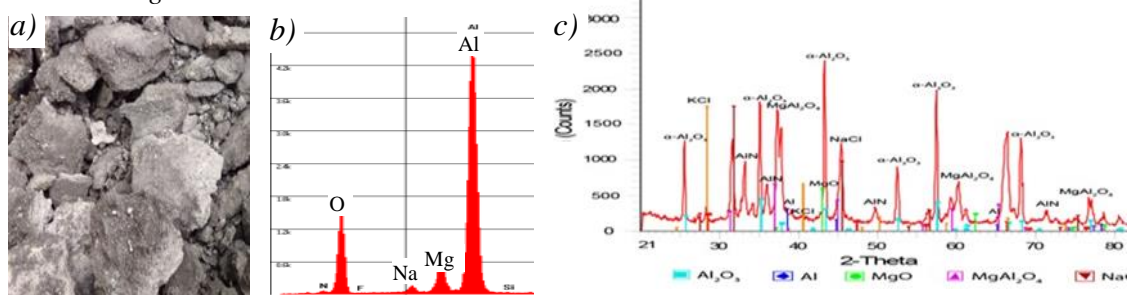


Figure 2

The macro (a), the EDS (b) and the XRD spectra of the light coloured residue from the thermo-mechanical treatment.

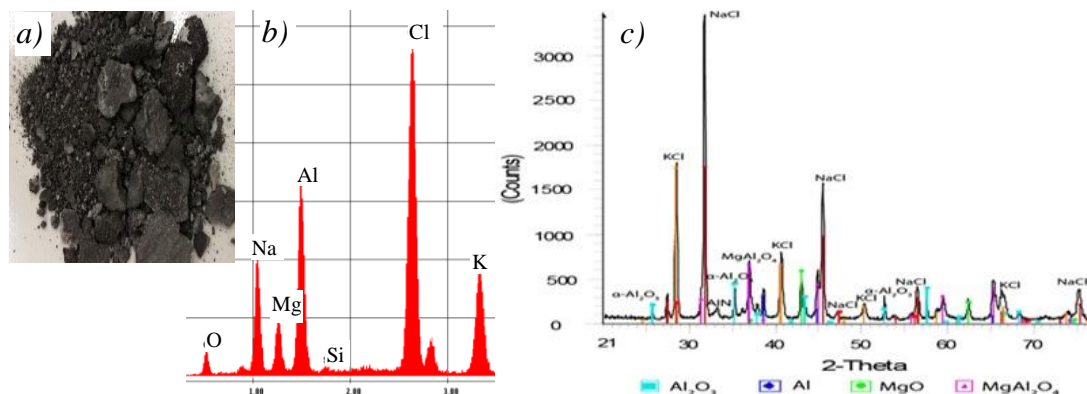


Figure 3

The macro (a), the EDS (b) and the XRD (c) spectra of the dark coloured residue from the thermo-mechanical treatment.

The EDS spectra reveal that the light coloured dross residue mainly consists of aluminium oxide, while the dark residue exhibits a relatively large proportion of the salt components and probably more metallic aluminium. However, the electron beam cannot penetrate below an oxide layer thicker than $\sim 5 \mu\text{m}$, thus not all the particles consisting of a metallic core can be detected as metal. The analytical method based on the collected volume of the H₂ evolved from reactions (4-5) could reveal the real metal content hidden under the oxide coatings of the fine particles (KULCSÁR and KÉKESI 2017). Shown by the XRD spectra, α -Al₂O₃ is dominant in the light coloured dross residue. The dominance of the simple oxides in the light coloured dross residue indicates the higher temperature probably reached during the thermo-mechanical treatment, which also enhances the evaporation of especially KCl and Mg and could cause the formation of AlN. However, the remaining NaCl and KCl salt content is significantly higher in the dark dross residue and the MgAl₂O₄-spinel component is also more evident.

Apart from the extreme types of the residual dross, samples were collected from the common grey coloured dross residues obtained from the industrial thermo-mechanical processing of primary dross batches generated in the melting of aluminium alloys of different Mg concentrations. The XRD spectra obtained with the residual dross samples from the thermo-mechanical processing of primary dross batches obtained from the melting of low and medium Mg containing aluminium alloys are compared in Figure 4.

The visual appearances of the two residual dross samples are quite similar, but the XRD spectra reveal some differences. The major phases found are marked in either or both diagrams in Figure 4. It is obvious that due to the Mg alloying in the metal, the spinel MgAl₂O₄ phase appeared in the residual dross, while the salt and metallic Al content diminished. It can be attributed to the exothermic reaction of Mg oxidation during the hot dross treatment.

Suggested by the observed compositions of the raw materials, it was preferred to use the primarily the dark coloured extreme type dross residue and that related to the treatment of the dross related to the low-Mg aluminium alloy in the hydrometallurgical processing experiments. These cases offered the highest concentrations of the salt and the metal to be recycled or eliminated.

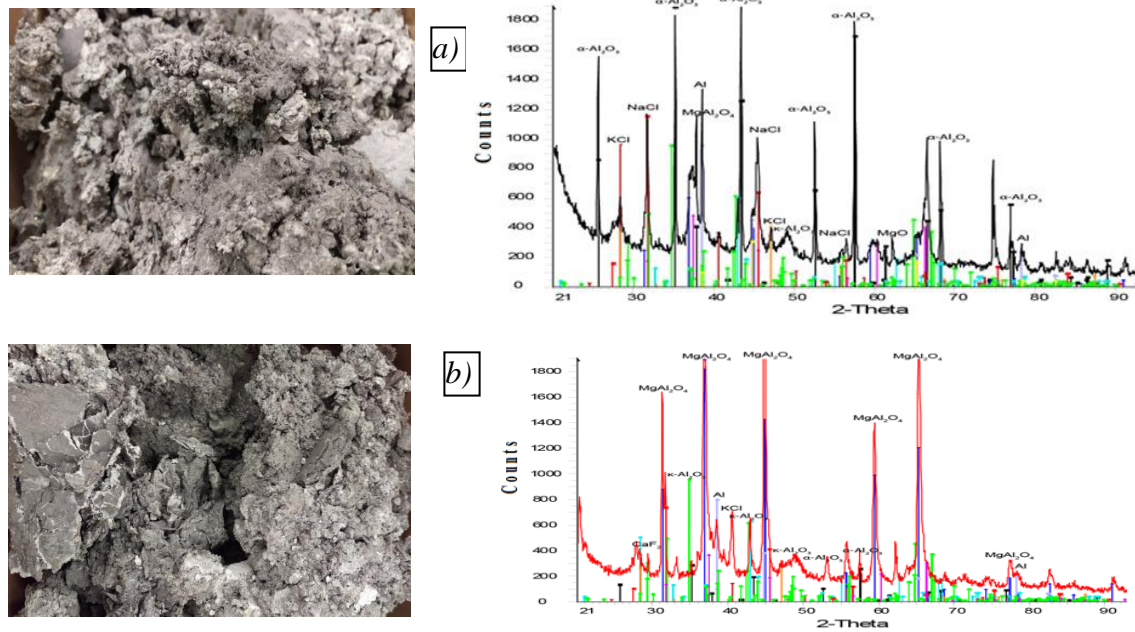


Figure 4

The pictures and XRD spectra of the residue from the hot treatment of primary dross batches obtained from the melting of low (a) and medium high (b) Mg containing aluminium alloys

The fine fraction ($<250\ \mu\text{m}$) of the ground residual dross samples – obtained from the industrial thermo-mechanical processing of aluminium melting dross – were leached with distilled water and 16.3 m/m % sulphuric acid, respectively, followed by washing and solid/liquid separation steps organised in different procedures. Control tests of high dissolving power for aluminium-oxide were carried out with 6 M NaOH too. Some pieces of equipment and the main steps of the laboratory leaching experiments are shown by Figure 5.



Figure 5

The main steps of the hydrometallurgical procedure (a – grinding, b – raw material, c – leaching, d – settling and washing, e – filtering, f – AAS analysis).

The applied sulphuric acid concentration corresponds to a 10 % by volume ratio, but beyond the convenience of preparation, it is preferred generally in hydrometallurgy (GILCHRIST 1979; BAR and BARKETT 2015). To examine the reaction rate, 10 g or 20 g samples, resp. were contacted with 100 cm³ of the solutions. It was a safe ratio to provide sufficient solubility. A horizontal shaking machine was used to provide a virtually homogeneous dispersion in reactor bottles of 300 cm³ in volume. The kinetic experiments were carried out for various times, but further examinations included set times of leaching (allowing equilibration). The larger scale experiments examining the elimination of the salt content in the various dross samples were carried out usually with 300 g material samples contacted with 500 cm³ of fresh solutions in each step of the complex hydrometallurgical procedure, applying 1000 cm³ reaction vessels (as shown in *Figure 5c*) for set total times allowing equilibrium dissolution at a shaking rate providing homogeneous dispersion. The concentrations of the chloride and the hydrogen ions were determined by classical titration, but the concentrations of the dissolved metals were analysed by Atomic Absorption Spectrometry (AAS). The results are given as yields of the indicated elements (or compounds) relative to the masses of the leached dross samples.

In order to check the analytical results and to demonstrate the possible recycling of the salt content removed by leaching, the brine solutions obtained from the aqueous treatment were evaporated to dryness by the application of a rotary vacuum distilling equipment. The process and the resulted salt products are shown in *Figure 6*.



Figure 6

Salt recovery (a – rotary vacuum evaporation, b – crystallized salt, c – drying in oven, d – products).

3. EXPERIMENTAL RESULTS AND DISCUSSION

3.1. Basic studies on the leaching behaviour of the extreme dross types

The kinetic characteristics of the dissolution process are illustrated by the yields of the analysed elements as functions of the time of leaching expressed in terms of the dissolved amount relative to the mass of the raw material. Although the principal aim is to recover the salt content, which can be achieved by applying water, it is of more information and interest to present the results of acid leaching. It is equally efficient in removing the chloride salts, but it may also dissolve the metallic aluminium content. Thus, beside showing the leaching behaviour, it may also reflect the

composition of the treated samples. These fundamental results obtained by water and acid leaching of the extreme types of the residual dross are given by the kinetic curves shown in *Figure 7*.

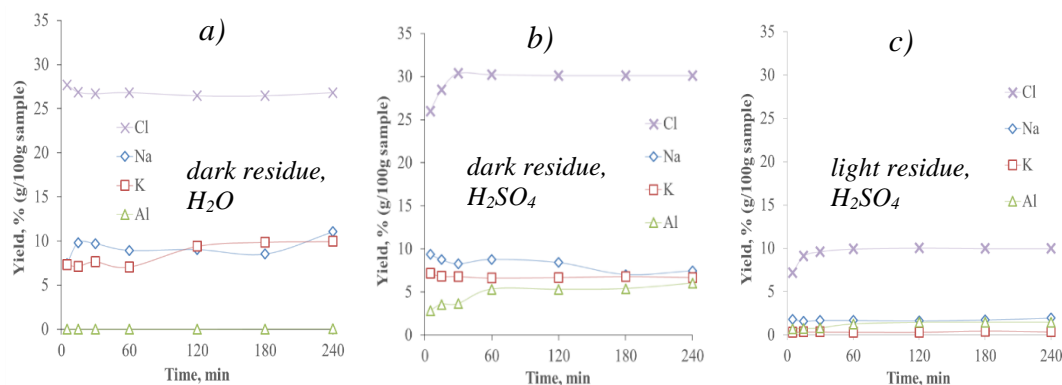


Figure 7

Dissolution rates of Na, K, and Al by distilled water (a) and 16.3% H₂SO₄ (b,c) leaching from the dark (a,b) and the light coloured (c) extreme-type dross samples obtained from the industrial hot treatment.

According to the plotted total metal concentrations, analysed by the AAS technique, the water leaching of the dark residual dross sample yielded an amount of ~ 40 % chloride salt removed, relative to the sample mass, which was ~ 48% according to the approximate argentometric analysis. The AAS based result is actually ~ 4% higher than the ~ 36% value obtained with sulphuric acid. It is not a significant difference, especially considering the heterogeneity of the mass of the powdery raw materials, but it indicates that water is not less efficient in dissolving the chloride salts than dilute sulphuric acid. However, the argentometric analysis of the acid solutions shows a higher chloride salt yield (of ~ 51 %) from the dark residual dross. Beyond the gradual degradation of the AgNO₃ test solution, the argentometric method is more likely to give positive errors in the acidic medium, where the potassium chromate indicator may be converted in a larger proportion to the inert chromic acid form. On the other hand, water leaching of the light coloured dross material yielded only ~ 5 % salt recovery by AAS and 6.4% by the less accurate argentometry. This corroborates the comparison of the two extreme residues by the relevant XRD spectra in *Figures 2* and *3*. The kinetic curves prove that the water leaching of the chloride salt can be completed within a few minutes.

As expected, it is noticeable that applying the sulphuric acid solution, metallic aluminium can be recovered too. This result shows a ~ 6 % recoverable aluminium metal content in the dark sample, which was only 1.5% in the case of the light coloured dross. It corresponds to the results obtained by the special method (KULCSÁR and KÉKESI 2017) determining the metal content in the fine fraction of this dross type. The light coloured dross yielded significantly lower amounts of dissolved salts and aluminium, corroborating expectations based on analytical and instrumental examination results shown above. As the analysed concentrations of the examined metals in the solutions reach their stabilized values, it is indicated that the dissolution of aluminium by the acid

leaching is completed within 60 minutes, while the total salt content is dissolved in less than 15 minutes under the applied technical conditions.

The compositions of the solid residues obtained after the 1 hour leaching treatments were dried at 105 °C and were analysed by the same instrumental techniques as applied for the raw materials. The SEM images revealed wrinkled surfaces of particles consisting of Al and O, indicating the presence of α - Al_2O_3 , while the Na, K and Cl peaks disappeared from the EDS spectra of all the treated samples. Although these results already confirmed the successful removal of the salt components, the remaining phases were also examined by XRD analysis. Because of the higher initial concentration of the salt components, the effects of leaching can be even more clearly demonstrated by the solid residues from the hydrometallurgical treatment of the dark coloured residual dross obtained from the industrial thermo-mechanical processing. The phases detected in the solid samples after leaching the dark residual dross with water, sulphuric acid and – for reference – with NaOH are marked on the XRD spectra of *Figure 8*.

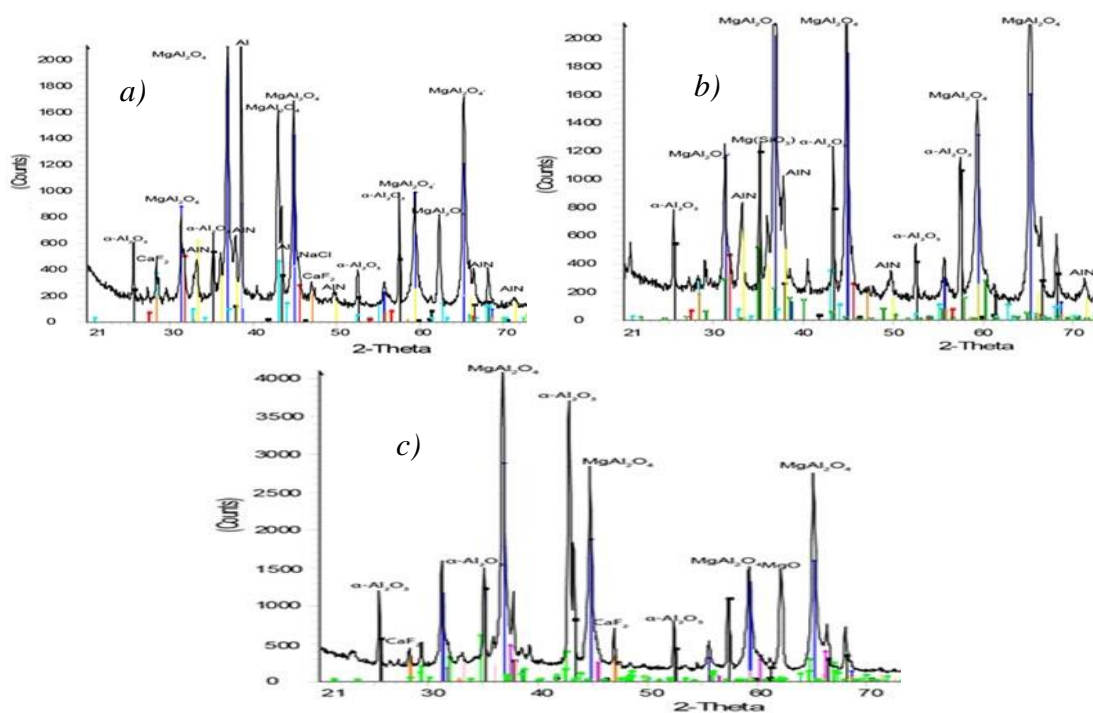


Figure 8

The XRD spectra of the solid residues obtained after 1 hour of leaching with water (a), 16.3% H_2SO_4 (b) and 6M NaOH (c) of the dark coloured residual dross samples from the industrial thermo-mechanical treatment.

A comparison of *Figures 3* and *8* shows that α - Al_2O_3 and the MgAl_2O_4 spinel are dominating in the solid residue after water leaching, as the previously dominant chloride salts have been removed from the dark coloured residual dross. The XRD spectrum obtained after the sulphuric acid leaching is similar, indicating the high chemical stability of the α - Al_2O_3 and the MgAl_2O_4

compounds. At the same time the intensity of the AlN peaks are slightly higher when the acid was used instead of water for leaching. It shows that the unpleasant evolution of NH_3 may be slightly depressed by the addition of sulphuric acid in the water for leaching the residual dross obtained from the high temperature thermo-mechanical treatment of the primary dross. The metallic Al phase still detected in the residue after water leaching is clearly removed by the acid treatment. The aggressive 6M NaOH solution – used as a reference - could even more efficiently dissolve the metallic Al, but it also involves a strong evolution of gas and heat, caused by the dissolution of metallic Al, producing H_2 and the dissolution of AlN enhanced by NaOH according to Eq. (2), generating of NH_3 . This unfavourable reaction is proved as the AlN peaks are removed after the NaOH leaching. Small amounts of the additive CaF_2 , which is not dissolved either in water nor in the alkaline solution, may remain in the residue. However, it may be gradually converted to the sulphate by applying sulphuric acid, but a noticeable, though relatively slight dissolution of Ca may be noticed only during a subsequent water rinsing.

The above results prove that the residual dross – obtained from the thermo-mechanical treatment of the primary dross of aluminium melting – may be successfully prepared for any further applications by a hydrometallurgical treatment. The simplest and cheapest treatment with water can remove the chloride salts. Applying dilute H_2SO_4 , which is another inexpensive option, Al and some other metallic components may also be eliminated. The process may consist of single or multiple steps of leaching, washing, solid/liquid separation and a final rinsing filtration. It is important to minimize the necessary process steps and to include the best suitable ones.

3.2. Hydrometallurgical purification of the usually obtained dross type

The technological examinations, carried out with a residual dross from the industrial thermo-mechanical treatment of the primary melting dross containing a metallic phase of low-Mg alloyed aluminium, were carried out with water, sulphuric acid and NaOH reagents in multiple leaching steps followed by repeated washing with distilled water, solid/liquid (S/L) separation by decantation or filtering and the final filtering was continued by rinsing with distilled water. In these experiments the starting material was always 300 g and each step involved 500 cm^3 of the fresh solution added. According to *Figure 7*, the chloride salts are dissolved almost instantaneously from the previously examined extreme-type residual dross samples. However, this had to be confirmed with the average-type of the residual dross examined in the here presented purification experiments. The results, confirming the same behaviour, are shown by the relative kinetic curves of *Figure 9a*. Here, the deviation from the average concentration in the solutions obtained after various times of leaching are plotted. While NaCl and KCl are dissolved after a few minutes completely, a slowly developing Al dissolution can also be observed, which can be attributed to reaction (1), although the maximum Al concentration was just around $50\text{--}100 \text{ mg/dm}^3$. It also implies that a very short water leaching can be applied to remove enough chloride salt before a significant volume of NH_3 is evolved. *Figure 9b* shows that changing the S/L mass/volume ratio (g dross/cm^3 water) from 10:100 through 100:100 did not have any appreciable effect. The solubility and the dissolution rate of NaCl and KCl are high. *Figures 9c* and *9d* show the results of repeated leaching steps with water lasting each for 10 minutes. The subsequent washing steps were carried out in a wide vessel agitated by manual shaking and the S/L separation applied was

simple settling and decanting. The final step was vacuum filtration combined with water rinsing (thus doubling the collected volume of the solution in this step).

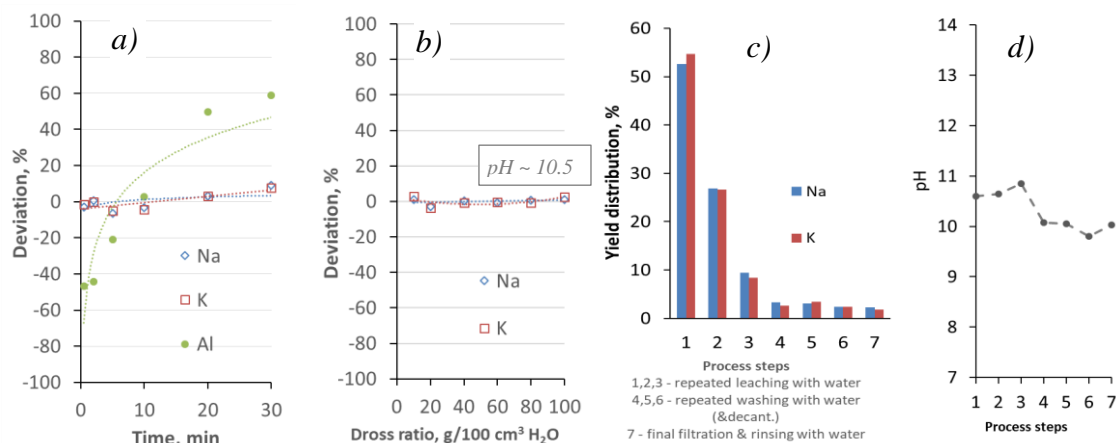


Figure 9

Dissolution of the common type of the residual dross by applying only water (a, b – deviation from the average of all the solutions, c – yield distribution among steps, d – pH of the solutions)

Most of the chloride salt content is dissolved in the first leaching step. However, the imperfect S/L separation by simple settling and decantation left a considerable amount of the liquid phase behind in the settled thick sludge in each step, therefore the salt content in the subsequent solutions could not be reduced efficiently. Even the last rinsing filtration – after six steps - could still remove some significant portion of the salt content. The alkaline pH generated is a result of the dissolution of AlN according to Eq. (1). Still applying the simple settling and decantation for separating the obtained solution in each step, Fig. 10.a shows the yields of the dissolved metals by water leaching and subsequent washing steps, as well as by the final rinsing filtration. As the S/L separation was still very rough, significant portions of the water-soluble NaCl and KCl were carried over among the subsequent steps. As water leaching did not result in any Al dissolution, AlCl₃ was not found to be present at a recognisable level in the common type of the residual dross, however the presence of AlN was confirmed by the alkalinity of the solutions obtained. In order to check the tendencies determined by the AAS analysis of the solution samples, the rest of the solutions were evaporated and the dissolved NaCl-KCl salt was crystallized and weighed. As shown in Fig. 10c, it yielded similar tendencies of salt removal in the multiple step procedure, although due to significant losses, the total yield of the directly crystallized salts (~ 33%) was less than that calculated from the analysed concentrations (~ 48%) taking the chloride molar mass ratios into account. A further discrepancy is caused – beyond the potential systematic error in the analysis of the concentrated samples – by the settling after the leaching step, leaving the more concentrated portions of the – not perfectly homogeneous - solution in the residue at the bottom of the reaction bottle. Nevertheless, the final elimination and the distribution of the yields of the salt content by the water treatment was confirmed.

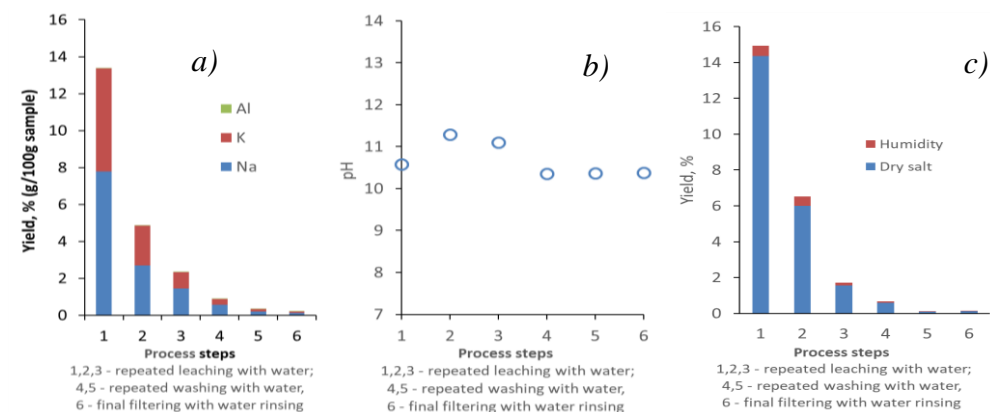


Figure 10

Metal yields (a), solution pH (b) and evaporated salt masses (c) obtained by water leaching of the common type residual dross in multiple steps, followed by washing and rinsing filtration

Applying dilute sulphuric acid for the leaching steps had the expected effect of removing aluminium and other impurity metals. In view of the slower dissolution reaction of the metallic phase, the acid leaching was carried out for longer (30 min) periods. However, it was repeated with fresh reagent only once, after decanting off the first solution. For a better separation of the acidic and the subsequent quasi-neutral steps, the last leaching step here was followed by a filtration, applying also water rinsing, instead of the simple decantation. Figure 11 shows the results of leaching with both the preferred dilute (16.3%) and with a more concentrated (23.5%) H_2SO_4 concentrations.

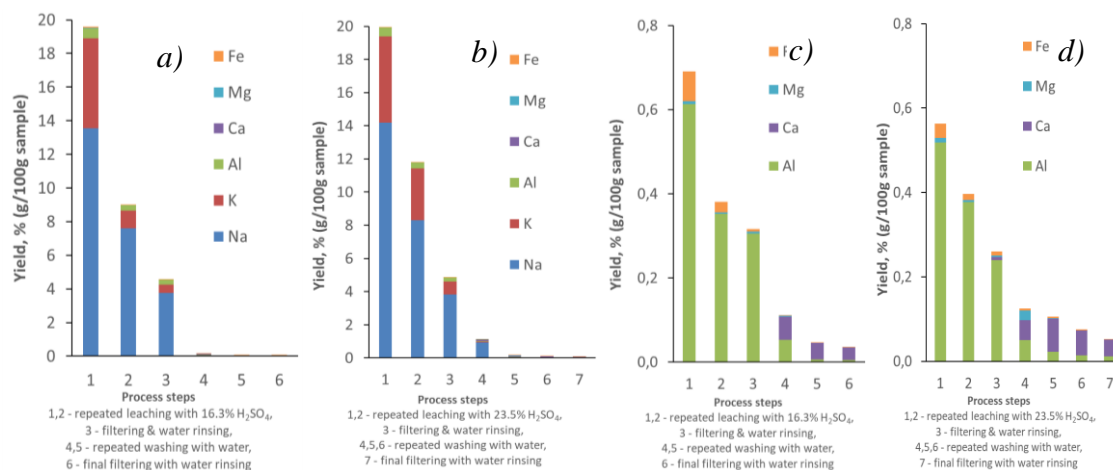


Figure 11

Metal yields obtained with 16.3 % (a,c), and 23.5% (b,d) H_2SO_4 solutions applied for leaching and water for the subsequent rinsing and washing steps to purify the common type residual dross

Despite fine grinding of the examined dross samples, some extent of heterogeneity cannot be excluded, therefore comparing the results of different experiments starting from nominally the same raw material cannot be made accurately. Nevertheless *Figure 11a* and *b* reveal that increasing the sulphuric acid concentration may not increase the yields of NaCl and KCl by leaching. In order to examine the effect of H_2SO_4 on the solubilisation of Al and the other impurity metals in it, results from the same experiments are plotted on a different scale in *Figure 11c* and *d*. It is seen that increasing the H_2SO_4 concentration did not improve the efficiency of metal dissolution. However, the latter two figures also show that some CaF_2 is solubilized as a result of the sulphuric acid treatment. It may be converted into the $CaSO_4$ form, which is however not dissolved – due to the solubility product – until the sulphate ions are removed by the water rinsing. Calcium appears significantly only in the neutral solutions of washing after the sulphuric acid leaching. In practice, it may be of reason to apply water leaching first and recover the salt content of the neutral solutions. The desalinated solid residue neutral procedure may be further treated by acid leaching to reach the necessary level of purity if any possible application requires it. This procedure has also been tested on the laboratory scale. A preliminary water leaching in three repeated steps followed by a double water washing was used to remove the chloride salt content from the common type of the residual dross samples. These pre-treated materials were then leached with sulphuric acid reagents of 8.5% (reduced), 16.3% (preferred) and 23.5% (increased) concentrations according to the procedure described above. The results are summarized in *Figure 12*.

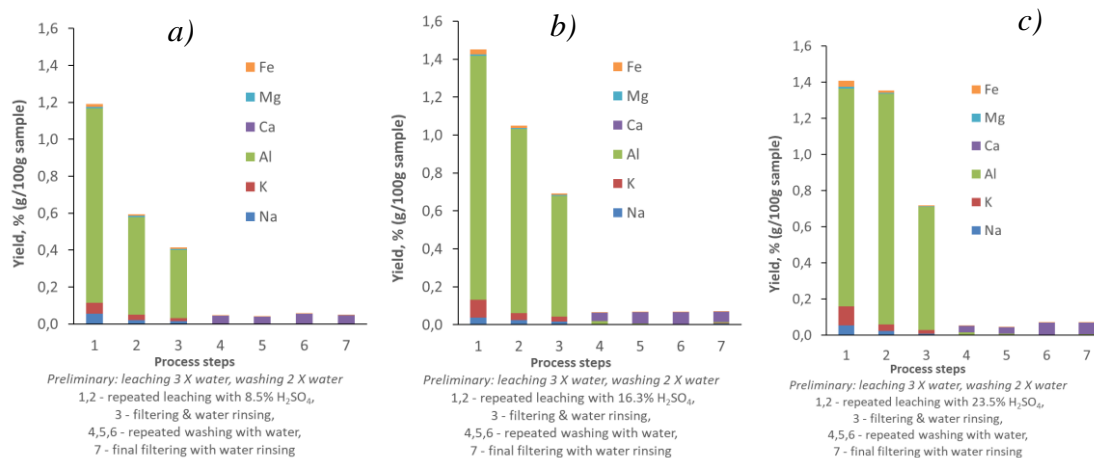


Figure 12

Metal yields obtained with 8.5%, (a), 16.3 % (a,c), and 23.5% (b,d) H₂SO₄ solutions applied for leaching and water for rinsing and washing steps, after preliminary water-leaching, to purify the common type residual dross.

The analysis of the minor components in the leachates was probably more accurate after the preliminary removal of the high salt content. The comparison of *Figures 11* and *12* suggests that the preliminary treatment of the residual dross with water (3 times leaching and twice washing in series) could remove more than 95% of the chloride salts. Especially the recovery of NaCl was

efficient. Some remaining KCl and NaCl were completely removed by the subsequent acid leaching steps. Increasing the sulphuric acid concentration from 8.5 % to 23.5 % could enhance the efficiency of removing the metallic Al, although the preferred dilute 16.3% H₂SO₄ concentration may be just satisfactory.

In order to compare the efficiency of a strong alkaline leaching, where the oxide coatings of the hidden aluminium particles may be more efficiently digested (GASTEIGER et al. 1992), experiments with different NaOH reagents were also carried out. Results are shown in *Figure 13*.

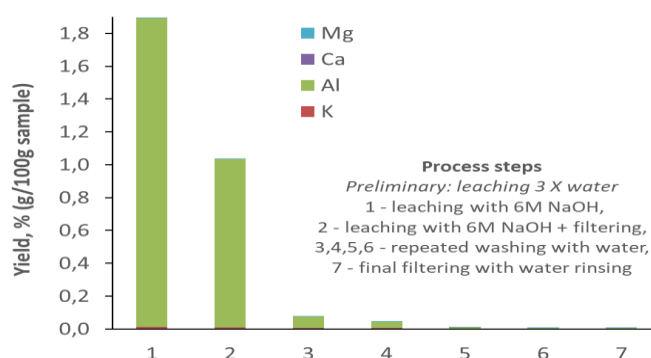


Figure 13

Metal yields obtained with 6M NaOH applied for leaching and water for the subsequent rinsing and washing steps, after preliminary water-leaching, to purify the common type residual dross

After a preliminary triple water-leaching treatment to remove the chloride salt content, the applied 6M NaOH leaching could remove virtually only aluminium, which may have been mostly in the metallic form, but some Al₂O₃ dissolution from the coatings of the particles may also have contributed to the analysed values. The second leaching was combined with filtering where a minute amount of rinsing water was also applied. It was followed by the usual washing and the final filtering steps, applying water to remove the remaining solution. Despite all the expectations, the aggressive alkaline leaching could remove significantly more metallic aluminium than the procedure applying 16.3% or 25.3% sulphuric acid solutions as leachants. Although the decantation steps involved in the preliminary water-leaching treatment may have wasted some of the starting material, which could reduce the overall amount of dissolved metal.

4. CONCLUSIONS

A thorough examination of the residual dross samples collected from the industrial thermo-mechanical processing of aluminium melting dross materials revealed that the salt content can reach as high a level as ~ 40 %, the major constituents being NaCl and KCl. The examinations proved that a multiple-step procedure consisting of leaching, rinsing filtering and washing steps with water at room temperature and applying shaking can remove the chloride components efficiently. The dissolution of chlorides may be completed in a few minutes and a such a high S/L mass to volume ratio as 1 g/1 cm³ can be still efficient. Thereby the cost of recovering the salt by evaporation and crystallization can be reduced. The reaction of AlN, also present in the residual dross from the hot treatment, can react with water, and especially with alkaline solutions, to produce

unpleasant NH_3 emission. It may be suppressed by acid media, but a practical way to diminish its evolution is to apply shorter leaching, which may be efficient to dissolve the salts, but prevent the development of unwanted reactions. Applying repeated leaching steps may not increase the efficiency of salt removal, however washing the residue with water and separating it by vacuum filtration, while rinsing the cake with water can usually guarantee at least a 95% efficiency in removing NaCl and KCl. If the S/L separation is carried out as much as technically possible, the product can be suitable for various new applications, such as cement and glass foams, geopolymer production, or asphalt conditioning, but the conventional use of a purified material in steel making is also advantageous. The residual minor amount of metallic aluminium in the product from the water-leaching procedure is mostly covered by an oxide layer making it virtually inert for applications in the construction materials industry, and it is even useful in steel making. Any practical metallic component content however, can be readily eliminated by applying dilute sulphuric acid leaching followed by the necessary washing and rinsing-filtering steps in a second purification procedure. Sodium hydroxide, although more efficient in digesting the Al_2O_3 layers, was not found significantly more efficient in removing the metallic aluminium from the residue of the water-leaching procedure.

ACKNOWLEDGEMENTS

The research was carried out in the Centre of Applied Materials Science and Nano-Technology at the University of Miskolc. The continuation is supported by the GINOP-2.2.1-15-2016-00018 project in the framework of the New Széchenyi Plan of Hungary, co-financed by the European Social Fund. The described study was carried out as part of the EFOP-3.6.1-16-2016-00011 “Younger and Renewing University – Innovative Knowledge City – institutional development of the University of Miskolc aiming at intelligent specialisation” project implemented in the framework of the Széchenyi 2020 program. The realization of this project is supported by the European Union, co-financed by the European Social Fund.

REFERENCES

- [1] HAN, Q. et al. (2003): Dross formation during remelting of aluminium 5182 remelt secondary ingot (RSI). *Materials Sci. Eng.*, A363 pp. 9–14.
- [2] TÓTH, G. B. et al. (2013): Metal content of drosses arising from the melting of aluminium. *XXVII MicroCad International Scientific Conference*, Miskolc, Hungary, 21–22 March, Section C-D/14, p. 12.
- [3] GILCHRIST, J. D. (1979): *Extraction Metallurgy*. Elsevier; 2Rev Ed., Pergamon Press, London.
- [4] HO, F. K.–SAHAI, Y.: Interfacial Phenomena in Molten Aluminium and Salt System. In: VAN LINDEN, J. H. L. et al. (eds.): *2nd. Int. Symp. Recycling of Metals and Engineered Materials*. Williamsburg, Va, 28–31 October, TMS, Warrendale, pp. 85–103.
- [5] XIAO, Y. et al. (2005): Aluminium Recycling and Environmental Issues of Salt Slag Treatment. *Journal of Environmental Science and Health*, 40, pp. 1861–1875.

-
- [6] OLPER, M.–KASPAR, T. (1994): The Engitec System for Treatment of Salt Slag from Secondary Aluminium Smelters. *Metal Bulletin's Fourth International Scrap & Secondary Metals Conference*, March, 21–23, Amsterdam, The Netherlands. <https://www.ips-engineering.net/Doc/Engitec/STE%20Process.pdf>
- [7] KULCSÁR, T.–KÉKESI, T. (2017): Thermo-mechanical extraction of aluminium from the dross of melting AlMg scrap. *MultiScienc-XXXI. microCAD Int. Multidisciplinary Scientific Conference*, Miskolc, Hungary, 20–21 April, Section D, p. 9.
- [8] GASTEIGER, H. A. et al. (1992): Solubility of aluminosilicates in alkaline solutions and a thermodynamic equilibrium model. *Industrial & Engineering Chemistry Research*, 31, pp. 1183–1190.



GLASS FOAM FROM WASTE HOLLOW GLASS

ROLAND SZABÓ¹–BENJÁMIN GULYÁS²–GÁBOR MUCSI³

¹University of Miskolc, H 3515 Miskolc-Egyetemváros, ejtszabor@uni-miskolc.hu

²University of Miskolc, H 3515 Miskolc-Egyetemváros, rekbenj@uni-miskolc.hu

³University of Miskolc, H 3515 Miskolc-Egyetemváros, ejtmucsi@uni-miskolc.hu

Abstract

Present paper deals with glass foam development from waste hollow glass. It is focused on the influence of glass particle size on the foaming process and physical characteristic of glass foam pellet. After the determination of the raw materials' properties, green pellets were produced in a pelleting table using optimal pelleting parameters (2.5 w/w% bentonite concentration, 20 w/w% moisture content, heat curing of 850 °C) developed in our previous research. Ground glass with different particle size distribution (<106; 80; 45 and 20µm), Na-bentonite (to improve the initial strength of pellet) and dolomite (as foaming agent) were used for the pellet production. The apparent density, and pore size (by optical microscope) of the resulted glass foam pellets were determined. The mechanical stability (abrasion resistance) was investigated by abrasion test in a Deval-drum. The use of finer glass particle size resulted smaller density of glass foam pellets. The lowest density of glass foam was 0.52 g/cm³. Based on the results of mechanical stability, it can be stated the abrasion of coarser size pellets was higher. The pore size of pellets was different, it changed between few micron and 1000 micron.

Keywords: *waste glass, particle size, glass foam pellet, foaming agent, dolomite*

1. INTRODUCTION

In Hungary, the glass waste is generated in approx. 180,000 tons/year, most of which (about 80%) is colored hollow glass. However, utilization of a significant ratio (60%) is not solved. Due to the technical and economic development of recent years, protection against the harmful effects of waste has become one of the most important economic and environmental factors. Waste should be properly collected, handled and disposed, otherwise it may have an adverse environmental impact. Along with recognizing the environmental impact of wastes, the role of wastes in the rational management of natural resources, material and energy management has become more apparent. In the developed countries, the significant part of waste is re-used as raw material, secondary raw material or secondary energy source [1].

According to the EU Waste Directive 2008/98 / EK: "The primary purpose of any waste policy is to minimize the negative effects of waste generation and waste management on human health

and the environment. Waste policy must be strived to reduce the use of resources and give preference to the use of the waste hierarchy”[1].

One of the positive property of glass is that it can be completely recycled theoretically.

According to the type of glass wastes can be recycled as packaging materials or raw materials.

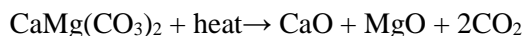
Part of the packaging waste glass is recycled. After separating and grading, the bottling plants receives the intact bottles after cleaning, and the glass industry receives the broken, defective pieces after appropriate grinding, milling and preparation, where they melt the glass and produce new bottles. This is a cost-effective and energy-saving solution. The prerequisite for recycling used glasses is the clean state of the bottles. Cleaning is carried out with water wash in a rotating drum. Waste glasses are used to make bottles and industrial glass panes after melting [2]. Hoffmann et al. found a solution for the use of increasingly accumulated, non-recyclable waste glass for example: cathode ray tube glasses [5]. Their invention is so called geofil glass foam. For this purpose, the waste glass should be ground to a suitable particle size. Depending on its composition, the foaming agent should be added to the glass and then it will be foamed at a suitable temperature by sintering [5]. Glass foam possess unique properties: lightweight, rigid, resistant, heat-insulating, antifreeze, non-flammable, chemically neutral and non-toxic, rodent and insect resistant, resistant to bacteria, water and vapor. Glass foam can be used in many ways in the construction industry and in many other areas [6].

The purpose of this study is to further develop the glass foam product, namely the investigation of the effect of ground glass powder fineness and glass foam pellet size on the abrasion resistance, pore structure and particle density.

2. MATERIALS AND METHODS

For the glass foam production were used ground hollow glass, dolomite and Na-bentonite. First the waste glass of brown, green and transparent was prepared for the laboratory tests. The mean particle size of initial glass were the following: 50% passing particle size (median particle size) $x_{50} = 6.3$ mm and 80% passing particle size $x_{80} = 10$ mm. The initial glass was crushed in three steps. The particle size distribution of ground glass and other raw materials (dolomite, Na-bentonite) was investigated by Horiba LA950 V2 type laser particle size analyzer, specific surface area was calculated from distribution data by software using shape factor 1. These results can be seen in *Figure 1*.

The fine-grained dolomite was used as foaming agent, because of thermal composition of dolomite released CO_2 resulting in pore structure and foam formation [5] [6].



The median size of dolomite powder was $x_{50} = 42.3$ μm and the 80% particle size was $x_{80} = 61.5$ μm . The particle size distribution of dolomite powder is shown in *Figure 1*.

Na-bentonite was used as pelleting agent in order to improve the strength of initial pellets. The characteristic particle sizes of bentonite were the following: $x_{50} = 29.9$ μm and $x_{80} = 65.5$ μm . The particle size distribution of bentonite can be seen in *Figure 1*.

Glass foam pellets were examined for abrasion resistance. The tests were performed for 10 minutes at 30 revolutions per minute.

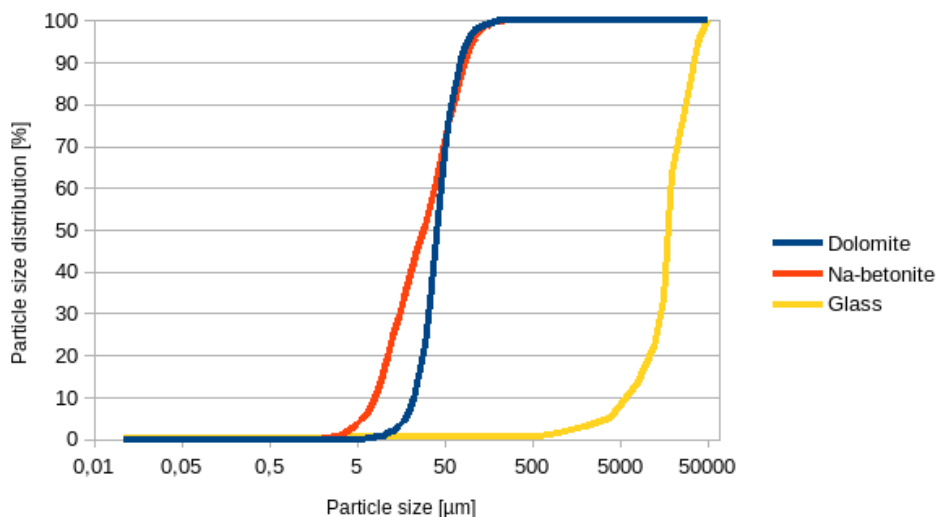


Figure 1

Particle size distribution of raw materials (glass waste, dolomite, Na-bentonite)

The green pellets were made using pelleting table. Additionally, Al_2O_3 was used to avoid aggregation of melted pellets. The mechanical stability (resistance of pellets to degradation by abrasion) of the glass foam pellets was tested with a conventional Deval drum ($\text{Ø}210 \times 340$ mm) apparatus. The tests were performed for 10 minutes at 30 revolutions per minute.

The cell structure of glass foam pellets were examined by Zeiss Axio Imager type optical microscopy using five-fold magnification.

3. EXPERIMENTS

In order to achieve the appropriate particle size, the glass waste was ground. The particle size of initial glass was below 50 mm, which was crushed in three steps. As a first step the material was crushed in a jaw crusher with gap size of 15 mm (crushing step 1) then followed the second crushing step in a roll crusher (the gap size of 6 and 1mm were between the rolls) and finally the glass was ground in a laboratory ball mill with the size of $\text{Ø}305 \times 305$ mm internal diameter (smooth walled), with steel balls (max. ball size 50 mm) as grinding media. The mill filling ratio of the grinding media was 30 v/v%, the material filling ratio was 110 v/v%. The operating revolution number to critical revolution number was 80%. The glass powder meant the base of the glass foam. After the grinding, the ground glass was classified (<106 ; 80; 45 and $20\mu\text{m}$). Then the raw materials were mixed in a ball mill for homogenization. The mixture contained the follows: ground (classified) glass of 92.5%, dolomite of 5% and Na-bentonite of 2.5%.

For the green pellets production was used ground glass with particle size of below $106\mu\text{m}$. The pellets were manufactured in a pelleting table using optimal pelleting parameters (2.5 w/w% bentonite concentration, 20 w/w% moisture content) which were developed in our previous research [8]. After preparing the green pellets, they were dried in a drying cabinet at $105\text{ }^\circ\text{C}$ for 2

hours. Then the pellets were fractionated by sieves. The fractions were the following: 2–4, 4–6.3, 6.3–8 and 8–10 mm. Then the fractionated pellets were sintered in an electric furnace.

In the preliminary experiments the sintering conditions (such temperature and residence time) were examined to find the optimal conditions for glass manufacturing.

The mechanical stability (resistance of pellets to degradation by abrasion) of the foam pellets was tested with a conventional Deval drum ($\text{Ø } 210 \times 340 \text{ mm}$) apparatus. Since the initial pellet size does not reach the standard size fraction (10–14 mm), the measurements were carried out using the manufactured pellets (4–6.3 mm, 6.3–8 mm, 8–10 mm and 12.5–16 mm) using 10 min residence time and then the product was sieved at 1.6 mm sieve aperture size, the evaluation used the mass of material finer 1.6 mm.

4. RESULTS

Preparation of glass

One of the most important steps in glass foam production is the preparation of glass powder. For this purpose the initial glass was crushed in three steps. The *Figure 2* shows particle size distribution of the glass after crushing on a jaw crusher (gap size value of 15 mm) and a roller crusher (gap size value of 1 mm).

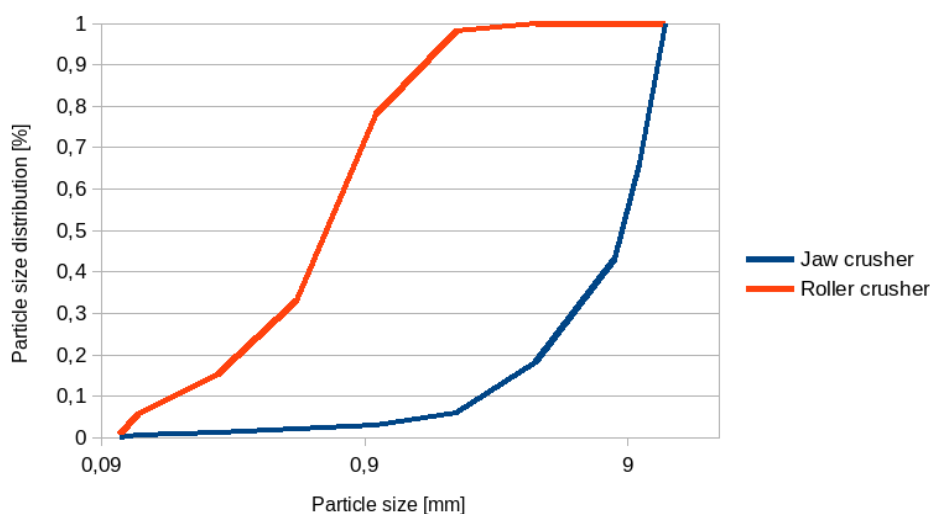


Figure 2

Particle size distribution of glass crushed by jaw crusher and roller crusher

Based on this *Figure* it can be stated that the median size $x_{50} = 9 \text{ mm}$ and the 80% particle size $x_{80} = 15.7 \text{ mm}$ was achieved by crushing the glass with jaw crusher while after the crushing in a roller crusher 0.75 mm median size was achieved from the initial value of 6.3 mm indicated a 8.4 size reduction rate. In this case the 80% particle size was 1.1 mm (size reduction rate 9.09).

The particle size distribution of the ground glass shown in *Figure 3*.

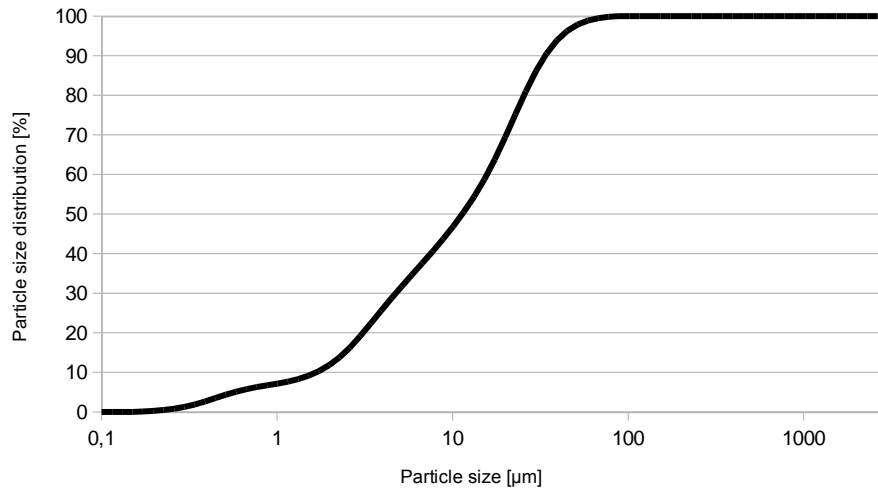


Figure 3
Particle size distribution of ground glass

Figure 3 shows that the 50% particle size (median) of $x_{50} = 12.9 \mu\text{m}$ and the 80% particle size $x_{80} = 27 \mu\text{m}$ was achieved by grinding in a ball mill. During the grinding the invested energy was measured, from which the specific grinding energy was calculated. Figure 4 shows the specific surface area and median particle size (x_{50}) as function of specific grinding energy. Based on this figure it can be stated, that SSA increasing almost linearly as function of specific grinding energy.

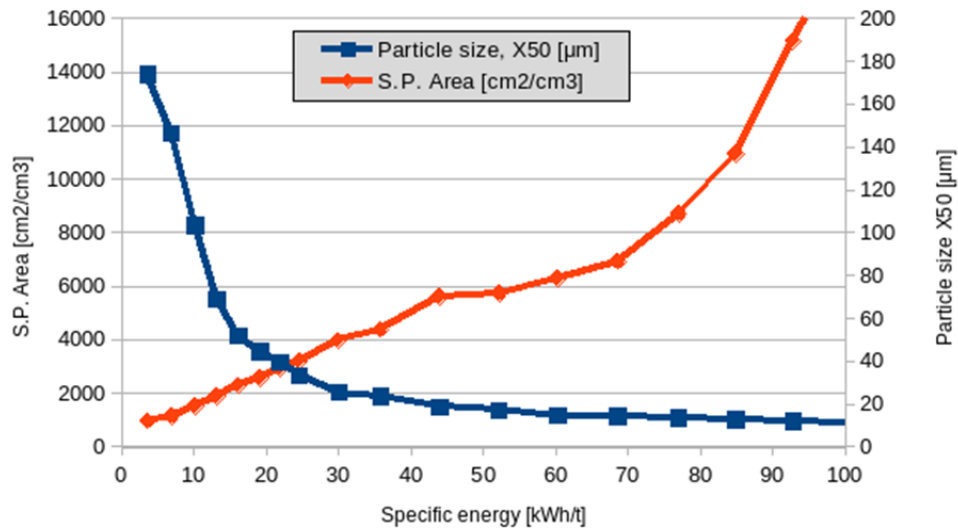


Figure 4
Grinding kinetics of glass

Glass foam pellet results

Based on the preliminary experiments it can be stated that at 800 °C sintered glass foam was developed not or only a few pores and these cell size were below 200 µm (mostly <100 µm). Increasing the temperature, the size of the pores increased in the pellet. When the pellets were sintered at 850 °C the cell size reached a maximum value of 800 µm but the most of cells were between 200–400 µm. In that case of the sintering was at 900 °C, the cells were coalesced and resulted in pores greater than 3 mm, which was positive in terms of density reduction, but at this point the pellet was foamed such an extent that the pellets were broken easily with the slightest mechanical stress. Due to the 900 °C temperature and the 9 min residence time, the pellet was already excessively foamed, the cell structure was unstable.

Based on the cell structure the optimal sintering temperature and residence time were at 850 °C and 8 min for glass foaming.

Based on the results of preliminary experiments the pellets were prepared at 850 °C for 8 min. According to the microscopy images (*Figure 5–7*) it can be stated the glass foam which made of a coarser initial pellet size contained bigger cell in larger quantities than which made of finer initial pellets.

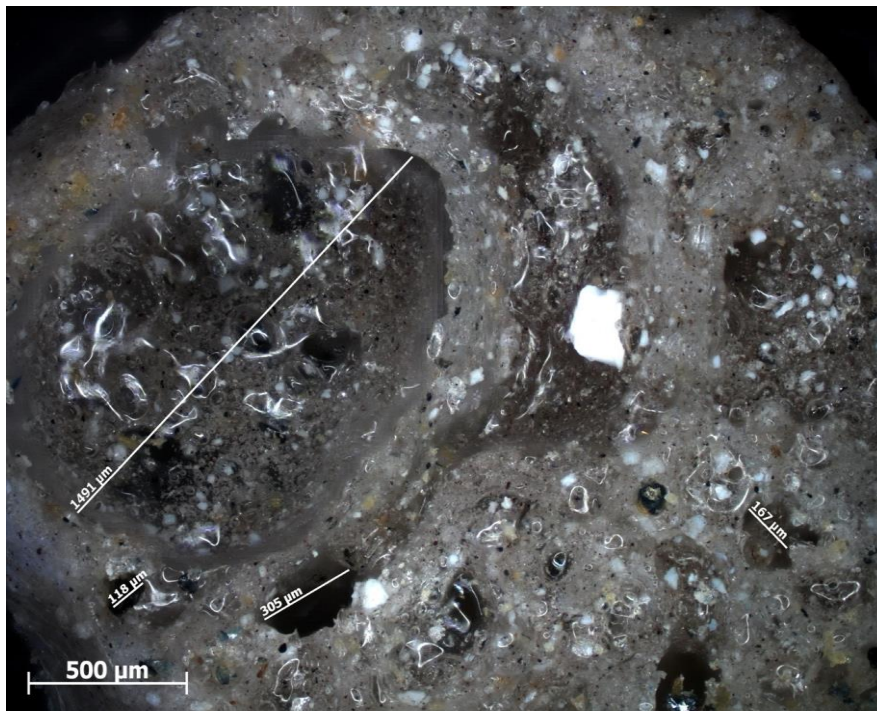


Figure 5
Optical microscopy image of 2–4 mm pellet at 850 °C

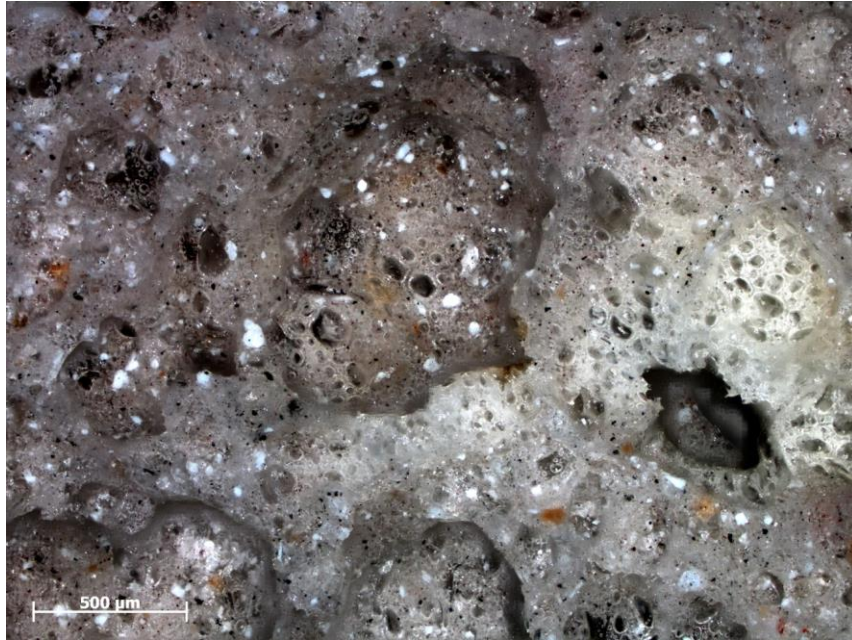


Figure 6
Optical microscopy image of 12.5–16 mm pellet (850 °C)

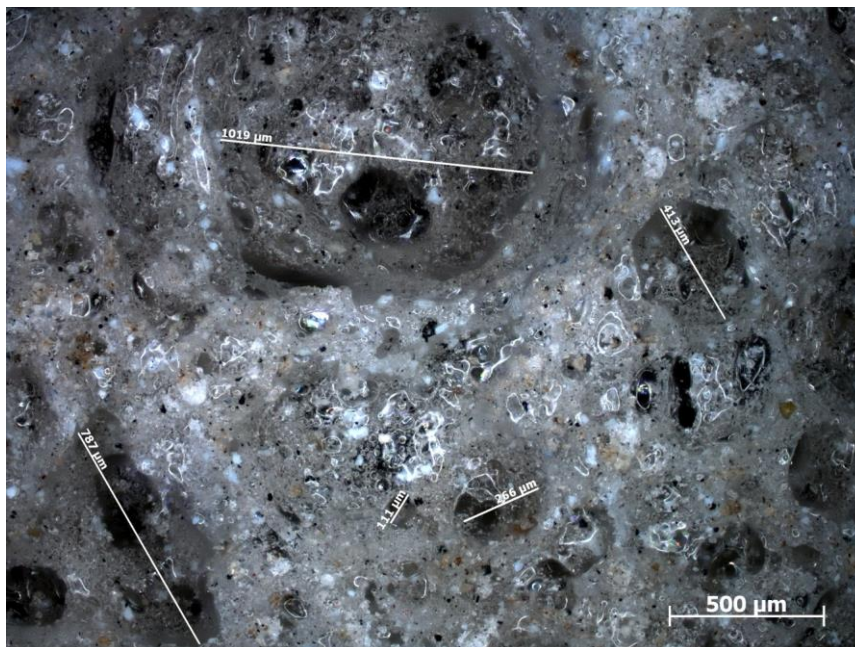


Figure 7
Optical microscopy image of 22.4–25 mm pellet (850 °C)

Density tests on glass foam pellets were performed. These data are shown in *Table 1*.

The optimal settings for foam glass manufacture taking into account the mechanical stability and particle density are determined: 850 °C temperature and 8 min residence time are suggested for ideal foam characteristics using the size fraction 8-10 mm. In this case, density reduced down to 0.52 g/cm³.

Table 1
Density of pellet made of <32 µm and <106 µm glass powder

<32 µm and <106 µm glass powder					
Initial pellet fraction [mm]	Glass foam pellet fraction [mm]	Density of pellets of <20 µm [g/cm ³]	Average of density of pellets of <20 µm [g/cm ³]	Density of pellets of <106 µm [g/cm ³]	Average of density of pellets of <106 µm [g/cm ³]
10-16 mm	10-16 mm	1.01	0.76535	1.46	0.859877
	16-20 mm	0.71		0.89	
	20-22.4 mm	0.65		0.68	
8-10 mm	8-10 mm	0.83	0.694236	1.26	0.875519
	10-12.5 mm	0.74		0.84	
	12.5-16 mm	0.57		0.55	
6.3-8 mm	6.3-8 mm	1.31	0.870645	1.02	0.746318
	8-10 mm	0.76		0.82	
	10-12.5 mm	0.58		0.56	
4-6.3 mm	4-6.3 mm	1.1	0.898502	1.37	0.938072
	6.3-8 mm	0.79		0.73	
	8-10 mm	0.52		0.59	
2-4 mm	2-4 mm	1.18	0.99796	1.28	1.175263
	4-6.3 mm	0.58		0.67	

The following chart (*Figure 8*) shows the data in the table.

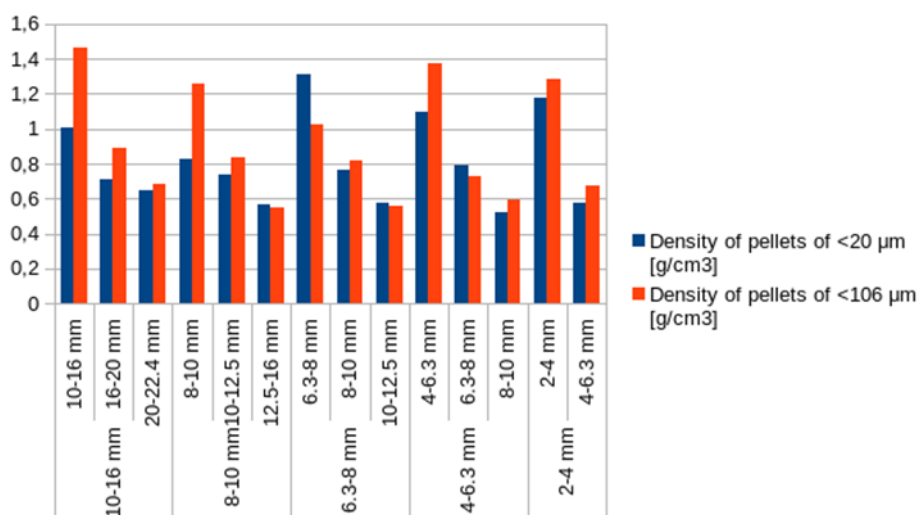


Figure 8
Density of pellet made of <32 µm and <106 µm glass powder

Result of abrasion test

The result of abrasion resistance can be seen in *Figure 9*. Based on this Figure it can be stated, the rate of abrasion considerably different depending on the particle size interval. The highest abrasion rate (3.56%) was observed at the size fraction of 10–16 mm. The lowest abrasion was to the size fraction of 4–6.3 mm. The relationship can be established between the particle size and the abrasion resistance: the lower the glass foam pellet size the higher its resistance to the abrasion. With the increase in the particle size fraction of glass foam pellets, the amount of collapsed mass increased. For the 4–6.3 mm fraction, only 0.32% was the rate of abrasion.

Table 2
Results of abrasion test

Particle size fraction [mm]	The feed weight [g]	Abrasion weight [g]	Rate of abrasion [%]
4–6.3	25	0.08	0.32
6.3–8	25	0.18	0.72
8–10	25	0.35	1.40
10–16	25.25	0.9	3.56

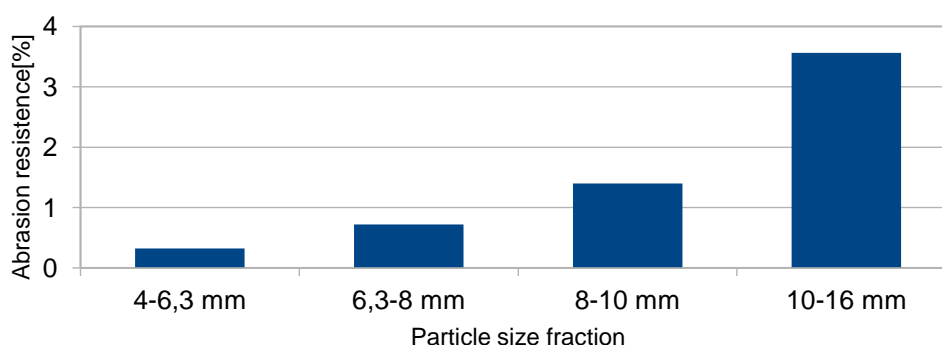


Figure 9
Results of abrasion resistance

5. CONCLUSIONS

According to our measurement data, the optimum glass powder particle size was $<32 \mu\text{m}$, because the most appropriate properties of the pellets (density, abrasion resistance) were achieved in this case. For the density and abrasion resistance the most favorable results were obtained from the 8–10 mm green pellet fraction, so this size is recommended for industrial production both as a thermal insulation additive and lightweight concrete additive.

Based on the results the following conclusions can be drawn.

1. The finer glass powder resulted lower particle density of green pellets.
2. Based on the experiments it can be concluded that the optimal glass foam pellets were obtained at 850 °C for 8 min. In this case, the density of the pellets was greatly reduced and their volume were doubled.
3. The density of glass foam pellets made of <32 µm glass powder were less than the density of glass foam made of glass powder <106 µm. The particle size of the ground glass waste plays the role changing the density of glass foam, which is confirmed by other literature [6].
4. Based on the abrasion test it can be stated that the higher the glass foam pellet size was the lower its resistance to abrasion stress (mechanical stability)

ACKNOWLEDGEMENTS

This research was supported by the European Union and the Hungarian State, co-financed by the European Regional Development Fund in the framework of the GINOP-2.3.4-15-2016-00004 project, aimed to promote the cooperation between the higher education and the industry.

REFERENCES

- [1] Netjogtár 2015/49.: A Kormány T/6984. számú, a hulladékról szóló 2012. évi CLXXXV. törvény módosításáról szóló törvényjavaslat (2015. október 29).
- [2] BARÓTFI I. (2000): *Környezettechnika*. pp. 562–564.
- [3] SZAKÁLL S. (2011): *Ásvány- és kőzettan alapjai*.
- [4] Chris PELLANT (1998): *Kőzetek és Ásványok*. Budapest, Egyetemi Nyomda Kft., 100, 241.
- [5] HOFFMANN László–JALSOWSZKY István–HOFFMANN Emma–ROSTÁS Rita–FEHÉR Jenő–FEJÉR Zsolt (2005): *Innovációs Környezetvédelmi Verseny – EKO 2005: Hulladéküveg hasznosítása – „Geofil habkavics”*.
- [6] M. SCHEFFLER–P. COLOMBO (2006): *Cellular Ceramics: Structure, Manufacturing, Properties and Applications*.
- [7] CSÖKE B.: *Aprítás, darabosítás és osztályozás: Mechanikai fizikai eljárások*.
- [8] G. MUCSI–B. CSÖKE–M. KERTÉSZ–L. HOFFMANN (2013): Physical characteristics and technology of glass foam from waste cathode ray tube glass. Hindawi Publishing Corporation, *Journal of Materials*.



SHORTER METHODS FOR DETERMINING BOND WORK INDEX

VLADIMIR NIKOLIĆ¹–MILAN TRUMIĆ¹–MAJA TRUMIĆ¹–LJUBIŠA ANDRIĆ²

¹University of Belgrade, Technical Faculty Bor, V.J. 12, 19210 Bor, Serbia,
vnikolic@tfbor.bg.ac.rs, mtrumic@tfbor.bg.ac.rs, majatrumic@tfbor.bg.ac.rs
²ITNMS, Franše d'Eperea 86, 11000 Belgrade, Serbia, andric.ljubisa@gmail.com

Abstract

In the mineral processing the grindability is one of the basic characteristics of materials which is important for calculation and selection of mills. The grindability expressed by Bond Work Index (W_i), as an energy parameter, represents the basis of the third theory of comminution – Bond comminution Law. The procedure of standard Bond test for Bond Work Index determination is a lengthy, complex and is therefore susceptible to procedural errors. For this reason many authors have outlined the procedures for Bond Work Index determination. The paper presents shorter procedures for determining the Bond Work Index value and a comparison of the values obtained by the shorter methods and the standard Bond test on different materials. The exact determination of Bond Work Index is essential for proper cost estimation related to the process of grinding, which is the area with the highest energy-saving potential, and mineral and recycling plant design.

Keywords: *Bond Work Index, grinding, grindability, shorter procedures.*

1. INTRODUCTION

Creation of new surface areas is generated by the process of crushing and grinding, which consumes a considerable amount of energy, and it is therefore very important that these processes be carried out in the most efficient way. Excessive grinding should be avoided due to high electricity costs, and finely grinding is further complicated by the process of grinding itself. The energy required for crushing and grinding is Bond work index and is determined by the Bond's test of grindability in Bond's ball mill. The numerical work index is the energy (kWh/sht) necessary for one short tone of the raw material to be infinitely large to the bulk, at which 80% of the raw material passes through a sieve of a square opening of size 100 μm .

Determining the Bond's work index is part of the design phase of a mining plant and can significantly affect the projected grinding problems. Grinding processes in mining are the most energy-efficient, and also the area with the highest energy-saving potential. The exact determination of Bond's work index is essential for proper design and cost estimation related to the process of grinding.

According to the standard Bond procedure, the work index is determined by simulation of dry milling in a closed cycle in Bond's mill with balls to reach 250% of the circulation load (BOND

1949, 1952, 1961). The Bond test requires 7–10 milling cycles, which indicates that the procedure is long and complex, and therefore subject to errors. For mills with rods, Bond's work index is obtained by testing in a standard mill in which 21 rods are inserted with a total mass of 33,380 grams. The determination procedure is the same as the mill with balls.

The Bond test and calculations of the results obtained through its equation proved to be extremely reliable for estimating the energy required for the grinding of raw materials in industrial conditions. Table 1 gives the values of Bond's work index for some raw materials.

The Bond work index is widely used to estimate the required power for grinding materials. Due to the difficulty in determining the Bond work index by the standard method, many researchers have developed alternative methods. The use of the Bond standard method in grinding plants is very common because it gives satisfactory results. Despite its advantages, this method also has some shortcomings, it takes a long time and requires a special milling mill. Therefore, the aim of this paper is to present other, shortened methods developed by other researchers to determine the Bond's work index.

2. MATERIALS AND METHODS/AREA DESCRIPTION

Methods for testing the grindability of the raw material are used to determine the energy consumption for grinding the product to the desired size. These procedures vary depending on the type of mills and the manufacturer. Mill mills usually use a Bond test to measure the size of the balls for grinding. The standard Bond test is not without limit. The test requires a specific preparation of the sample for work and a precisely defined bulk of the starting sample. For a Bond test, a 10 kg sample is needed, and usually a professional technical assistant is required to perform one test, which can last for more than 8 hours. According to the standard Bond test, the work index (W_i) is determined by simulation of dry milling in a closed cycle in Bond's mill with balls up to a circulation load to 250% (Bond, 1949, 1952, 1961). The Bond work index is calculated using the equation:

$$W_i = 1,1 \cdot \frac{44,5}{P_k^{0,23} \cdot G^{0,82} \cdot \left(\frac{10}{\sqrt{P_{80}}} - \frac{10}{\sqrt{F_{80}}} \right)}, [kWh/t] \quad (1)$$

where:

W_i – Bond work index, (kWh/t),

P_k – test sieve mesh size, (μm),

G – weight of the test sieve fresh undersize per mill revolution, (g/rev),

F_{80} – sieve mesh size passing 80 % of the feed before grinding, (μm),

P_{80} – opening of the sieve size passing 80 % of the last cycle test sieve undersize product, (μm).
(TODOROVIC et al. 2016)

Bond equation is widely applied in the preparation of mineral raw materials for comparison of resistance to grinding in a mill with balls of different types of materials, estimation of the required energy in industrial crushing and grinding plants and for adjusting the parameters of the grinding process.

Table 1
The value of Bond work index for some raw materials

Material	Work index	Material	Work index
Andesite	18,25	Graphite	43,56
Barite	4,73	Magnetite	9,97
Basalt	17,10	Lead ore	11,90
Bauxite	8,78	Lead-zinc ore	10,93
Cement clinker	13,45	Limestone	12,74
Cement raw material	10,51	Manganese ore	12,20
Clay	6,30	Magnesite	11,13
Coal	13,00	Molybdenum	12,80
Coke	15,13	Nickel ore	13,65
Copper ore	12,72	Oil shale	15,84
Diorite	20,90	Pyrrhotite ore	9,57
Dolomite	11,27	Quartzite	9,58
Emery	56,70	Quartz	13,57
Feldspar	10,80	Zinc ore	11,56
Hematite	12,84	Titanium ore	12,33
Ferro-manganese	8,30	Slag	10,24
Ferro-silicon	10,01	Slate	14,30

(METSO, 2015)

3. RESULTS AND DISCUSSION

Determining the Bond index by the standard method gives very accurate and reliable results, but the method is very boring and takes a long time. Due to the complexity and length of the Bond test and the ability to make mistakes during its performance, many scientists have tried more or less to simplify this procedure and sketch (WEISS 1985; TODOROVIC et al. 2016). This section will describe some of these methods.

BERRY and BRUCE (1966) devised an approximate procedure comparing the data on the alignment of an unknown ore with a reference ore whose data on the grindability are known and determined in Bond's ball mill. This procedure can be performed in any laboratory mill with balls. The reference ore and ore samples of an unknown grindability of 2 kg mass, (– 1.651) mm were milled in a wet mill in a mill with 305 mm diameter balls under identical conditions. They concluded that the energy needed for grinding is approximately the same for both samples, so:

$$W_{ir} \cdot \left[\frac{10}{\sqrt{P_r}} - \frac{10}{\sqrt{F_r}} \right] = W_i \cdot \left[\frac{10}{\sqrt{P}} - \frac{10}{\sqrt{F}} \right] \quad (2)$$

where:

- W_{ir} – work input of reference ore, (kWh/t),
- P_r – 80 % of product (reference ore) passes, (μm),

F_r	– 80 % of feed (reference ore) passes, (μm),
W_i	– work index of test, (kWh/t),
P	– 80 % of product (test ore) passes, (μm),
F	– 80 % of feed (test ore) passes, (μm).

From equation (2) it follows that Bond's work index of ore whose grindability is determined:

$$W_i = W_{ir} \cdot \frac{\left[\frac{1}{\sqrt{P_r}} - \frac{1}{\sqrt{F_r}} \right]}{\left[\frac{1}{\sqrt{P}} - \frac{1}{\sqrt{F}} \right]}, [\text{kWh/t}] \quad (3)$$

HORST and BASSAREAR (1977) gave a slightly longer procedure similar to that of **BERRY and BRUCE (1966)** in which the reference and ore data for which the Bond index value is sought are compared. The difference in this procedure with respect to the Berry-Bruce process is that it does not take into account the granulometric composition of the inputs and grinding products of the test sample, but starts from the granulometric composition of the reference ore input, and the granulometric composition of the grinding product of an unknown ore is calculated by the equation of the law of the kinetics of the first order. The test is carried out on samples of a bulk density of ($- 1.651$) mm in any laboratory mill with balls. The sample of the reference ore weighing 1 kg is ground for so long to achieve the desired granulometric composition of the mill. Three samples of ore whose grindability is determined as 1 kg weighed in the same mill as the reference sample under the same conditions and with different grinding times. The grinding times of these three samples should include the grinding time of the reference ore. On grinding products, granulometric analysis is continued. The obtained data is plotted graphically ($t; \ln R$) and hence the constants of grinding speed k_i are calculated for different sieve openings. The granulometric composition of the grinding ore whose grindability is determined is calculated using the granulometric composition of the reference ore input, the grinding time of the reference ore to the desired fineness, and the rate of grinding velocity k_i for the various sieves of the sieves determined by the opacity tests of the ore whose grindability is determined. From the granulometric composition calculated in this way, the value of P is determined, and the value of F is taken to be equal to F_r . The Bond work index is calculated according to equation (3). By using copper ore as a reference ore, comparative results using the Berry-Bruce method and the standard Bond method show that the biggest error was 14.21% and at least 1.36%, while the comparative results using the Horst-Bassarear method and the standard method showed that the largest the error amounted to 2.16%, and the smallest 1%.

SMITH and LEE (1968) compared the data obtained with the standard Bond test and the data from the open grinding cycle, or the first grinding cycle of the standard Bond test (TODOROVIC et al. 2016). The tests were carried out on eight different raw materials at different openings of the comparative sieve according to the standard Bond test for the grindability. They found that the parameter G_e (g/rev) of the last grinding of the standard Bond test and the G_0 open grinding cycle parameter under the same conditions are in the direct correlation bond $G_0 = f(G_e)$ (TODOROVIC et al. 2016). This correlation link is established on smaller openings and for tests carried out with less than 300

rotation of mill. Using this correlation, it is possible to determine the G_0 value using one grinding in the open cycle and evaluate the value of the parameter G_e of the standard Bond procedure on the basis of it, and calculate the Bond work index using equation (1). The correlation between parameters G is valid only for certain material and it takes a lot of work to determine it. Smith and Lee argued that the differences between the values of W_i obtained by the standard Bond method and their shortened procedure did not exceed 15%.

Kapur (1970) concluded that estimating the Bond index can be derived from data from the first two grinding cycles of the standard Bond test. This conclusion was reached by analyzing the standard grinding cycles using a mathematical algorithm based on the first order grinding kinetics. He noticed that there was not much difference between the rate constant of grinding class $+P_k$ in the second and final grinding cycle of the standard Bond test. He proposed that the rate of grinding in the second cycle serve to estimate the value of Bond work index using the equation:

$$W_i = 1,1 \cdot 2,648 \cdot P_k^{0,406} \cdot k_2^{-0,81} \cdot (XM)^{-0,853} \cdot (1 - X)^{-0,099}, [kWh/t] \quad (4)$$

where:

- P_k – test sieve mesh size, (μm),
- k_2 – the rate of grinding speed of the class $+P_k$ from the second experiment of the standard Bond test,
- X – content of the class $+P_k$ in the starting sample, (fractions of unity),
- M – mass of the sample in the mill, (g).

Comparative values of Bond work index according to the standard Bond test and Kapur's procedure show that the largest error at the copper ore was 15.47%, and the smallest 0.30%.

KARRA (1981) modified the Kapura method by taking into account that the circular load with a standard Bond test is harder than a fresh sample and that it is slower and slower. This method simulates the Bond test using a mathematical algorithm based on the results obtained from the first two grinding stages of the standard test until a stable circulating load of 250% is established. From the last simulated experiment, the value of the parameter G is obtained. The value of the parameter P can not be estimated in this way, so the Bond equation that includes this parameter can not be used to calculate the Bond index. To calculate the Bond index, the empirical formula obtained from the statistical data processing is used:

$$W_i = 1,1 \cdot 9,934 \cdot P_k^{0,308} \cdot G^{-0,696} \cdot F^{-0,125}, [kWh/t] \quad (5)$$

where:

- P_k – test sieve mesh size, (μm),
- G – estimated newly created prospect of the comparative sieve after rotating the mill in the last experiment, (g/rev),
- F – 80 % passing size of the feed, (μm).

The Karra algorithm is performed by performing the first two grinds, and the further simulation is carried out by calculation. The obtained benchmark values of the Bond work index according to the standard Bond test and the Karra procedure show that the biggest error for quartzite was 5.5 % and at least 1.4%.

MULAR and JERGENSEN (1982) have devised a procedure called ,“Anakonda procedure” which is performed in any laboratory mill with balls that is calibrated with a reference ore or ores in relation to the Bond work index. For the calibration of a mill, it is necessary to determine the values of the Bond work index W_i at the given size of the opening of the comparative sieve on the reference ore or ores by the standard Bond procedure. The reference ore or ores of the same mass and volume should be further grounded in a laboratory mill that is calibrated for the same time t and determined for each F and P . The obtained results determine the calibration constant of the mill A :

$$A = W_i \cdot \left(\frac{1}{\sqrt{P}} - \frac{1}{\sqrt{F}} \right), [kWh/t] \quad (6)$$

where:

- A – calibration constant of the mill, (kWh/t),
 - F – sieve mesh size passing 80 % of the feed before grinding, (μm),
 - P – opening of the sieve size passing 80 % of the grinding product, (μm).
- (TODOROVIC et al. 2016)

For multiple values A obtained on different raw materials, the mean value is taken, or the value A is calculated using the least squares method. Bond work index W_i is calculated according to equation (7):

$$W_i = \frac{A}{\left(\frac{1}{\sqrt{P}} - \frac{1}{\sqrt{F}} \right)}, [kWh/t] \quad (7)$$

By comparing the value of the work index with the standard Bond method and the Anakonda method copper ore process, the biggest error was 7.02% and the minimum 0.87%.

MAGDALINOVIĆ (1989) gave a shortened method for determining the Bond work index, which includes two grinding (TODOROVIC et al. 2016). This method relies on the law of the first order of kinetics by which the comminution of the raw material in the Bond mill with balls takes place. The procedure is performed on a 100 % (– 3.35) mm sample in the Bond mill with balls. The granulometric composition, the parameter F (μm) and the weight of the mill feed M (g) 700 cm^3 is determined. The weight of the new feed $U = M / 3.5$ (g) is calculated. The first grinding sample is formed by combining the weight of the test sieve over-size $R = 2.5 / 3.5 \cdot M$ (g) and the weight of the new feed U . The grinding of this formed sample for the arbitrary chosen number of mill revolutions ($N_1 = 50, 100$ or 150). After grinding, the entire sample is screened on a test sieve and the over-size is weighed (R). The over-size grinding rate constant (k) is calculated from eq. (8).

$$k = \frac{n(\ln R_0 - \ln R)}{N} \quad (8)$$

The total number of mill revolutions (N_2) for the second grinding test is based on this constant which is required to obtain a circular load of 250% (TODOROVIC et al. 2016). The sample for the second grinding is formed in the same way as the sample for the first grinding and is grounded to calculate the (N) number of rotation of the mill. After grinding, the entire sample is screened on the test sieve. Both the over-size and the under-size are weighed. The weight of the over-size should be equal or approximately equal to $(2.5/3.5) \cdot M$ whereas the weight of the under-size (m) should be: $m = (1/3.5) \cdot M$. Size distribution of the under-size from the second test is determined by means of screen analysis and the value (P) is determined graphically. The weight (G) of the new under-size obtained per mill revolution in the second test is calculated. The work index (W_i) is derived from the Bond formula (eq. 1). Comparative results obtained with the standard Bond method and Magdalinovic shortened copper ore method show that the largest error is 7.0% and the smallest 1.3%.

MAGDALINOVIĆ (2003) gave a shortened method similar to the previously described, but it includes three millings. This method also relies on the law of the first order of kinetics by which the comminution of raw materials in the Bond mill with balls takes place. The procedure is performed on a 100 % (– 3.35) mm sample in the Bond mill with balls. Determine the size distribution of the sample and the starting size F (μm) and contribution of sample of larger size than the mesh of comparative test-sieve (X) (fractions of unity). Take the sample of volume 700 cm^3 , determine its weight M (g) charge it into Bond's ball-mill and grind at arbitrary mill RPM N_2 ($N_1 = 50, 100$ or 150 revolutions) (TODOROVIC et al., 2016). After grinding, screen the sample on comparative test-sieve and determine the weight of the over-size R_1 (g). By using a class fraction greater than the opening of the comparative sieve before and after grinding and equation (9), the grinding rate constant k_1 for the given sample is determined.

$$k_1 = \frac{\ln MX - \ln R_1}{N_1} \quad (9)$$

Based on this constant, is calculated the number of revolutions of the mill N_2 (rev) for the second grinding test. Add fresh sample to the over-size (R_1) of weight ($M - R_1$), charge it into the mill and grind it for duration of N_2 mill RPM. After grinding, screen the sample on comparative test-sieve and determine its weight R_2 (g). By using a class fraction larger than the opening of the comparative sieve before and after grinding and the formula $R = R_0 \cdot e^{-kt}$, the grinding rate constant for the given sample is determined. Based on this constant, is calculated the number of revolutions of the mill N_3 (rev) for the third grinding test. Add fresh sample of weight ($M - R_2$) to the over-size (R_2) charge into mill and grind for the duration of mill RPM, N_3 . After grinding, screen the sample on comparative test-sieve and determine the weight of under-size of comparative test-sieve m_3 (g). Determine granulometric composition of over size of comparative test sieve from the third grinding test and determine the size of the over- size product P (μm). Calculate the weight of newly formed over size product per one mill revolution in the third grinding test (G_3). Calculate

work index (W_i) according to Bond's equation (1). The obtained comparative results with the standard Bond method and this shortened method on copper ores show that the biggest error was 3.50 %, and the smallest 1.49%.

LEWIS et al. (1990) gave a mathematical algorithm that simulates a standard Bond test (TODOROVIC et al. 2016). A computer simulation based on a mathematical algorithm is divided into two distinct parts. The first part of the simulation uses experimental data from the first grinding cycle of the standard Bond test to form the initial model parameters (TODOROVIC et al. 2016). The initial model parameters together with the description of the starting material are then stored in the database used in the second phase of the prediction simulation. The simulation method simulates the traditional procedure. For each grinding cycle, the material smaller than the opening of the comparative sieve is replaced with a representative amount of the starting sample (TODOROVIC et al. 2016). Calculation is continued using parameters that are set according to the current grinding cycle. The four grinding cycles are counted automatically. In the fourth and subsequent cycles, the parameter G (g/rev) is constant (within 3%) for the last three grinding cycles. If it is, then a stable state is achieved, otherwise the computer simulation continues with the next grinding cycle. When a stable state is reached, the parameters obtained in the last grinding cycle are used and Bond's work index is calculated using equation (1). A comparison of the results obtained with the standard Bond method and the results obtained by the computer simulation of Bond's limestone test show that the biggest error was 6.18%, and the smallest 0.39%.

NEMATOLLAHI (1994) designed a smaller mill to determine the Bond index, and called it a calibrated Bond mill with balls. The diameter of the mill was 200×200 mm and used 85 steel balls for grinding. The weight of the ball was 5.9 kg, and the balls were in the range of 16–38 mm in diameter. The initial sample had a volume of 207 cm^3 instead of 700 cm^3 , which is standard in the Bond test. The test is performed by grinding to dry in a closed cycle until reaching a 250% circulating load. Grinding is repeated until the produced sample of the control sieve after one rotation of the mill does not become constant in the last three grinding. The Bond work index is calculated by equation (10):

$$W_i = \frac{11,76}{P_k^{0,23}} \cdot \frac{1}{G^{0,75}} \cdot \frac{1}{\frac{10}{\sqrt{P}} - \frac{10}{\sqrt{F}}}, [kWh/t] \quad (10)$$

By comparing the value of Bond work index with Bond's balls and new balls, it was found that the greatest error for various raw materials was 11.90% and at least 1.62%.

AKSANI and SONMEZ (2000) gave a computer simulation of Bond's grindability test that relies on a cumulative kinetic model (FINCH and RAMIREZ-CASTRO 1981). In this cumulative kinetic model, the grinding constant constant $k = C \cdot x^n$, where C and n constants depend on the characteristics of the mill and material characteristics, and x represents the size of the screen opening. The process is performed by grinding 700 cm^3 of a 100 % (– 3.35) mm sample in a Bond mill with balls with grinding time (0.5; 1; 2 and 4) minutes. After each grinding cycle, the sample is emptied from the mill and its granulometric analysis is done. The obtained granulometric analysis products are merged and returned to the mill for the next grinding cycle. On the basis of the obtained data of the

cumulative reflection in relation to the grinding time, a constant of the grinding rate k is calculated by nonlinear regression. In order to calculate the parameters C and n , both sides of the above equations are logarithmic and then linear regression is applied. The simulation program uses data on the granulometric composition, the input mass, the parameters of the kinetic model and the number of rotations of the mills of the first grinding cycle. The simulation method simulates the traditional procedure. For each grinding cycle, the parameter G (g/rev) is calculated and the material smaller than the opening of the comparative sieve is replaced with a representative quantity of the starting sample. Calculation continues until parameter G becomes constant for the last three grinds. When a stable state is reached, the parameters obtained in the last grinding cycle are used and Bond work index is calculated using equation (1). Comparison of the results obtained with the standard Bond method and the results obtained by computer simulation show that the largest error for different samples is 4.01%, and the smallest 0.25%.

TÜZÜN (2001) stated that the scope of the activities included in the Bond test can produce errors that can easily result in results due to ignorance of the volume and the limits of the end of the test itself. It came to the conclusion that when a sieve size of 53 μm is used as a comparative sieve, the values obtained for Bond work index are higher than expected. The values of the Bond work index that are obtained on that occasion are generally higher due to errors that can arise during dry screening. The procedure for determining the Bond index by wet procedure is followed by the standard Bond test, but 1 kg of water is added to each grinding, and the screening is done in a wet process for a period of 10 minutes. Then the reflection is filtered, dried and its mass measured, in order to calculate the mass of the asterisks needed to determine the mass of the newly created reaches after one rotation of the mill. The test is finished when the mass of the averages of the comparative sieve is constant during the three experiments and is approximately equal to the mass of the products of the ideal grinding product. Then Bond work index according to Bond equation (1) is calculated, and the obtained value is multiplied by a correction factor of 1.3, determined by Bond. Comparative results of Bond work index obtained by wet and dry grinding process on the quartz sample show that the biggest error was 5.70% and at least 0.56%.

DENIZ and OZDAG (2002) investigated the relationship between the parameters of the Bond method W_i (kWh/t) and G (g/rev) and the dynamic elastic parameters of the raw material (shear modulus G_d , the elasticity modulus E_d and the bulk modulus K_d). They found that the best correlation can be established between the Bond index and the bulk module K_d , also called the brittleness module. This module takes into account the state of porosity and discontinuity, such as compounds of a certain material. They performed measurements on several different raw materials and obtained results that the biggest error for the bulk modulus K_d was 20.53%, for the elasticity modulus E_d 28.40%, for the shear modulus G_d 32.40% and the smallest error for the bulk modulus K_d was 0.08%, for elasticity modulus E_d 3.12% and for shear modulus G_d 2.59%.

MENÉNDEZ-AGUADO et al. (2005) examined the possibility of determining the work index in Denver's laboratory mill. The research was carried out on a bulk class of 100% (-3.35) mm, and the starting volume of the sample was 326 cm^3 . A milling test in the Denver mill followed Bond's methodology, but some corrections were made. In Denver and Bond's mill, the method followed

three grinding cycles. Due to the volume difference between Denver and Bond's mill, grinding balls of other dimensions were used in the mill. The Bond work index is calculated by equation (11):

$$W_i = \frac{44,5}{P_k^{0,233} \cdot (2,15 \cdot G)^{0,82} \cdot \left(\frac{10}{\sqrt{P}} - \frac{10}{\sqrt{F}} \right)}, [kWh/t] \quad (11)$$

By comparing the results of Bond work index in Bond and Denver's mill, the biggest mistake for the difference in raw materials was 6.77%, and the smallest 0.67%.

SWAIN and RAO (2009) have investigated the possibility of determining the Bond's work index based on the Hardgrove grindability index. The Hardgrove grindability index is determined by the method described by FASBENDER et al. (1975). Grinding is performed on a representative sample of 50 g of the class $(- 1.18 + 0.6)$ mm at 60 rpm. The Hardgrove index is calculated according to the following equation (12):

$$H = 13 + 6,93 \cdot m_H \quad (12)$$

where:

- H – Hardgrove index,
- m_H – of the particles smaller than 74 μm (g).

FASBENDER et al. (1975) modified the equation that binds Hardgrove index and Bond's index of work and gave the following equation:

$$W_i = \frac{435}{H^{0,82}}, [kWh/t] \quad (13)$$

By comparing the results obtained with the standard Bond method and the results obtained by the Hardgrove index, the largest bauxite ore deficiency was 4.04% and the smallest 2.13%.

SAEDI et al. (2013) used a special mill to determine the Bond work index, which was designed by NEMATOLLAHI (1994). The number and diameter of the balls used in this experiment is the same as used by NEMATOLLAHI (1994), and the Bond's work index is calculated by equation (10). On a representative sample of 2 kg a granulometric composition was determined, and then a representative sample was milled at time intervals of (20, 60, 120 and 180) seconds. After each grinding, the sample is average, the parameter P and Bond's work index is determined (TODOROVIC et al. 2016). Due to the large deviations in the values of the Bond work index, obtained from the equation (10), the authors defined a new equation (14) for determining the Bond's work index based on the obtained results. They came to the new formula by examining the relationship between G and P with the time of grinding. It was necessary to create a relationship between these parameters, which could replace G and P . The relationship between G and P indicates that they are dependent on the grinding time. Based on the obtained iron ore results, the error was 0.41%.

$$W_i = \frac{5,6}{(-1E - 0,6 \cdot t^2 + 0,0004 \cdot t + 0,3397)^{0,75}} \cdot \frac{1}{\frac{10}{\sqrt{-0,1085 \cdot t + 122,56}} - \frac{10}{\sqrt{F_{80}}} } \quad (14)$$

FORD and SITHOLE (2015) gave a shortened method for determining a Bond's work index consisting of two tests. The first test was done with only one grinding experiment, and the second test with three grinding experiments. A sample of 700 cm³ of a class of 100 % (– 3.35) mm is ground in a standard Bond mill with balls for a predetermined number of rings, at time intervals of (0.5; 1; 2; and 4) minutes. After each grinding, the mass of the sample is measured and the granulometric composition is determined. These data are then used to calculate the parameters k for each granulometric composition according to equation (15):

$$W_{(x,t)} = W_{(x,0)} \cdot \exp(-k \cdot t) \quad (15)$$

where:

- t – grinding time (minutes),
- $W_{(x,t)}$ – the cumulative percentage of oversize material of particle size x at time t in the product,
- $W_{(x,0)}$ – the cumulative percentage of oversize material of particle size x in the feed, corresponding to $t = 0$,
- k – the cumulative breakage rate constant (min⁻¹).

The model describes a mathematical simulation in a closed grinding cycle. In simulation, the number of turns varies until a re-circulating load of 250% is achieved. The mass of the newly created screen is calculated after one rotation of the mill G , F and P , and the Bond work index is calculated from the equation (1). Based on the results obtained from the first and second copper-cobalt ore tests, the biggest error was 20.81% for the first test and 3.74% for the second test, and the smallest 0.21 % for the first test and 0.46% for the second test.

GHAREHGESHLAGH (2015) gave a method for estimating a Bond work index that relies on monitoring the grinding kinetics in Bond mill with balls and establishing a series of the ratio of grinding parameters and parameters of the Bond equation (TODOROVIC et al. 2016). The process is performed by grinding 700 cm³ of a 100% (– 3,35) mm sample in a Bond mill with balls with grinding time (0.33; 1; 2; 4 and 8) minutes. After each grinding cycle, the sample is emptied from the mill and its granulometric analysis is done. The obtained granulometric analysis products are merged and returned to the mill for the next grinding cycle. Based on the data obtained by kinetic milling and granulometric analysis of the grinding product, the numerical method of the smallest squares determines the functional dependence of the number of rotations of the mill and the mass of the averages of the comparative sieve m_p (g), as well as the number of rotations of the mill G (g/rev) and the parameter P (μm). On the basis of the first function, the number of rotations of the mill $N_{250\%}$ (rotation) that is required to obtain the mass of the sieve is such that the circular load is 250%. The parameters G (g/rev) and P (μm) are calculated using $N_{250\%}$ and functional dependencies determined. The Bond work index is calculated using the obtained values and equation (1). Gharegheshlagh stated that the error between the results obtained by this method

and the results obtained by the standard Bond test does not exceed 2.6% for different raw materials (TODOROVIC et al. 2016).

TODOROVIC et al. (2016) gave a shortened method that can be done with two, three or four grinding cycles. Each grinding cycle is done identically as with the standard Bond process. In the shortened procedure with two grinding cycles, the granulometric composition of the starting sample is determined, the value F (μm) as well as the participation of a larger size and the comparative sieve openings X (fractions of unit). A sample of a volume of 700 cm^3 of a 100% ($- 3.327$) mm is taken, its mass M (g) is determined, and the sample is ground in a Bond mill with balls for an arbitrary number of rotations of the mill ($N_1 = 50, 100$ or 150 revolutions). After grinding, screen the sample on the comparative sieve and determine undersize mass D , (g) and oversize R , (g) (TODOROVIC et al. 2016). Undersize D consists of a undersize mass D_u , which is entered with fresh feed and newly formed undersize in mill D_n . Calculate the newly formed undersize mass $D_n = D - D_u$. In first grinding cycle it is: $D_u = M \cdot (1 - X)$, (g), while in subsequent cycles it is: $D_u = D_{(n-1)} \cdot (1 - X)$, (g), where $D_{(n-1)}$ is the undersize mass from the previous cycle, (g) (TODOROVIC et al. 2016). Then, calculate the newly formed undersize mass per mill revolution G (g/rev) and the mill revolutions for following grinding cycle N_n according to equation (16).

$$N_n = \frac{\frac{M}{3,5} - D_{(n-1)} \cdot (1 - X)}{G}, [\text{revolution}] \quad (16)$$

Add to comparative sieve oversize fresh sample a mass equal to the undersize mass from the previous cycle $D_{(n-1)}$. Thus, the formed feed sample is charged into the mill and ground for N_n revolutions. After grinding, screen the sample on the comparative sieve and measure the oversize mass R (g). (TODOROVIC et al. 2016) Then the constant k is calculated using formula (17):

$$k = \frac{n \cdot (\ln R_0 - \ln R)}{N} = \frac{n \cdot \left[\ln \left(\frac{R_{(n-1)}}{M} + \frac{D_{(n-1)}}{M} \cdot X \right) - \ln \frac{R}{M} \right]}{N}, \quad (17)$$

Calculate the required mill revolutions number N . In the case the grinding material quantity is the same as when the equilibrium was reached (circulating load 250%), with grinding rate constant as in the second grinding, using formula (18). (TODOROVIC et al. 2016)

$$N = \frac{n}{k} \left[\ln \left(\frac{2,5}{3,5} \cdot 100 + \frac{X}{3,5} \cdot 100 \right) - \ln \left(\frac{2,5}{3,5} \cdot 100 \right) \right] \quad (18)$$

Calculate parameter G (g/rev) with formula (19). Obtained value G is multiplied by the constant of 1.158, giving value G_e , which should be approximately equal to the value of G at the last grinding cycle during the execution of the standard Bond test. (TODOROVIC et al., 2016)

$$G = \frac{\frac{M}{3,5} \cdot X}{N} \quad (19)$$

Determine the grain size distribution and parameter P_2 for the second grinding undersize. The obtained value is multiplied by constant 1.035. Calculated result should be approximately equal to the P value of undersize from the last grinding cycle during the execution of the standard Bond test. Using the achieved values of G_e , P and formula (1) an approximate value of W_i (kWh/t) is obtained. In case of a quick method with three or four grinding, three or four grinding cycles should be carried out, in the same way as the standard Bond procedure. Parameters G_e and P are calculated as in the procedure with two grinding, except for being multiplied by the appropriate parameters for three or four cycles grinding. During the performance of the two, three and four grinding tests and the standard Bond test on a composite sample of limestone and andesite in various mass relations, the biggest error was 8.93% and the minimum 0.51%. (TODOROVIC et al. 2016)

CHANDAR et al. (2016) attempted to determine the Bond's work index using ore characteristics, such as density of rock (ρ), Protodyakonov's strength index (PSI), and rebound hardness number (RHN). Determination of the Bond work index was carried out on samples of the class ($- 3.35$) mm by the standard Bond method until reaching a circulating load of 250%. Two mathematical models for the analysis of laboratory results, artificial neural networks (Artificial Neural Networks – ANN) and regression analysis were used. Artificial neural networks were used to check the accuracy of data on the basis of experimental results, and regression analysis were used to find correlation mathematical factors. The access of artificial neural networks were used to ensure that the results obtained from the laboratory experiments were error-free. It was found that the percentage of the error between the actual values of the Bond work index, obtained from laboratory experiments and the predicted results obtained from artificial neural networks between the maximum deviation of 5.44% and the minimum deviation of 0.05%. The correlation coefficient is determined individually for relations between the density, the Protodyakonov's strength index and rebound hardness number with the Bond work index. A combined ratio between Bond's work index and all other parameters was also determined. Models obtained by regression analysis are given in the equations (20), (21), and (22).

$$W_i = 8,85 \cdot \rho - 12,58 \quad (20)$$

$$W_i = 4,32 \cdot (PSI) - 2,2 \quad (21)$$

$$W_i = 0,34 \cdot (RHN) - 6,61 \quad (22)$$

By comparing the results obtained with the standard Bond method and using the equations (20), (21) and (22) for different raw materials, it was found that the largest equation error (20) is 7.46%, for the equation (21) 9.91% and for the equation (22) 5.34%, while the smallest error for the equation (20) was 0.27%, for the equation (21) 0.09% and for the equation (22) 0.02%.

MENÉNDEZ et al. (2017) wanted to point out that changing the standard Bond balls with new balls influenced the Bond's work index. The dimensions of some of the balls were ejected, and they inserted balls of new dimensions, and they changed the number of balls. After each ten test they checked the weight of the balls, and each ball that was less than 10 g was replaced with a new ball. Before grinding, all samples were reduced to ($- 3.15$) mm, and screened on sieves

(2,800; 2,000; 1,400, 1,000; 710; 500; 355; 250; 180; 125; 90; 63; 45 36 and 25) μm . The Bond work index is calculated by equation (1). They used the comparative sieve of the holes (500, 250, 125, 90 and 63) μm . Minimum 4 grinds were made, while the mass of the comparative sample was not constant. When the grinding product is screened on the sieves (90 and 63) μm , the screening is done in a wet process. Three mathematical models for calculating P (μm) were proposed:

$$P = 0,8133 \cdot P_k - 3,4562 \quad (23)$$

$$P = 0,7704 \cdot P_k^{1,0051} \quad (24)$$

$$P = 0,0001 \cdot P_k^2 + 0,7539 \cdot P_1 + 1,681 \quad (25)$$

By comparing the values obtained with the standard Bond test and the values obtained from the equations (23), (24), and (25) on various raw materials, it was found that the greatest error for the equation (23) is 3.69%, for the equation (24) 3.42% and for the equation (25) 5.00%, while the smallest error was 0.08% for equation (23), for equation (24) 0.08% and for equation (25) 0.09%.

MENÉNDEZ et al. (2018) gave a corrected formula for determining the Bond work index. The tests were carried out on samples of the class ($- 3.35$) mm, and comparative sieves of (500, 250, 125, 90 and 63) μm were used. On comparative sieves of (90 and 63) μm , the screening was carried out using a wet process, in order to accurately determine the mass of the comparative sample and the granulometric composition. The method follows the standard Bond procedure, given the corrected formulas for the weight of the test sieve fresh undersize per mill revolution G (g/rev), and the corrected formula for determining the Bond's work index (W_i). They have come to the conclusion that the weight of the test sieve fresh undersize per mill revolution G (g/rev) depends on the percentage of fine classes of fresh sample added to the mill for the new grind milling, and based on this, the corrected formula (26) for the weight of the test sieve fresh undersize per mill revolution:

$$G_f = \frac{G}{\left(1 - \left(0,01 \cdot \frac{U}{3,5}\right)\right)} \quad (26)$$

where:

- G_f – the corrected weight of the test sieve fresh undersize per mill revolution, (g/rev),
- G – weight of the test sieve fresh undersize per mill revolution, (g/rev),
- U – sample mass, (g).

Since the Bond work index is based on a constant sample volume of 700 cm^3 , but the results are presented in grams, two samples of the same grindability but different densities have to have different values for the parameter G . They have proposed a new equation (27) for calculating the parameters G :

$$G_{\gamma} = \frac{G_f}{\gamma} = \frac{G}{\gamma \cdot \left[1 - \left(0,01 \cdot \frac{U}{3,5}\right)\right]} \quad (27)$$

where: γ – sample density.

The Bond work index is calculated by equation (28):

$$BWi_c = \left[\frac{49,1}{P_k^{0,23} \cdot \left\{ \frac{G}{\gamma \cdot \left[1 - \left(0,01 \cdot \frac{U}{3,5}\right)\right]} \right\}^{0,82} \cdot \left(\left(\frac{10}{\sqrt{P_{80}}} \right) - \left(\frac{10}{\sqrt{F_{80}}} \right) \right)} \right], [kWh/t] \quad (28)$$

By comparing the results obtained with the standard Bond method and the results obtained using the corrected formula for different raw materials, the largest error was found to be 30.16% and at least 10.21%.

4. CONCLUSIONS

The paper deals with existing methods for determining the grindability of mineral and secondary raw materials, which were proposed by the authors. Several laboratory methods have been developed to determine the grindability of mineral and secondary raw materials, and some of them have been described in the paper. The aim of all the methods described in the paper is to give as close to Bond's work index as possible a comparison with Bond's standard method and to reduce the very process of work that lasts very long and requires professional personnel to work. The described methods are quick and practical, since they eliminate individual steps in the work itself and reduce the number of grinding steps. Some methods also require a lower initial mass compared to the Bond method, where about 10 kg of the initial sample is required. Regardless of the Bond's defects in determining the Bond's work index, the defects observed in fine grinding and the defects related to the replacement of spent balls in a ball mill, the original Bond procedure remains an industry standard.

ACKNOWLEDGMENTS

This investigation was supported by Serbian Ministry of Education, Science and Technological Development and it was conducted under following project: TR 33007.

REFERENCES

- [1] AKSANI, B.–SONMEZ, B. (2000): Technical note – Simulation of Bond grindability test by using cumulative based kinetic model. *Mineral Engineering*, 13 (6), pp. 673–677.
- [2] BERRY, T. F.–BRUCE R. W. (1966): A simple method of determining the grindability of ores. *Canadian Mining Journal*, 87, pp. 63–65.
- [3] BOND, F. C. (1949): Standard grindability test tabulated. *Transactions of the American Institute of Mining and Metallurgical Engineers*, 183, pp. 313–329.

-
- [4] BOND, F. C. (1952): The third theory of comminution. *Transactions of the American Institute of Mining and Metallurgical Engineers*, 193, pp. 484–494.
- [5] BOND, F. C. (1961): Crushing and grinding calculation part I and II. *British Chemical Engineering*, 6 (6 and 8), pp. 378–385, 543–548.
- [6] CHANDAR, R. K. et al. (2016): Prediction of Bond's work index from field measurable rock properties. *International Journal of Mineral Processing*, 157, pp. 134–144.
- [7] DENIZ, V.–OZDAG, H. (2002): A new approach to Bond grindability and work index: dynamic elastic parameters. *Minerals Engineering*, 16, pp. 211–217.
- [8] FASBENDER, H. et al. (1975): Mahlbarkeitspruefung und rohrmuehlenauslegung bei zementrohstoffen. *Zem.-Kalk-GipsZement Kalk-Gips*, 28 (8), pp. 316–324.
- [9] FINCH, J. A.–RAMIREZ-CASTRO, J. (1981): Modelling mineral size reduction in the closed-circuit ball mill at the Pine Point Mines concentrator. *International Journal of Mineral Processing*, 8 (1), pp. 61–78.
- [10] FORD, E.–SITHOLE, V. (2015): A Comparison of Test Procedures for Estimating the Bond Ball Work Index on Zambian/DRC Copper–Cobalt Ores and Evaluation of Suitability for Use in Geometallurgical Studies. *Copper Cobalt Africa, incorporating the 8th Southern African Base Metals Conference*, Livingstone, Zambia, 6–8 July, pp. 65–68.
- [11] GHAREHGESHLAGH, H. H. (2015): Kinetic grinding test approach to estimate the ball mill work index. *Physicochemical Problems of Mineral Processing*, 52 (1), pp. 342–352.
- [12] HORST, W. E.–BASSAREAR, J. H. (1977): Use of simplified ore grindability technique to evaluate plant performance. *Transactions of the Metallurgical Society of AIME*, 260, pp. 348–351.
- [13] KAPUR, P. C. (1970): Analysis of the Bond grindability test. *Transactions of the Institution of Mining and Metallurgy*, 79, pp. 103–108.
- [14] KARRA, V. K. (1981): Simulation of the Bond Grindability test. *CIM Bulletin*, 74 (827), pp.195–199.
- [15] LEWIS, K. A. et al. (1990): Computer Simulation of the Bond Grindability test. *Minerals Engineering*, 3 (1–2), pp. 199–206.
- [16] MAGDALINOVIĆ, N. (1989): A procedure for rapid determination of the Bond work index. *International Journal of Mineral Processing*, 27, pp. 125–132.
- [17] MAGDALINOVIĆ, N. (2003): Abbreviated test for quick determination of Bond's Work index. *Journal of Mining and Metallurgy*, 39 (1–4) A, pp. 1–10.
- [18] MENÉNDEZ-AGUADO, J. M. et al. (2005): Determination of work index in a common laboratory mill. *Minerals & Metallurgical Processing*, 22 (3), pp. 173–176.
- [19] MENÉNDEZ, M. et al. (2017): A Bond Work index mill ball charge and closing screen product size distributions for grinding crystalline grains. *International Journal of Mineral Processing*, 165, pp. 8–14.

-
- [20] MENÉNDEZ, M. et al. (2018): The comminution energy-size reduction of the Bond Mill and its relation to Vickers Hardness. *Minerals Engineering*, 119, pp. 28–235.
- [21] MULAR, A. L.–JERGENSEN, G. V. (Eds.) (1982): *Design and installation of comminution circuits*. New York, Society of Mining Engineers of the American Institute of Mining, Metallurgical, and Petroleum Engineers, pp. 176–203.
- [22] NEMATOLLAHI, H. (1994): New size laboratory ball mill for Bond work index determination. *Mining Engineering*, 46 (4), pp. 352–353.
- [23] SAEIDI, N. et al. (2013): A developed approach based on grinding time to determine ore comminution properties. *Journal of Mining & Environment*, 4 (2), pp. 105–112.
- [24] SMITH, R. W.–LEE, K. H. (1968): A comparison of data from Bond type simulated closed-circuit and batch type grindability tests. *Transactions of the Metallurgical Society of AIME*, 241, pp. 91–99.
- [25] SWAIN, R.–RAO, R. B. (2009): Alternative Approaches for Determination of Bond Work Index on Soft and Friable Partially Laterised Khondalite Rocks of Bauxite Mine Waste Materials. *Journal of Minerals & Materials Characterization & Engineering*, 8 (9), pp. 729–743.
- [26] TODOROVIC, D. et al. (2017): A quick method for Bond work index approximate value determination. *Physicochemical Problems of Mineral Processing*, 53 (1), pp. 321–332.
- [27] TÜZÜN, M. A. (2001): Wet bond mill test, *Minerals Engineering*, 14 (3), pp. 369–373.
- [28] WEISS, N. L. (1985): *Mineral Processing Handbook*. New York, Society of Mining Engineers, AIMM.



COATING AS A POSSIBLE WAY TO IMPROVE THE RECYCLABILITY OF WASTE AGGREGATES

ALENA SICAKOVA¹–KAROL URBAN²

¹Technical University of Kosice, Faculty of Civil Engineering, Vysokoskolska 4, 042 00 Kosice, Slovakia, alena.sicakova@tuke.sk

² Technical University of Kosice, Faculty of Civil Engineering, Vysokoskolska 4, 042 00 Kosice, Slovakia, karol.urban@tuke.sk

Abstract

The paper is aimed at the construction and demolition waste (C&DW) aggregate, mainly recycled concrete aggregate (RCA), and its utilization for concrete production. While the environmental benefits of using recycled aggregates are well accepted, some unsolved problems prevent this type of material from wide application in structural concrete. The main problems with the use of RCA in structural concrete are connected with the presence of old mortar adhered onto the grains, thus the variability of its composition and microstructure. As a consequence, such aggregate is of irregular shape, surface, it possesses the porous nature and high water absorption capacity; also cracks are presented ... Generally, the parameters of RCA affect negatively the bond between the grains and cement paste when used in new concrete. This fact directly influences the properties of fresh and hardened concrete; that is why the poorer quality of RCA often limits its utilization.

The research and development of techniques which can minimize this adverse effect of RCA are taking place worldwide. These techniques are expected to consolidate the adhering mortar layer and reduce the porosity of RCA, thereby improving the interfacial bond between RCA and new cement paste in the new concrete. Excepting various cleaning methods (cleaning such aggregates from adhered mortar), the methods dealing with surface treatments (impregnation, coating) are investigated, too. In the paper, the coating of grains is presented as a currently progressive method, while various techniques are described. Next, some own results of the coating of recycled concrete aggregate using triple mixing approach and its effect on the properties of hardened concrete are presented, too.

Keywords: *recycled aggregates, surface improvement, coating, triple mixing, concrete.*

1. INTRODUCTION

Concrete is a specific construction material – a composite mixture made up of an assembly of particles of different sizes. Like all materials, the performance of concrete is determined by its microstructure, which, in turn, is determined by its composition (the granular composition of a wide variety of cements, sands, fillers and aggregates of different chemical compositions, mean sizes, size dispersions, shapes, densities, surface properties etc.), its curing conditions, and the mixing method and mixer conditions used to process the concrete. The mixing process can be very significant and can affect the final properties of concrete (JÉZÉQUEL and COLLIN 2007).

The environmental impact of production of the components of concrete (such as cement, coarse and fine aggregate) warrants close consideration. The scale of the problem makes it prudent to investigate other sources of raw materials in order to reduce the consumption of energy and available natural resources (OIKONOMOU 2005).

The idea of using recycled concrete aggregate (RCA) in new concrete production appears to be an effective utilization of concrete waste. RCA falls into the group of recycled aggregates (RA) which comes from reprocessing materials that have previously been used in construction. Examples of recycled aggregate include recycled concrete from construction and demolition waste material and railway ballast. The composition of the demolition waste varies according to the country where is generated. The construction techniques and materials differ from country to country and consequently the type of residues produced. Demolition waste composition varies according to the type of building or structure and also with the age of the building. The material reflects the construction techniques and materials used at the time they were built.

The composition of these aggregates can vary substantially and consequently the varying properties have a significant influence on the properties of the concrete (SPAETH and DJERBI 2013). The main technical problems of RCA can be specified as follows (TAM 2007; DESCARREGA 2011; SIVAKUMAR 2014; KARTINI 2012):

- high content of cement paste/mortar,
- weak interfacial transition zones between cement paste and aggregate,
- porosity and traverse cracks within demolished concrete,
- high level of sulphate,
- high levels of chlorides,
- impurity,
- poor grading,
- high variations in quality.

While only one type of interfacial transition zone (ITZ) exists in normal concrete, lying between the virgin aggregate and the new cement mortar, three types of ITZ occur in RCA-based concrete – see *Figure 1*: between the natural aggregate and the new mortar, inside the RCA between the old virgin aggregate and the old mortar, and between the old mortar and the new mortar (ZHANG and ZHAO 2015; PAUL 2018).

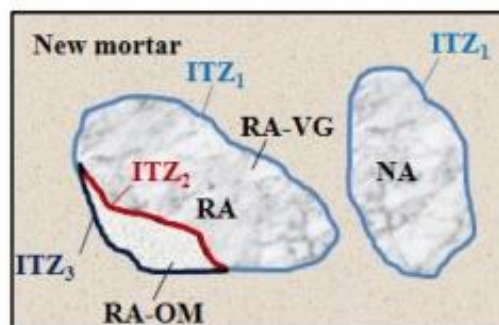


Figure 1
 Illustration of interfacial transition zones in RCA-based concrete
 (ZHANG and ZHAO 2015)

It is clear that different qualities of various ITZ create an increased risk of unfavourable impact on concrete quality. According to (SIDOROVA 2014; RYU 2002; LI 2016; XIAO 2013), this suggests that the properties of recycled aggregate concrete can be enhanced by improving the new ITZ.

The research and development of techniques which can minimize this adverse effect of RCA are taking place worldwide. Excepting various cleaning methods (cleaning such aggregates from adhered mortar), the methods dealing with surface treatments of RA (impregnation, coating) are investigated, too.

As for coating methods, the surface of aggregate is coated with an inorganic material (fly ash, slag, etc.), thus improving the surface properties of RCA and enhancing the mechanical properties of the resultant concrete (ANN 2008; CORINALDESI and MORICONI 2009; SUNAYANA and BARAI 2017). There are two basic ways to coat the aggregate:

- coating in advance before mixing the concrete (RYOU and LEE 2014; KIM 2005; CHOI 2016; LI 2009) and
- coating during the mixing using specific mixing methods (KONG 2010; URBAN and SICAKOVA 2016; FERRARIS 2001; REJEB 1996).

In the paper, the coating of grains of aggregate directly during the mixing process is presented as a currently progressive method, while various techniques are described. Next, some own results of the coating the recycled concrete aggregate and its effect on the properties of hardened concrete are presented and discussed, too. Results are given by changes in properties according to change of mixing technique, as well as change of aggregate type.

2. PRINCIPLE AND KINDS OF COATING METHODS

The efficiency of the mixing operation often determines the homogeneity of the produced concrete. The mixing procedure includes the type of mixer, the order of introduction of the materials into the mixer (loading method), the energy of mixing (duration and power), and the discharge method. These parameters of mixing procedures are generally undergoing widespread investigation to evaluate their impact on the concrete properties (FERRARIS 2001; PRASITTISOPIN and TREJO 2015; TAM and TAM 2005).

The loading method includes the order of loading of the constituents into the mixer and also the duration of the loading period. The duration of this period depends on how long the constituents are mixed before the addition of the next one and how fast the constituents are loaded. The loading period extends from the time when the first constituent is introduced in the mixer to when all the constituents are in the mixer. The loading period is important because some of the concrete properties depend on the order in which the constituents are introduced in the mixer (FERRARIS 2001).

With the exception of standard single-stage mixing, in which the entire mixing process is done in one stage, several mixing approaches are under investigation, such as the two-stage mixing approach, and the three-stage mixing approach. The principle of dividing the mixing process into two/three steps lies in the different timings of concrete's components loading; the coating of aggregate occurs in the first stage in principle, and can continue in the second one, depending on kind of components being added in this mixing sequence. Several examples are given below and also in *Figures 2 and 3*, which show that despite of the same principle, the details of mixing process are different.

2.1. Double-mixing method (DM) or two-stage mixing approach

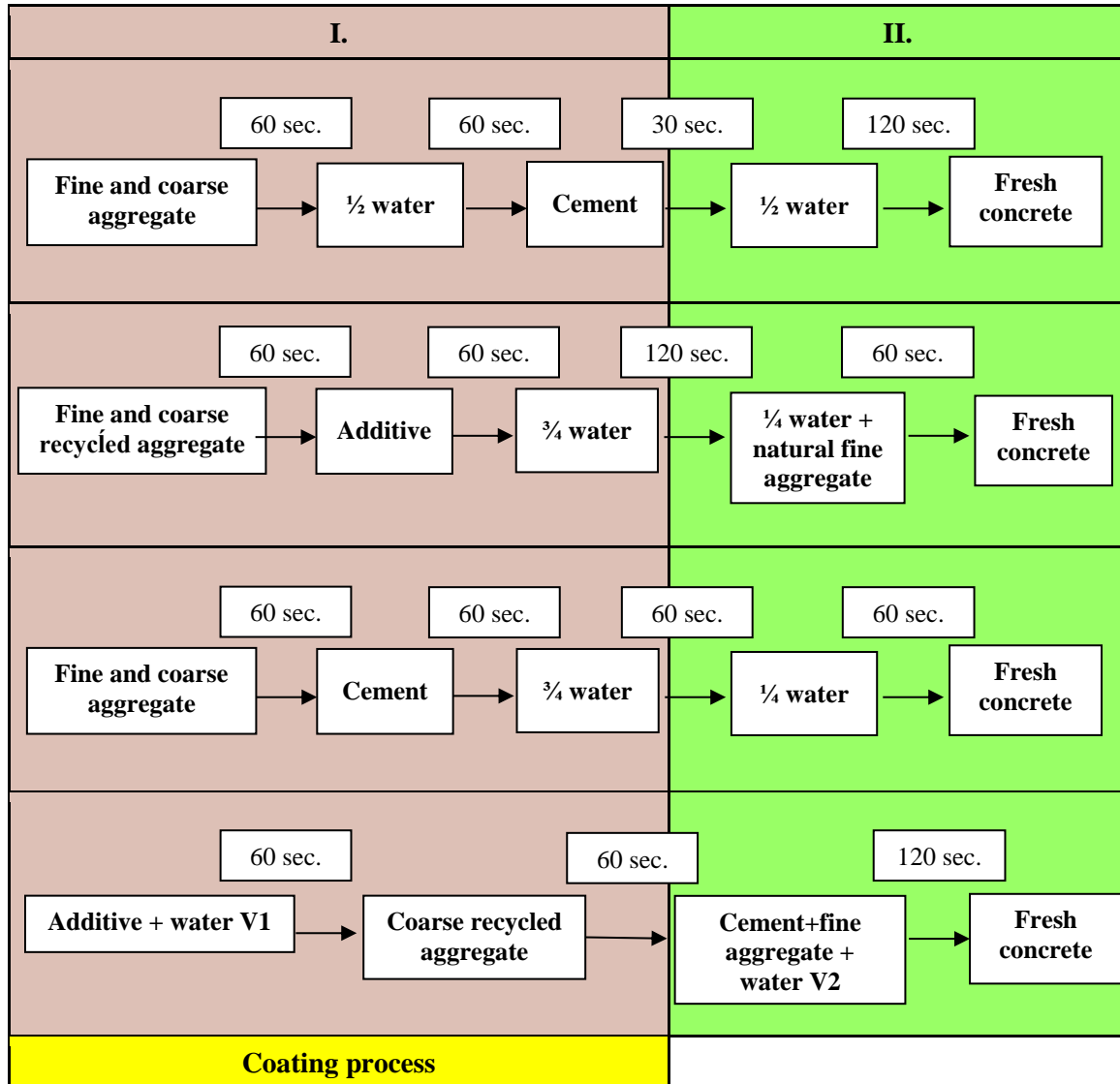


Figure 2

Comparison of various models of Two-stage mixing approach according to (TAM and TAM 2005; JEONG 2011; HYUNGU 2011; LI 2009).

The principle lies in dividing the mixing operation into two steps to improve both the concrete uniformity and the aggregate coating. However, the exact order of loading the concrete components can also be varied and several procedures are presented. TAM and TAM (2005) developed DM for improving the quality of recycled aggregate concrete (RAC). In DM, the mixing process is sequenced as follows: first, fine and coarse aggregates are mixed for 60 s before half of the water required is added

and mixed for another 60 s; then cement is added and mixed for 30 s before the remaining half of the water is added and mixed for 120 s. During the first stage of mixing, half of the required water is used for mixing, leading to the formation of a thin layer of cement slurry on the surface of the RCA, which permeates into the porous old cement mortar, filling up old cracks and voids. At the second stage of mixing, the remaining water is added to complete the concrete mixing process. This basic method has been modified to also use pozzolanic materials like silica fume.

Other modifications of DM are also present, as illustrated in *Figure 2*. According to Jeong (2011), the steps are as follows: first coarse and fine recycled aggregates are mixed for 60s and cementitious materials are added and mixed for another 60s; second, three quarters of the total water are supplemented and mixed for 120s; lastly, the rest of the total water and natural fine aggregates are added and mixed for 60s. HYUNGU (2011) also give cementitious material before the first dosage of water. The DM presented by LI (2009) involves mixing a slurry of cementitious materials and water first and then adding the slurry to coarse and fine aggregate to form concrete, while this slurry coats the aggregate. Research indicates that this process might facilitate the dispersion of cementitious materials and improve cement hydration, the characteristics of the Interfacial Transition Zone (ITZ) between aggregate and paste, and concrete homogeneity.

2.2. Triple mixing method (TM):

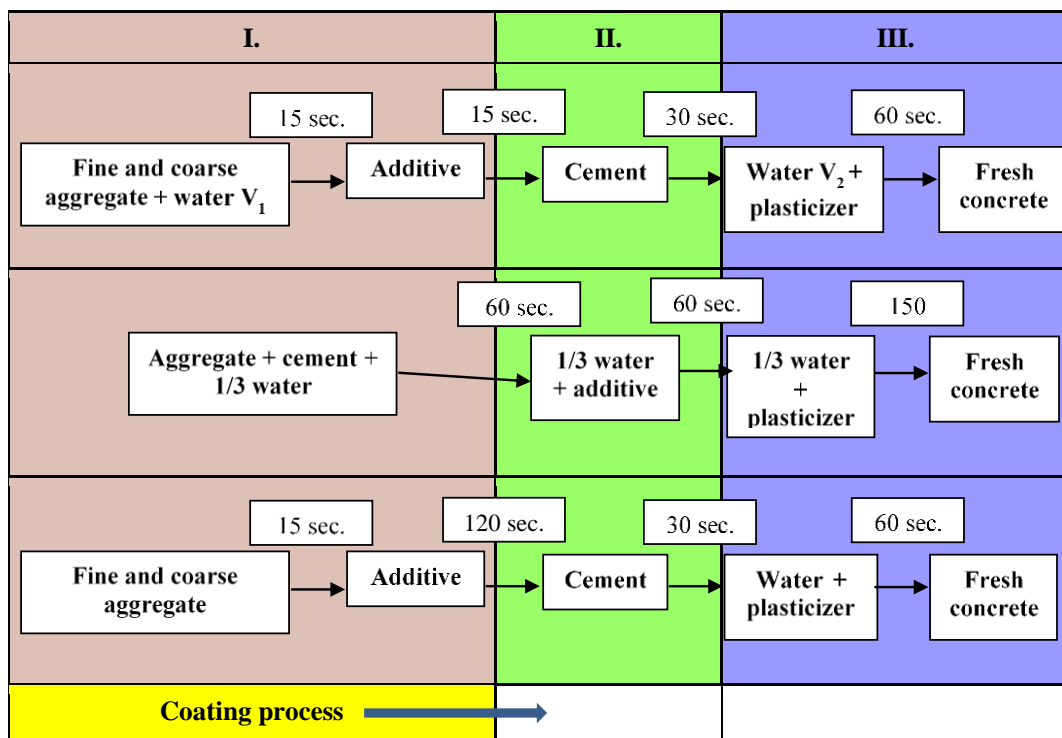


Figure 3

Comparison of various models of Three-stage mixing approach according to (KONG 2010; PREETHA 2012; LEE 2014)

As given by KONG (2010), the principle lies in dividing the mixing operation into the three steps to further enhance ITZ and thus properties of the RAC by the surface-coating of pozzolanic materials such as fly ash, slag, and silica fume. It is designed as follows: the coarse and fine aggregates are mixed for 15s with the addition of a certain amount of water to obtain the wet aggregates. Then, the additive used is added and agitated for another 15s to get the surface-coated aggregates. The cement is then added and mixed for a further 30s. Finally, the remaining water, together with superplasticizer, is added for the last 60s of mixing. Thus, a portion of the water is added to the aggregate first to moisten it, followed by the mineral additive and cement, while PREETHA et al. (2012) mention adding cement and additive first. Part of the water is added after them or with them. Lee et al. (2014) give another modification of TM: Coarse and fine aggregates are mixed for 15s, then the additive is added (120s), followed by cement (30s); thus a ‘dry coating’ occurs here. Then, the water, together with superplasticizer, is added for the last 60s of mixing. The total mixing time periods presented in the three examples are also different: 120s (Kong, 2010), 270s (PREETHA, 2012), and 225s (LEE, 2014). *Figure 3* presents some examples of TM models.

Generally, these techniques are intended to be beneficial for properties of hardened concrete. Their main benefit lies in the fact that the RCA treatment (coating) takes place directly in the concrete mixing process, thus simplifying the entire technological process of concrete production. Looking at the basic summary of DM and TM, it is clear that they provide many optimization options, e.g. in the selection of the ingredients, their sorting into individual mixing steps, or scheme of mixing time for each step.

3. MATERIALS AND METHODS

In this paper, our own triple mixing course is presented (*Figure 4*), along with its influence on the hardened concrete properties. Two kinds of additives (fly ash and recycled concrete powder) were used to coat the coarse fraction of RCA in the first step of mixing. While fly ash is considered worldwide to be a standard additive, recycled concrete powder is not widely used; it even represents a problematic part of recycled concrete. It was included in the experiment from environmental reasons to check whether it is suitable to play the role of coating material in the triple-mixing technology. Although it is porous in character, the size fractions of <0.15 and 0.3–0.6mm (active fractions) are most likely to be the principal cause of the self-cementing properties of the fine RCAs, as presented by POON (2006). Thus, it may probably form a solid coating layer. As a control mixture, the concrete of standard composition was tested as well, having natural aggregate (NA) and cement (CEM), while the cement meets both functions within the triple-mixing: coating the coarse aggregate and filling the voids between grains. The following technical parameters of concrete were tested after 28 days of setting and hardening: compressive strength, splitting tensile strength, water absorption capacity, and depth of penetration of water under pressure. To find the advantages of triple mixing technology, adequate samples and tests were performed using the normal mixing (NM) approach (*Figure 5*).

3.1. Materials and mixing method

The actual mixing method is specific in the following aspects:

- the sequence of adding aggregate,
- the method of calculating the coating layer thickness and volume,

- the model of saturation of RCA and method of calculating the water amounts (W_1 and W_2).

These aspects, as well as characterisation of concrete's components were presented by Sicakova and Urban (2018).

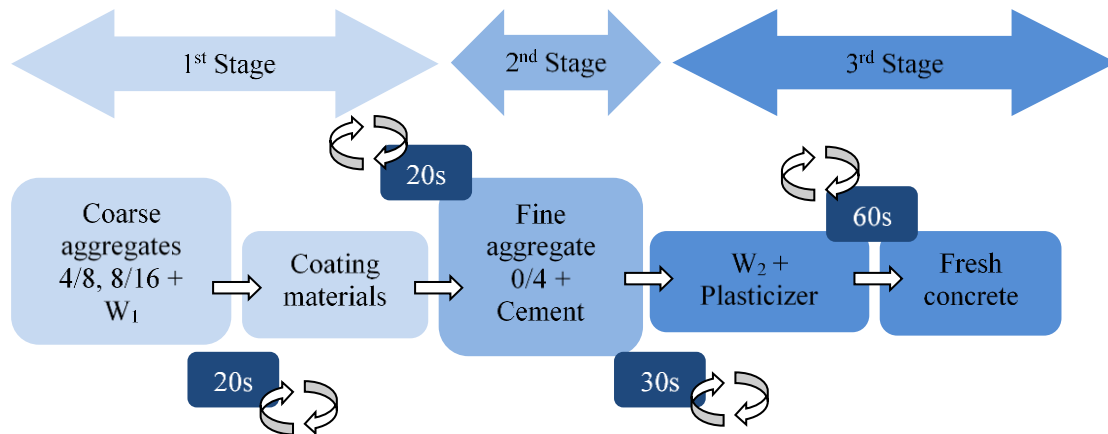


Figure 4
Experimental triple mixing procedure

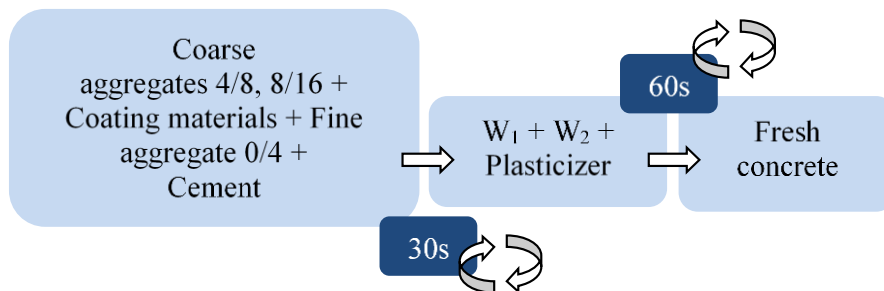


Figure 5
Experimental normal mixing procedure

The principle of composition of concrete mixtures is given in *Table 1*, where components are specified for the 3M approach. In normal mixing, adequate samples of the same compositions were prepared, differing only in the order of the components' dosage. Mixtures were intended to achieve the S4–S5 consistency class according to EN 206 (2016), so it was necessary to adjust the amount of plasticizer for RCA-based mixtures.

Table 1
The principle of mix compositions, according to kind of aggregate and kind of coating material

Component [kg]	RCA - coarse aggregate			NA - coarse aggregate		
	RCA _{CEM}	RCA _{FA}	RCA _{RCP}	NA _{CEM}	NA _{FA}	NA _{RCP}
NA	0/4	•	•	•	•	•
	4/8	–	–	–	•	•
	8/16	–	–	–	•	•
RCA	4/8	•	•	•	–	–
	8/16	•	•	•	–	–
Paste to coat aggregates	Coating material	CEM	FA	RCP	CEM	FA
	Water	W ₁	W ₁	W ₁	W ₁	W ₁
Paste to fill voids	CEM I 42.5 R	•	•	•	•	•
	Water	W ₂	W ₂	W ₂	W ₂	W ₂
	Admixture	•	•	•	•	•

3.2. Methods of Testing the Properties of Hardened Concrete

Six different samples (see Table 1), varying in terms of the kind of aggregate (RCA and NA) and the kind of coating additives (FA, RCP and CEM), were prepared by 3M and cured under standard conditions EN 12390-2 (2010). In parallel, six corresponding samples were prepared by NM. The cube samples (150 × 150 × 150 mm for depth of penetration and splitting tensile strength, and 100 × 100 × 100 mm for compressive strength and water absorption capacity) were used for testing the following properties after 28 days of setting and hardening, while each of parameter was measured using three samples:

- compressive strength according to EN 12390-3 (2010),
- splitting tensile strength according to EN 12390-6 (2009),
- total water absorption capacity according to STN 73 1316 (1989) – trivial gravimetric method, wherein samples are dried at 105 °C and then immersed in water up to constant mass. Water absorption capacity is then calculated on the basis of mass of saturated sample and mass of the dry sample in (%),
- depth of penetration of water under pressure according to EN 12390-8 (2011).

4. RESULTS AND DISCUSSION

The results of 28-day density, compressive and splitting tensile strength, total water absorption capacity, and depth of penetration of water under pressure of concrete samples are evaluated by changes in properties depending on mixing technique (expressed as difference between results of samples prepared by NM and TM), as given in Table 2, and by changes in properties depending on

the kind of aggregate (expressed as difference between results of samples prepared with NA and RCA), as given in Table 3. Here, samples are divided according to mixing technique (NM and TM). Upon **changing normal mixing to the triple one** (Table 2), several positive effects can be seen (highlighted in bold). TM is beneficial for concrete based on RCA in the case the cement (CEM) is used for coating the aggregate.

In the case of NA-based samples, the benefit of TM is again clear for water absorption and depth of penetration, when CEM is used for coating the aggregate. Positive effect on strength parameters is here clear when coating by fly ash.

Based on this, the **effect of individual coating materials**, when changing mixing methods, can be observed given as follows: cement works better for all properties, while fly ash can be beneficial only for strength properties. Positive effect of TM on properties of concrete, when using FA in the first stage of mixing, was also presented by (LI 2009; KONG 2010; PREETHA 2012).

Table 2

Changes in properties of samples according to change in mixing technique [%]

Samples according to kind of aggregate	Change in values according to change in mixing (NM/TM) [%]			
	f_c – compressive strength	f_s – splitting tensile strength	WA – water absorption capacity	Depth of penetration of water under pressure
RCA _{CEM}	49	3	-4	-14
RCA _{FA}	-19	-13	23	100
RCA _{RCP}	-24	-23	5	60
NA _{CEM}	-14	4	-1	-20
NA _{FA}	1	2	16	150
NA _{RCP}	-13	-7	4	0

* note the decrease in both the water absorption and depth of penetration values means, the change is positive

When **changing natural aggregate to RCA** (Tab. 3), negative effect is determined practically in all cases, both in normal and triple mixing (note that the ‘plus’ change in the case of water absorption and depth of penetration means negative effect on the property). This worsening of concrete properties corresponds to the character of RCA and is obvious; however, the rate of this change is a subject of interest here. The smallest negative effect (up to 20%) on strength characteristics was recorded for samples prepared by normal mixing and coated by FA and RCP (NM-_{FA} and NM-_{RCP}), and for sample prepared by triple mixing and coated by cement (TM-_{CEM}). The smallest negative effect on water absorption was recorded for samples coated by RCP (NM-_{RCP} and TM-_{RCP}), and smallest negative effect on depth of penetration was recorded for sample NM-_{RCP}.

The **effect of individual coating materials** when changing aggregates can be described as follows: FA and RPC work similarly for strength characteristics within each group of mixing, while cement is more beneficial for triple-mixing, having 0% impact on compressive strength. For water absorption, the RCP has the least negative impact in both mixing methods (28% and 29% respectively). For depth of penetration, this material can again be mentioned as having no negative effect

when normal mixing is used; effect in the case of triple-mixing is practically the same as provided by other materials.

Table 3
Changes in properties of samples according to change in kind of aggregate [%]

Samples according to mixing technique	Change in values according to change in aggregates (NA/RCA) [%]			
	f_c – compressive strength	f_s – splitting tensile strength	WA – water absorption capacity	Depth of penetration of water under pressure
NM-CEM	–42	–19	40	40
NM-FA	–9	–15	33	100
NM-RCP	–14	–2	28	0
TM-CEM	0	–20	36	50
TM-FA	–27	–27	41	60
TM-RCP	–25	–19	29	60

* note the increase in both the water absorption and depth of penetration values means, the change is negative

5. CONCLUSIONS

The mixing course presented in the paper was specific mainly in the design of mixing water (consisting of water for full saturation of aggregate and water for creation of paste) and in the design of coating layer, which—being of the same thickness for aggregates of different quality—needed different volumes of coating paste. However, all samples were based on the same volume of aggregates and same total volume of binder. The fly ash (FA) and fine fraction of recycled concrete (RCP) were used to coat the recycled concrete aggregate (RCA), while the triple mixing technology was applied for this purpose. The cement (CEM) for coating and natural aggregate (NA) instead of RCA were included in the experiment as control samples. The compressive strength, splitting tensile strength, total water absorption capacity, and depth of penetration of water under pressure were evaluated, with attention being paid to the type of mixing, type of aggregate, and type of coating material. The following conclusions oriented on triple-mixing and RCA can be formulated:

- Triple mixing does not seem to be generally beneficial for concrete based on RCA compared to normal mixing approach; its impact depends on the coating material used:
 - cement works the best better for all properties, while fly ash can be beneficial for strength properties.
- Type of aggregate influences the results of all tested parameters—using RCA instead of NA leads to worsening of all tested properties, although the rates of worsening are different and depend on the coating material used:
 - using RCP for coating the aggregate was often found to cause the least negative impact on properties of samples.

Generally, all evaluated aspects (triple-mixing, RCA, and both the fly ash and recycled concrete powder), were found to be suitable for giving positive results of concrete properties—their impact

depends on the actual combination of these three factors. Exact conditions for the application of triple-mixing technology should be studied further to be beneficial for production of recycled aggregate-based concrete.

ACKNOWLEDGEMENTS

The results presented in this article have been carried out within the project of Slovak Scientific Grant Agency VEGA (grant number 1/0524/18) and by the project NFP 26220220051 Development of progressive technologies for utilization of selected waste materials in road construction engineering (European Union Structural funds).

REFERENCES

- [1] ANN, K. Y. et al. (2008): Durability of recycled aggregate concrete using pozzolanic materials. *Waste Management*, 28, pp. 993–999.
- [2] CEN EN 12390-2:2010 (2010): Testing hardened concrete. Part 2: Making and curing specimens for strength tests. *Eur. Comm. Stand. Bruss. Belg.*
- [3] CEN EN 12390-3:2010 (2010): Testing Hardened Concrete. Part 3: Compressive Strength of Test Specimens. *Eur. Comm. Stand. Bruss. Belg.*
- [4] CEN EN 12390-6:2009 (2009): Testing Hardened Concrete. Part 6: Tensile Splitting Strength of Test Specimens. *Eur. Comm. Stand. Bruss. Belg.*
- [5] CEN EN 12390-8: 2011 (2011): Testing Hardened Concrete. Part 8: Depth of Penetration of Water Under Pressure. *Eur. Comm. Stand. Bruss. Belg.*
- [6] CEN EN 206:2013 + A1:2016 (2016): Concrete. Specification, performance, production and conformity. *Eur. Comm. Stand. Bruss. Belg.*
- [7] CORINALDESI, V.–MORICONI, G. (2009): Influence of mineral additions on the performance of 100% recycled aggregate concrete. *Construction and Building Materials*, 23, pp. 2869–2876.
- [8] DEHN, F. (2006): Influence of mixing technology on fresh concrete properties of HPFRCC. *Proc. Intl RILEM Workshop HPFRCC Struct. Appl.*, pp. 1–8.
- [9] DESCARREGA, A. (2011): Quality improvement of the recycled aggregates through surface treatment. *Master theses*, Barcelona.
- [10] FERRARIS, Ch. F. (2001): Concrete mixing methods and concrete mixers: State of Art. *Jou Res Natl Bur Stand*, 106, pp. 391–399.
- [11] HYUNGU J. (2011): Processing and properties of recycled aggregate concrete. <http://citeseerx.ist.psu.edu/>
- [12] CHOI, H. et al. (2016): Evaluation on the mechanical performance of low-quality recycled aggregate through interface enhancement between cement matrix and coarse aggregate by surface modification technology. *IJCSM* 2016, 10, pp. 87–97.

-
- [13] JEONG, H. (2011): Processing and properties of recycled aggregate concrete. Master of Science, University of Illinois, Urbana.
- [14] JÉZÉQUEL, P. H.–COLLIN, V. (2007): Mixing of concrete or mortars: Dispersive aspects. *Cem. Concr. Res.*, 37, pp. 1321–1333, doi:10.1016/j.cemconres.2007.05.007.
- [15] KARTINI, K., et al. (2012): Performance of Ground Clay Bricks as Partial Cement Replacement in Grade 30 Concrete. *World Academy of Science, Engineering and Technology*, 68, pp. 312–315.
- [16] KIM, N.-W. et al. (2005): A study on the mechanical properties of concrete using the recycled aggregates by surface coating. *Journal of the Korean society of Civil engineering*, 25, pp. 387–393.
- [17] KONG, D. et al. (2010): Effect and mechanism of surface-coating pozzalanic materials around aggregate on properties and ITZ microstructure of recycled aggregate concrete. *Construction Building Materials*, 24, pp. 701–708.
- [18] LEE, S. H. et al. (2014): Influence of Aggregate Coated with Modified Sulfur on the Properties of Cement Concrete. *Materials*, 7, pp. 4739–4754, doi:10.3390/ma7064739.
- [19] LI, J. et al. (2009): Influence of coating recycled aggregate surface with pozzolanic powder on properties of recycled aggregate concrete. *Construction and Building Materials*, 23, pp. 1287–1291.
- [20] LI, T. et al. (2016): Hydration process modeling of ITZ between new and old cement paste. *Construction and Building Materials*, 109, pp. 120–127.
- [21] OIKONOMOU, N. D. (2005): Recycled concrete aggregates. *Cement and Concrete Composites*, 27 (2), pp. 315–318. DOI:10.1016/j.cemconcomp.2004.02.020
- [22] PAUL, S. CH., et al. (2018): A novel approach in modelling of concrete made with recycled aggregates. *Measurement*, 115, pp. 64–72.
- [23] POON, C. S. et al. (2006): The cause and influence of self-cementing properties of fine recycled concrete aggregates on the properties of unbound sub-base. *Waste Management*, pp. 1166–1172, doi:10.1016/j.wasman.2005.12.013.
- [24] PRASITTISOPIN, L. TREJO, D. (2015): Effects of Mixing Variables on Hardened Characteristics of Portland Cement Mortars. *ACI Mater. J.*, 112, pp. 1–10, doi:10.14359/51686973.
- [25] PREETHA, R. et al. (2012): Effect of mixing methods in behavior of fly ash concrete. <https://www.nbmw.com>.
- [26] REJEB, S. K. (1996): Improving compressive strength of concrete by a two-step mixing method. *Cement and Concrete Research*, 26, pp. 585–592.
- [27] RYOU, J. S.–LEE, Y. S. (2014): Characterization of Recycled coarse aggregate (RCA) via a surface coating method. *IJCSM*, 8, pp. 165–172.

-
- [28] RYU, J. S. (2002): Improvement on strength and impermeability of recycled concrete made from crushed concrete coarse aggregate. *Journal of Materials Science Letter*, 21, pp. 1565–1567.
- [29] SICAKOVA, A.–URBAN, K. (2018): The influence of discharge time, kind of additive, and kind of aggregate on the properties of three-stage mixed concrete. *Sustainability*, 10 (11), pp. 1–13. doi:10.3390/su10113862.
- [30] SIDOROVA, A. et al. (2014): Study of the recycled aggregates natures influence on the aggregate-cement paste interface and ITZ. *Construction and Building Materials*, 68, pp. 677–684.
- [31] SIVAKUMAR, N. et al. (2014): Experimental Studies on High Strength Concrete by using Recycled Coarse Aggregate. *International Journal of Engineering And Science*, 4 (1), pp. 27–36, ISSN (e): 2278-4721.
- [32] Slovak Standards Institute STN 73 1316:1989 (1989). Determination of Moisture Content, Absorptivity and Capillarity of Concrete. *Slovak Stand. Inst. Bratisl. Slovak*.
- [33] SPAETH, V.–DJERBI-TEGGUER, A. (2013): Treatment of recycled concrete aggregates by Si-based polymers. *International Journal of Civil and Environmental Engineering*, 7 (1), 16–20.
- [34] SUNAYANA, S.–BARAI, S. V. (2017): Recycled aggregate concrete incorporating fly ash: Comparative study on particle packing and conventional method. *Construction and Building Materials*, 156, pp. 376–386.
- [35] TAM, V. W. Y.–TAM, C. M. (2005): Microstructural analysis of recycled aggregate concrete produced from two-stage mixing approach. *Cement and Concrete Research*, 35 (6), pp. 1195–1203. doi:10.1016/j.cemconres.2004.10.025
- [36] TAM, W. Y. V, et al. (2007): Removal of cement mortar remains from recycled aggregate using pre-soaking approaches. *Resources, Conservation and Recycling*, 50, pp. 82–101.
- [37] URBAN, K.–SICAKOVA, A. (2016): Impact of specific mixing method on the properties of concrete with BFS aggregate. Proceeding of SGEM, Albena, Bulgaria, 28 June-6 July 2016; STEF92: Sofia, Bulgaria, pp. 49–56.
- [38] XIAO, J. et al. (2013): Properties of interfacial transition zones in recycled aggregate concrete tested by nanoindentation. *Cement and Concrete Composites*, 37, pp. 276–292.
- [39] ZHANG, H.–ZHAO, Y. (2015): Integrated interface parameters of recycled aggregate concrete. *Construction and Building Materials*, 101, pp. 861–877.



INVESTIGATION OF RHEOLOGICAL BEHAVIOUR OF DIFFERENT BENTONITE-WATER SUSPENSIONS FOR TUNNEL BORING APPLICATION

GUILLERMO UQUILLAS GIACOMETTI

MSc Student,

University of Miskolc, Institute of Raw Material Preparation and Environmental Processing
Hungary, 3515 Miskolc - Egyetemváros, ejtfajtj@uni-miskolc.hu

Abstract

A project called “Genova Bypass” is going to be developed with a slurry conveyance circuit. It will transport the spoil from the job site to the seaside within 9 km of slurry pipes. Weir Minerals Hungary Ltd. and the Institute of Raw Materials Preparation and Environmental Processing of the University of Miskolc made a frame contract for carrying out physical material testing. In this framework the physical and rheological testing of different waters and solid materials had been conducted by the Institute. Two types of bentonites have been analysed mixing them with sea and fresh water at different concentrations. Bentonites were examined to get physical properties as the particle size distribution, moisture content, and density. Six types of combinations “water-bentonite” are in the research: 1. Marine bentonite-tap water, 2. Marine bentonite-sea water, 3. Marine bentonite-mixed water, 4 “100” bentonite-tap water, 5. “100” bentonite-sea water, and 6. “100” bentonite-mixed water. Two different methods have been utilized to do the analysis: rotational rheometer and tube rheometer, where the rotational rheometer has been used mainly to get qualitative data. In the rotational rheometer, two samples of ten different volumetric concentration were prepared (2, 4, 6, 8, 10%) which later were corrected with the moisture content of the bentonite. After the qualitative data was available, tube rheometer was utilized to obtain the rheological properties of the different combination. Tube rheometer was focused only in the concentration which were closer to the aim of the investigation. From the six possible combinations, only the most adequate ones were chosen to develop a numerical relation between the concentration and both, plastic viscosity and yield stress. The aim of this investigation is to measure physical and rheological parameters of all the possible combinations that are available with the materials provided for the interested party to subsequently find a particulate numerical model to predict the behaviour of the suspensions and design the technology for the tunnelling project.

Keywords: *Rotational rheometer, tube rheometer, bentonite – sea water suspension, Bingham plastics suspension.*



PROPERTIES OF RECYCLED CONCRETE AGGREGATE PRODUCED BY DIFFERENT COMMINUTION METHODS

PAULA FIGUEIREDO¹–CARINA ULSEN²–MAURÍCIO BERGERMAN³–GÁBOR MUCSI⁴

¹University of Sao Paulo, Polytechnic School, Mining and Petroleum Engineering Department, Brazil,
paulafigueiredo@usp.br

²University of Sao Paulo, Polytechnic School, Mining and Petroleum Engineering Department, Brazil,
carina.ulsen@usp.br

³University of Sao Paulo, Polytechnic School, Mining and Petroleum Engineering Department, Brazil,
mbergerman@usp.br

⁴University of Miskolc, Faculty of Earth Science and Engineering, Hungary, ejtmucsi@uni-miskolc.hu

Abstract

Due to the scarcity of aggregate natural in large metropolises, the abundance of construction and demolition waste (CDW) and the high costs for landfill deposition are factors that encourage the development of new processing technologies, however, few studies offer a comparative analysis of the different production processes applied in the CDW. Thus, this paper compares the use of jaw and impact crushers configured to generate two products with the same top-size, consecutively, the crushed products were subjected to selective milling. The results show that the aggregates produced in both crushing routes have similar properties particle size distribution, particle shape, chemical and mineralogy composition and content of attached cement paste, this tendency intensified after selective milling. Thus, minor differences observed do not justify the common belief in the industry that impact crushers provide an improvement in the quality of RA; furthermore, selective milling indicates additional removal of cement paste from aggregates surface, improving the properties of recycled aggregates.

Keywords: *Recycled concrete aggregates. Concrete aggregates properties. Liberation comminution. Jaw crusher. Impact crusher. Selective milling.*

1. INTRODUCTION

Civil construction is one of the activities that most demand raw materials [1] and is a relevant parameter to indicate the economic and social situation of a country; it also generates significant amounts of waste (CDW – construction and demolition waste). Waste generation increases along with the economic development, which led to the development of scientific studies regarding the recycling and use of CDW in substitution of scarce raw materials in urban networks. However, to generate recycled aggregates (RA) to be used as building materials, mineral processing operations of CDW must be improved and adapted to each context, materials source and composition.

The CDW recycling plants are similar to those of natural aggregate production [2] in which the commonly used equipment are jaw, impact, cone or a combination of crushers. In order to

control the quality of the product, it is necessary to carry out characterization procedures to aid in the decisions regarding operational conditions and the choice of equipment.

Mineral processing aims to detach mineral phases and, in parallel, to generate a product suitable for use. However, for a more efficient separation of aggregates and cement paste in CDW, comminution should induce ruptures along the grain boundaries to release both phases [3]. The literature states that jaw crushers tend to remove lower proportions of cement paste adhered to recycled aggregates, while impact and cone crushers are more effective for the same goal [4]. However, these studies were not conclusive regarding the role of a crusher type concerning RA characteristics. The literature also reports that concrete breakage by impact machines generates a high proportion of natural aggregates with low content of mortar [5] but does not present comparative data among other crushing methods. Abrasion comminution generates high quality RA with lower energy consumption [6] if compared to methods involving heating and rubbing [7]. An example of such a mechanism is selective milling, in which the aggregate remains intact while the cement paste coupled to the surface is broken. It should be highlighted that the larger the number of crushing stages to which the material is subjected, the lower is the cement paste content (liberation by comminution) [8]. However, this number is limited by the cost of production and mass losses at ultrafine fractions.

Different mineral processing operations and routes are feasible in recycling processes to achieve the desired content of cement paste in RA [9], but few studies offer a comparative analysis of these methods [10]. In addition, the recycling industry usually selects crushers based on acquisition costs, capacity and availability of second-hand machines, but very rarely considers essential parameters, such as the desired properties of the product. Therefore, we here present comparative data about the use of jaw crusher, impact crusher and selective milling for recycling CDW to produce recycled aggregates.

2. MATERIALS AND METHODS/AREA DESCRIPTION

The CDW, composed of cement-based materials, was collected in a landfill of inert material. In order to have representative aliquots for laboratory studies, a homogenization-elongated pile was formed to obtain sample for an eccentric jaw crusher (JC) and a horizontal axis impact crusher (IC); the crushers were configured to obtain products with a top size of 80% by mass passing at 4.8 mm (maximum particle size for sand).

Subsequently, the products were again disposed in a pile and sampled in duplicate. That is, the characterization analyses occurred in duplicate with opposite samples of the pile, denominated A and B, to minimize the compositional variability. For this confirmation, chemical composition (quantitative X-Ray Fluorescence -XRF in fused beads) and particle size distribution (dynamic image analysis at Camsizer equipment – Retsch Technology brand) were evaluated.

The material produced in each crusher was subjected to a low energy Selective Milling (SM) in a conventional lab-scale jar mill; at low spin or low energy milling, the kinetics of fragmentation occurs by abrasion, in which the milling balls slides on the sample. Therefore, the experimental purpose is to keep the original aggregates intact while the cement paste adhered to particles surface is released by the abrasion with grinding balls.

The experiment was carried out at 1 kg of crushed recycled aggregates and 0.5 kg of 17 mm balls in a jar mill 8x10", with a rotation at 50 rpm for 30 minutes. Preliminary tests were initially conducted before setting the experimental conditions.

Then, the recycled aggregates after abrasion tests were again characterized in terms of chemical composition (XRF), particle size and shape distribution (dynamic image at Camsizer equipment). In addition, mineralogical composition (X-Ray powder Diffraction - XRD), water absorption (C128 standard [11]) and binder content (assessed by HCl leaching [12]) were carried out.

A schematic flowchart of the process is shown in Figure 1.

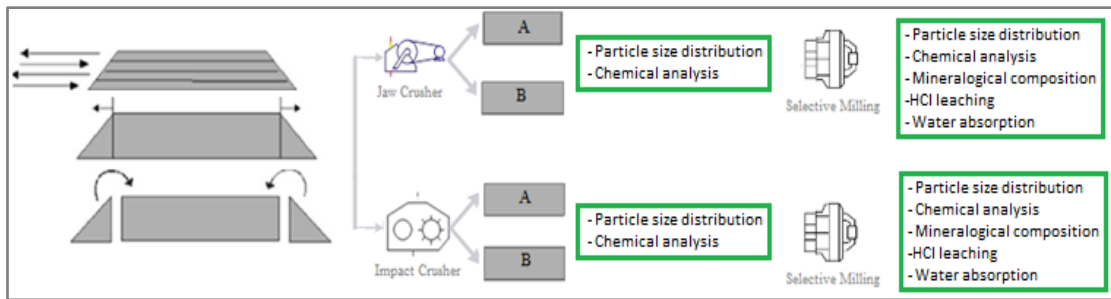


Figure 1
Schematic flowchart of CDW processing and characterization

3. RESULTS AND DISCUSSION

3.1. Crushing

Figure 2 shows the comparative result of the particle size distribution of samples A and B comminuted in JC and IC.

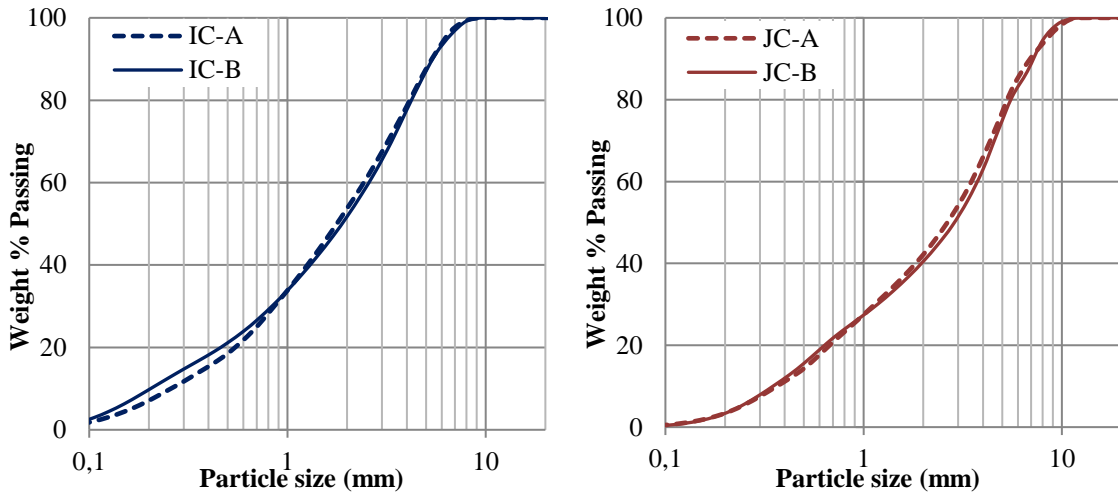


Figure 2
Particle size distribution of products from impact and jaw crusher

The equipments were configured to obtain a product with the same top-size ($P_{80} = 4.8$ mm), but the grading curve clearly indicates a displacement between the curves. Considering that the curves displacement occurred in parallel, if the configuration was reached, possibly the products of both crushers would have a similar particle size distribution and parallel curves would overlap. This difference is explained by aliquots heterogeneity; despite all difficulties for setting the impact crusher conditions, the pre-test with a reduced sample succeeded and the curves were equal, while the test with a higher amount of sample diverge from the preliminary one.

Samples A and B in both crushers had similar grading curves. However, to confirm the representativeness and homogenization, chemical composition was also analysed.

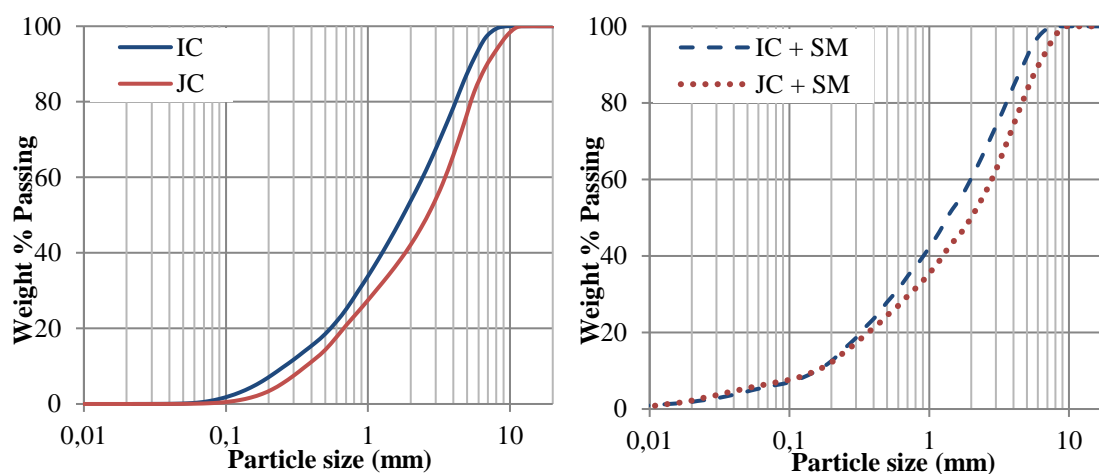
The chemical composition summary and the sieve fractions is shown in *Table 1*. The chemical composition for aliquots A and B of each crushing process are very similar, consequently, it is verified that homogenization procedure was successfully carried out.

Table 1
Comparative chemical analysis between aliquots A and B

Aliquots/ crusher	Mass (%)	Grade (%)										
		SiO ₂	Al ₂ O ₃	Fe ₂ O ₃	CaO	LOI	Na ₂ O	K ₂ O	TiO ₂	P ₂ O ₅	MnO	MgO
JC-A	100	66.5	10.4	2.7	7.6	6.2	2.2	3.2	0.4	0.2	0.1	1.2
JC-B	100	67.1	10.5	2.9	7.6	5.7	2.2	3.1	0.4	0.1	0.1	1.2
IC-A	100	66.6	10.3	3.0	7.8	5.8	2.2	3.1	0.4	0.1	<0.1	1.3
IC-B	100	66.1	10.1	3.3	8.0	6.0	2.1	3.1	0.5	0.2	<0.1	1.3
Average		66.6	10.3	3.0	7.8	5.9	2.2	3.1	0.4	0.2	0.1	1.3
Standard deviation		0.4	0.2	0.3	0.2	0.2	0.1	0.1	0.0	0.1	0.0	0.1

3.2. Crushing and selective milling

The particle size distribution curves of JC, JC + SM, IC and IC + SM are shown in *Figure 3*.



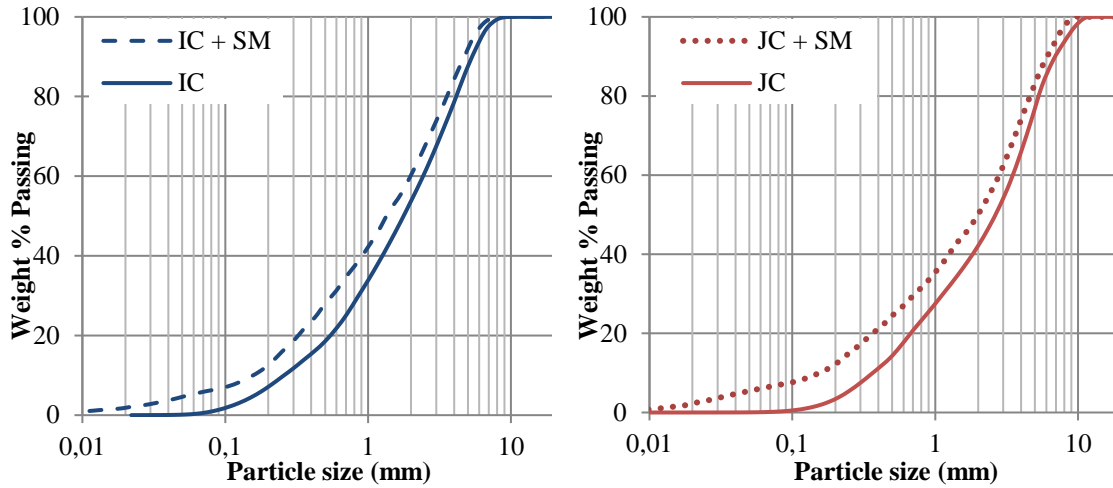


Figure 3
Particle size distribution between different comminution methods

The particle size distribution after selective milling, in both processes, presented a finer particle size curve compared to the crushing curve, as expected. However, the JC + SM curve started with coarser fractions than IC + SM and in 0.3 mm (20% of the particles) the curves overlapped. In addition, dynamic image analysis evaluates the shape of the particles (for fractions greater than 0.15 mm); the result is shown in the Figure 4.

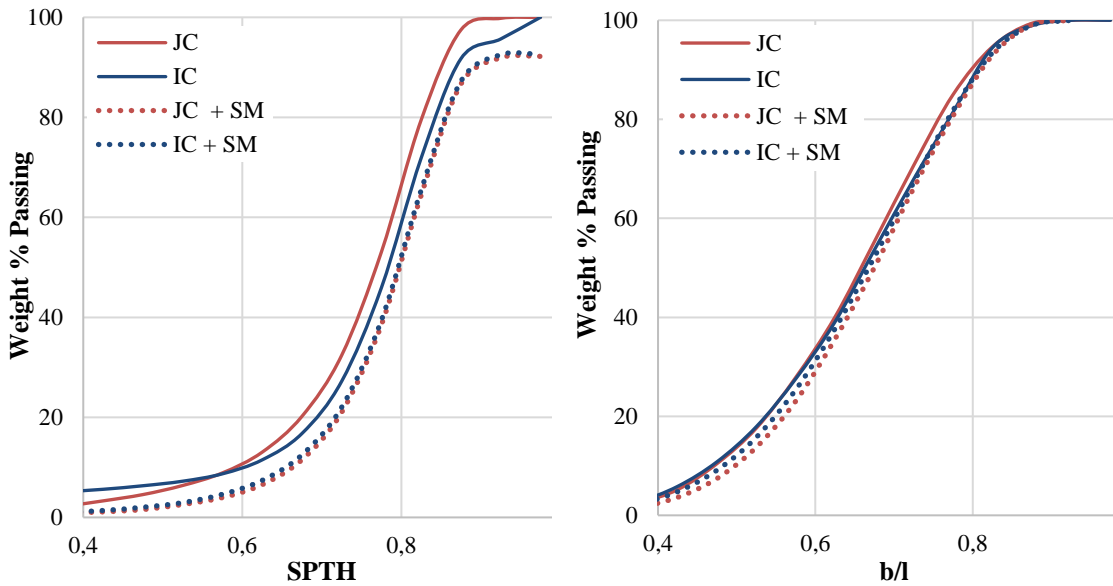


Figure 4
Comparison of particle shapes

The shape of the particles is related to the parameters of sphericity (SPHT) and aspect ratio (b/l) of the particles. This value varies from 0 to 1, therefore values of b/l tending to 0 the particles approximate an elongated aspect while tending to 1 a spherical aspect; SPHT is related to the angularity of the particle and the irregularity its projected perimeter [13]. The results demonstrate that the difference particles shape are subtle but there is a tendency to improve after SM.

The contents of the main oxides attained by XRF and LOI by sieve fraction are shown in Table 2.

Table 2
Comparative chemical analysis by sieve fraction between different comminution methods

Fraction (mm)	Mass (%)	Grades (%)							
		SiO ₂	Al ₂ O ₃	Fe ₂ O ₃	CaO	LOI	Na ₂ O	K ₂ O	MgO
JC	100	66.5	10.4	2.7	7.6	6.2	2.2	3.2	1.2
9.5–4.8	23.5	64.6	13.3	3.6	5.5	3.6	3.2	3.9	1.4
4.8–1.2	43.5	65.8	10.5	3.2	7.5	5.8	2.2	3.2	1.2
1.2–0.075	24.0	71.5	7.7	2.6	7.5	6.2	1.3	2.4	1.1
< 0.075	9.0	52.7	10.1	3.7	15.7	12.2	1.4	2.6	1.9
JC + SM	100	65.8	10.9	2.9	7.3	5.1	2.2	3.3	1.2
9.5–4.8	19.4	65.4	13.5	3.8	4.9	2.9	3.3	3.9	1.1
4.8–1.2	38.3	65.8	10.4	3.0	7.3	5.5	2.2	3.2	1.2
1.2–0.075	32.6	71.7	7.4	2.8	7.0	5.4	1.3	2.4	1.0
< 0.075	9.8	45.2	10.5	4.2	17.6	15.4	1.2	2.4	2.2
IC	100	66.6	10.3	3.0	7.8	5.8	2.2	3.1	1.3
9.5–4.8	12.9	62.6	12.8	3.6	7.7	5.1	3.0	3.4	1.5
4.8–1.2	47.3	65.0	12.1	3.3	6.9	4.8	2.8	3.5	1.3
1.2–0.075	31.1	70.9	8.2	2.7	7.0	5.8	1.5	2.6	1.2
< 0.075	8.7	53.5	10.1	4.6	13.7	11.4	1.5	2.6	2.1
IC + SM	100	65.8	10.5	3.1	7.4	5.1	2.4	3.2	1.3
9.5–4.8	10.1	62.1	12.9	4.3	7.1	4.4	3.2	3.3	1.4
4.8–1.2	40.4	65.1	11.3	3.3	6.9	5.4	2.5	3.4	1.2
1.2–0.075	44.0	70.4	8.0	3.3	6.8	5.4	1.5	2.6	1.1
< 0.075	5.4	45.3	10.2	4.9	16.8	15.8	1.3	2.5	2.2

The chemical composition of the products, IC compared to JC and both after SM, are similar. The silica content is lower in the fine fractions, while the CaO+LOI (estimative of cement paste content [14]) content is higher; indicating a preferential concentration of cement paste in the finer fraction and natural aggregates in the coarser fractions. The increasing of those content after SM indicates a higher liberation of cement paste.

The mineralogical composition is consistent with the chemical composition; there is a higher concentration of cement paste (peaks at 29.5 °2theta) in the fractions below 0.075 mm while in the fractions 1.2–0.075 mm there is a higher content of quartz (mainly related to SiO₂) and feldspar (associated with Na₂O+K₂O [15]), related to the natural aggregate.

In addition to estimating the cement paste by the CaO+LOI, the content was also estimated by the HCl leaching [12] - cement paste and carbonates react with acidic and minerals from aggregates remains at the insoluble residue (IR). Therefore, the content of the IR is measured and the soluble (addressed to the cement paste) is calculated (1-IR).

The water absorption of the recycled aggregates is the parameter of greater control according to the international standards and that determines its application. Therefore, the water absorption and the content of soluble phases at HCl (1-IR) in the fraction 4.8-0.075 mm is shown in *Table 3*.

Table 3

Water absorption and HCl leaching of products in the fraction 4.8-0.075 mm

Comminution route	Water absorption (%)		1-IR (%)	
	average	standard deviation	average	standard deviation
JC	4.58	0.4060	21.2	0.0009
JC + SM	4.49	0.4953	21.5	0.0015
IC	3.98	0.1126	22.8	0.0016
IC + SM	3.84	0.5645	20.8	0.0007

The amount of soluble phases are consistent with the estimated cement paste reported in previous studies (23% g/g) [14]. The recommendations of RILEM (International Union of Laboratories and Experts in Construction Materials, Systems and Structures) accept the use of recycled aggregates with up to 10% water absorption in concrete with a maximum strength of 50 MPa. Thus, the water absorption values for all comminution methods are close to 5%, within those acceptable.

4. CONCLUSIONS

The separation of enriched cement paste particles through mineral processing can be attained only if a reasonable degree of liberation between this material and natural aggregates has been achieved through a previous treatment.

Although CDW is a heterogeneous material, the present work minimized by homogenizing the whole sample and getting enough sample mass for the studies. After this confirmation, comparative studies were carried out between the jaw crusher and the impact and, in sequence, the products attained at each comminution route were subjected to a selective milling. In the end, the results demonstrated that the products for both crushers are similar in terms of cement paste content, particle size distribution, particle shape, chemical and mineralogical composition. The additional step of selective milling after crushing increased slightly the liberation between cement paste and natural aggregates. Further studies must be carried out to optimize selective milling conditions to maximize cement paste removal without milling the aggregates.

ACKNOWLEDGEMENTS

The authors gratefully acknowledge CNPq-CAPES process 88881 068109 2014-01 and the laboratories: Technological Characterization Laboratory (LCT-USP), Mineral and Industrial

Waste Processing Laboratory (LTM-USP). The information and views set out in this study are those of the authors and do not necessarily reflect the opinion of the funding agencies.

REFERENCES

- [1] MATOS, G. R.: *Use of Minerals and Materials in the United States From 1900 Through 2006*. USGS Fact Sheet 2009-3008. Doi: 10.17226/12034
- [2] MOMBER, A. W.: *The fragmentation of cementitious composites in a jaw breaker*. *Theor Appl Fract Mech* 2002;38:151–64. doi:10.1016/S0167-8442(02)00092-7.
- [3] KIM, K. H.–CHO, H. C.–AHN, J.W.: Breakage of waste concrete for liberation using autogenous mill. *Miner Eng.*, 2012; 35:43–5. doi:10.1016/j.mineng.2012.05.011.
- [4] GRESS, D. L.–SNYDER, M. B.–STURTEVANT, J. R.: Performance of rigid pavements containing recycled concrete aggregates. *Transp Res Rec.*, 2009, 2113:99–107.
- [5] ETXEBERRIA, M.–VAZQUEZ, E.–MARI, A.–BARRA, M.: Influence of amount of recycled coarse aggregates and production process on properties of recycled aggregate concrete. *Cem Concr Res*, 2007, 37:735–42. doi:10.1016/j.cemconres.2007.02.002.
- [6] QUATTRONE, M.–ANGULO, S. C.–JOHN, V. M.: Energy and CO2 from high performance recycled aggregate production. *Resour Conserv Recycl*, 2014, 90:21–33. doi:10.1016/j.resconrec.2014.06.003
- [7] SHIMA, H.–TATEYASHIKI, H.–MATSUHASHI, R.–YOSHIDA, Y.: An advanced concrete recycling technology and its applicability assessment through input-output analysis. *J Adv Concr Technol.*, 2005, 3:53–67.
- [8] DE JUAN, M. S.–GUTIERREZ, P. A.: Study on the influence of attached mortar content on the properties of recycled concrete aggregate. *Construction and Building Materials*. doi: 10.1016/j.conbuildmat.2008.04.012
- [9] ULSEN, C.–KAHN, H.–HAWLITSCHKE, G.–MASINI, E.A.–ANGULO, SC. Separability studies of construction and demolition waste recycled sand. *Waste Manag* 2013;33:656–62. doi:10.1016/j.wasman.2012.06.018.
- [10] BRAYMAND, S.; ROUX, S.; FARES, H.; DÉODONNE, K.; FEUGEAS, F. Separation and quantification of attached mortar in recycled concrete aggregates. *Waste and Biomass Valorization* 1393–1407, 2017. doi: 10.1007/s12649-016-9771-2.
- [11] ASTM C128. Standard test method for density, relative density and absorption of fine aggregate, 2003.
- [12] QUARCIONI, V. A.–CINCOTTO, M. A.: Optimization of calculation method for determination of composition of hardened mortars of Portland cement and hydrated lime made in laboratory. *Construction and Building Materials*, 1069–1078, 2006. doi: 10.1016/j.conbuildmat.2005.02.028.

-
- [13] HAWLITSCHKEK, G. Caracterização das propriedades de agregados miúdos reciclados e a influência no comportamento reológico de argamassas. Departamento de Engenharia de Minas e de Petróleo. Mestrado, 2014.
- [14] ANGULO, S. C.–ULSEN, C.–JOHN, V. M.–KAHN, H.–CINCOTTO, M. A.: Chemical-mineralogical characterization of C&D waste recycled aggregates from Sao Paulo, Brazil. *Waste Manag* 2009;29:721–30. doi:10.1016/j.wasman.2008.07.009.
- [15] ULSEN, C.–KAHN, H.–FRANÇA, R. R.–ULIANA, D.–CAMPBELL, F. S.: 2012. Microstructural characterization of fine recycled aggregates by Sem-Mla. In: BROEKMANS, M. A. T. M. (ed.): *Proceedings of the 10th International Congress for Applied Mineralogy (ICAM)*, Springer, Berlin Heidelberg, pp. 725–732.



ALKALI ACTIVATED CEMENT PRODUCTION FROM AIR-COOLED SLAG INDUSTRIAL WASTE

IDA BALCZÁR¹–TAMÁS KORIM²

¹Institute of Materials Engineering, University of Pannonia,
H-8200, Veszprém, Egyetem Street 10., Hungary, balczari@almos.uni-pannon.hu

²Institute of Materials Engineering, University of Pannonia,
H-8200, Veszprém, Egyetem Street 10., Hungary, ktm042@almos.uni-pannon.hu

Abstract

Alkali activated cements play an increasing role as a successful substitute of ordinary Portland cements due to their superior durability and environment friendliness. Based on the chemical composition of these binders, alkaline cements can be divided to two basic categories: high- and low-calcium cements. Most commonly used starting material for high-calcium system is blast furnace slag (BFS), which can be activated using alkali hydroxides, carbonates or silicates.

This study introduces a novel activation method to manufacture high-calcium alkali-activated cements (AACs) based on inactive air-cooled blast furnace slag (ACS), which is well-crystallized and hydraulically unreactive. To enhance its reactivity, we developed a new procedure, called mechanochemical activation. Mechanochemical activation is technically an intensive grinding, where the formed amorphous phase reacts later with the alkaline solution.

During experiment grinding parameters were altered (grinding time, the mass ratio of sample to grinding body, and rotation speed), and the effect of storage time on the activated samples was investigated. The structural and morphological changes of mechanochemically activated ACS were followed by X-ray diffraction (XRD), and Fourier transform infrared (FTIR) spectrometry, scanning electron microscopy (SEM), as well as determination of particle size distribution. The applicability of activated ACS in alkali activated cements was characterised using compressive strength at 28 days.

The ACS partially amorphised by mechanochemical activation proved to be a valuable component for AACs with its compressive strength around 50 MPa in mortar (even with 180 days of storage time before use) surpassing that of granulated slag (30 MPa).

Keywords: alkali activated cements, mechanochemical activation, grinding, compressive strength, air-cooled slag, storage time

We acknowledge the financial support of Széchenyi 2020 under the EFOP-3.6.1-16-2016-00015.



CHARACTERIZATION OF GEOPOLYMER COMPOSITES REINFORCED WITH PLASTIC WASTES

KINGA KORNIJEJENKO¹–JANUSZ MIKUŁA²–MICHAŁ ŁACH³–FLORENCIA MOURE⁴–
LUCÍA MOREIRA⁵–MARTÍN DUARTE GUIGOU⁶

¹Institute of Materials Engineering, Faculty of Mechanical Engineering, Cracow University of Technology, Jana Pawła II 37, 31-864 Cracow, Poland, kinga.korniejenko@mech.pk.edu.pl

²Institute of Materials Engineering, Faculty of Mechanical Engineering, Cracow University of Technology, Jana Pawła II 37, 31-864 Cracow, Poland, janusz.mikula@pk.edu.pl

³Institute of Materials Engineering, Faculty of Mechanical Engineering, Cracow University of Technology, Jana Pawła II 37, 31-864 Cracow, Poland, michal.lach@pk.edu.pl

⁴Engineering and Technology School, Catholic University of Uruguay, 8 de Octubre 2738, CP 11600, Montevideo, Uruguay, florencia.moure111@gmail.com

⁵Engineering and Technology School, Catholic University of Uruguay, 8 de Octubre 2738, CP 11600, Montevideo, Uruguay, lucia.moreiragarmendia@gmail.com

⁶Engineering and Technology School, Catholic University of Uruguay, 8 de Octubre 2738, CP 11600, Montevideo, Uruguay, martin.duarte@ucu.edu.uy

Abstract

The main objective of the article is to analyse the possibilities of using plastic wastes as the reinforcement for geopolymer composites. The mechanical properties of fly-ash based geopolymer reinforced with three different kinds of plastic wastes have been investigated. The samples were prepared using sodium promoter and plastic wastes (1% by mass of the composite). The following kind of waste have been used for manufacturing the composites: post processing waste - basalt fibres with polystyrene, waste form plastic pallet utilization and mixing of waste polyolefin materials such as polyethylene, polypropylene and other waste packing materials. The empirical part of the research is based on the compressive strength tests, flexural strength tests and detailed microstructure examination. The results show the addition different waste polymers materials to geopolymer matrix can be promising way of its utilization. The best results for compressive strength are achieved for the matrix reinforced by post processing waste - basalt fibres with polystyrene – 57,6 MPa. It is better value than for plane geopolymer – 55,6 MPa. The results for other samples have also very high values of compressive strength is 56 MPa for composites with waste form plastic pallet utilization and 54,5 MPa for composites with mixing plastic waste form packing. The best results for flexural strength are achieved for the matrix without reinforcement – 9,7 MPa. However the results for other reinforced composites are also very good. There are between 7 and 8,3 MPa. Based on waste materials it is possible to receive the composite with good mechanical properties that could be used for different applications in construction industry.

Keywords: *Geopolymer, Composite, Plastic Waste.*

1. INTRODUCTION

Construction industry it is very important field in the world and as well as EU economy. At world level, civil works and building construction consumes 60% of the raw materials extracted from the lithosphere and in Europe, the mineral extractions per capita intended for building amount to 4.8 tonnes per inhabitant per year (BRIBIÁN 2011). Innovations in this branch have a strongly impact on the sustainable development of Europe's competitiveness. Contemporary, materials in construction industry should not only improved safety and functionality, but they also have reasonable prices and taking under consideration the final product recyclability (ARULRAJAH 2017; IUCOLANO 2013). In Europe buildings are responsible for more than 40% of the energy consumption and greenhouse gas emissions (CRAWLEY 2009; PACHECO-TORGAL 2014). The main goal of the research was develop the eco-friendly material for construction industry with using geopolymer matrix and waste material. The article present the research that try to determinate the possibilities of utilization the plastic waste to create the composites based on geopolymer matrix. Especially the mixed waste that are hard to processing.

Nowadays, geopolymers can be the solution of the problem high CO₂ emission and another environmental aspects connected with using traditional Portlant cement in the construction industry (CELIK 2018; NAZARI 2013; PALOMO 2014). In comparison to the traditional materials, such as concrete, geopolymers have a number of advantages. There are not only eco-friendly but the production of such composites, compared to the other cementitious materials is economically more beneficial including the low energy consumption of the their manufacturing (ŁACH 2017). Additional environmental benefit is connected with using to producion process waste materials: for example fly ashes and mine talings (SEIDRA 2017; MIERZWIŃSKI 2018a). At the same time, the obtained materials have better properties than the conventional ones (CHENG 2011; OGUNDIRAN 2013) i.a.: high initial strength, reduced shrinkage and low thermal conductivity, a good fire resistance (up to 1000 °C) and lack of emission of toxic fumes when heated, high level of resistance to a variety of acids and salts, good resistance to abrasion, adherence to the new and old concrete, steel, glass and ceramics, lack of corrosion of the steel reinforcement in a geopolymer matrix and a high level of adhesion to steel inherent protection of reinforcing steel due to high residual pH as well as low diffusion rates chloride, high resistance to atmospheric conditions, lower costs and wide availability of the raw materials required for their manufacturing and possibility of hazardous waste immobilization by shutting them in geopolymers composites.

Moreover, the positive environmental influence can be even higher if the waste materials will be applied to production this composites. Some of the attempting will be conducted with natural and synthetic reinforcement. Among the natural additions some waste form plant production has been successfully tested, especially waste from abaca (MALENAB 2017), coir (PALANISAMYA–SURESH KUMAR 2018) and coffee grounds (MIERZWIŃSKI 2018b). Among the synthetic waste the invastigation has been provided on: waste form production carbon (LUNA-GALIANO 2018) and glass (NOVAIS 2017) fibres, waste Rockwool (KINNUNEN 2017), waste form used tires (ŁACH 2017; MUCSI 2018) and other plastic waste (VISHWAKARMA–RAMACHANDRAN 2018).

One of the most problematic waste for recycling are mixing plastic waste (SINGH 2017; WANG–XU 2014). They are non-biodegradable and takes many years to degrade. The previous investigations made on cementitious materials show that this kind of waste can be successfully applied for replacement for fine aggregate as substitution of sand in the formulation of concrete

(ISMAIL–AL–HASHMI 2008; GHERNOUTI 2014). The replacement materials reduce the weight of final product which reduces the costs of transport (ISMAIL–AL–HASHMI 2008) and gives a good approach to reduce the cost and problems posed to dispose plastics (GHERNOUTI 2014). The further research show that this kind of additive can be also beneficial for geopolymer concrete (COLANGELO 2013).

2. MATERIALS AND METHODS

The geopolymer matrix was based on fly ash from CHP plant located in Skawina, Poland. This kind of fly ash is proper for geopolymer production because of its physical properties and chemical composition (KORNIEJENKO 2018). The three different types of reinforcement were applied:

- basalt fibres with polystyrene (FA1),
- waste form plastic pallet utilization (FA2),
- and mixing of waste polyolefin materials such as polyethylene, polypropylene and other waste packing materials (FA3).

The samples were prepared using sodium promoter, fly ash, sand to create geopolymer matrix and reinforcement form waste plastic particles (1% by mass). The matrix was based on fly ash and fine sand at a ratio of 1:1. The process of activation was made by 12M sodium hydroxide solution combined with the sodium silicate solution (liquid glass at a ratio of 1:2.5). To manufacture geopolymers, flakes of technical sodium hydroxide were used and an aqueous solution of sodium silicate (R-145) which molar module was 2.5 and density - about 1.45 g/cm³. The tap water was used instead of the distilled one. The alkaline solution was prepared by means of pouring the aqueous solution of sodium silicate over the solid sodium hydroxide. The solution was mixed and left until its temperature became stable and the concentrations equalized, which took, about 2 hours. The fly ash, sand, alkaline solution and fibres were mixed about 15 minutes by using mixing machine Varimixer Bear (to receive the homogeneous paste). Next, it was poured into sets of plastic moulds and were heated in the laboratory dryer for 24h at 75 °C. Then, the samples were un moulded and cured in laboratory condition during 14 days. Next, the mechanical properties were investigated.

Compressive strength tests were carried out according to the methodology described in the standard EN 12390-3. ('Testing hardened concrete. Compressive strength of test specimens'). The tests involved 4 cubic samples: 50 x 50 x 50 mm.

Scanning electron microscope (SEM) type JEOL JSM 820 has been used for microstructure research. The research has been made for the samples previously broken during compressive or flexural strength tests. The samples were covered with a thin layer of gold with JEOL JEE-4X vacuum sputter. The investigations were made at various magnifications (between 20–100x).

Flexural strength tests were carried out according to the methodology described in the standard EN 12390-5. ('Testing hardened concrete. Flexural strength of test specimens'). The tests involved 2 prismatic samples: 50 × 50 × 150 mm. Tests were performed on an concrete press – MATEST 3000kN with speed 0,5 [MPa/s].

3. RESULTS AND DISCUSSION

The micro- and macro-observation for the prepared samples have been done. The particles distribution was evaluated. Macro-observations showed that the composites with basalt fibres with polystyrene (FA1) as well as the composites with waste from plastic pallet utilization (FA2) have the regular particular distribution by volume and they have not a tendency to create the agglomerates. The composites reinforced by mixing of waste polyolefin materials such as polyethylene, polypropylene and other waste packing materials (FA3) the distribution was irregular. The vibration process applied during the manufactured the specimens happens that most of particles was on the upper surface of the sample (*Figure 1*). This irregular distribution in the matrix heavily influences the mechanical properties of the composite.



Figure 1
The irregular distribution of plastic particle in the geopolymer matrix,
crosssection trough the samples after compressive strength test

The SEM observations were made for composition reinforced by three different kinds of plastic particles (FA1, FA2 and FA3). The images were made at various magnifications – between 20 – 100× for each composition. The observation of microstructure of composites gave a preliminary information about the coherency of the reinforcements with the geopolymer matrix.

In the *Figure 2*, there is presented the morphology of the composite with waste: basalt fibres with polystyrene (FA1). The figure shows polystyrene particle and geopolymer matrix below. The observation do not show any basalt fibres, they probably be dissolved during production process because of high molar ratio of the sodium hydroxide solution (12M). The microstructural observation also allows to notice that the structure is coherent (good adhesion the polystyrene particles to the matrix).

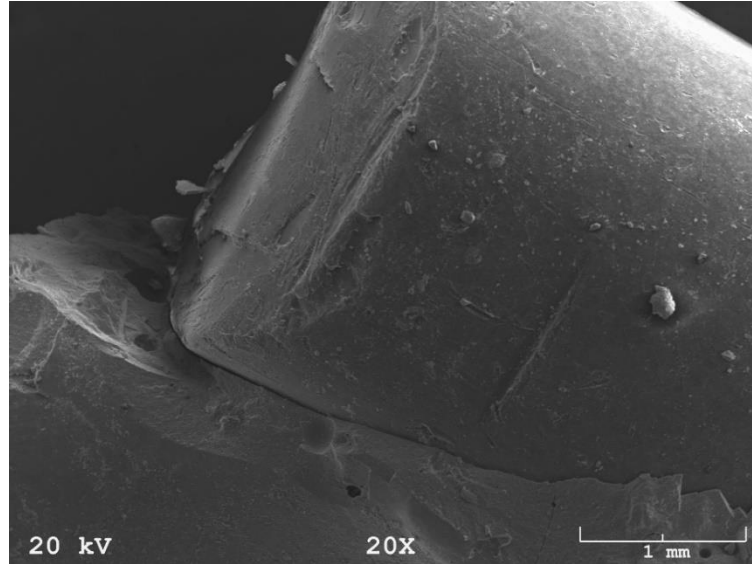


Figure 2

SEM image of composite: geopolymer matrix with basalt fibres with polystyrene (FA1)

The results from the scanning electron microscopy analysis for composite with waste form plastic pallet utilization (FA2) are shown in *Figure 3*. The figure shows plastic particle and the parts of geopolymer matrix. The observations do not show any problems with coherence particles – matrix.

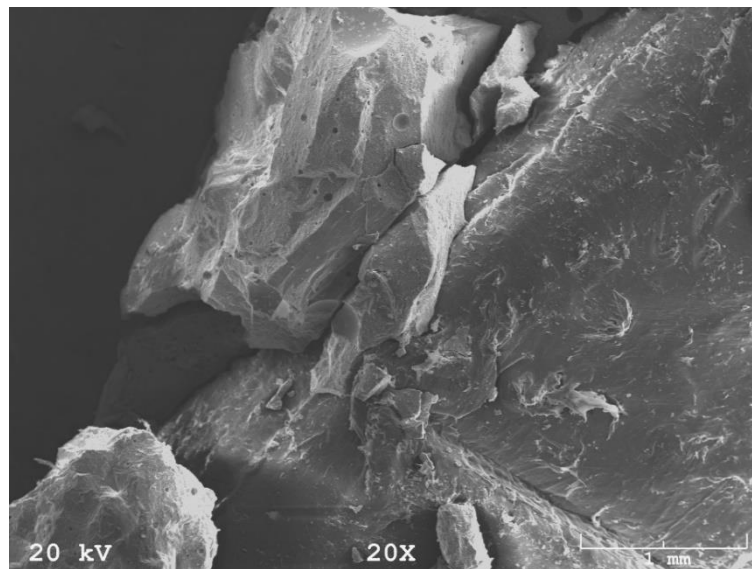


Figure 3

SEM image of composite: geopolymer matrix with waste form plastic pallet utilization (FA2)

Composite with additive mixing of waste polyolefin materials such as polyethylene, polypropylene and other waste packing materials (FA3) is presented in *Figure 4*. The observations confirm the cohesiveness between particles and matrix. The coherent structure has a positive impact on the mechanical properties of the composites.

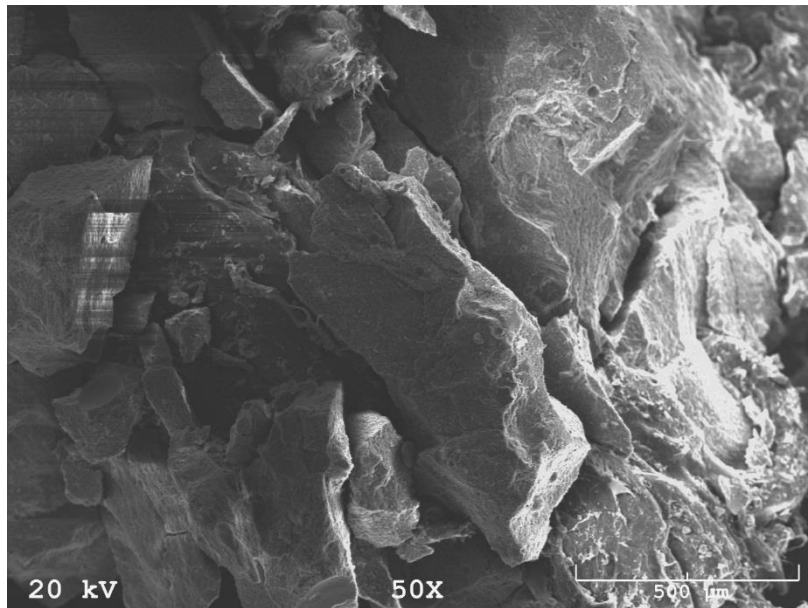


Figure 4

SEM image of composite: geopolymer matrix with mixing of waste polyolefin materials such as polyethylene, polypropylene and other waste packing materials (FA3).

Results for mechanical properties tests are presented in *Table 1* and 2. The results of the compressive strength test are shown in *Table 1*. The results of the reinforced composites and for comparison the plain (without reinforcement) specimens are presented.

Table 1
Results of compressive strength tests.

Samples	Compressive strength [MPa]	Standard deviation
FA0	55.6	7.7
FA1	57.6	14.2
FA2	56.0	7.7
FA3	54.5	3.1

The best results for compressive strength have been achieved for the composite with waste from basalt fibres with polystyrene (FA1) – 57.6 MPa and composite with waste form plastic pallet utilization (FA2) – 56 MPa. There are better than for the plain geopolymer matrix – 55.6 MPa. The

results for composition with mixing of waste polyolefin materials - waste packing materials (FA3) are slightly worse than for the plain material – 54.5 MPa. However, it should be noted that the results of compressive strength for different kind of reinforcements are very similar. The differences are statistically not important.

The results from the flexural strength tests are shown in *Table 2*. The results of the reinforced composites and for comparison the plain (without reinforcement) specimens are presented.

Table 2
Results of flexural strength tests.

Samples	Flexural strength [MPa]	Standard deviation
FA0	9.7	0.9
FA1	8.1	1.4
FA2	8.3	0.2
FA3	7.0	0.1

The best results for flexural strength are achieved for the matrix without reinforcement – 9.7 MPa. However the results for other reinforced composites are also very good. The differences between plain matrix and composites with basalt fibres with polystyrene (FA1) – 8.1 MPa, and composites with waste form plastic pallet utilization (FA2) – 8.3MPa are statistically not important. The composition with mixing of waste polyolefin materials such as polyethylene, polypropylene and other waste packing materials (FA3) has worse properties than plain matrix – 7.0 MPa. However they are still acceptable taking under consideration application this material in civil engineering.

4. CONCLUSIONS

Geopolymer composites reinforced with various waste have been produced and characterized. The samples were prepared using sodium promoter and three various types of waste additives (1% by mass of the composite): basalt fibres with polystyrene (FA1), waste form plastic pallet utilization (FA2), and mixing of waste polyolefin materials such as polyethylene, polypropylene and other waste packing materials (FA3). The matrix was geopolymer cement (fly ash and sand in ratio 1:1).

The observation of macrostructure gives the information about particles distributions. In case of additive basalt fibres with polystyrene (FA1) and waste form plastic pallet utilization (FA2), the particles distribution was regular. For the composites reinforced by mixing of waste polyolefin materials such as polyethylene, polypropylene and other waste packing materials (FA3) the particles was cumulate in the upper part of the composite. The microstructure analysis of composites gave a preliminary information about the coherency of the reinforcements with the geopolymer matrix. The results of compressive strength tests for different kind of reinforcements as well as plain matrix are very similar. The differences are statistically not important. The results of flexural strength tests show that the differences between plain matrix and composites with basalt fibres with polystyrene (FA1) and composites with waste form plastic pallet utilization (FA2) are statistically not important. The composition with mixing of waste polyolefin (FA3) has slightly worse properties, however they are still acceptable taking under consideration application this material in civil engineering.

This study presents that it is possible to produce the composites of reasonable properties from the industrial wastes (fly ash and waste polymers). However the results show the addition different waste polymers materials to geopolymer matrix do not increasing significantly the mechanical properties of the composites it still can be promising way of its utilization. The investigated materials work in the composites as a fillers not as an reinforcement. Based on this kind of waste materials it is possible to receive the composite with good mechanical properties that could be used for different applications. Additionally, using the plastic waste has positive impact on environment. Thus, the designed composites have potential to be used as new eco-friendly material e.g. in construction industry. The industrial application in this area required further research such as: water absorption, durability, cost-effectiveness and corrosion resistance.

ACKNOWLEDGEMENTS

This work was supported by the ERANet-LAC 2nd Joint Call (<http://www.eranet-lac.eu>) and funded by National Centre for Research and Development, Poland, under the grant: “Development of eco-friendly composite materials based on geopolymer matrix and reinforced with waste fibers”.

REFERENCES

- [1] ARULRAJAH, A. et al. (2017): Recycled plastic granules and demolition wastes as construction materials: Resilient moduli and strength characteristics. *Construction and Building Materials*, 147, pp. 639–647. DOI: <https://doi.org/10.1016/j.conbuildmat.2017.04.178>.
- [2] BRIBIÁN, I. Z. et al. (2011): Life cycle assessment of building materials: Comparative analysis of energy and environmental impacts and evaluation of the eco-efficiency improvement potential. *Building and Environment*, 46, pp. 1133–1140. DOI: 10.1016/j.buildenv.2010.12.002.
- [3] CELIK, A. et al. (2018): High-temperature behavior and mechanical characteristics of boron waste additive metakaolin based geopolymer composites reinforced with synthetic fibers. *Construction and Building Materials*, 187, pp. 1190–1203. DOI: <https://doi.org/10.1016/j.conbuildmat.2018.08.062>.
- [4] CHENG, T. W. et al. (2011): The heavy metal adsorption characteristics on metakaolin-based geopolymer. *Applied Clay Science*, 56, pp. 90–96. DOI: <https://doi.org/10.1016/j.clay.2011.11.027>.
- [5] COLANGELO, F. et al. (2013): Experimental and Numerical Analysis of Thermal and Hygrometric Characteristics of Building Structures Employing Recycled Plastic Aggregates and Geopolymer Concrete. *Energies*, 6, pp. 6077–6101; DOI:10.3390/en6116077.
- [6] CRAWLEY (2008): Estimating the impacts of climate change and urbanization on building performance. *Journal of Building Performance Simulation*, 1, pp. 91–115. DOI: <https://doi.org/10.1080/19401490802182079>.
- [7] GHERNOUTI Y., et. al. (2014). Use of recycled plastic bag waste in the concrete. *Journal of International Scientific Publications: Materials, Methods and Technologies*, 8, pp. 480–487.

-
- [8] ISMAIL, Z. Z-AL-HASHMI, E. A. (2008): Use of waste plastic in concrete mixture as aggregate replacement. *Waste Management*, 28 (11), pp. 2041–2047. DOI: <https://doi.org/10.1016/j.wasman.2007.08.023>.
- [9] IUCOLANO, F. et al. (2013): Recycled plastic aggregate in mortars composition: Effect on physical and mechanical properties. *Materials & Design*, 52, pp. 916–922. DOI: <https://doi.org/10.1016/j.matdes.2013.06.025>.
- [10] KORNIEJENKO, K. et al. (2018): The mechanical properties of flax and hemp fibres reinforced geopolymer composites. *IOP Conference Series: Materials Science and Engineering*, 379 (2018) 012023, p. 9. DOI: [10.1088/1757-899X/379/1/012023](https://doi.org/10.1088/1757-899X/379/1/012023).
- [11] KINNUNEN, P. et al. (2017): Rockwool waste in fly ash geopolymer composites. *Journal of Material Cycles and Waste Management*, 19, pp. 1220–1227. DOI: [10.1007/s10163-016-0514-z](https://doi.org/10.1007/s10163-016-0514-z).
- [12] LUNA-GALIANO, Y. et al. (2018): Carbon fiber waste incorporation in blast furnace slag geopolymers composites. *Materials Letters*, 233, pp. 1–3. DOI: <https://doi.org/10.1016/j.matlet.2018.08.099>.
- [13] ŁACH, M. et al. (2017): The possibilities of use granulates made from tires as an additive to geopolymer concretes. In: HAGER I. (ed.): *Energy Efficient, Sustainable Building Materials and Products*. Cracow: Wydawnictwo Politechniki Krakowskiej, pp. 63–78.
- [14] MALENAB, R. A. J. et al. (2017): Chemical Treatment of Waste Abaca for Natural Fiber-Reinforced Geopolymer Composite. *Materials*, 10, pp. 579–598. DOI: [10.3390/ma10060579](https://doi.org/10.3390/ma10060579).
- [15] MIERZWIŃSKI, et al. (2018a): Stabilization of ash and slag from combustion of medical waste in the geopolymers matrix. *E3S Web of Conferences*, 44, p. 8. DOI: [10.1051/e3sconf/20184400110](https://doi.org/10.1051/e3sconf/20184400110).
- [16] MIERZWIŃSKI, et al. (2018b): Effect of Coffee Grounds Addition on Efflorescence in Fly Ash-based Geopolymer. *IOP Conference Series: Materials Science and Engineering*, 416 (2018) 012035, p. 7. DOI: [10.1088/1757-899X/416/1/012035](https://doi.org/10.1088/1757-899X/416/1/012035).
- [17] MUCSI, G. et al. (2018): Fiber reinforced geopolymer from synergetic utilization of fly ash and waste tire. *Journal of Cleaner Production*, 178, pp. 429–440. DOI: <https://doi.org/10.1016/j.jclepro.2018.01.018>.
- [18] NOVAIS, R. M. et al. (2017): Effective mechanical reinforcement of inorganic polymers using glass fibre waste. *Journal of Cleaner Production*, 166, pp. 343–349. DOI: <https://doi.org/10.1016/j.jclepro.2017.07.242>.
- [19] OGUNDIRAN, M. B. et al. (2013): Immobilisation of lead smelting slag within spent aluminate-fly ash based geopolymers. *Journal of Hazardous Materials*, 248–249 (1), pp. 29–36. DOI: <https://doi.org/10.1016/j.jhazmat.2012.12.040>.

- [20] NAZARI (2013): Compressive strength of geopolymers produced by ordinary Portland cement: Application of genetic programming for design. *Materials and Design*, 43, pp. 356–366. DOI: <https://doi.org/10.1016/j.matdes.2012.07.012>.
- [21] PACHECO-TORGAL (2014): Eco-efficient construction and building materials research under the EU Framework Programme Horizon 2020. *Construction and Building Materials*, 51, pp. 151–162. DOI: <https://doi.org/10.1016/j.conbuildmat.2013.10.058>.
- [22] PALANISAMYA, P.–SURESH KUMAR, P. (2018): Effect of Molarity in Geopolymer Earth Brick Reinforced with Fibrous Coir Wastes Using Sandy Soil and Quarry Dust as Fine Aggregate. (Case Study). *Case Studies in Construction Materials*, 8, pp. 347–358. DOI: <https://doi.org/10.1016/j.cscm.2018.01.009>.
- [23] PALOMO, A. et al. (2014): A review on alkaline activation: new analytical perspectives. *Materials de Construcción*, 64 (315), p. 22. DOI: <http://dx.doi.org/10.3989/mc.2014.00314>.
- [24] SEDIRA, N. et al. (2017): A Review on Mineral Waste for Chemical-Activated Binders: Mineralogical and Chemical Characteristics. *Mining Science*, 24, pp. 29–58. DOI: [10.5277/msc172402](https://doi.org/10.5277/msc172402).
- [25] SINGH, N. (2017): Recycling of plastic solid waste: A state of art review and future applications. *Composites Part B*, 115, pp. 409–422. DOI; <https://doi.org/10.1016/j.compositesb.2016.09.013>.
- [26] VISHWAKARMA, V.–RAMACHANDRAN, D. (2018): Green Concrete mix using solid waste and nanoparticles as alternatives – A review. *Construction and Building Materials*, 162, pp. 96–103. DOI: <https://doi.org/10.1016/j.conbuildmat.2017.11.174>.
- [27] WANG R.–XU, Z. (2014): Recycling of non-metallic fractions from waste electrical and electronic equipment (WEEE): A review. *Waste Management*, 34 (8), pp. 1455–1469. DOI: <https://doi.org/10.1016/j.wasman.2014.03.004>.



HIGH-PERFORMANCE GEOPOLYMERS BY WET MILLING OF BLAST FURNACE SLAGS

THOMAS MÜTZE–URS ALEXANDER PEUKER

Institute of Mechanical Process Engineering and Mineral Processing, TU Bergakademie Freiberg,
Agricolastraße 1, 09599 Freiberg (Germany), thomas.muetze@mvtat.tu-freiberg.de

Abstract

Since more than 100 years blast furnace slags are used as additive material or substitute material in cementitious systems like mortar and concrete. Due to their different syntheses, the slag systems have binding properties which differ from conventional clinker. Some properties like limited heat generation and heat transfer due to a slow reaction kinetics are advantageous for certain applications. Other properties like a low short-term strength of the corresponding concrete are limiting the use of blast furnace slags in applications like the pre-manufacturing of building parts.

With the help of mechanical activation due to fine grinding the properties of blast furnace slags can be shifted towards conventional clinker systems. Therefore a common blast-furnace slag cement was used to study the influence of the grinding regime in media mills on the binding properties of the corresponding cement. The grinding regime of conventional wet ball milling has been compared to a planetary ball mill and a stirred media mill circuit. Since finely ground slag reacts with the process medium water, several strategies have been tested to remove the process water as quickly as possible in order to evaluate the particle properties like specific surface area and size.

Fine grinding with the stirred media mill produced a hydraulic reactive material with similar properties as conventional clinker cement. The fineness of the material, which is described by the specific surface area, increased its reactivity. Nevertheless, the reactivity of the slag was still low enough that it can be processed in aqueous suspensions.

Keywords: *blast furnace slags, fine grinding, stirred media mill*

1. INTRODUCTION

The application of secondary raw materials from anthropogenic high temperature processes in building material has a long tradition [1]. With a proper processing of the secondary raw material like slags and ashes it is possible to substitute cement [2, 3]. Some application properties even are improved due to the special properties and reaction behavior of the secondary raw materials. One example is the construction of large concrete structures like dams, which require the slow reaction of slag-based concrete mixtures due to heat generation and heat transfer limitations. When combined with conventional cement in defined mixing ratios, slag- and ash-based concretes and mortars can be used in a broad field of building applications. Since the reactivity of cement as well as of secondary raw materials is a function of the particle size, comminution is the key to generate

an sufficient amount of highly reactive fines. Furthermore ashes or slags can be chemically treatment to activate the silica structure. Typical modifiers and activators are sodium and potassium-hydroxide [4–7].

The relatively low reaction rate of secondary raw materials leads to several applications of ash and slag based concretes, especially if short-term strength of the concrete is necessary, e.g. for pre-manufactured parts. Beside chemical activation, mechanical activation is also possible. Mechanical activation can be due to size reduction and the increase in reactive particle surface or due to mechanical alteration of the internal crystal structure of the material. The latter determines the velocity of ionic or aqueous attack to the solids structure. The main problem of such a size reduction step for secondary raw materials derives from the field of operation of typical mills used in cement grinding. Conventional ball mills or roller mills are not suited to generate ultra fine products. The alternatives are high-pressure grinding rollers (HPGR), vertical roller mills [8], or stirred media mills (SMM) [9-11] which are known from pigment [12] and re-grinding applications.

2. MATERIALS AND METHODS

A common blast-furnace slag cement was used to study the influence of the grinding regime on the binding properties of the corresponding cement. The slag was produced by conventional ball milling (*Figure 2*: BM). Particle properties like size and specific surface were measured in order to evaluate the process function. The particle size analysis utilized the laser diffraction system Helos (Sympatec, Clausthal-Zellerfeld, Germany) with either the dry dispersing system RODOS or with the wet dispersing system SUCELL. In order to avoid the hydration reaction in the wet dispersing mode, isopropanol was used as carrier liquid.

The comminution experiments used a planetary ball mill PULVERISETTE 5 (Fritsch, Idar-Oberstein, Germany) and the lab scale stirred media mill Perl Mill (Draiswerke Mannheim, Germany). The planetary ball mill (PBM) is a high energetic mill type, which promised both a small final particle size and an optional mechanical activation, due to the high energy milling mechanism. The stirred media mill (SMM) is known for the capability to produce nano-sized materials [9, 13]. It is typically operated in wet mode, where a slurry is pumped through the grinding chamber. With a suitable size of grinding balls and a stabilizing physico-chemical milieu as well as with high specific energy input, it is possible to produce ultra fine particle systems.

The PULVERISETTE 5 has a milling chamber of 0.25 l volume and was operated at a media filling degree of 30 %. The processing consisted of three subsequent grinding stages with different grinding balls (see *Table 1*) and used triethanolamine and diethylene glycol as grinding aids at a concentration of 0.02 %. The Perl Mill (*Fig. 1*) operated in a closed circuit with a mass concentration of the feed slurry $c_m = 0.3$. The grinding chamber was filled with ceramic balls (see *Table 1*) at a filling ratio of 60%.

Since finely ground slag reacts with the process medium water especially during storage after comminution, several strategies have been tested to remove the process water as quickly as possible and to preserve the material properties for analytics. The removal strategies included convective thermal drying, spray drying, filter cake washing with organic liquids (isopropanol or ethanol), and subsequent low temperature drying. The latter method proofed to be sufficient to

stop unwanted changes of the material properties and has been used for the experiments presented here (except *Figure 5*).

Table 1

Grinding conditions in the planetary ball mill (PBM) and stirred media mill (SMM)

Equipment	Grinding stage	Grinding time in min	grinding media	Diameter of grinding media in mm
PBM	1	30	Steel balls	10
	2	20		6–7
	3	20		1–2
SMM		15	Ceramic balls	1–1.6
		60		

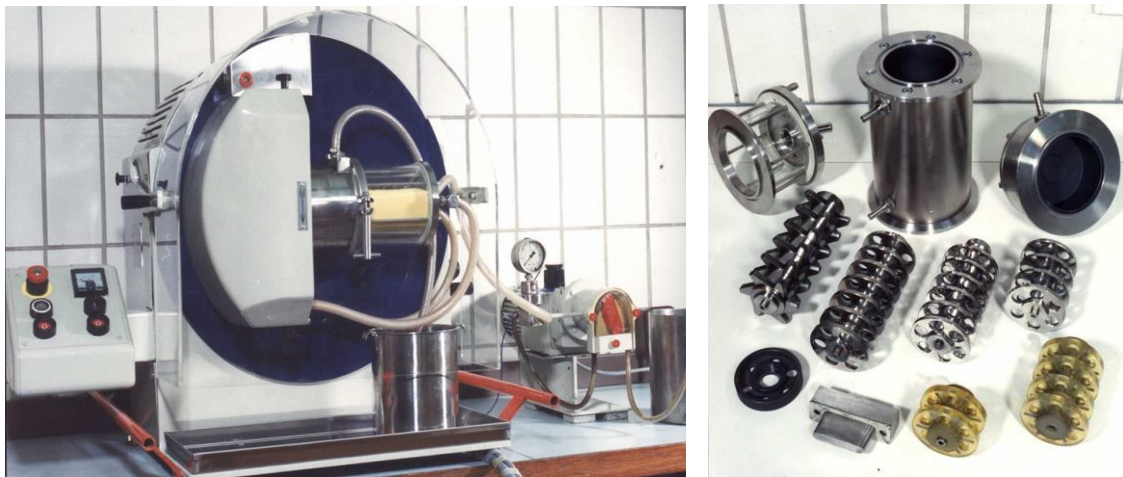


Figure 1

Left: Stirred Media Mill (SMM) type Drais Perl Mill, with a 0,75 l processing chamber; right: milling chamber and used stirrer geometries.

3. RESULTS AND DISCUSSION

The investigation of different types of fine grinding equipment showed that dry processing of the slag comes quickly to a grinding limit. At this limit agglomeration and breakage kinetic reach an equilibrium state and the particle size does not decrease further. The PSD shows, that the different concepts of fine grinding can be applied to blast furnace slags to produce superfine geopolymer material. The experiences during the aqueous grinding of the blast furnace slag in the SMM demonstrated, that the binding kinetic is sufficiently low. During one hour of wet processing no gelation/ binding could be observed. Nevertheless, it was necessary to remove the water after

processing because longer contact times to water got the binding reaction more and more accelerating.

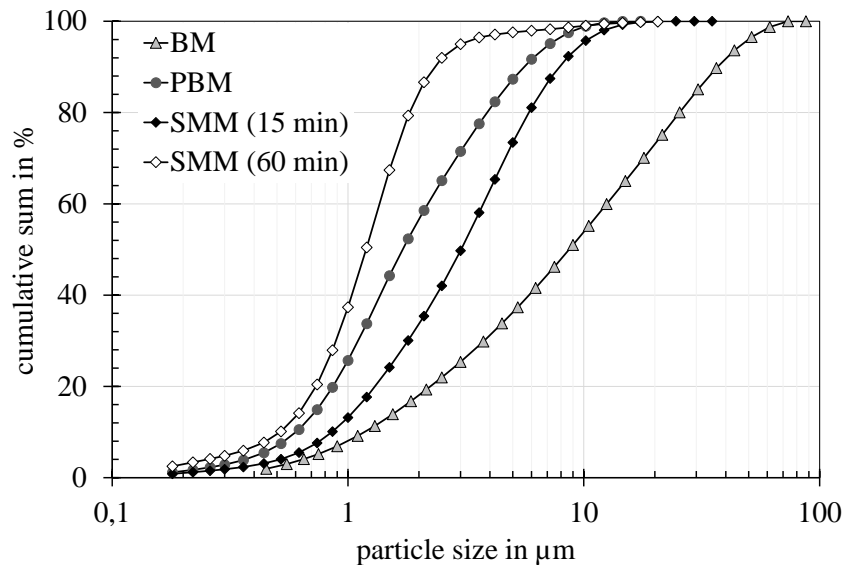


Figure 2

Particle size distribution of the feed material and grinding products (BM: ball mill product (feed), PBM: product of planetary ball mill, SMM: products of stirred media milling after defined grinding times)

Selected samples of both the PBM and the SMM products were used in a mortar test (Figure 3), which shows the relative compressive strength of a defined mortar sample as a function of the binding time. Characteristic values of this function are the ones after one day (1 d), two days (2 d) and 28 days (28 d). The last value corresponds approximately to the final strength. The one-day strength is relevant for the production of prefabricated parts.

The higher fineness of the finely milled material leads to an increased compressive strength. The data is normalized to the compressive strength (28 d) of mortar produced with standard cement CEM. Both mortars which contain fine slag reach a higher final strength compared to pure CEM. The increase in final strength amounts to more than 10 %. Even more relevant for the application of fine slag are the values of the compression strength after one-day. The SMM product reaches after one day already 80 % of the final strength of the CEM, whereas the BM and PBM products are much weaker. Especially in comparison with the PBM product, the differences in strength do not derive from the final PSD only. During the milling a chemical activation occurs, which is due to the interaction between the silicates in the slag structure and the aqueous carrier fluid.

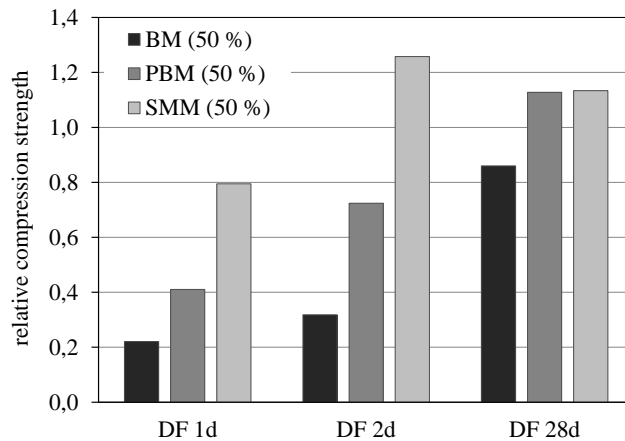


Figure 3

Compression strength of concrete manufactured of 50 % CEM and 50 % of milled slag fraction (testing according DIN EN 12390-3) relative to 100 % CEM.

The increase of compression strength of the material depends on the reactivity of the hydraulic active component. The mechanical and chemical activation leads to a higher reactivity, which allows a faster reaction, which finally provides higher early phase compression strength (1 d). The reactivity becomes visible in the plot of the heat of reaction and heat of hydration respectively (Figure 4), when differently processed slag materials are mixed with water and CEM. The reference is the pure cement system “CEM”. The transient heat flux shows an inhibition of about 5 h before the hydration reaction begins to start. The reaction itself shows a fast kinetic, which is comparable to the CEM system.

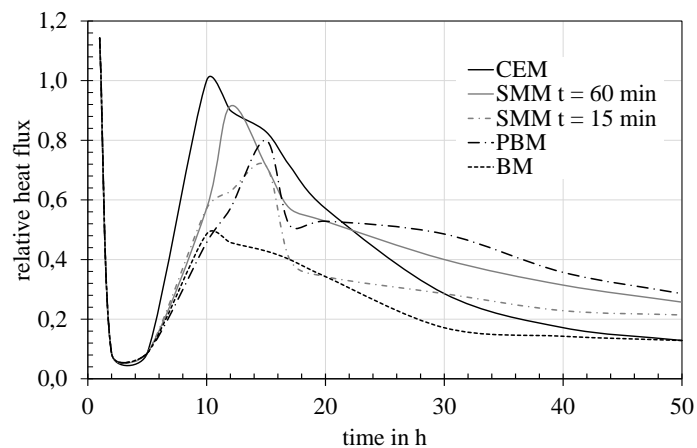


Figure 4

Heat flux of the hydration reaction of pure CEM compared the ones of slag mixtures (50 % fine blast furnace slag mixed with 50 % conventional CEM, slag to water ratio 2:1; BM: ball mill; SMM: stirred media mill; PBM: planetary ball mill).

The maximum of the heat flux depends on the processing of the slag, which means the fineness and the chemical activation of the milled material. The finer the slag is, the closer the maximum comes to the data of the CEM system. The overall reactivity can be taken from the integral of the curves, the larger the integral area is the more binding occurs within the system. The area of the BM slag is smaller since the quite coarse material does not react completely. Also, the curves of the finely milled slags (PBM and SMM) show a longer-lasting reactivity. These systems have a significant heat flux in the period 20–50 h, which is even higher than that of the CEM system.

Thus the conventional processing provides a slow reaction kinetic, which explains the low compression strength after one day. The other slag fractions have been further processed with either the planetary ball mill (PBM) as dry material or with the stirred media mill (SMM) as aqueous suspension. For the SMM two different milling times have been investigated (15 and 60 min). These times are at least one order of magnitude smaller than the inhibition time of the hydraulic reaction shown in *Figure 4*. This explains why there is no significant setting of the reaction during the wet comminution and why a smooth replacement of the grinding environment from aqueous to organic (isopropanol) allows to study the particle characteristics of the grinding products.

Bringing all comminution data together, it becomes clear that an increase in fineness also increases the reactivity of the slag system. The inhibition time decreases and the initial as well as the overall heat flux becomes much higher. When looking at the integral of reaction heat, it can be stated, that more CSH phases are formed in a shorter period. The increased processing time of the SMM product, 60 min compared to 15 min, supports this finding, since the longer milling results in a finer product (*Figure 2*). Furthermore *Figure 5* illustrates that the specific surface of the slag system determines the mechanical properties of the final mortar system. This effect is more significant in the early stage (1 d and 2 d), where the difference of the strength amounts up to a factor of three to four between a specific surface of 1 m²/g to 6 m²/g. Fine milling of slags therefore enables the application of the material where early stage strength is needed, e.g. for prefabricated parts.

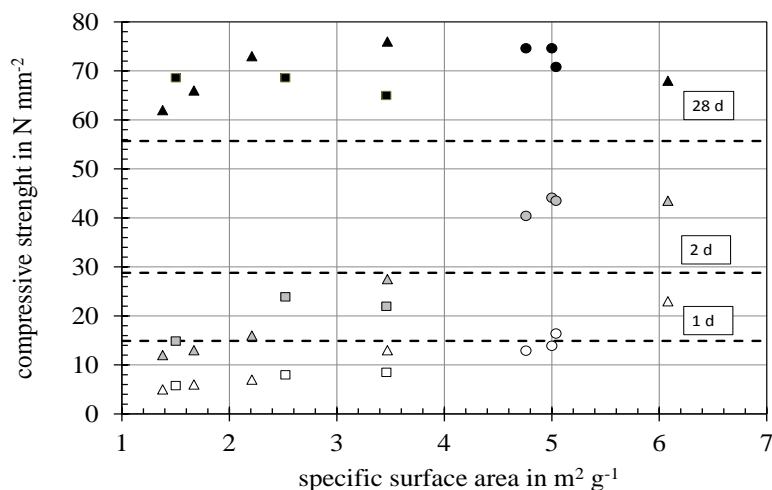


Figure 5
Compressive strength (1d; 2 d; 28 d) as a function of specific surface of the activated slag material for different milling strategies, measured in the system 50 % slag and 50 % CEM (dashed lines: pure CEM).

The comminution of the slag material definitely consumes energy. Bringing together the data sets of different processing machines and concepts, they do all follow the breakage law of the slag system which can be described by a power law (*Figure 6*). The high quantity of mechanical energy which is needed to enhance the reactivity of the slag has to be counterbalanced with the saving of CO₂-emissions during CEM production from limestone.

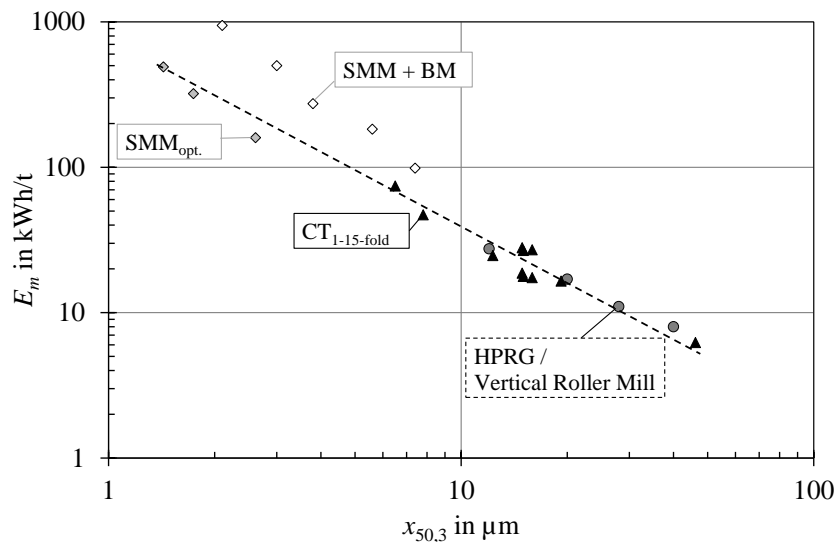


Figure 6

Evaluation of the comminution performance (SMM – stirred media mill; SMM + BM – sum of comminution energy of ball mill (BM) plus stirred media mill (SMM); CT – compression in piston-die system (lab scale – typically used to simulate HPRG [14, 15]); HPRG – high pressure grinding roller).

4. CONCLUSIONS

Fine milling with SMM allows the production of a hydraulic reactive material from blast furnace slags, which has similar properties as conventional Portland cement. The fineness of the material, which is described by the specific surface, increases its reactivity. The reactivity of the slag is still low enough that it can be processed in aqueous suspension. For further application, the water has to be removed from the finely milled material as it has been done in the lab-scale tests here. An alternative would be milling the slag directly prior to the application in the cementous system, thus to feed a (thickened) SMM slurry in the mortar / concrete production process.

ACKNOWLEDGEMENTS

The authors would like to acknowledge the financial support from the Federal Government of Germany in the scope of the research project ECO-Zement (BMBF-No. 0327477 B).

REFERENCES

- [1] W. MATTHES et al.: *Ground granulated blast-furnace slag*. 252018
- [2] Z. SEKULIC et al. (2004): Mechanical activation of various cements. *International Journal of Mineral Processing*, 74, SUPPL., S355-S363
- [3] A. EHRENBERG (2010): Current developments in the manufacturing and utilization of granulated blast furnace slag. *ZKG International*, 63/3, pp. 52–66.
- [4] V. TOMKOVÁ et al. (2011): Potential modification of hydration of alkali activated mixtures from granulated blast furnace slag and fly ash. *Ceramics – Silikaty*, 56/2, pp. 168–176
- [5] P. AYTURAN–M. TOKYAY (2011): *Alkali activation of granulated blastfurnace slag and fly ash. 33rd International Conference on Cement Microscopy 2011*.
- [6] R. TÄNZER et al. (2012): Concrete based on alkali-activated granulated blast-furnace slag (Part 1). *Betonwerk und Fertigteil-Technik/Concrete Plant and Precast Technology* 78/3, pp. 25–33.
- [7] R. TÄNZER et al. (2012): Concrete based on alkali-activated granulated blast-furnace slag (Part 2). *Betonwerk und Fertigteil-Technik/Concrete Plant and Precast Technology* 78/4, pp. 44–57.
- [8] H. WEIMAR et al. (2017): Mobilization of the hydraulically active phases in LD slags by producing ultrafine material. *Cement International*, 15/4, pp. 76–86.
- [9] S. MENDE et al. (2004): Production of sub-micron particles by wet comminution in stirred media mills. *Journal of Materials Science*, 39/16–17, pp. 5223–5226.
- [10] F. STENGER et al.(2005): The influence of suspension properties on the grinding behavior of alumina particles in the submicron size range in stirred media mills. *Powder Technology*, 156/2–3, pp. 103–110.
- [11] K. OHENOJA et al. (2014): Ultrafine grinding of limestone with sodium polyacrylates as additives in ordinary portland cement mortar. *Chemical Engineering and Technology*, 37/5, pp. 787–794.
- [12] F. FLACH et al. (2018): Model based process optimization of nanosuspension preparation via wet stirred media milling. *Powder Technology*, 331, pp. 146–154.
- [13] M. SCHÄFER et al. (2016): The grinding of porous ion exchange particles. *Powder Technology*, 291, pp. 14–19.
- [14] T. MÜTZE (2014): Modellhafte Beschreibung des Beanspruchungsverhaltens geschlossener Gutbetten, Modeling of the Stress Behavior of Confined Particle Beds. *Chemie Ingenieur Technik*, 86/6, pp. 814–820.
- [15] T. MÜTZE (2015): Energy dissipation in particle bed comminution. *International Journal of Mineral Processing*, 136, pp. 15–19.



INFLUENCE OF MOISTURE CONTENT AND TEMPERATURE ON BRIQUETTING OF SOLAR DRIED SEWAGE SLUDGE

SÁNDOR NAGY¹–QUYEN V. TRINH²–LJUDMILLA BOKÁNYI³–
ANETT PINTÉR⁴–TAMÁS FÁBRIK⁵

¹University of Miskolc, H-3515, Miskolc Egyetemváros, ejtnagys@uni-miskolc.hu

²University of Miskolc, H-3515, Miskolc Egyetemváros, trinhquyennd@gmail.com

³University of Miskolc, H-3515, Miskolc Egyetemváros, ejtblj@uni-miskolc.hu

⁴Trandanebian Regional Waterworks Corporation DRV, Siófok

⁵Trandanebian Regional Waterworks Corporation DRV, Siófok

Abstract

DRV Plc. and the Institute of Raw Material Preparation and Environmental Processing carry out a R&D project in which the by-products of wastewater treatment process, such as sewage sludge and other organic waste, are the input materials. The by-products are processed on various ways, to transform them to products, which can be used either as fuel, or soil conditioner. Solar dried sewage sludge sample originated from DRV Plc was investigated in course of this research work. The main material parameters of sewage sludge sample dried in solar drier were determined: particle size distribution and moisture content. The sample material was agglomerated into cylinder form tablets in an experimental hydraulic piston press with 25 mm diameter. Effect of various parameters on tablet quality were determined, such as pressure, temperature and moisture content. The investigated pressure range was 50 to 300 MPa. The highest tablet density was achieved by the 8.7 wt.% moisture content raw material at 100°C. According to the results, proper quality of agglomerated products can be achieved.

Keywords: *Agglomeration, briquetting, tableting, sewage sludge*

1. INTRODUCTION

The utilization of biosolids/sewage sludge in agriculture is gaining popularity as a source of waste treatment and utilisation. Biosolids/sewage sludge generally contains useful compounds of potential environmental value. It also contains useful concentration of organic matter, nitrogen, phosphorus and potassium and to lesser extent, calcium, sulphur and magnesium (USMAN et al. 2012).

Sewage is municipal wastewater composed of domestic liquid wastes, often in admixture with runoff and industrial and commercial effluents. When this undergoes treatment the particulate and colloidal matter is concentrated to form sludge. The physical properties and chemical composition of sewage sludge vary widely according to the source and the type of sewage treatment (DEAN and SUESS 1985). Sludge is processed further, either to render them more acceptable for disposal or to

reduce water content. No particular treatment or combination of treatments can be said to be typical (MATTHEWS 1984). Sewage sludge may be used in many ways, particularly in agriculture, forestry, gardens, and for the reclamation of infertile land (DEAN and SUESS 1985).

The „Development of bio raw materials products range with a special regard to the local technology – research on the possibility of utilisation by technological“ optimisation GINOP-2.2.1-15-2017-00069 R&D Project was generated aiming at the development of new products from sewage sludge to be utilized in agriculture and energy production. The DRV Plc. and the Institute of Raw Material Preparation and Environmental Processing, University of Miskolc are engaged in this project. One such a product can be briquettes obtained from solar dried sludge. This paper is dealing with the research on this option.

Describing of agglomeration process

Parameters of materials and agglomerate production are especially important in aspects related to product quality and economics. On the one hand, the reduction of moisture content and increasing temperature usually results in better quality agglomerates; it is possible to achieve higher density and strength. On the other hand, moisture content reduction (drying) and increasing temperature is related to a high energy demand. To find the optimal production parameters, the exact relationship between moisture content, temperature and briquetability (applied pressure, agglomerate density) should be known. Furthermore, it was reported that an increase in temperature reduces the friction in the press channel of the mill (STELTE et al. 2011) and lowers the energy required for different components of the pelletizing process (Nielsen et al. 2009). Other process parameters might influence the result of agglomeration too. CSÓKE et al. (2000) and (2003) investigated the effect of different feed methods (screw feed and gravity feed) on compacting. Another serious issue is the de-airing, because if the outflow of the displaced air from the agglomerated particles is too intense, that might break down the newly formed briquettes (TARJÁN et al. 1999).

Different approaches have been taken in order to calculate the connection between applied pressure and agglomerate density. The Johanson equation (1965) can take two forms:

$$\frac{\rho}{\rho^*} = \left(\frac{p}{P^*}\right)^{1/\kappa} ; \frac{F}{F_0} = \left(\frac{V_0}{V}\right)^\kappa$$

where κ is compressibility factor, ρ is agglomerate density, p is tableting pressure, F is tableting force, V is tablet volume, and p^* , ρ^* , F_0 , V_0 are reference values (if surface perpendicular to force and mass of tablet are constant) (STIEB 1997).

LIU and WASSGREN (2016) modified the Johanson model for improved relative density

$$\text{predictions: } \frac{P}{P_{\text{initial}}} = \left(\frac{\eta}{\eta_{\text{initial}}}\right)^\kappa$$

where η_{initial} is the inlet relative density, P_{initial} is the corresponding pressure according to the fit data; η is the powder's relative density.

Effect of temperature: The effect of temperature on the composting reaction of sewage sludge was investigated at 50, 60, and 70°C. The total amount of CO₂ evolved and the final conversion of volatile matter were maximum at 60°C, suggesting that the optimal temperature for composting was around 60°C (NAKASAKI et al. 1985). Temperature is a crucial parameter in the final stage of utilization and transportation of sewage sludge (WOLSKI et al. 2011).

Effect of moisture content: In industrial application, the moisture content and combustion characteristic of the received sewage sludge depends on the waste water treatment process and dewatering method. It is recognized that the sludge with different water content should be burned with different types of furnace (HUANG et al. 2016).

2. MATERIAL AND METHODS

2.1. Material

5 kg of solar dried sewage sludge was being selected as the raw material for our experiments (in May, 2018). It originated from Siófok, Hungary (DRV Ltd). It was ground using a cutting mill (Retsch SM2000) in one step (screen size 2 mm) at original moisture content of 8.7 wt.%. The particle size of sewage sludge was determined as < 1.6 mm and bulk density as high as 698 kg/m³. Raw material sewage sludge can be seen in *Figure 1*. It can be observed that sewage sludge is not a homogeneous material. *Figure 2* shows that although screen size of 2 mm was used, 100 % particles are smaller than 1.6 mm.

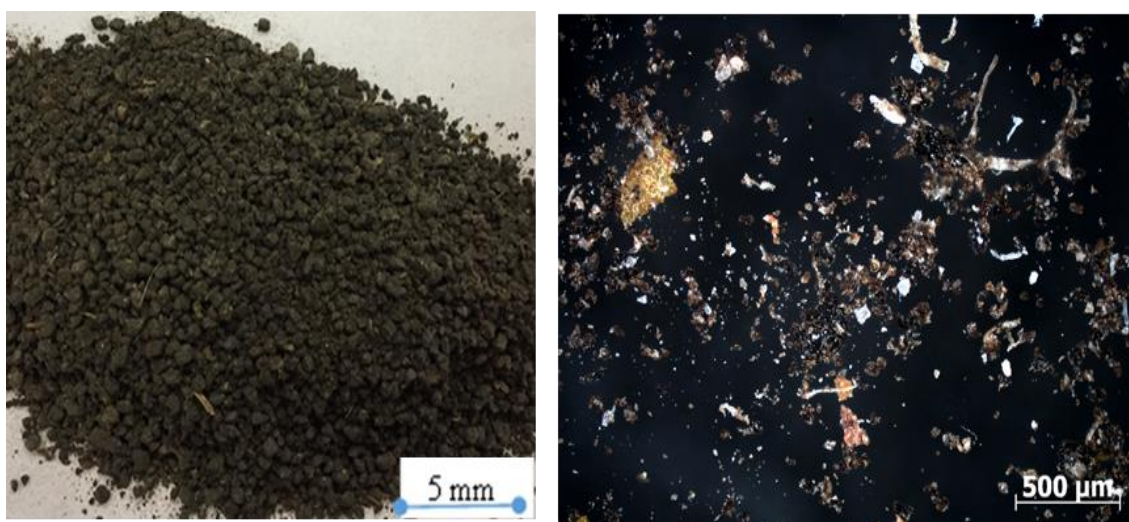


Figure 1
Solar dried sewage sludge with particle size < 1.6 mm; (left) optical camera;
(right) optical microscope: Zeiss AXIO Imager.M2m

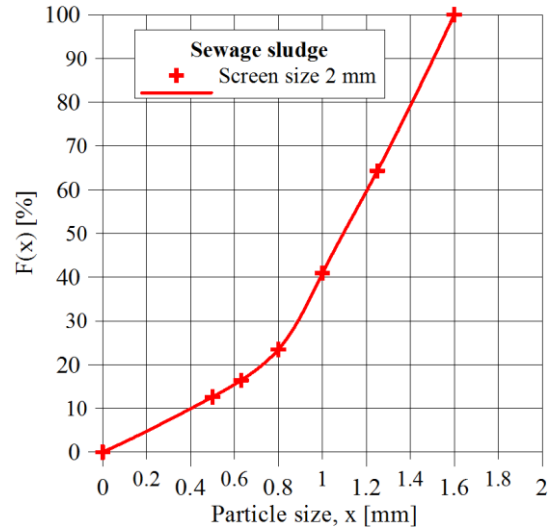


Figure 2

Particle size distribution of comminuted solar dried sewage sludge

2.2. Methods

Hydraulic piston press. The hydraulic piston press (Figure 3) was designed by the University of Miskolc. The press is supported by a pump motor unit with a pressure limiter and a heat-able load cell (20–140°C). The maximum force is 200 kN and the maximum velocity of the piston feed-rate is 30 mm s⁻¹. The measuring of the piston position is done with an incremental encoder.



Figure 3

Hydraulic piston press

Experimental procedure. The hydraulic piston press with 25 mm diameter was used for two different kinds of tests and each tablet was made by the compression of 5 g material. Applied pressures on the surface of tablets were 50, 100, 150, 200, 250 and 300 MPa with the same particle size < 1.6 mm and compression time of 5 seconds.

In the first test, the applied moisture contents were 4.7, 8.7, 14.8, and 19.6 wt.% with temperature of 25°C.

In the second test, the applied temperature was 25, 40, 60 and 100°C with moisture content of 8.7 wt.%, and spring-back ratio was also determined.

The springback ratio (SBR) of a tablet can be determined by:

$$SBR = \frac{H_t - H_{tp}}{H_{tp}} 100 \%$$

where H_t is the height of the produced tablet, H_{tp} is minimum height of the tablet under pressure.

The quality of tablets can be described easily by their density. The diameters and heights of the tablets product were measured by Vernier caliper (diameter of tablets can be shrunken after agglomeration in the case of 60°C, 100°C and 19.6 wt.%). The mass was measured and density was calculated for each test. The minimum height of tablets under pressure was measured by the incremental distance measurement method.

The determination of tablet strength was carried out by the well-known falling test method. Tablets were released by freefall from a height of 2 m onto a concrete floor repeatedly until they broke. The falling number is the number of falls the sample survived undamaged. In each experiment three tablets were tested.

Raw material particles and surfaces of tablets were investigated with an optical microscope Zeiss AXIO Imager M2m.

3. RESULTS AND DISCUSSION

Tablet density, spring-back ratio, tablet strength, and the structure of tablets were determined in our investigations.

3.1. Tablet density and compressibility

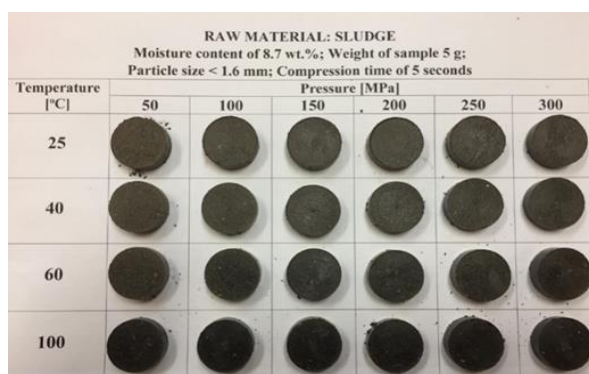


Figure 4
Tablets made from particle size < 1.6 mm

Tablets produced by processes with different parameters are shown in *Figure 4*. The tablet density values are recorded as an average of three measurements with particle size < 1.6 mm.

Figure 5 (left) shows the pressure density values and the fitted Johanson curves in the case of particle size < 1.6 mm raw material at 4.7, 8.7, 14.8 and 19.6 wt.%. Table 1 shows the constants of the fitted curves and coefficient of determination (R^2), residual mean square (σ) and calculated deviation (V_s). Results for different temperatures are introduced in *Figure 5* (right) and *Table 2*.

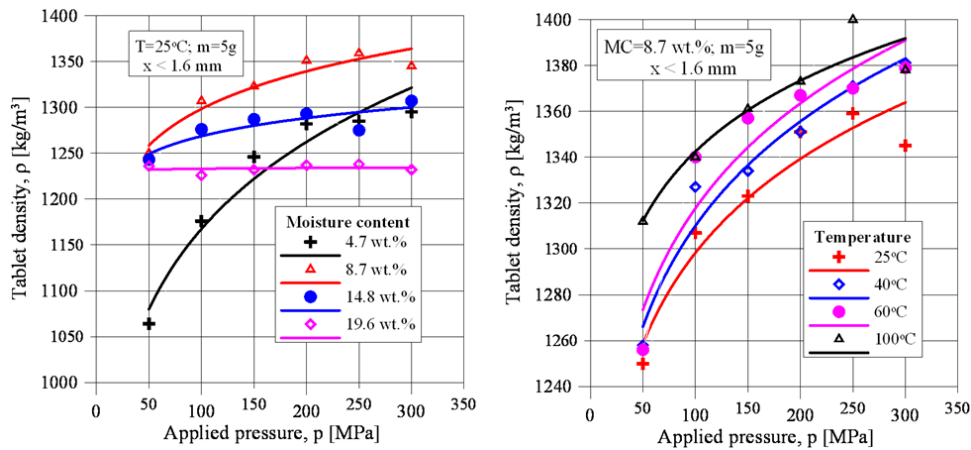


Figure 5

Compressibility data for solar dried sewage sludge with different moisture content (left); obtained at different temperature (right)

Table 1.

Constants of Johanson's equation ($\rho = ap^{1/\kappa}$) for sewage sludge with different moisture contents

Moisture contents [wt.%]	Constant a [$\text{kg}^{1-1/\kappa} \text{m}^{(1/\kappa)-3} \text{s}^{2/\kappa}$]	Constant κ [-]	Spread deviation: V_s Coefficient of determination: R^2 Residual mean square: σ
4.7	694.90	8.87	$R^2 = 0.9539$; $\sigma = 0.000335$; $V_s = 1.6$ %
8.7	1056.04	22.30	$R^2 = 0.9202$; $\sigma = 0.000095$; $V_s = 0.8$ %
14.8	1144.97	44.94	$R^2 = 0.7486$; $\sigma = 0.000091$; $V_s = 0.8$ %
19.6	1227.65	1063.83	$R^2 = 0.8852$; $\sigma = 0.000015$; $V_s = 0.3$ %

Table 2

Constants of Johanson's equation for sewage sludge with different temperatures

Temperatures [°C]	Constant a [$\text{kg}^{1-1/\kappa} \text{m}^{(1/\kappa)-3} \text{s}^{2/\kappa}$]	Constant κ [-]	Spread deviation: V_s Coefficient of determination: R^2 Residual mean square: σ
25	1056.04	22.30	$R^2 = 0.9202$; $\sigma = 0.000095$; $V_s = 0.8$ %
40	1044.03	20.28	$R^2 = 0.9598$; $\sigma = 0.000055$; $V_s = 0.6$ %
60	1050.40	20.31	$R^2 = 0.8865$; $\sigma = 0.000170$; $V_s = 1.1$ %
100	1153.93	30.43	$R^2 = 0.9067$; $\sigma = 0.000060$; $V_s = 0.7$ %

Tablets compressed at lower pressure have a lower density. In the case of different moisture contents and the same temperature of 25°C, tablets made from raw material (MC = 8.7 wt.%) have the highest density values, tablets made from raw material (MC = 19.6 wt.%) have a constant density with increasing pressure and lower density than those made from raw material (MC = 14.8 wt.%). For instance, at 200 MPa and T = 25°C, the tablet densities were 1282 kg/m³ (MC = 4.7 wt.%), 1351 kg/m³ (MC = 8.7 wt.%), 1293 kg/m³ (MC = 14.8 wt.%), 1237 kg/m³ (MC = 19.6 wt.%). In the case of different temperature, an increased temperature resulted in a higher tablet density. For instance, at 150 MPa and MC = 8.7 wt.%, the tablet densities were 1323 kg/m³ (25°C), 1334 kg/m³ (40°C), 1357 kg/m³ (60°C), 1361 kg/m³ (100°C).

Spread deviation values (V_s) of fitted Johanson’s equations are calculated in *Table 1* and *Table 2*, with all values smaller than 1.6% (different moisture contents) and 1.1% (different temperature) respectively. At the same moisture content the increasing of temperature results in not higher constants a and κ . A linear equation can’t be found that described the temperature dependence of values a and κ . Therefore, it can not be described by modified Johanson’s equation containing temperature as a parameter.

3.2. Spring-back ratio

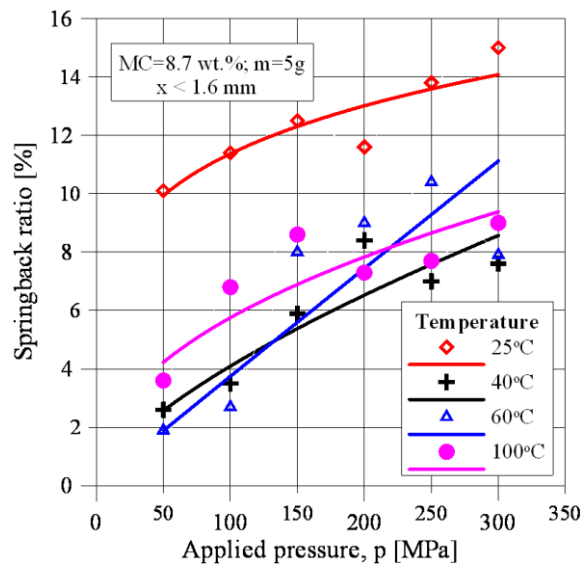


Figure 6
 Relationship between spring-back ratio and pressure for different temperatures of solar dried sewage sludge

Figure 6 shows the relationship between applied pressure and SBR in the case of different temperatures of raw material (25, 40, 60 and 100 °C). This relationship can be described by the following function: $SBR=bp^c$, the constants c and b are corresponding to each temperature. SBR

of tablet increases with the increased pressure, tablets made from the raw material with lower temperature have higher SBR (at the same pressure, moisture content and particle size). In the case of 25 °C temperature, the range of SBR from 10 to 15 % was measured. Tablets had only 1.9 to 10.4% SBR depending on pressure at temperature from 40 to 100 °C.

3.3. Structure of tablets

The surfaces of tablets are shown in *Figure 7*. The tablets made at 25 °C have more space between particles (porosity is higher) than the tablet made at 100 °C, with the same moisture content of 8.7 wt.% and pressure of 100 MPa. The tablets made at MC= 19.6 wt.% have more space between particles than those made at MC = 8.7 wt.% at the same temperature of 25 °C and pressure of 200 MPa. In the case of the same moisture content of 8.7 wt.% and temperature of 25 °C, tablets made at 100 MPa have more space than those made at 200 MPa. The reasons for that are that generally, with increasing external forces acting upon the particulate matter during size enlargement, porosity and characteristics related to this parameter decrease, while density and strength increase (PIETSCH 1991).

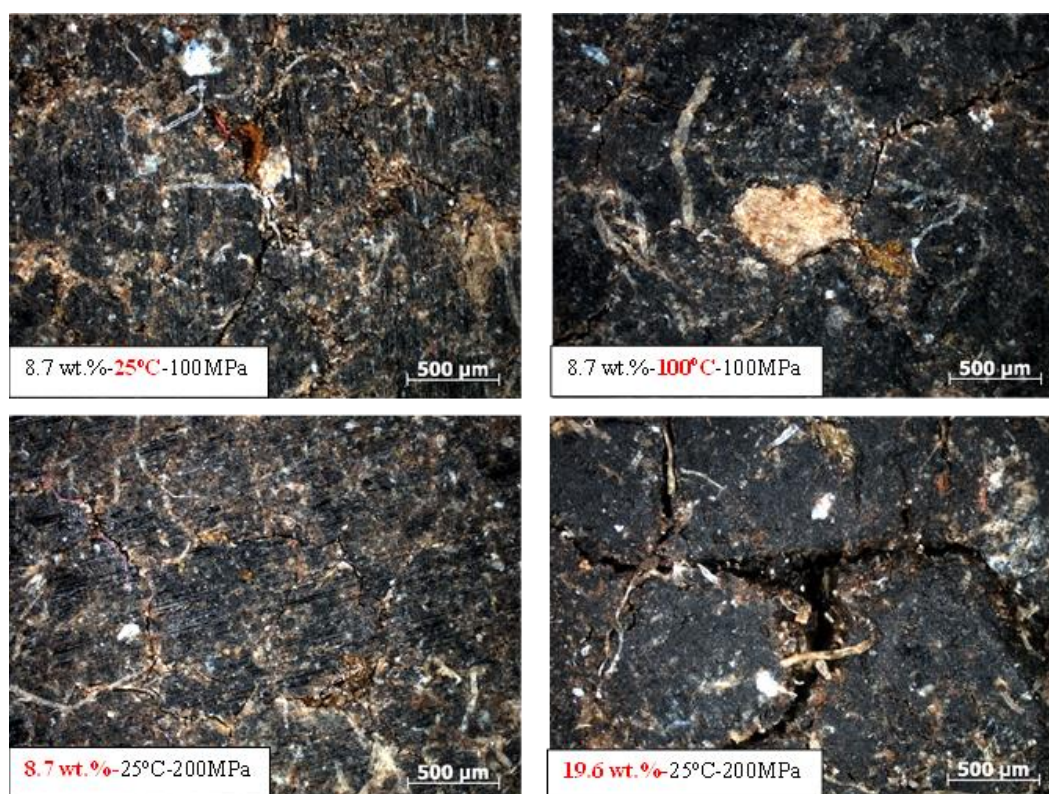


Figure 7

Surface of tablets made from solar dried sewage sludge
(optical microscope: Zeiss AXIO Imager.M2m)

3.4. Tablet strength

Falling number values in the case of different temperatures with the same particle size < 1.6 mm are shown in *Figure 8*. Increasing temperature resulted in higher tablet strength at the same pressure and particle size. For instance, at the same pressure of 200 MPa and moisture content of 8.7 wt.%, falling number 5.3 (25 °C), 18.6 (40 °C), 28 (60 °C), 50.3 (100 °C).

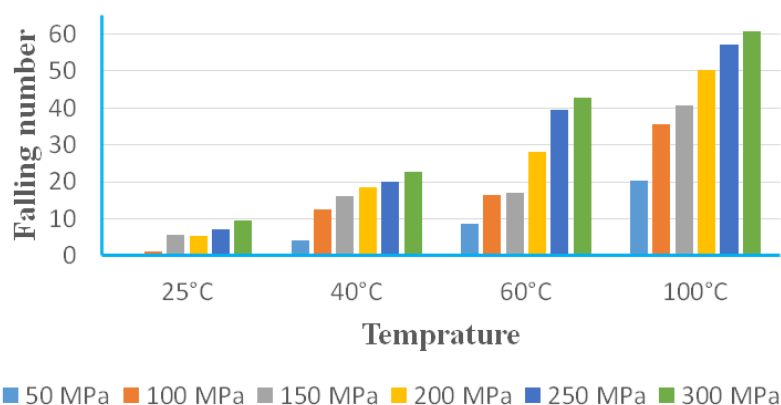


Figure 8
Falling number values in the case of tables made from solar dried sewage sludge with different temperature and pressure

4. CONCLUSIONS

This paper has presented tools and methods to evaluate the effect of temperature, moisture content and pressure with the same particle size < 1.6 mm on tablet density in the case of solar dried sewage sludge. The description of the processes is essential to be able to determine the optimal production parameters (moisture content of 8.7 wt.%, temperature of 100 °C).

While the applied Johanson functions describe the processes well (at 4.7 wt.%, in the case of the same temperature of 25 °C, $V_s = 3.0\%$). In the case of 60°C temperature and same moisture content of 8.7 wt.%, $V_s = 2.2\%$). Experiments found that if pressure and moisture content are kept constant, increasing temperature results in higher density of tablets. If pressure and temperature are kept constant, tablet density has maximum value at 8.7 wt.%, in the examined range; and increasing moisture content results in lower density of tablets. Increasing temperature resulted in higher tablet strength at the same pressure and particle size.

The experimental method can be used for other materials as well to find the optimal conditions of temperature, moisture content and pressure during agglomeration. The determination of compression time and tablet drying time are to be studied in further work.

ACKNOWLEDGEMENTS

The experimental work was carried out as a part of “Development of bio raw materials products range with special regard to the local technology – research on the possibility of utilisation by technological” optimisation GINOP-2.2.1-15-2017-00069 R&D Project. The described article was carried out as part of the “Sustainable Raw Material Management Thematic Network – RING 2017”, EFOP-3.6.2-16-2017-00010 project in the framework of the Széchenyi2020 program. The realization of these projects is supported by the European Union, co-financed by the European Social Fund.

REFERENCES

- [1] CSÖKE, B. et al. (2000): Experimental investigation of compacting in roll press with gravity and screw feed. In: LAKATOS, I. (ed.): *Progress in Mining and Oilfield Chemistry. Novelities in Enhanced Oil and Gas Recovery*. Budapest, Akadémiai Kiadó, pp. 241–254.
- [2] CSÖKE, B. et al. (2003): Experimental study of the compacting phenomena in roll presses using screw feed. In: LAKATOS, I. (ed.): *Progress in Mining and Oilfield Chemistry. Advances in Incremental Petroleum Production*. Budapest, Akadémiai Kiadó, pp. 413–424. (Progress in Mining and Oilfield Chemistry, 5)
- [3] DEAN, B. R. et al. (1985): The risk to health of chemicals in sewage sludge applied to land. *Waste management & research*, 3. pp. 251–278.
- [4] HUANG, Q. et al. (2016): Effect of moisture on sewage sludge combustion temperature profile and heavy metal leaching. *Drying Technology an International Journal*.
- [5] JOHANSON, J.R. (1965): A rolling theory for granular solids. *American Society of Mechanical Engineers*, 32. pp. 842–848.
- [6] LIU, Y. et al. (2016): Modifications to Johanson’s roll compaction model for improved relative density predictions. *Powder Technology*, 297. pp. 294–302.
- [7] MATTHEWS, P. J. et al. (1984): Methods for the application and incorporation of sludge. In *Processing and Use of Sewage Sludge* (P. L’Hermite & H. Ott, Eds), pp. 244–258. D. Reidel, Dordrecht, Holland.
- [8] NAKASAKI, K. et al. (1985): Effect of Temperature on Composting of Sewage Sludge. *Applied and Environmental Microbiology*, Vol 50, No 6, pp. 1526–1530.
- [9] NIELSEN, N.P.K. et al. (2009): Importance of temperature, moisture content, and species for the conversion process of wood residues into fuel pellets. *Wood Fiber Sci*, 41 (4), pp. 414–425.
- [10] PIETSCH, W. (1991): Size Enlargement by Agglomeration. *John Wiley & Sons Ltd*, p. 115.
- [11] STELTE, W. et al. (2011): Fuel pellets from biomass: The importance of the pelletizing pressure and its dependency on the processing conditions. *Fuel*, 90 (11), pp. 3285–3290.
- [12] STIEB, M. (1997): *Mechanische Verfahrenstechnik 2*. Springer Lehrbuch.

- [13] USMAN, K. et al. (2012): Sewage Sludge: An Important Biological Resource for Sustainable Agriculture and Its Environmental Implications. *American Journal of Plant Sciences*, 3, pp. 1708–1720.
- [14] WOLSKI, P. et al. (2011): Impact of Temperature on Viscosity of Sewage Sludge after Conditioning. *Ecological chemistry and engineering*, Vol 18, No 12.

COMPRESSION TIME AND TEMPERATURE EFFECTS ON PUR AGGLOMERATION

SÁNDOR NAGY¹–QUYEN V. TRINH²–GÁBOR DÓRA³

¹University of Miskolc, H-3515, Miskolc Egyetemváros, ejtnagys@uni-miskolc.hu

²University of Miskolc, H-3515, Miskolc Egyetemváros, trinhquyennd@gmail.com

³Gazdaságfejlesztő és Tanácsadó Kft, 7400 Kaposvár, Füredi utca 1

Abstract

Improve living conditions worldwide has focused on environmental issues in all areas of activity. During processing of end of life refrigerators, fine polyurethane (PUR) bulk material is arising as by product. Agglomerated form of PUR material can be prosperous in several solutions, especially in thermal utilization. The introduced research work is focusing on the determination of optimal agglomeration conditions of PUR originated from Elektronikai Hulladékhasznosító Ltd, Hungary. This paper demonstrates the effects of applied pressure, temperature and compression time on PUR agglomerates and also identifies the optimal conditions of the process for producing tablets with high density. The PUR with a moisture content of 1.8 wt.% was compressed in a load cell by a hydraulic piston press with 25 mm diameter, applied pressure range were 50 to 300 MPa. Results showed that the optimal conditions during agglomeration process are 60°C temperature and a compression time of 5 seconds. A new compression equation can be introduced, which contains temperature as a parameter.

Keywords: *Agglomeration, PUR, Polyurethane, compression time, compressibility, recycling.*

1. INTRODUCTION

The necessity to care for the natural environment and to improve the quality of human life has been enforcing relevant steps to be undertaken in terms waste management. In principle, the problem involves the recovery of raw materials through the application of recycling processes (THORARK 2002; BLENGINI 2009; LUIZ et al. 2013). Agglomeration of recycling materials such as briquetting, extrusion, tableting, pelletizing can increase bulk density, improves storability, reduces transportation costs, makes easy the handling and increase the quality of products.

During the process of wrecking the refrigerators in a closed system the PUR insulation material is grounded and washed so as to release it from the harmful gas (freon, pentane) and other contaminants. Fragmentation reduces the volume of the material therefore the storage and transportation of it would be more economical. It can be divided into further components by chemical wrecking, adsorption and recycling into production. For example in Elektronikai Hulladékhasznosító Ltd, every year there will be 6,500 to 7,000 tonnes refrigerators of scrap and about 1,000 to 1,200 tonnes of PUR powder was produced each year. Incineration is one way through the burning waste polyurethane materials for heat recovery. 1 kg polyurethane burning can produce calorific value of about 29,307 kJ/kg, which can provide heat equivalent to the same

weight of coal provides energy (LIU et al. 2010). Through burning, it can make the wastes volume reduced by 99 %. Polyurethane foam wastes can shattered into grain, as fuel alternative coal, oil and natural gas recovery energy, and applied to cement or power (WENQING et al. 2012).

The parameters of recycling materials agglomerate production are especially important in aspects related to product quality and economics. On the one hand, the reduction of moisture content and increasing temperature usually results in better quality agglomerates; it is possible to achieve higher density and strength. On the other hand, moisture content reduction (drying) and increasing temperature have a large energy demand. To find the optimal production parameters, the exact relation between moisture content, temperature and briquetability (applied pressure agglomerate density) should be known. Furthermore, it was reported that an increase in temperature reduces the friction in the press channel of the mill (STELTE et al 2011b) and lowers the energy required for different components of the pelletizing process (NIELSEN et al 2009a). Other process parameters might influence the result of agglomeration too. CSŐKE et al. (2000) and (2003) investigated the effect of different feed methods (screw feed and gravity feed) on compacting. Another serious issue is the de-airing, because if the outflow of the displaced air from the agglomerated particles is too intense, that might break down the newly formed briquettes (TARJÁN et al. 1999).

Different approaches have been taken in order to calculate the connection between applied pressure and agglomerate density. The Johanson equation (1965) can take two forms:

$$\frac{\rho}{\rho^*} = \left(\frac{p}{P^*}\right)^{1/\kappa} ; \frac{F}{F_0} = \left(\frac{V_0}{V}\right)^\kappa$$

where κ is compressibility factor, ρ is agglomerate density, p is tableting pressure, F is tableting force, V is tablet volume, and p^* , ρ^* , F_0 , V_0 are reference values (if surface perpendicular to force and mass of tablet are constant) (STIEB 1997).

The mechanical strength of agglomerates is one of the main features determining their further applicability or processing. There are many methods of defining and measuring the strength. Depending on needs, impact, wear, compression, bend and tensile tests are used (SCHUBERT 1975; KRISTENSEN et al 1985; GLUBA and ANTKOWIAK 1988). This study investigates the effects of temperature and compression time on the density and strength of PUR tablets with the same particle size < 1.25 mm and moisture content of 1.8 wt.%.

Temperature dependence, novelty: There are studies regarding the compaction equation between density and applied pressure, no equation was found in the literature that includes the temperature as a parameter of PUR materials. The objective of the current work is also to supplement the original Johanson equation with the parameter temperature. The spring-back ratio (SBR) was also investigated because it has an effect on the density of tablets.

2. MATERIAL AND METHODS

2.1. Materials

Polyurethane rigid foam is the insulating material which is most widely used throughout the world for refrigerators and freezers. Therefore, polyurethane (PUR) was being selected as the raw material for our experiments. It is originated from Electronic Waste Management Ltd. with

original particle size $x < 2.5$ mm. The sieve was used to remove particle size from 1.25 to 2.5 mm. The moisture content of PUR ($x < 1.25$ mm) was determined as 1.8 wt.% and bulk density of 270 kg/m^3 . Raw material PUR can be seen in *Figure 1*. It can be observed that PUR is an inhomogeneous material.

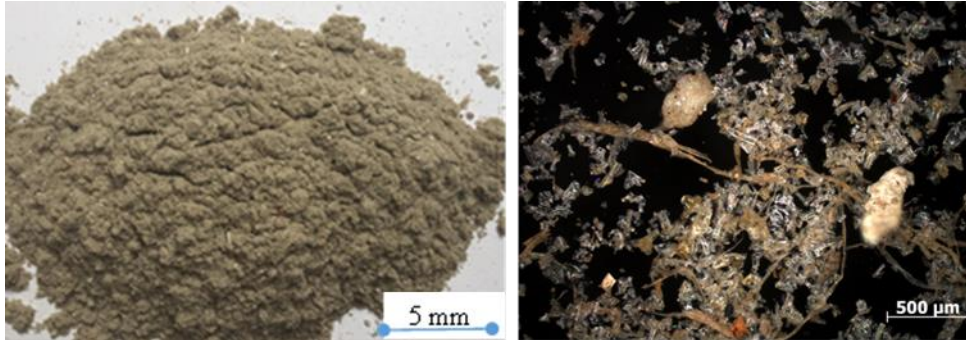


Figure 1
PUR with $x < 1.25$ mm; (left) optical camera;
(right) optical microscope: Zeiss AXIO Imager.M2m

Figure 2 shows the particle size distribution of PUR. The x_{95} , x_{80} and x_{50} values are 860 μm , 530 μm and 280 μm respectively.

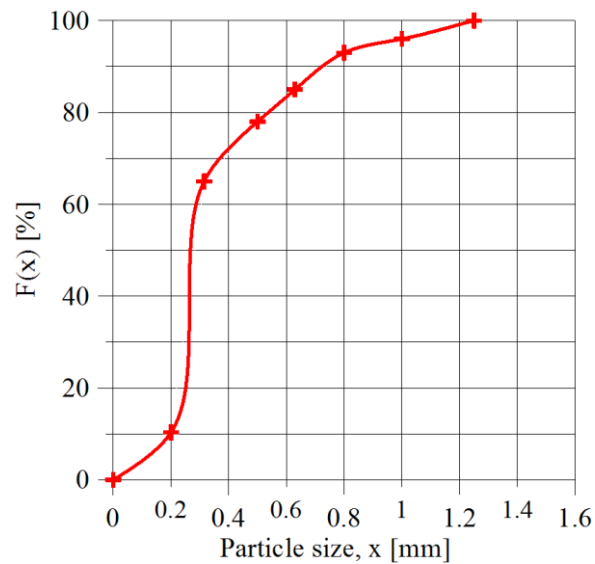


Figure 2
Particle size distribution of PUR

2.2. Hydraulic piston press

The hydraulic piston press (*Figure 3*) was designed by the University of Miskolc. The press is supported by a pump motor unit with a pressure limiter and a heat-able load cell (20–140°C). The maximum force is 200 kN, and the maximum velocity of the piston is 30 mm/s. The measuring of the piston position is done with an incremental encoder.



Figure 3
Hydraulic piston press

2.3. Experimental procedure

The hydraulic piston press with diameter 25 mm was used for two different kinds of tests and each tablet was made by the compression of 5 g PUR. Applied pressures on the surface of tablets were 50, 100, 150, 200, 250 and 300 MPa, moisture content of 1.8 wt.% and particle size < 1.25 mm.

In the first test, the applied temperatures were 20, 40, 60 and 100°C with compression time of 5 seconds.

In the second test, spring-back ratio experiments were carried out with compression time were 2, 5 and 10 seconds with the same temperature of 60°C.

The springback ratio (SBR) of a tablet can be determined by:

$$SBR = \frac{H_t - H_{tp}}{H_{tp}} \cdot 100 \%$$

where H_t is the height of the produced tablet, H_{tp} is minimum height of the tablet under pressure.

The quality of tablets can be described easily by their density. The diameters and heights of the tablets product were measured by Vernier caliper (a tablet can be extended after agglomeration).

The mass was measured and density was calculated for each test. The minimum height of tablets under pressure was measured by the incremental distance measurement method.

The determination of tablet strength was carried out by the well-known falling test method. Tablets were released by freefall from a height of 2 m onto a concrete floor repeatedly until they broke. The falling number is the number of falls the sample survived undamaged. In each experiment three tablets were tested.

Raw material particles and cross sectional surfaces of tablets were investigated with an optical microscope Zeiss AXIO Imager.M2m.

3. RESULTS AND DISCUSSION

Compression time, tablet density, spring-back ratio, tablet strength, and the structure of tablets were determined in our investigations.

3.1. Tablet density and compressibility

Tablets produced by processes with different compression times and the same production conditions are shown in *Figure 4*. The tablet density values are recorded as an average of three measurements in the case of different temperatures (at the same compression time of 5 seconds), and also with different compression times (at the same temperature of 60°C).

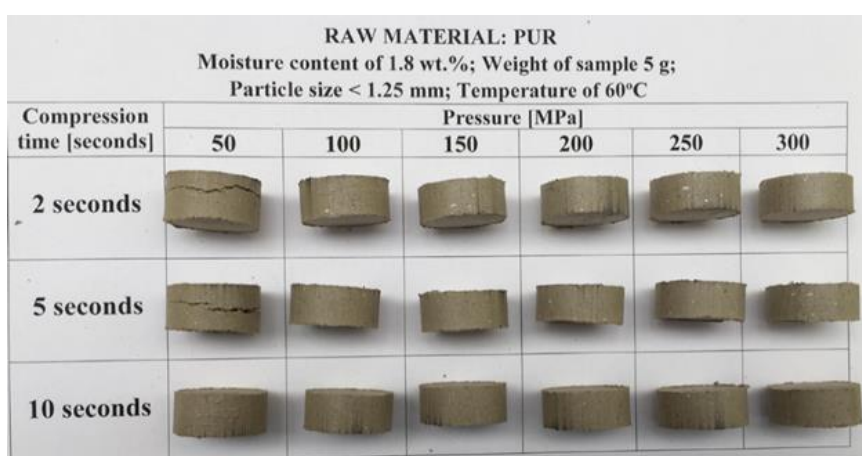


Figure 4

Tablets made from PUR with different compression time and the same production conditions

Figure 5 shows the pressure density values and the fitted Johanson curves in the case of particle size < 1.25 mm raw material at 20, 40, 60 and 100°C and different compression times. *Table 1* shows the constants of the fitted curves and coefficient of determination (R^2), residual mean square (σ) and calculated deviation (V_s).

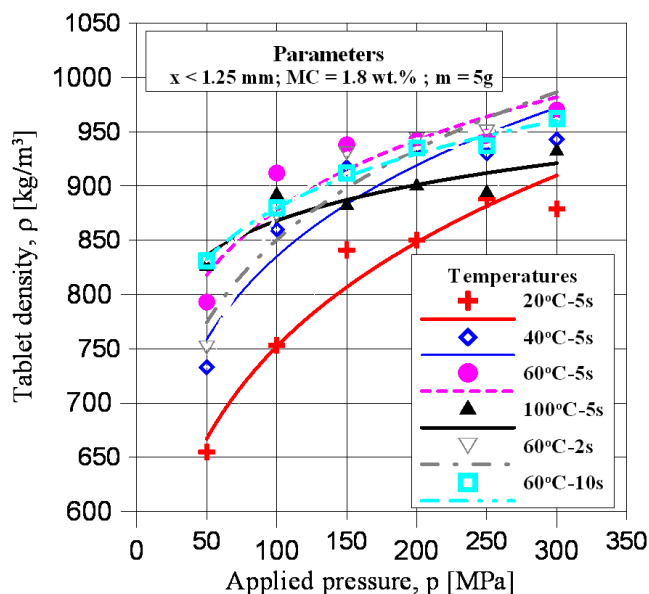


Figure 5
Compressibility data for PUR with different temperatures and compression time

Tablets compressed at lower pressure have a lower density with the same production conditions. In the case of the same compression time of 5 seconds, the tablet density value has a maximum at 60°C temperature (for instance at 250 MPa, tablet densities: 888 kg/m³ (T = 20°C), 930 kg/m³ (T = 40°C), 945 kg/m³ (T = 60°C), 894 kg/m³ (T = 100°C)).

In the case of different compression times, tablet made at 5 seconds compression time have higher density than those made at 2 seconds and 10 seconds compression time with the same production conditions (for example at 150 MPa, tablet densities: 938 kg/m³ (5 seconds), 930 kg/m³ (2 seconds), 912 kg/m³ (10 seconds)). The reason for that could be the temperature dependence of the viscoelastic properties in the solid, initially they increased with increasing temperature up to 60°C and then decrease at the temperature was increased to 100°C.

Table 1
Constants of Johanson’s equation for different temperatures and compression time

Temperature – Compression time	Constant a [$\text{kg}^{1-1/\kappa} \text{m}^{(1/\kappa)-3} \text{s}^{2/\kappa}$]	Constant κ	Spread deviation: V_s Coef of determination: R^2 Residual mean square: σ
20°C-5s	338.6500	5.77	$R^2 = 0.9523$; $\sigma=0.0008$; $V_s = 2.6 \%$
40°C-5s	441.5794	7.23	$R^2 = 0.8928$; $\sigma = 0.0012$; $V_s = 3.1 \%$
60°C-5s	548.9211	9.81	$R^2=0.8645$; $\sigma=0.0008$; $V_s = 2.5 \%$
100°C-5s	676.9574	18.55	$R^2= 0.8134$; $\sigma=0.0003$; $V_s = 1.7 \%$
60°C-2s	456.1195	7.39	$R^2=0.9128$; $\sigma=0.0009$; $V_s = 2.7 \%$
60°C-10s	609.9893	12.57	$R^2=0.9891$; $\sigma=0.00003$; $V_s = 0.5 \%$

To describe the compressibility of PUR, the Johanson equation was used. As the original equation for describing compressibility, it is universal. It is possible to insert other parameters in it, such as temperature. The spread deviation values (V_s) of fitted Johanson's equations are calculated (Table 1) and shown to have a value smaller than 3.1 %. At the same compression time of 5 seconds, the higher temperature results in higher constants a and κ . A linear equation can be found, that describes the temperature dependence of values a , and κ , and so compression can be described by an equation based on the original Johanson's equation and containing temperature as a parameter.

Johanson's equation: $\rho = ap^{1/\kappa} = ap^b$
where

$$a = f(t) = a_1 t + a_2 = 4.2089 \cdot t + 270.0359$$

$$b = f(t) = b_1 t + b_2 = \frac{1}{\kappa} = -0.0014 \cdot t + 0.1986$$

The new equation for particle size < 1.25 mm:

$$\rho = (4.2089 \cdot t + 270.0359) p^{(-0.0014 \cdot t + 0.1986)}$$

where t is temperature [$^{\circ}\text{C}$]

The processes were well described by the applied Johanson functions at each temperature.

The modified Johanson equation, which contains temperature t as a parameter, provides only a small deviation of the density of approximately 0.15 %.

Thus, we conclude that the modified Johanson equation gives accurate results, at 100°C temperature, MC = 1.8 wt.%, $p = 200 \text{ MPa}$, compression time 5 seconds, density of Johanson's equation 900 kg/m^3 ; density of modified Johanson's equation 899 kg/m^3 .

3.2. Spring-back ratio

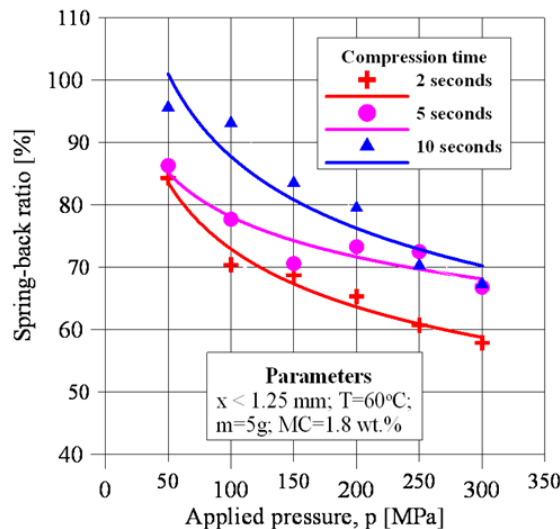


Figure 6

Relationship between pressure, spring-back ratio and compression time

Figure 6 shows the relationship between applied pressure and SBR in the case of different compression time and the same production conditions ($T = 60^{\circ}\text{C}$, $x < 1.25$ mm, MC = 1.8 wt.%, the weight of sample $m = 5$ g). This relationship can be described by the following function: $SBR = c \cdot p^d$. The constants c and d are corresponding to each compression time.

Tablets made at higher pressure had lower SBR at the same production conditions. Tablets made with compression time of 10 seconds resulted in highest SBR, while those made at 2 seconds compression time had lowest SBR (SBR of tablets at 200 MPa: 65.3 % (2 seconds), 73.3 % (5 seconds), 79.5 % (10 seconds)).

3.3. Tablet strength

Falling number values are shown in Figure 7 as a function of temperature at different pressures for both the same compression time and different compression times.

In the case of the same compression time of 5 seconds, increasing temperature resulted in higher tablet strength (except at 100°C), for example falling number at 150MPa: 5.3 ($T = 20^{\circ}\text{C}$), 12.6 ($T = 40^{\circ}\text{C}$), 14.3 ($T = 60^{\circ}\text{C}$), 7.3 ($T = 100^{\circ}\text{C}$).

In the case of different compression times, tablets made at compression time of 5 seconds resulted in higher tablet strength than those made at 2 seconds and 10 seconds compression time, for instance, falling number at 250 MPa: 15.6 (5 seconds), 7.6 (2 seconds), 14.3 (10 seconds). The reason for this may be the viscoelastic properties of PUR are decreases with time, while that compression time at 2 seconds is not enough time for connecting particles.

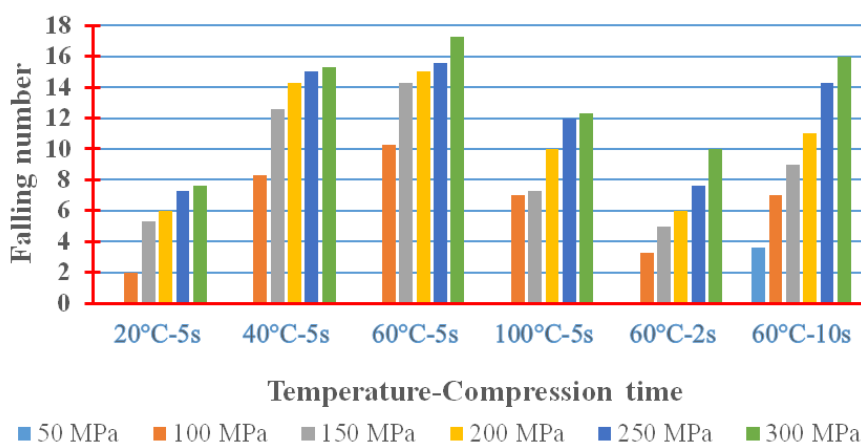


Figure 7

Relationship between falling number, temperature, compression time and pressure

4. CONCLUSIONS

This paper has presented tools and methods to evaluate the effect of temperature and compression time on tablet density in the case of PUR. The description of the processes is essential to be able to determine the optimal production parameters (at 60°C temperature and compression time of 5 seconds).

While the applied Johanson functions describe the processes well (at 60°C, in the case of 5 seconds compression time $V_s = 2.5\%$, when using 2 seconds compression time $V_s = 2.7\%$) the modified Johanson's equation for compression introduced here contains also temperature as a parameter.

Experiments found that if pressure, compression time, moisture content and particle size are kept constant, increasing temperature results in the higher density of tablets and strength (except at 100°C).

An effect of compression time was also identified: tablets made at 5 seconds compression time resulted in higher strength and density of tablets than those made at 2 seconds and 10 seconds when temperature, pressure, particle size and moisture content are kept constant.

The experimental method can be used for other materials as well to find the optimal conditions of pressure, temperature and compression time during agglomeration. Effect of moisture content and particle size on agglomeration of PUR in the further work.

ACKNOWLEDGEMENTS

The described work/article was carried out as part of the “Sustainable Raw Material Management Thematic Network – RING 2017”, EFOP-3.6.2-16-2017-00010 project in the framework of the Széchenyi 2020 program. The realization of this project is supported by the European Union, co-financed by the European Social Fund. Electronic Waste Management Ltd is thanked for supporting with PUR.

REFERENCES

- [1] BLENGINI, G. (2009): Life cycle of buildings, demolition and recycling potential: a case study in Turin Italy. *Build. Environ.* 44. p. 319–330.
- [2] CSÖKE, B. et al. (2000): Experimental investigation of compacting in roll press with gravity and screw feed. In: LAKATOS, I. (ed.): *Progress in Mining and Oilfield Chemistry. Novelties in Enhanced Oil and Gas Recovery*. Budapest, Akadémiai Kiadó, pp. 241–254.
- [3] CSÖKE, B. et al. (2003): Experimental study of the compacting phenomena in roll presses using screw feed. In: LAKATOS, I., (ed.): *Progress in Mining and Oilfield Chemistry. Advances in Incremental Petroleum Production (Progress in Mining and Oilfield Chemistry, 5)*. Budapest, Akadémiai Kiadó, pp. 413–424.
- [4] GLUBA, T. et al. (1988): Effect of wetting on granule abrasion resistance. *Aufbereitungs Technik*, 2. pp. 76–80.
- [5] JOHANSON, R. (1965): A rolling theory for granular solids. *American Society of Mechanical Engineers*, 32. pp. 842–848.
- [6] KRISTENSEN, G. et al. (1985): Mechanical Properties of Moist Agglomerates in Relation to Granulation Mechanisms. *Powder Technology*, 44. pp. 227–237.
- [7] LIU, J.P. et al. (2010): The reuse of polyurethane wastes. *New Chemical Materials*, 38 (12): pp. 21–23.

-
- [8] LUIZ, H. et al. (2013): Recycling concepts and the index of recyclability for building materials. *Resour. Conserv. Recycl.*, 72, pp. 127–135.
 - [9] NIELSEN, N. P. K. et al. (2009a): Importance of temperature, moisture content, and species for the conversion process of wood residues into fuel pellets. *Wood Fiber Sc*, 41 (4), pp. 414–425.
 - [10] SCHUBERT, H. (1975): Tensile strength of agglomerates. *Powder Technology*, 11. p. 107–119.
 - [11] STELTE, W. et al. (2011b): Fuel pellets from biomass: The importance of the pelletizing pressure and its dependency on the processing conditions. *Fuel*, 90 (11). p. 328–3290.
 - [12] STIEB, M. (1997): *Mechanische Verfahrenstechnik 2*. Springer Lehrbuch.
 - [13] TARJÁN, I. et al. (1999): Investigation of airing out at compacting fine granular material. In: LAKATOS, I., (ed.): *Progress in Mining and Oilfield Chemistry. Challenges of an Interdisciplinary Science*. Budapest, Akadémiai Kiadó, pp. 275–284.
 - [14] THORMARK, C. (2002): A low energy building in a life cycle-its embodied energy, energy need for operation and recycling potential. *Build. Environ*, 37. p. 429–435.
 - [15] WENQING, Y. et al. (2012): Recycling and disposal methods for polyurethane foam wastes. *Procedia Environmental Sciences*, 16. p. 167–175.

COMPARISON OF BAUXITE AND RED MUD LEACHABILITY

JÁNOS LAKATOS

Assoc. Prof., University of Miskolc, Institute of Chemistry,
Miskolc-Egyetemváros, Hungary, mtasotak@uni-miskolc.hu

Abstract

The transformation of the mobility of the elements which are present in different mineral forms in the red mud compared to the bauxite were tested by the sequential extraction technique, using salt solutions, weak and strong acids, complexing agents, reductive and oxidative media. Beside the Al extraction during the Bayer process a considerable mineral transformations will happen which modify considerable the remaining elements mobility compared to the bauxite.

Due to this transformations a part of the elements which are present in the red mud (e.g. Fe, Mn) will get a less soluble, less mobilisable forms, while others (e.g. Al, Cr. etc) mobility will increase. As a result of this mineral transformations the difference of the solubility of iron and aluminium in the red mud became larger in low acidic medium, which offers an efficient way for recovery for the aluminium content of the red mud without considerable iron dissolution. Unfortunately the trial of this low acidic media for selective removal of rare earth elements from red mud was not successful. It can probably be due to that the rare earth elements bearing minerals have not go through such kind of transformation which could help their selective dissolution.

Keywords: *bauxite, red mud, mobility of elements, recovery of rare earth elements*

1. INTRODUCTION

The recovery of valuable elements from the red mud has improving interest worldwide. In Hungary approx. 50×10^6 t red mud are in deposited form near Ajka, Almasfüzitő and Mosonmagyaróvár. This contains lot of valuable elements: approx. $8 - 10 \times 10^6$ t Al, $15 - 18 \times 10^6$ t Fe, 1×10^6 t Ti, 5×10^4 t V, 100 – 150 t Ga and 50 t rare earth elements (most valuable among them are Ce, La, Nd, Gd, (SZEPVÖLGYI, J. 2010). Many of papers of us made attempts to characterize the red mud looking for the best solution for recovery of the above nominated components (BARANYAI, V. ZS. and LAKATOS, J. (2009); LENGYEL, A. and LAKATOS, J. 2011). At the present state of the researches are focused to the extraction of the rare earth. The difficulty is that no clear picture has formed about which way and where the rare earth remained back in the red mud. Efficient separation can be done if someone can highlight of this problem.

2. SAMPLES AND EXTRACTION MEDIA

Hungarian bauxite and red mud samples were tested. The total Al and Fe content of the samples was measured in the solutions achieved by lithium-metaborate-digestion. This data was considered as a reference in comparison of the data have got at the leaching tests. *Table 1* shows the

humidity, Al and Fe content of the bauxite and red mud samples determined after complete dissolution.

Table 1

Moisture, Al and Fe content of the tested samples. Litium-metaborate-digestion was used, m/m%.

Samples	Moisture m/m%	c(Al) m/m%	c(Fe) m/m%
MOTIM bauxite, dry	0	28.8	9.6
MOTIM red mud, dry	0	8.8	23
MAL bauxite, dried at 105 °C	0	27.3	10.8
MAL red mud, dried at 105 °C	0	11.4	19.4
MAL red mud, filtered, dried at 105 °C	0	11.4	19.4
MAL bauxite, wet	19.32	27.3	10.8
MAL red mud, filtered, wet	57.62	11.4	19.4

The leaching test for rare earth elements were carried out a different wet samples, which sources were Ajka (sampling was at the last washing unit) and Almásfüzitő (sampling were taken from the VI, VII. storage palace). Humidity of these slurries are given in *Table 2*. Since this case the detection limits of the rare earth elements determination require higher sample amounts, for the dissolution a combination of HCl and HF was used. Finally boric- acid was add to the mixture for elimination of excess of HF and liberate the Ca from the CaF₂ precipitate.

The total concentration of the rare earth elements of these red mud samples are given in *Table 3–4*.

Table 2

Humidity content of the tested red muds originated from Ajaka and Almasfuzito.

Sample	m(slurry), g	m(water), g	m (humidity.) m/m%
Ajka last washing unit 300g/l slurry (2007 07 06)	34,8582	12,9384	37,1
Almásfüzitő VI (2017 04 20)	33,0348	12,7948	38,7
Almásfüzitő VII (2017 04 21)	57,005	21,6801	38,0

Table 3
Rare earth elements concentrations in the solutions have got from tested red muds, c mg/l

Sample	m (slurry), g	V, ml	Dilutions x	Humidity%	Ce 407,5	Dy 353,1	Er 349,9	Eu 397,1	Gd 335,0	Ho 389,9	Lu 261,5	Nd 401,2	Pr 410,0	Sm 356,8	Tb 370,2	Tm 336,2	Yb 222,4
Ajaka	1,5448	50	2	37,1	4,42	0,2	0,21	0,05	1,09	0,18	0,03	7,88	0,77	0,27	0,1	0,78	1,44
Alamsfuzito VI.	1,2511	50	2	38,7	3,39	0,18	0,16	0,05	0,85	0,15	0,013	5,69	0,61	0,24	0,064	0,54	1,12
Almasfuzito VII	1,5923	50	2	38,03	5,002	0,36	0,34	0,1	1,46	0,27	0,05	9,63	0,96	0,45	0,15	0,95	1,63
Almasfuzito VI (only HCl diss)	1,05	50	1	38,7	2,89	0	0,13	0,04	0,75	0,12	0,003	5,01	0,52	0,18	0,05	0,48	0,97

Table 4
Rare Earth elements concentrations in the tested red muds (mg/g dry base)

Sample	c, mg/g(dry)												
	Ce 407,5	Dy 353,1	Er 349,9	Eu 397,1	Gd 335,0	Ho 389,9	Lu 261,5	Nd 401,2	Pr 410,0	Sm 356,8	Tb 370,2	Tm 336,2	Yb 222,4
Ajaka	0,455	0,0206	0,0216	0,0051	0,1122	0,0185	0,0031	0,8110	0,0792	0,0278	0,0103	0,0803	0,1482
Alamsfuzito VI.	0,442	0,023	0,021	0,007	0,111	0,020	0,002	0,742	0,080	0,031	0,008	0,070	0,146
Almasfuzito VII	0,507	0,036	0,034	0,010	0,148	0,027	0,005	0,976	0,097	0,046	0,015	0,096	0,165
Almasfuzito VI (only HCl diss)	0,2245	0,0000	0,0101	0,0031	0,0583	0,0093	0,0002	0,3892	0,0404	0,0140	0,0039	0,0373	0,0754

3. RESULTS AND DISCUSSION

The sequential extraction is a well applicable tool for determination of the forms of elements in different solids and often used for determination of the manner of the environmental hazard (TESSIER, A. et al. 1979; URE, A. M. et al. 1993; POLYÁK, K. et al. 1995). The technique can be used also in planning of hydrometallurgical process for determine the proper leaching agent. The solutions used for mobilisation of elements in case of bauxites and red mud are given in the Table 5.

Table 5
Composition of solution used for leaching tests and the mobilised form of the elements.

Extraction step	Type of solution	Forms of the mobilised component
1	Distilled water (H ₂ O)	Water soluble
2	1 mol/l magnesium-chloride (MgCl ₂)	1. step + ion-exchangable
3	1 mol/l acetic-acid (HAc)	2. step + carbonate /composed by carbonates
4	0,1mol/l hydroxil-amin-hydrochloride + 1mol/l acetic-acid (NH ₂ OH-1M HAc)	3. step + reducible
5	20 m/m% hydrogen peroxide + 1 mol/l nitric acid (H ₂ O ₂ -HNO ₃)	4. step + oxidizable
6	3 vol. cc.HCl + 1vol. cc HNO ₃ (aqua regia)	All form, except silicate
7	HF-HClO ₄ -digestion (HF)	5. step + composed by silicates

The results of the dissolution of Al and Fe are given in the *Figure 1–2*. This figures indicate the difference of the Al and Fe leachability in bauxite and red mud and the modification of dissolution character of elements are in the bauxite during the Bayer process.

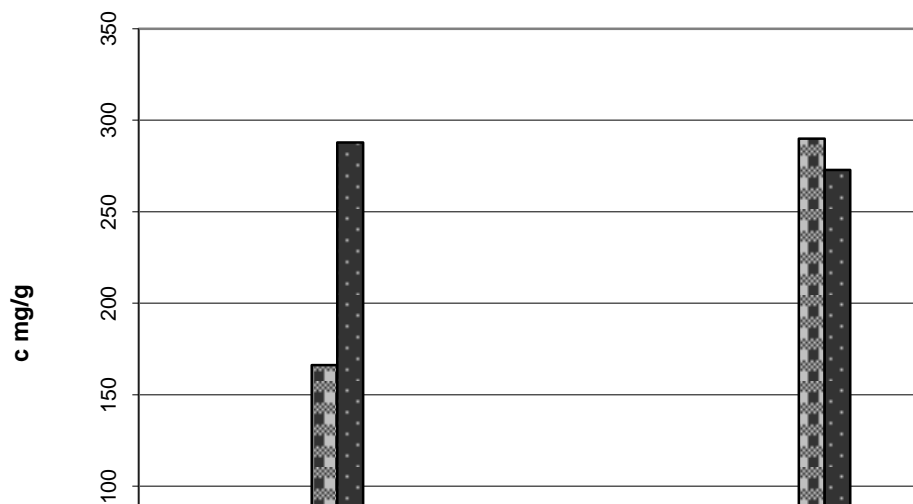


Figure 1

Dissolution of aluminum content of MAL and MOTIM samples (0.4 g solid sample; 20 ml solvent; dissolution time: 8 days)

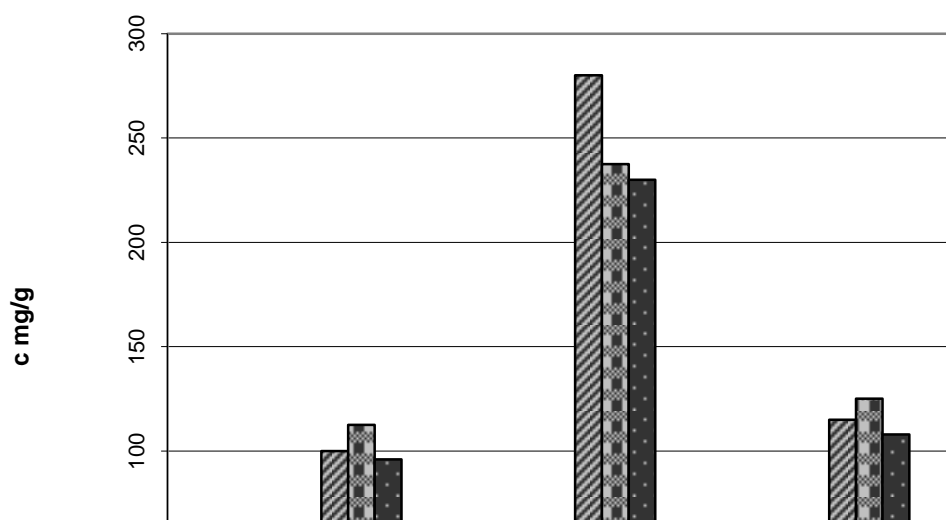


Figure 2

Dissolution of iron content of MAL and MOTIM samples (0.4 g solid sample; 20 ml solvent; dissolution time: 8 days)

Since the low strength of acids e.g. Acetic-acide was found to useful for selective solution of Al from red mud an attempt has been done to check how this system work in case of rare earth element. *Figures 3, 4* shows the dissolution of rare earth elements using acetic acid compared to the strong acids and the total rare earth contents. Unfortunately no significant rare earth elements can be selectively dissolved while the recovery of Al was significant compared to the Fe dissolution. Selective dissolution can be achieved with diluted sulfuric acid since the Ca concentration will remains low due to the gypsum formation.

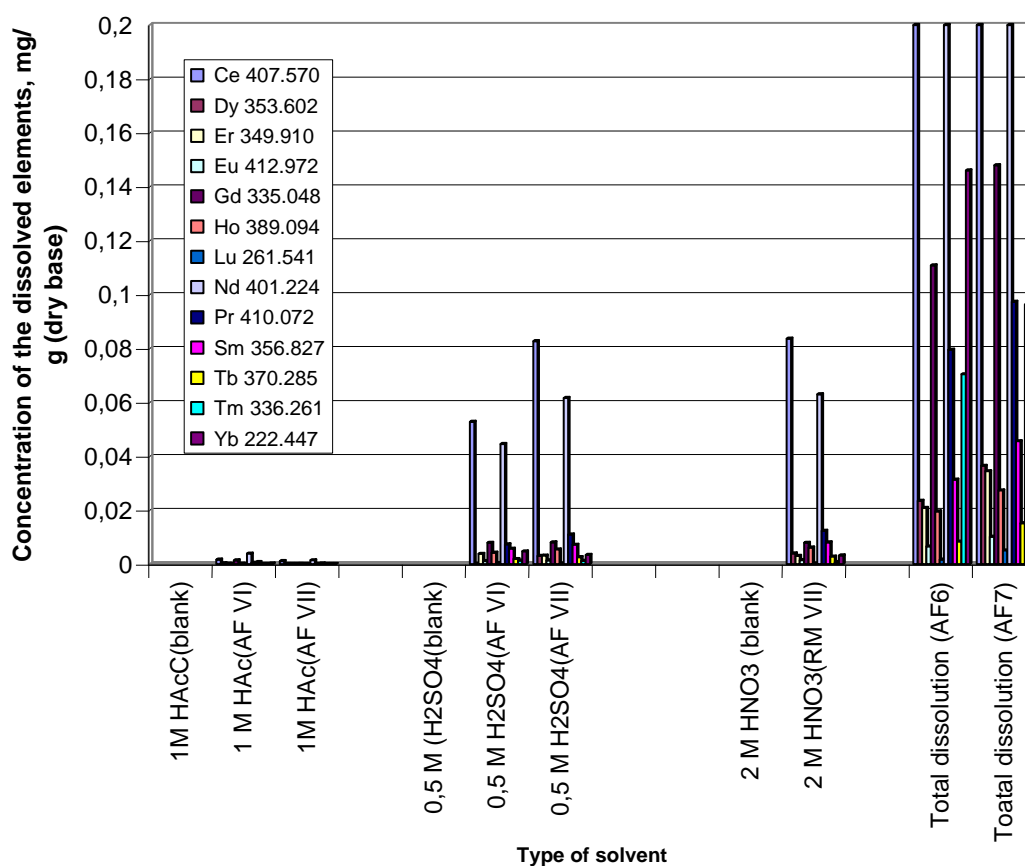


Fig. 3

Comparison of mobilisation of rare earth elements from red muds *Almásfüzitő* (AF) by weak and strong acids. (10 g wet red mud + 40 ml solvent, contact time 5 days).

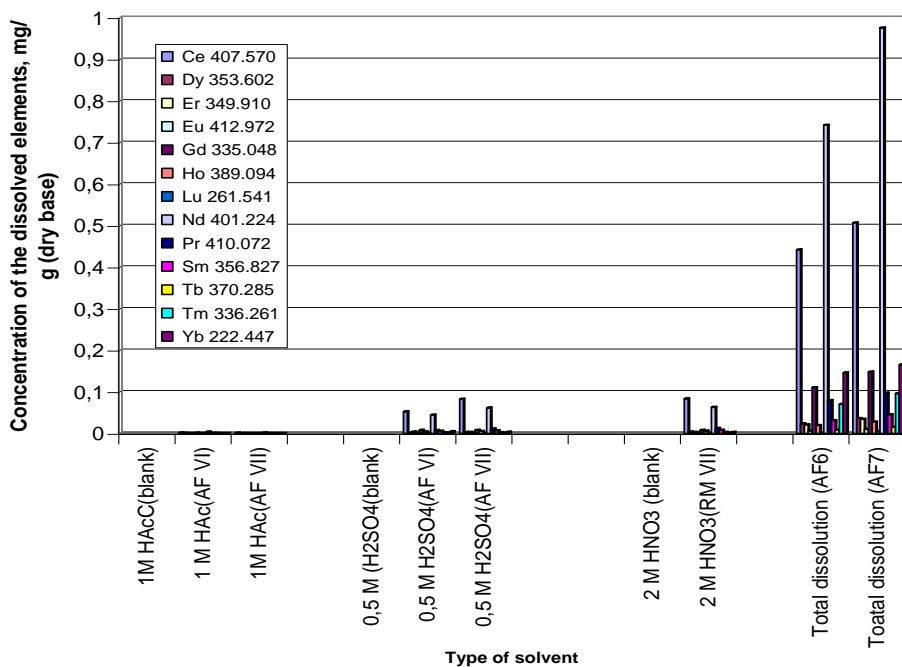


Figure 4

Comparison of mobilisation of rare earth elements from red muds *Almásfüzitő* (AF) by weak and strong acids. (10 g wet red mud + 40 ml solvent, contact time 5 days).

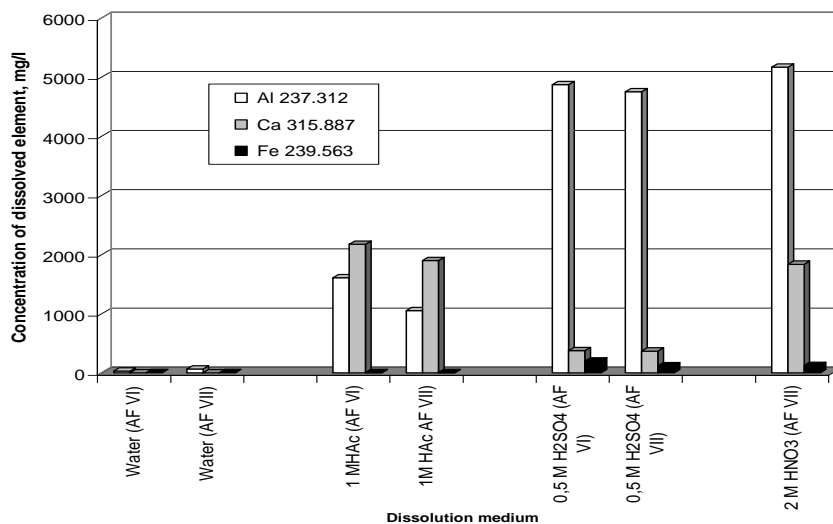


Figure 5

Comparison of mobilisation Al, Ca, and Fe from red muds *Almásfüzitő* (AF) by weak and strong acids. (10 g wet red mud + 40 ml solvent, contact time 5 days)

4. CONCLUSIONS

The main aim of these leaching tests was to determine the effect of the Bayer process for the mobility of the elements are in the bauxite and red mud.

It was proved that beside the Al extraction during the Bayer process a considerable mineral transformations will happen which modify considerable the remaining elements mobility.

Due to this mineral transformations a part of the elements are present in the red mud (Fe, Mn) will get a less soluble, less mobilisable forms compared to the bauxite, while others (Al, Cr etc) mobility will increase. As a results of the mineral transformations the difference of the solubility of iron and aluminium in the red mud became large in low acidic medium, which offers an efficient way for recovery for the aluminium content of the red mud without considerable iron dissolution. Unfortunately the trial of this low acidic media for selective removal of rare earth elements from red mud was not successful. It can probable due to that the rare earth elements bearing minerals did not go through such kind of transformation which could help their selective dissolution. The diluted strong acid e.g. H₂SO₄ also can apply for selective recovery of Al since the dissolved Ca will precipitated in gypsum form. Since the acid almost consumed for the Al and Ca no considerable Fe can dissolved. This acid also could not provide good rare earth recovery at the applied partial dissolution.

REFERENCES

- [1] BARANYAI, V. Zs.–LAKATOS, J. (2009): Reparability of aluminium and iron content of red mud via selective extraction. *Material Sci and Eng. Univ of Miskolc*, Proceedings 34, pp. 21–30.
- [2] LENGYEL, A.–LAKATOS, J. (2011): A vörösiszap hasznosításának lehetőségei. Possibilities of utilisation of red mud, *Anyagmérnöki Tudományok*, Miskolc, 36/1. kötet, pp. 35–48.
- [3] SZÉPVÖLGYI J. (2010): https://24.hu/belfold/2010/10/18/milliardok_hevernek_vorosiszap_tarozokban/
- [4] POLYÁK, K.–BÓDOG, I.–HLAVAY, J. (1995): Fémionok fizikai-kémiai formájának meghatározása szilárd anyagokban. I–II. *Magyar kémiai folyóirat*, 1 01, 17–23, pp. 24–30.
- [5] TESSIER, A.–P. G. C. CAMPBELL–M. BISSON (1979): Sequential Extraction Procedure for the Speciation of Particle Trace Metals. *Analytical Chemistry*, 51, pp. 844–851.
- [6] URE, A. M.–P. H. QUEVAUVILLER–H. MUNTAU–B. GRIEPNIK (1993): Speciation of Heavy Metals in Soils and Sediments. *Inter J Environ. Anal.* 51, pp. 135–151.



CHANGES AND LEADING TRENDS IN CONTAMINATED SITE REMEDIATION

TAMÁS MADARÁSZ¹

¹University of Miskolc, H-3515 Miskolc-Egyetemváros, hgmt@uni-miskolc.hu

Abstract

Contaminated site remediation has gone through remarkable changes since the late 1980's when environmental legacy sites has been catalogued and prioritized first in North-America and then across Europe. The first ground breaking change in the remediation practice was the shift from generic and threshold value-based concept to a new risk based, site specific approach. The paradigm change demanded a new mindset from all involved stakeholders, including problem holders, remediation specialists and especially from authorities. The changes in remediation industry did not cease there but were further fostered as contaminated site clean up was replaced by brownfield rehabilitation and later by sustainable site management concept. This change was driven mainly by the change in financing scheme as the tardy state liability financing was replaced by the flexible real-estate market driven investor financing. In the technological context one can observe that passive, more cost-effective remediation techniques replaced conventional active remediation actions. The industry these years experiences a dynamic spreading of bio-, and nanotechnology solutions while the chemical, physical and hydraulic methods more often play secondary role in cleaning processes. The more accurate and high resolution site investigation gained everyday practice to optimise resource use during the technical intervention. These and several other trends continue to shape the remediation business even today. The paper discusses these changes in detail

Keywords: *contaminated site remediation, change in concept, risk based and site specific approach, brownfield rehabilitation, change in financing schemes*



TESTING OF LEACHABILITY OF ELEMENTS OF EAF DUST BY ACIDIC AND ALKALINE MEDIA

JANOS LAKATOS¹–TAMAS TÖRÖK²–LJUDMILLA BOKANYI³

¹Assoc. Prof., University of Miskolc, Institute of Chemistry, Miskolc-Egyetemváros, Hungary, mtasotak@uni-miskolc.hu

²Prof., Institute of Metallurgy, University of Miskolc, fekt@uni-miskolc.hu

³Assoc. Prof., University of Miskolc, Institute of Raw Material Preparation and Environmental Processing, Miskolc-Egyetemváros, Hungary, ejtblj@uni-miskolc.hu

Abstract

EAF dusts sources were used from the different steel plants of Germany (10) and Hungary (2) along with the standard reference materials (EAF dust: No 876-1; and SPF dust (Steel Plant Furnace dust). DK No12-1-05). The chemical environments were distilled water, salty solutions, complexing medium, weak and strong acids or different alkaline media. Complete dissolution of EAF dusts was achieved only in case of alkaline fusion. It was considered as a reference for getting the maximal yield of leaching. It was found that: the distilled water unable to dissolve zinc ($c_{Zn(mob)} < 0,03 \text{ mg g}^{-1}$), however NH_4NO_3 solution is able to dissolve approx. 10% of total zinc content, due to the zinc-amine complex formation. The weak acids and weak acid + complex forming agents are able to dissolve approx. 80% of total Zn. The disadvantage of this method is the moderate iron dissolution. Strong acid solutions (1 M HCl, HNO_3) and aqua-regia can dissolve approx. 90% of the EAF dusts but can dissolve almost all of the Zn and Pb content. The dissolved iron concentration can be kept low using alkaline media but only less than the half of the zinc content can be mobilised. The most effective alkali solution was the ammonium-carbonate. The less effective was the saturated $\text{Ca}(\text{OH})_2$ and the 1 M K_2CO_3 solutions. In case of the alkaline media selection for the Zn and Pb recovery which can offer efficient separation from the iron one of the way of improvement of the efficiency can be the transformation of the EAF dusts into better leachable state.

Keywords: *EAF dust, Zn and Pb leaching, acidic and alkaline medium*

1. INTRODUCTION

The steel scrap recycling using electric furnace represents about 30 % of the world steel production, 40% in Europe.

Getting 1 t steel in this way will produce 15–20 kg dust. Due to the high Zn content (15–25% ZnO) of the EAF dust almost 50% of the produced amount is recycled, which is equivalent with the 6% of the world Zn production/year. The recycling uses generally only thermal process; unfortunately the hydrometallurgical methods are still not feasible. Both, the determination of the risk caused by the Zn and Pb leaching from the landfilled portion, and the establishing an effective hydrometallurgical process, require to investigate the mobilization manner of these

elements at the circumstances of different chemical environments (ANTREKOWITCH and RÖSLER 2015, BUZINA et al. 2017).

2. SAMPLES AND EXTRACTION MEDIA

EAF dusts sources were used from the different steel plants of Germany (10) and Hungary (2) (Ózd and Diósgyőr) along with the standard reference materials (EAF dust: No 876-1; and (SPF dust (Steel Plant Furnace dust). DK No12-1-05). All of them also were investigated as a part of the REDILP Projekt (REDILP). The chemical environments were distilled water, salt solutions, complexing medium, weak and strong acids or different alkaline media. Complete dissolution of EAF dusts was achieved only in case of alkaline fusion. It was considered as a reference for getting the maximal yield of leaching.

The investigations done consisted from two parts: determination of elemental composition of the samples and determination of the mobility of the elements using the sequential extraction procedure. For this investigation the samples were used in as received form, however to check the sample dryness, humidity and the ignition loss were determined.

Determination of humidity: Approx. 5 g of sample was heated at 105 °C till achieved constant weight.

Determination of ignition loss: Approx. 1 g of sample was heated in Pt crucible at 750 °C. Duration of heating was one hour.

Determination of acid insoluble fraction: Approx. 0.5 g sample was heated up with 20 cm³ of cc. hydrochloric –acid till boiling, then 5 cm³ cc. nitric acid was added. The boiling was stopped when the gas formation has finished. Then the system was left standing for a day, and was washed into 50 cm³ volumetric flask with distilled water. The remaining solid was separated by filtering, it was washed, dried and the insoluble fractions were determined from the mass of ash of filter papers. (The ashing was taken at 700 °C. Ashless paper was used).

This dissolution has been referred later as aqua regia solution.

Dissolution of sample by alkali fusion: To achieve complete dissolution of EAF dusts approx.0.2 g of samples were weighted into Pt crucible and were mixed with 2 g of mixture of fluxing agent (2 part Na₂CO₃, K₂CO₃, 1 part Na₂B₄O₇), then the crucible was heated up with Bunsen flame till clear melt has been formed. Dissolution was carried out with 75 ml 1:3 HCl and was transferred into volumetric flask and made up to 100 ml. Complete dissolution was achieved in all the tested cases. (Dissolution of flux with nitric acid was preferred to decrease the risk of lead precipitation in presence of chloride, but using nitric acid instead of hydrochloric acid insoluble iron compound has formed).

Using the procedure described above the two standard reference materials were analysed. Compared the received values to the certificated ones given in *Table 1* the adequacy of the used analytical procedure has been proved, see *Tale 2*. In case of the SPF standard reference material the Zn, and Pb concentration much lower to compare with the values expected in the EAF dust. Therefore the recovery of these elements is not suitable for validate the EAF dust analysis.

Table 1
Elemental composition of Standard reference materials No 876-1 EAF dust (Electric Arc Furnace dust) and DK-12-1-05 SPF dust (Steel Plant Furnace dust).

Component	EAF dust standard (876-1)	SPF dust standard (2012 01 05)
	c, m/m%	c, m/m %
Fe	24.85	53.4
Zn	23.29	0.84
Pb	7.82	0.21
Mn	2.84	0.77
Si	1.72	
Ca	3.43	6.91
Mg	1.31	0.35
Na	1.98	0.69
K	1.63	0.34
Al	0.34	
Cr	0.17	
Cu	0.42	
Cd	0.13	
Sn	0.094	
As	0.023	
C	0.26	
S	0.87	
P	0.128	
Cl	3.63	
F	0.24	

Table .2
Determination of Fe, Zn, Pb of Standard reference materials No 876-1 EAF dust (Electric Arc Furnace dust) and DK-12-1-05 SPF dust (Steel Plant Furnace dust) by FAAS (Flame atomic Absorption Spectroscopy) after alkaline fusion.

Element	C determined m/m%	Deviation from the certified value $100(C-C^*)/C^*$ %	RSD of determination %
No 876-1 EAF dust			
Fe	24,05	-3,21	0,3
Zn	22,95	-1,47	0,6
Pb	7,92	+1,33	0,7
DK-12 SPF dust			
Fe	51,6	-3,45	0,5
Zn	1,13	+34,9	2,1
Pb	0,23	+25,5	18,7

3. RESULTS AND DISCUSSION

The humidity and the Fe, Zn, and Pb concentration in the EAF dust samples determined by AAS after alkaline fusion are given in *Table 3*. The *Table 3* shows that except a few cases the Zn content in the dusts varied between 20–30 m/m%, the Pb concentrations can be found between 2–4 m/m%. No correlation occurs between the Zn and the Pb content of the dusts, *Figure 1*. The ignition loss for the first seven samples varied between 1–7 m/m%, the acid insoluble fraction using aqua-regia varied between 2–8 %.

Table 3

Determination of humidity, Fe, Zn, Pb contents of EAF dusts by FAAS using alkaline fusion

Code	Sample source	Humidity, %	C Fe m/m%	C Zn m/m%	C Pb m/m%
EAF Dust 1	Lechstahlwerke Meitingen	0,53	27,1	25,85	2,38
EAF Dust 2	Stahlwerke Thuringen	0,54	28,6	23,93	3,08
EAF Dust 3	Badische Stahlwerke Kehl	2,09	29,7	15,30	1,00
EAF Dust 4	Stahlwerke Bous Saarland	0,47	20,4	37,51	1,93
EAF Dust 5	GM Hutte	4,32	26,2	31,25	2,26
EAF Dust 6	Hungarian sample 1	0,73	25,5	20,47	7,18
EAF Dust 7	Hungarian sample 2	4,95	30,5	8,53	2,05
EAF Dust 8.1	Stahlwerke Thuringen cont. s.	1,74	27,8	23,40	3,70
EAF Dust 8.2	Stahlwerke Thuringen cont. s.	1,19	28,7	21,89	4,13
EAF Dust 8.3	Stahlwerke Thuringen cont. s.	1,45	27,0	23,10	3,63
EAF Dust 8.4	Stahlwerke Thuringen cont. s.	0,86	29,1	22,83	3,57
EAF Dust 8.5	Stahlwerke Thuringen cont. s.	3,22	25,0	24,71	3,64
EAF Dust 8.6	Stahlwerke Thuringen cont. s.	4,40	25,2	24,75	3,77
EAF Dust 8.7	Stahlwerke Thuringen cont. s.	2,25	27,7	23,80	3,46
EAF Dust 8.8	Stahlwerke Thuringen cont. s.	3,21	24,7	24,39	3,45
EAF Dust 8.9	Stahlwerke Thuringen cont. s.	2,18	27,5	23,11	3,22
EAF Dust 8.10	Stahlwerke Thuringen cont. s.	0,68	29,2	21,81	4,35
EAF Dust 9	Hamburger Stahlwerke ISPAT	0,91	37,1	4,73	0,53
EAF Dust 10	Thuringer Stahlwerke 22.12.2004	0,83	26,0	25,89	4,38
EAF Dust 11	Lechstahlwerke meitingen	0,93	23,3	16,02	0,27
EAF Dust 12	Stahlwerke Bous Saarland	0,78	25,9	34,75	1,09
St 876	French standard	0,71	24,5	22,63	7,75

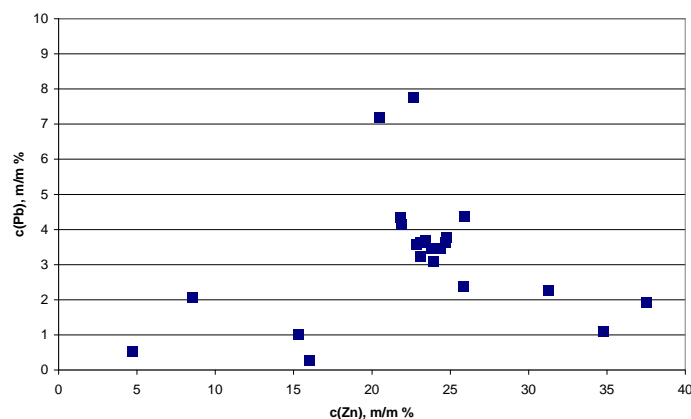


Figure 1

Correlation between the Zn and Pb content of the tested EAF dust samples

During the leaching tests 0.5 g samples were mixed with 50 ml of leaching solution. They were left standing for three weeks to achieve the dissolution equilibrium. The system was shaken up only occasionally (every 2-3 days). The separated liquid phases were analysed by AAS method. The compositions of leaching solutions are given in Table 4.

Table 4

Composition of solution used for leaching tests

No	Leachate	Composition	Expected mobilised fraction
1	Dist. Water	Distilled water	water soluble
2	1 M NH_4NO_3	1 mol dm^{-3} NH_4NO_3	No1+ ion-exchangeable, (NH_3 can act as well as complex forming)
3	1 M Hac	1 mol dm^{-3} acetic- acid solution	No2+ acid soluble oxides carbonates
4	Lak-Erv	Lakanen Ervio solution (0,1 mol dm^{-3} EDTA-1 mol dm^{-3} acetic acid solution)	No3+ complex forming
5	Ham-Hac	0,04 mol dm^{-3} Hydroxil-amin-hydrochlorid – 25 m/m% acetic- acid solution	No3+ loaded to component need reduction
6	1M HNO_3 -15% H_2O_2	1 mol dm^{-3} nitric-acid 15 m/m% hydrogen-peroxide solution	Strong acid soluble+ loaded to component need oxidation
7	2 M HCl	2 mol dm^{-3} hydrochloric-acid solution	Strong acid soluble
8	Aqua regia	Mixture of cc. hydrochloric and cc. nitric-acide*	Total acid soluble
9	Alkalic fusion	Fusion with mixture of two part Na_2CO_3 , K_2CO_3 , one part $\text{Na}_2\text{B}_4\text{O}_7$ T~800 C	Total content
10	Sat $\text{Ca}(\text{OH})_2$	Saturated calcium-hydroxide solution	
11	2 M NH_4OH	2 mol dm^{-3} ammonium-hydroxide	

No	Leachate	Composition	Expected mobilised fraction
		solution	
12	1 M NaOH	1 mol dm ⁻³ sodium-hydroxide solution	
13	1 M KOH	1 mol dm ⁻³ potassium- hydroxide solution	
14	1 M (NH ₄) ₂ CO ₃	1 mol dm ⁻³ ammonium-carbonate solution	
15	1 M Na ₂ CO ₃	1 mol dm ⁻³ sodium-carbonate solution	
16	1 M K ₂ CO ₃	1 mol dm ⁻³ potassium- carbonate solution	

*no complete dissolution occurs, the dissolution residue varied between 2–8 m/m%.

The Fe, Zn and Pb ion concentrations mobilised by acidic and alkali leaching solutions are given in *Figures 2–6*. For simplification only the first seven EAF dust samples data were plotted in the figures.

Dissolution of Fe: *Figures 2–3* show that distilled water, NH₄NO₃ solution is unable to mobilise iron ($c_{\text{Fe (mob)}} < 0.05 \text{ mg g}^{-1}$). Weak acids and complex forming agents can mobilise 10–20% of total iron. However, strong acids in one molar concentration were able to dissolve almost all of the EAF dust iron content. (The nitric-acid-peroxide system was found less effective than hydrochloric acid). The hydroxides are unable to mobilise iron ($c_{\text{Fe (mob)}} < 0.05 \text{ mg g}^{-1}$), however carbonates are already able to dissolve low quantity, the mobilised Fe varied between 0.5–5 mg g⁻¹ ($c_{\text{Fe (mob)}} 0,5\text{--}5 \text{ mg g}^{-1}$). To avoid the iron dissolution the alkaline solutions seems to be the best option.

Dissolution of Zn: *Figures 4–5* show that distilled water is unable to dissolve zinc ($c_{\text{Zn (mob)}} < 0.03 \text{ mg g}^{-1}$), however NH₄NO₃ solution is able to dissolve approx. 10% of total zinc content, due to the NH₃ complex formation. The weak acids and weak acid + complex forming agents are able to dissolve approx. 80% of total Zn. Strong acid solutions (1 M HCl, HNO₃) and aqua-regia can dissolve almost all of the Zn content. Less than half of the zinc content was mobilised by alkaline media. The most effective alkaline solution was the ammonium-carbonate. The less effective was the saturated Ca(OH)₂ and the 1 M K₂CO₃ solutions.

Dissolution of Pb: *Figures 6–7* show that the water soluble fraction of lead is low ($c_{\text{Pb(mob)}} < 0.3 \text{ mg g}^{-1}$). NH₄NO₃ solution is also unable to mobilise significant amount of lead ($c_{\text{Pb(mob)}} < 0.3 \text{ mg g}^{-1}$). Lead was almost completely mobilised by all of the weak and strong acidic media. More than 50% of lead is able to dissolve in alkaline media, except in NH₄OH and NH₄CO₃. The ammonium containing solutions are less effective than the sodium, potassium, and calcium-hydroxide and carbonates.

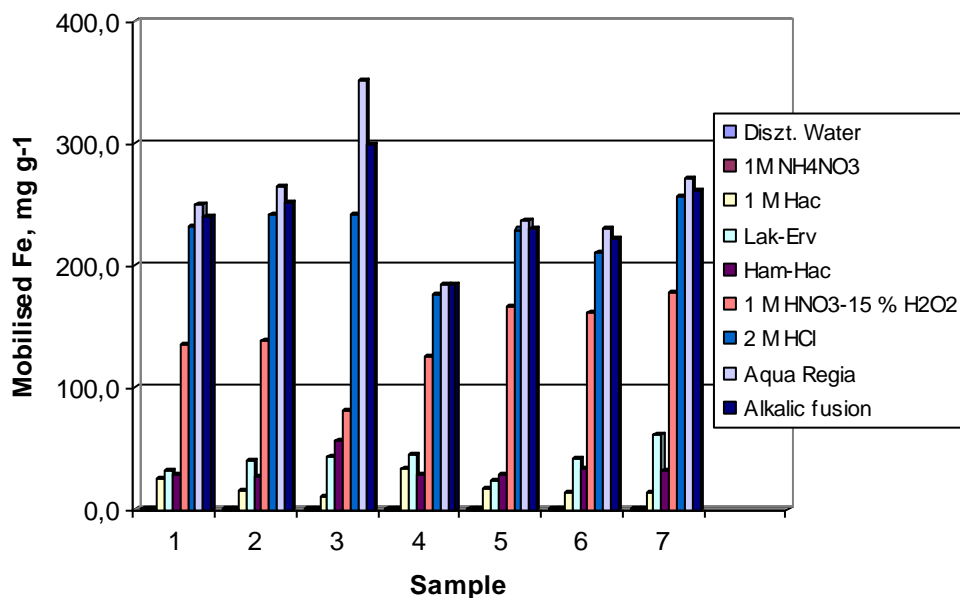


Figure 2

Mobilised Fe from EAF dusts by distilled water, complex forming materials and acidic leaching media. Alkalic fusion can be considered as the reference

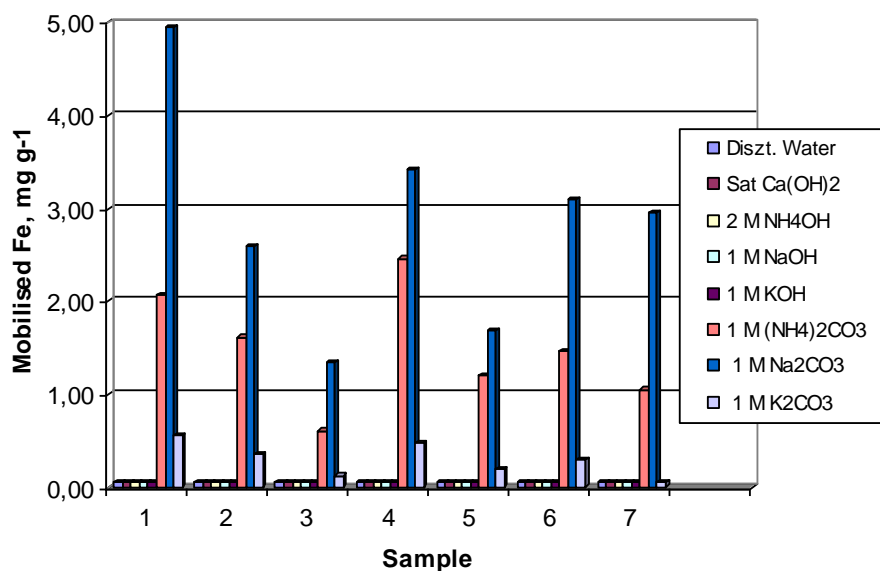


Figure 3

Mobilised Fe from EAF dusts by alkali leaching media. The maximum soluble Fe approx. 250 mg/g. See Fig 2, as a reference.

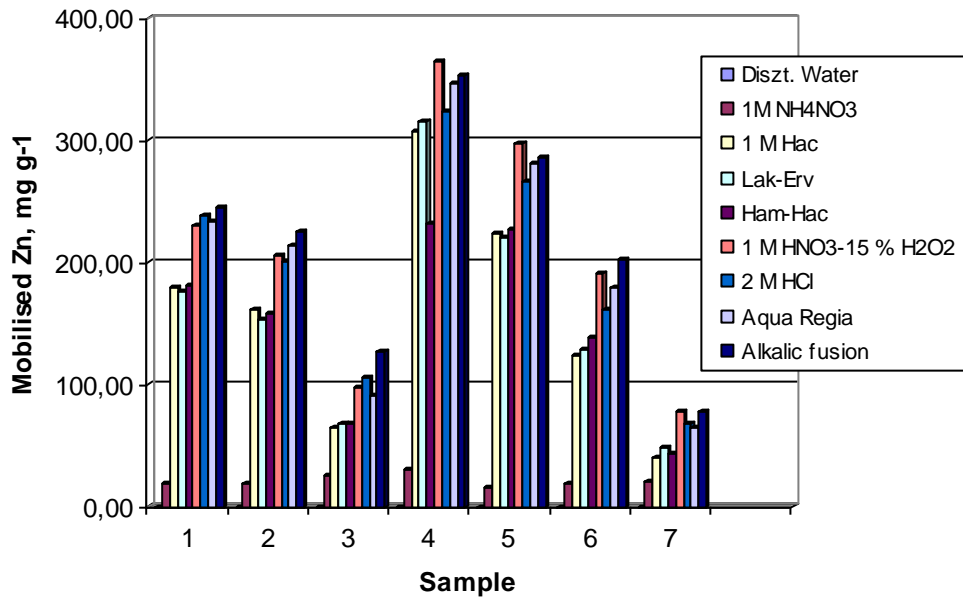


Figure 4

Mobilised Zn from EAF dusts by water, complex forming materials and acidic leaching media. Alkalic fusion can be considered as the reference.

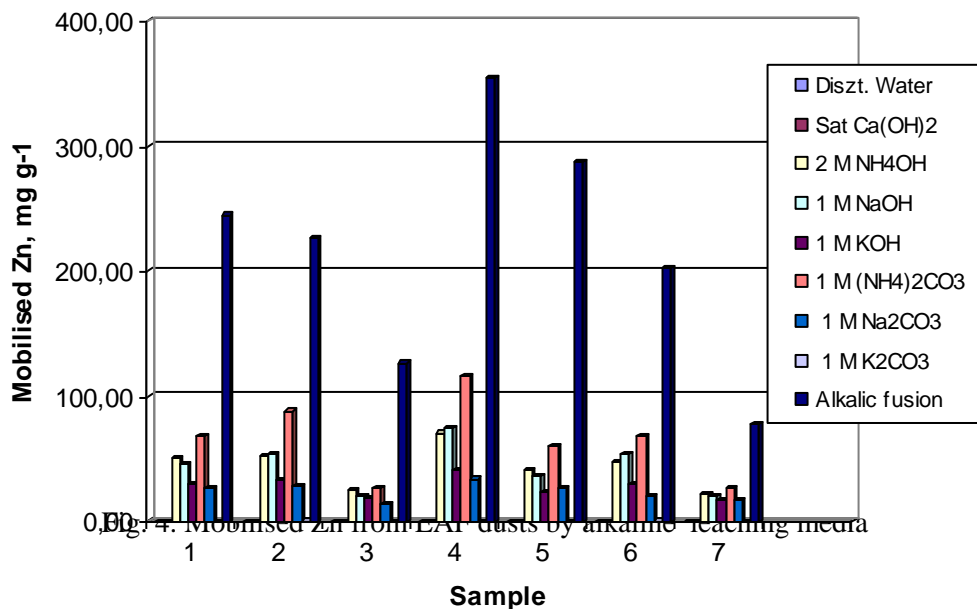


Figure 5

Mobilised Zn from EAF dusts by alkaline leaching media. Alkalic fusion can be considered as the reference.

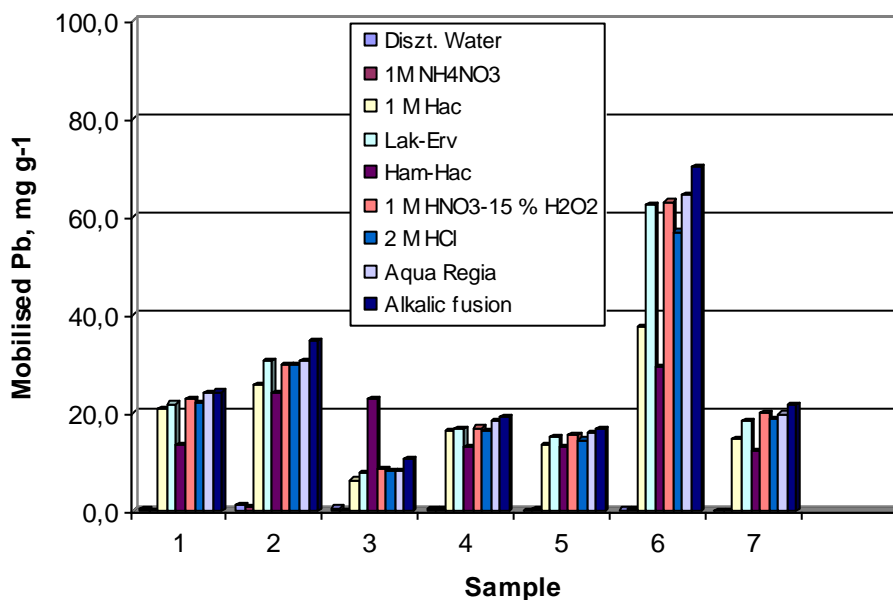


Figure 6

Mobilised Pb from EAF dusts by water, complex forming materials and acidic leaching media. Alkalic fusion can be considered as the reference.

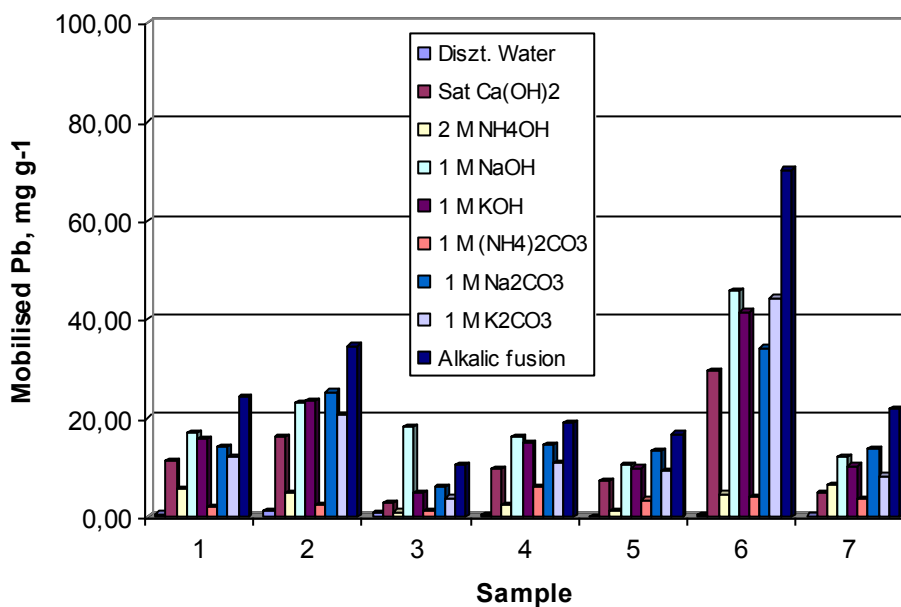


Figure 7

Mobilised Pb from EAF dusts by alkaline leaching media. Alkalic fusion can be considered as the reference.

4. CONCLUSIONS

The main aim of these leaching tests was to determine the manner of the mobilisation of Fe, Zn and Pb from EAF dusts. Leaching without Fe dissolution can be carried out only by alkaline solutions, but the efficiency achieved for Zn leaching was less than 50%. The Zn and Pb behaves differently in alkaline medium: the best leaching agent (the ammonium –carbonate) for Zn was found ineffective for Pb. High dissolution yields of Zn and Pb were found in weak acids, which unfortunately occurs along with a moderate Fe dissolution. This hinders the weak acid application if the iron free Zn and Pb extraction is the demand. At the same time good mobilisation of Zn and Pb in weak acids demonstrates that high environmental risk can occur at the sites of the EAF dust storage place if it can be contacted with these chemicals. Transformation of the EAF dust structure making the iron insoluble in acids or improving the alkaline solubility of Zn and Pb content can provide solutions for efficient recovery of Zn and Pb from EAF dusts.

ACKNOWLEDGEMENTS

The described article was carried out as part of the „Sustainable Raw Material Management Thematic Network – RING 2017”, EFOP-3.6.2-16-2017-00010 project in the framework of the Széchenyi 2020 Program. The realization of this project is supported by the European Union, co-financed by the European Social Fund.

REFERENCES

- [1] ANTREKOWITSCH J.–RÖSLER G. (2015): Steel Mill dust recycling in the 21st century.
- [2] www.uni-miskolc.hu/~microcad/publikaciok/2015/B2_Jurgen_Antrekowitsch.pdf, (DOI: 10.26649/musci.2015.018)
- [3] BUZINA, B. J. V. K.–HECKB, N. C.–VILELAC, A. C. F. (2017): EAF dust: An overview on the influences of physical, chemical and mineral features in its recycling and waste incorporation. *J. Mater Res. Techn.*, 6, pp. 194–202.
- [4] REDILP: Recycling of Electric Arc Furnace (EAF) Dust by Integrated Leach grinding Process. EU 6 Nemzetközi Projekt (2004–2006).